

New gold(I) and gold(III) coordination complexes derived from N and S heterocycles

by

TESFAMARIAM KIFLE HAGOS

Thesis

submitted in fulfilment of the requirements

for the degree of

Master of Science

in

CHEMISTRY

in the

FACULTY OF SCIENCE

at the

UNIVERSITY OF STELLENBOSCH

SUPERVISOR: PROF. H. G. RAUBENHEIMER

CO-SUPERVISOR: DR. S. CRONJE

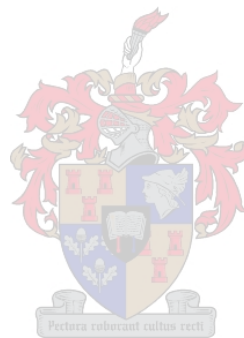
APRIL 2006

Declaration

I, the undersigned, hereby declare that the work contained in this thesis is my own original work and that I have not previously in its entirety or in part submitted it at any university for a degree.

Signature:

Date:



Abstract

An aqueous solution of tetrachloroaurate, HAuCl_4 reacted with 4-methylthiazole or 4,4-dimethyl-2-phenyloxazole in acetonitrile to give the cationic complexes $[\text{Cl}_2\text{Au}\{\overline{\text{N}=\text{C}(\text{Ph})\text{OCH}_2\text{C}(\text{CH}_3)_2}\}_2][\text{AuCl}_4]$, **4b** or $[\text{Au}\{\overline{\text{N}=\text{CHSCH}=\text{C}(\text{CH}_3)_2}\}_2][\text{AuCl}_4]$, **6a** compounds that each contain gold in two oxidation states. The molecular structures of these cationic complexes show that the heterocyclic ligands are bonded to gold(I) *via* the imine-N. The Au(I)-Au(III) separation of 3.3626 Å in complex **6a** is diagnostic for weak and alternating aurophilic interaction. An immonium tetrachloroaurate(III) salt of the type $[\text{LH}][\text{AuCl}_4]$ [L = 4,4-dimethyl-2-phenyl-oxazolyl] was also isolated from the reaction mixture containing **4b** and its crystal and molecular structure were determined. Analogous reactions of tetrachloroaurate(III) with various other imine ligands such as thiazole, benzothiazole, 4,4-dimethyl-2-thienyl-oxazole, 1-methyl-2-phenyl-imidazole, 1-methyl-2-(2-pyridinyl)imidazole and benzoxazole led to the formation of other immonium tetrachloroaurate(III) compounds belonging to this class; crystal and molecular structures of $[\overline{\text{HN}=\text{C}(\text{Ph})\text{OCH}_2\text{C}(\text{CH}_3)_2}][\text{AuCl}_4]$ (**4b'**), $[\overline{\text{HN}=\text{CHSC}=\text{CHCH}=\text{CHCH}=\text{C}}][\text{AuCl}_4]$, **8a** and $[\overline{\text{N}(\text{mes})\text{CHN}(\text{mes})\text{CH}_2\text{CH}_2}][\text{AuCl}_4]$ (mes = 2,4,6-trimethylphenyl), **12** were obtained.

A series of gold(III) complexes of the general type $[\text{AuCl}_3(\text{L})]$ were prepared from aqueous solutions of AuCl_3 and selected ligands, L (L = 1-methyl-2-phenyl-imidazole, 4,4-dimethyl-2-phenyl-oxazole, thiazole and its benzo- and methyl-substituted derivatives). ^1H and ^{13}C NMR spectra and mass spectrometry were utilised to characterise these products. The molecular structures of two of these products, **5b** and **7**, were determined by X-ray analysis, but only the structure of $[\text{Cl}_3\text{Au}\{\overline{\text{N}=\text{CHSC}(\text{CH}_3)=\text{C}(\text{CH}_3)_2}\}_2]$, **7**, appears in this thesis as an example: the five-membered N,N-, N,S- and N,O-heterocyclic ligands are bound to Au(III) through nitrogen. A mixed complex of silver and gold, $[(\text{Ag}\{\overline{\text{N}=\text{C}(\text{Ph})\text{OCH}_2\text{C}(\text{CH}_3)_2}\}_2)(\text{AuCl}_4)]$, **4d**, was obtained after an attempt to prepare the cationic complex $[(\text{Cl})_2\text{Au}\{\overline{\text{N}=\text{C}(\text{Ph})\text{OCH}_2\text{C}(\text{CH}_3)_2}\}_2][\text{AuCl}_4]$, **4c**, *via* exchange of the anion of $[\text{AgL}_2]\text{BF}_4$ with that of NaAuCl_4 . This product was mainly investigated using FAB MS, although ^1H and ^{13}C NMR spectroscopy measurements are included.

Displacement of the weakly-coordinating tetrahydrothiophene (tht) in the gold(I) precursor $\text{Au}(\text{C}_6\text{F}_5)(\text{tht})$ by the heterocyclic thiones [tetramethylimidazole-2(3H)-thione ($\text{S}=\text{CN}(\text{Me})\text{C}(\text{Me})=\text{C}(\text{Me})\text{N}(\text{Me})$), 1,3-diisopropyl-4,5-dimethyl-1,3-dihydro-imidazole-2-thione ($\text{S}=\text{CN}(i\text{-Pr})\text{C}(\text{Me})=\text{C}(\text{Me})\text{N}(i\text{-Pr})$) and 2-imidazolidinethione ($\text{S}=\text{CNHCH}_2\text{CH}_2\text{NH}$)] furnished $\text{Au}(\text{C}_6\text{F}_5)(\text{thione})$ complexes **13a**, **13b** and **13c**. The crystal and molecular structures of **13a** and **13b** were established by X-ray diffraction methods and show a linear coordination at Au *via* the thione sulfur.

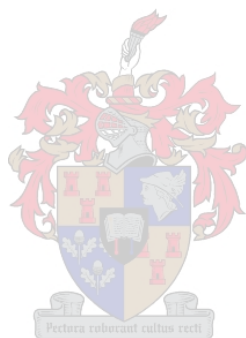
The gold(III) source, HAuCl_4 , reacted with the thiones, 1,3,4,5-tetramethyl-1,3-dihydro-imidazole-2-thione and 1,3-diisopropyl-4,5-dimethyl-1,3-dihydro-imidazole-2-thione, in ethanol to form stable complexes [$\text{AuCl}_3\{\text{S}=\text{CN}(\text{Me})\text{C}(\text{Me})=\text{C}(\text{Me})\text{N}(\text{Me})\}$], **14a** and [$\text{AuCl}_3\{\text{S}=\text{CN}(i\text{-Pr})\text{C}(\text{Me})=\text{C}(\text{Me})\text{N}(i\text{-Pr})\}$], **14b** respectively both of the type $\text{AuCl}_3(\text{thione})$. Physical methods as well as a crystal and molecular structure determination of **14b** indicated coordination *via* the exocyclic sulfur atom.

The reaction of $[(\text{AuCl})_2(\text{dppm})]$ with *in-situ*-prepared dilithio-1,3-dithiane-2-carbodithioate, [$\text{Li}_2\text{S}_2\text{C}=\text{CSCH}_2\text{CH}_2\text{CH}_2\text{S}$], promoted an oxidation reaction yielding the novel multinuclear, tetracationic sulphonium gold(I) cluster complex, $[\text{Au}_{12}(\mu\text{-dppm})_6(\mu_3\text{-S})_4]\text{Cl}_4$, (**15a**) and the by-product di(1,3-dithian-2-yl)methanol. Similar reactions were also carried out using the phosphine precursors $[(\text{AuCl})_2(\text{dppe})]$ or $[\text{AuCl}(\text{PPh}_3)]$.

Tetranuclear and dinuclear cationic complexes of $[\{\text{Ph}_3\text{PAu}(\text{BT}-N)\}_2\text{C}=\text{C}\{\text{BT}-N\}\text{AuPPh}_3\}_2]^{4+}4[\text{BF}_4]^-$ (BT = benzothiazolyl), **16** and $[\{\text{Ph}_3\text{PAu}(\text{BT}-N)\}_2\text{CH}_2]^{2+}2[\text{BF}_4]^-$, **17** were obtained as a mixture, by consecutive treatment of bis(2-benzothiazolyl)methane (HBBTM) with $\text{AuCl}(\text{PPh}_3)$ and AgBF_4 . The former complex was formed due to oxidative dimerisation of the ligand by an unspecified oxidising agent (probably air). The ^{31}P NMR spectroscopy investigation indicated that the relative concentrations of **16** and **17** may be varied by changing the reaction conditions. Single crystal X-ray structures of **16** and **17** showed that only imine-*N* donor atoms of 2-(1,2,2-tri(benzo[*d*]thiazol-2-yl)vinyl)benzo[*d*]thiazole and HBBTM coordinate to the gold(I) centres.

Neutral, tri-coordinated complexes $[(\text{PPh}_3)\text{Au}\{\text{BT}-N,N\}_2\text{CH}]$, **18** and $[(\text{PPh}_3)\text{Au}\{\text{BO}-N\}_2\text{CH}]$ (BO = benzoxazolyl), **20** were synthesised in reasonable yields by reacting $\text{Au}(\text{acac})(\text{PPh}_3)$ with bis(2-benzothiazolyl)methane (HBBTM) and bis(2-

benzoxazolyl)methane (HBBOM) respectively, at room temperature. The crystal and molecular structure of $[(\text{PPh}_3)\text{Au}\{\text{BO}-N,N\}_2\text{CH}]$, **20**, determined by X-ray analysis confirmed that the ligand is coordinated bidentately *via* the N-atoms to the gold(I) centre. Another neutral but dinuclear complex $[(\text{Ph}_3\text{P})\text{Au}-\overline{\text{NC}=\text{CHCH}=\text{CHCH}=\text{CSC}=\text{C}(\text{BT})-(\text{BT})\text{C}=\text{CSC}=\text{CHCH}=\text{CHCH}=\text{CN}}-\text{Au}(\text{PPh}_3)]$, **19** was obtained by reacting $\text{AuCl}(\text{PPh}_3)$, with deprotonated HBBTM. The molecular structure obtained by single crystal X-ray analysis showed that oxidative dimerisation had occurred. Similar attempts using *n*-BuLi promoted oxidative dimerisation of the carbanion of the deprotonated ligands of HBBTM and HBBOM to afford 2-(1,2,2-tri(benzo[*d*]thiazol-2-yl)vinyl)benzo[*d*]thiazole and 2-(1,2,2-tri(benzo[*d*]oxazol-2-yl)vinyl)benzo[*d*]oxazole, respectively.



Opsomming

'n Waterige oplossing van waterstof tetrachloroauraat, HAuCl_4 , reageer met 4-metiel-tiasool of 4,4-dimetiel-2-fenieloksasool in asetonitriël om onderskeidelik die kationiese komplekse $[\text{Cl}_2\text{Au}\{\overline{\text{N}=\text{C}(\text{Ph})\text{OCH}_2\text{C}(\text{CH}_3)_2}\}_2][\text{AuCl}_4]$, **4b**, en $[\text{Au}\{\overline{\text{N}=\text{CHSCH}=\text{C}(\text{CH}_3)_2}\}_2][\text{AuCl}_4]$, **6a**, te lewer. Beide komplekse bevat goud in tweeoksidasie toestande. Die molekulêre struktuur van hierdie kationiese komplekse toon dat die heterosikliese ligande *via* die imien-*N*-atome gebind is. Die Au(I)-Au(III) afstand van 3.3626 Å in kompleks **6a** gee 'n aanduiding van swak en afwisselende aurofiliese interaksie. 'n Immonium tetrachloroauraat(III) sout van die tipe $\text{LH}[\text{AuCl}_4]$ (L = 4,4-dimetiel-2-fenieloksasool) is ook uit die reaksiemengsel van **4b** geïsoleer en die kristal- en molekulêre struktuur daarvan bepaal. Soortgelyke reaksies van die tetrachloroauraat(III)-kompleks met verskeie imienligande soos tiasool, bensotiasool, 4,4-dimetiel-2-tioenieloksasool **4b'**, 1-metiel-2-feniel-imidasool, 1-metiel-2-(2-piridinil)imidasool en benso-oksasool lei tot die vorming van ander immonium tetrachloroauraat(III)-verbindings wat aan dié klas behoort; kristal- en molekulêre strukture van $[\text{HN}=\overline{\text{C}(\text{Ph})\text{OCH}_2\text{C}(\text{CH}_3)_2}][\text{AuCl}_4]$ **4b'**, $(\overline{\text{HN}=\text{CHSC}=\text{CHCH}=\text{CHCH}=\text{C}})[\text{AuCl}_4]$, **8a**, en $[\text{N}(\text{mes})\overline{\text{CHN}(\text{mes})\text{CH}_2\text{CH}_2}][\text{AuCl}_4]$ (mes = 2,4,6-trimetylphenyl), **12**, is bepaal.

'n Reeks goud(III)komplekse van die algemene tipe $[\text{AuCl}_3(\text{L})]$ is berei uit waterige oplossings van AuCl_3 en onderskeie ligande, L (L = 1-metiel-2-feniel-imidasool, 4,4-dimetiel-2-fenieloksasool, tiasool en hul benso- en metiel-gesubstitueerde derivate). ^1H - en ^{13}C -KMR-spektra, asook massaspektrometrie is gebruik om die produkte te karakteriseer. Die molekulêre strukture van twee van die produkte, **5b** en **7**, is met behulp van met X-straal analise bepaal, maar slegs die struktuur van $[\text{Cl}_3\text{Au}\{\overline{\text{N}=\text{CHSC}(\text{CH}_3)=\text{C}(\text{CH}_3)_2}\}_2]$, **7**, verskyn as voorbeeld in die tesis: die vyflid N,N-, N,S- en N,O-heterosikliese ligande is deur die stikstowwe aan Au(III) gebind. 'n Gemengde kompleks van silwer en goud, $[\text{Ag}\{\overline{\text{N}=\text{C}(\text{Ph})\text{OCH}_2\text{C}(\text{CH}_3)_2}\}_2\text{AuCl}_4]$, **4d**, is verkry tydens die poging om die kationiese kompleks $[(\text{Cl})_2\text{Au}\{\overline{\text{N}=\text{C}(\text{Ph})\text{OCH}_2\text{C}(\text{CH}_3)_2}\}_2][\text{AuCl}_4]$, **4c**, te berei deur die uitruiling van die anioon in $[\text{AgL}_2]\text{BF}_4$ met AuCl_4^- . Die produk is hoofsaaklik ondersoek deur gebruik te maak van FAB MS, alhoewel die ^1H - en ^{13}C -KMR-data ook ingesluit word.

Die verplasing van die swak-gekoördineerde tetrahidrotiofeen (tht) in die goud(I) uitgangstof $\text{Au}(\text{C}_6\text{F}_5)(\text{tht})$ deur die heterosikliese tione tetrametielimidiasool-2(3H)-tioon, $\text{S}=\overline{\text{CN}(\text{Me})\text{C}(\text{Me})=\text{C}(\text{Me})\text{NMe}}$, 1,3-di-isopropiel-4,5-dimetielimidiasool-2(3H)-tioon, $\text{S}=\overline{\text{CN}(i\text{-Pr})\text{C}(\text{Me})=\text{C}(\text{Me})\text{N}(i\text{-Pr})}$ en $\text{S}=\overline{\text{CNHCH}_2\text{CH}_2\text{NH}}$ lewer $[\text{Au}(\text{C}_6\text{F}_5)(\text{tioon})]$ -tipe komplekse (**13a**, **13b** en **13c**). Die kristal- en molekulêre strukture van **13a** en **13b** is bepaal deur X-straaldiffraksiemetodes en toon liniêre koördinasie aan die Au *via* die tioonswawels aan.

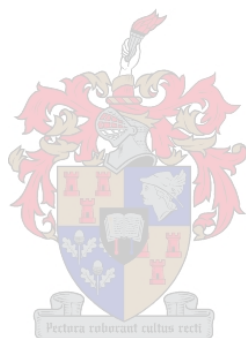
Die goud(III)bron, HAuCl_4 , reageer ook met die tione 1,3,4,5-tetrametielimidiasool-2(3H)-tioon en 1,3-di-isopropiel-4,5-dimetielimidiasool-2(3H)-tioon in etanol en vorm onderskeidelik die stabiele komplekse $[\text{AuCl}_3\{\text{S}=\overline{\text{CN}(\text{Me})\text{C}(\text{Me})=\text{C}(\text{Me})\text{N}(\text{Me})}\}]$, **14a**, en $[\text{AuCl}_3\{\text{S}=\overline{\text{CN}(i\text{-Pr})\text{C}(\text{Me})=\text{C}(\text{Me})\text{N}(i\text{-Pr})}\}]$, **14b**, albei van die tipe $[\text{AuCl}_3(\text{tioon})]$. Fisiese metodes asook kristal- en molekulêre struktuur bepaling van **14b** dui op koördinasie *via* die eksosikliese swawel atoom.

Die reaksie van $[(\text{AuCl})_2(\text{dppm})]$ met *in-situ*-bereide di-litio-1,3-ditiaan-2-karboditioaat, $\text{Li}_2(\text{S}_2\text{C}=\overline{\text{CSCH}_2\text{CH}_2\text{CH}_2\text{S}})$, bevorder 'n oksidasie-reaksie en lewer die nuwe, meerkernige, tetrakationiese sulfoniumgoud(I) klusterkompleks, $[\text{Au}_{12}(\mu\text{-dppm})_6(\mu_3\text{-S})_4]\text{Cl}_4$, **15a**, en 'n neweproduk, bis[2-(1,3-ditiaan)metanol]. Soortgelyke reaksies is ook uitgevoer met die fosfienvoorlopers $[(\text{AuCl})_2(\text{dppe})]$ en $[\text{AuCl}(\text{PPh}_3)]$.

Tetrakernige en dikernige kationiese komplekse van $[\{\text{Ph}_3\text{PAu}(\text{BT}-N)\}_2\text{C}=\text{C}\{\text{BT}-N\}\text{AuPPh}_3\}_2][\text{BF}_4]_4$ (BT = bensotiasoliel), **16**, en $[\{\text{Ph}_3\text{PAu}(\text{BT}-N)\}_2\text{CH}_2][\text{BF}_4]_2$, **17**, is as 'n mengsel verkry deur die opeenvolgende behandeling van bis(2-bensotiasoliel)metaan (HBBTM) met $[\text{AuCl}(\text{PPh}_3)]$ en AgBF_4 . Die eersgenoemde kompleks vorm as gevolg van oksidatiewe dimerisering van die ligand deur 'n ongespesifiseerde oksideermiddel (heel moontlik lug). Die ^{31}P -KMR-spektroskopiese ondersoek toon dat die relatiewe konsentrasies van **16** en **17** gevarieer kan word deur die reaksiekondisies te verander. Enkelkristal X-straalstrukture van **16** en **17** toon dat slegs imien-*N* donoratome van tetrakis(2-bensotiasoliel)eteen en HBBTM aan die goud(I)kern koördineer.

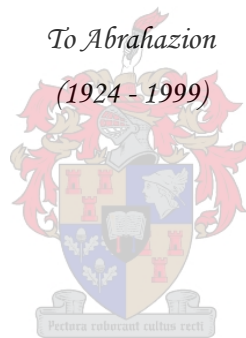
Neutrale, tri-gekoördineerde komplekse $[(\text{PPh}_3)\text{Au}\{\text{BT}-N,N\}_2\text{CH}]$, **18**, en $[(\text{PPh}_3)\text{Au}\{\text{BO}-N\}_2\text{CH}]$ (BO = benso-oksasoliel), **20**, is in redelike opbrengste

gesintetiseer deur $[\text{Au}(\text{acac})(\text{PPh}_3)]$ met onderskeidelik bis(2-bensotiasoliel)metaan en bis(2-bensoksasoliel)metaan (HBBOM) by kamertemperatuur te reageer. Die kristal- en molekulêre struktuur van $[(\text{PPh}_3)\text{Au}\{\text{BO-}N,N\}_2\text{CH}]$, **20**, bepaal deur X-straal analise, bevestig dat die ligand bidentaats gekoördineer is aan die goud(I)kern *via* die imien-*N*-atome. 'n Ander neutrale, maar dikernige kompleks $[(\text{Ph}_3\text{P})\text{Au}(\overline{\text{NC}=\text{CHCH}=\text{CHCH}=\text{CSC}=\text{C}(\text{BT})-(\text{BT})\text{C}=\text{CSC}=\text{CHCH}=\text{CHCH}=\text{CN}})\text{Au}(\text{PPh}_3)]$, **19**, is verkry deur $[\text{AuCl}(\text{PPh}_3)]$ met gedeprotoneerde HBBTM te laat reageer. Die molekulêre struktuur verkry deur enkelkristal X-straalanalise toon dat oksidatiewe dimerisering plaasgevind het. Soortgelyke pogings met *n*-BuLi, bevorder oksidatiewe dimerisering van die karbanioon met die gedeprotoneerde ligande van HBBTM en HBBOM om onderskeidelik tetrakis(2-bensotiasoliel)eteen en tetrakis(2-bensoksasoliel)eteen te lewer.



Dedication

*To Abrahazion
(1924 - 1999)*



Acknowledgements

I would like to express my sincerest gratitude to all who have encouraged, supported and advised me during the work presented in this thesis. In particular I would like to thank the following people and institutions.

My brother Tewelde for the endless love, support and care.

Prof. Raubenheimer for the excellent leadership, guidance and always having time for discussion.

Dr. S. Cronje for the continuous support, encouragement and meticulous follow-up.

Dr. S. Nogai and Mr. B. Barnard for the recording of crystal data and solving the structures. In particular Stephan for carefully checking the structures and friendship.

Elsa Malharbe and Jean McKenzie for recording excellent NMR spectra.

Dr. U. E. I. Horvath and Dr. O. Schuster for kindly proof-reading this thesis.

All my colleagues (Andrew, Anneke, Elzet, Gerrit, Jacorein, Julia, Karolien, Christoph, Phillip, William and staff members and students of the Inorganic building) for making the environment in the laboratory conducive and pleasant. Especially, Gerrit for the friendship and talks other than Chemistry.

My family for their prayers and encouragement.

All Eritrean friends for making the journey enjoyable.

The Government of Eritrea (GoE), Prof. Raubenheimer and University of Stellenbosch for the financial support.

My Heavenly Father

Part of this study has been presented in the form of:

Presentations:

- Lectures presented by Prof. Helgard Raubenheimer at various European Universities, July - December 2005.

Poster:

- A poster at the Cape Organometallic Symposium in Cape Town at the Waterfront, 28 October 2004. Gold(I) a versatile coordination centre, U. E. I. Horvath, W. F. Gabrielli, K. Coetzee, T. K. Hagos, S. Cronje and H. G. Raubenheimer.

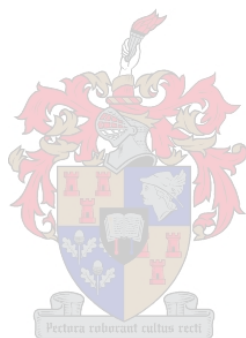


Table of Contents

Abstract	i
Opsomming	iv
Dedication.....	vii
Acknowledgements.....	viii
Table of Contents.....	x
Abbreviations.....	xvii
Chapter – 1 Introduction and Aims.....	1
1.1 Introduction.....	1
1.2 Research goals and thesis outline	12
Chapter – 2 Synthesis and characterisation of imine compounds of gold(III)	14
2.1 Introduction and aims	14
2.1.1 General.....	14
2.1.2 Aims and objectives.....	18
2.2 Results and discussions	19
2.2.1 Synthesis of immonium tetrachloroaurate(III) salts, neutral and cationic complexes.....	19
2.2.2 Spectroscopic characterisation of compounds 1 – 4	24
2.2.2.1 $[\text{HN}=\text{C}(\text{Ph})\text{NMeCH}=\text{CH}][\text{AuCl}_4]$, 1	24
2.2.2.2 $[\text{HN}=\text{C}(\text{py})\text{NMeCH}=\text{CH}][\text{AuCl}_4]$, 2a and $[\text{Cl}_3\text{Au}\{\text{N}=\text{C}(\text{py})\text{NMeCH}=\text{CH}\}]$, 2b	25
2.2.2.3 $[\text{HN}=\text{C}(\text{C}=\text{CHCH}=\text{CHS})\text{OCH}_2\text{C}(\text{CH}_3)_2][\text{AuCl}_4]$, 3	27

2.2.2.4	$[\text{Cl}_3\text{Au}\{\overline{\text{N}=\text{C}(\text{Ph})\text{OCH}_2\text{C}(\text{CH}_3)_2}\}]$, 4a and $[\text{Au}\{\overline{\text{N}=\text{C}(\text{Ph})\text{OCH}_2\text{C}(\text{CH}_3)_2}\}_2][\text{AuCl}_4]$, 4b	28
2.2.2.5	$[\text{Cl}_2\text{Au}\{\overline{\text{N}=\text{C}(\text{Ph})\text{OCH}_2\text{C}(\text{CH}_3)_2}\}_2][\text{AuCl}_4]$, 4c and $[(\text{Ag}\{\overline{\text{N}=\text{C}(\text{Ph})\text{OCH}_2\text{C}(\text{CH}_3)_2}\})_2][\text{AuCl}_4]$, 4d	30
2.2.3	Spectroscopic characterisation of compounds 5 - 12	34
2.2.3.1	$[\text{HN}=\overline{\text{CHSCH}=\text{CH}}][\text{AuCl}_4]$, 5a and $[\text{Cl}_3\text{Au}\{\overline{\text{N}=\text{CHSCH}=\text{CH}}\}]$, 5b	34
2.2.3.2	$[\text{Au}\{\overline{\text{N}=\text{CHSCH}=\text{C}(\text{CH}_3)}\}_2][\text{AuCl}_4]$, 6a and $[\text{Cl}_3\text{Au}\{\overline{\text{N}=\text{CHSCH}=\text{C}(\text{CH}_3)}\}]$, 6b	35
2.2.3.3	$[\text{Cl}_3\text{Au}\{\overline{\text{N}=\text{CHSC}(\text{CH}_3)=\text{C}(\text{CH}_3)}\}]$, 7	36
2.2.3.4	$[\text{HN}=\overline{\text{CHSC}=\text{CHCH}=\text{CHCH}=\text{C}}][\text{AuCl}_4]$, 8a and $[\text{Cl}_3\text{Au}\{\overline{\text{N}=\text{CHSC}=\text{CHCH}=\text{CHCH}=\text{C}}\}]$, 8b	37
2.2.3.5	$[\text{HN}=\overline{\text{CHOCH}=\text{CH}}][\text{AuCl}_4]$, 9 and $[\text{HN}=\overline{\text{CHOC}=\text{CHCH}=\text{CHCH}=\text{C}}][\text{AuCl}_4]$, 10	39
2.2.4	Spectroscopic characterisation of compounds 11 - 12	42
2.2.4.1	$(\text{BT})_2\text{C}=\text{C}(\text{BT})_2$, BT = benzothiazolyl, 11	42
2.2.4.2	$[\text{N}(\text{mes})\text{CHN}(\text{mes})\text{CH}_2\text{CH}_2][\text{AuCl}_4]$ (mes = 2,4,6-trimethylphenyl), 12	43
2.3	Crystal and molecular structure determinations by means of X-ray diffraction	45
2.3.1	The crystal and molecular structure of 4b	46
2.3.2	The crystal and molecular structures of 4,4-dimethyl-2-phenyl-oxazoline tetrachloroaurate(III) salt, 4b'	49
2.3.3	The crystal and molecular structure of 6a	52
2.3.4	The crystal and molecular structure of 7	55
2.3.5	The crystal and molecular structure of 8a	58
2.3.6	The crystal and molecular structure of 12	60
2.4	Conclusions and future work	63
2.5	Experimental	65
2.5.1	Materials and methods	65
2.5.2	Preparations	66

2.5.2.1 Preparation of tetrachloroaurate(III) imine salts [LH][AuCl ₄], 1 , 2a and 3 and cationic complex [AuL ₂][AuCl ₄], 4b	66
2.5.2.2 Preparation of adducts [AuCl ₃ (L)], 2b and 4a	67
2.5.2.3 Preparation of cationic complex [AuCl ₂ (L ₂)] [AuCl ₄]	68
2.5.2.4 Preparation of tetrachloroaurate(III) imine salts 5a and 8a , adduct 7 and cationic complex 6a	68
2.5.2.5 Preparation of adducts of [AuCl ₃ (L)], 5b , 6b , 7 and 8b	69
2.5.2.6 Preparation of tetrachloroaurate(III) imine salts, 9 and 10	70
2.5.2.7 (BT) ₂ C=C(BT) ₂ , 11	71
2.5.2.8 Preparation of 1,3-bis(2,4,6-trimethylphenyl)-imidazolium tetrachloroaurate(III) salt, 12	71
2.5.3 X-ray structure determinations	71

Chapter – 3 Thione complexes of gold(I) and gold(III); cationic sulphonium complexes of gold(I) 75

3.1 Introduction and aims	75
3.1.1 General	75
3.1.2 Aims and objectives	79
3.2 Results and discussions	80
3.2.1 Preparation of thione complexes of gold(I) and gold(III)	80
3.2.2 Spectroscopic characterisation of the new thione-coordinated gold(I) and gold(III) compounds 13a - 14b	82
3.2.2.1 [Au(C ₆ F ₅) {S=CN(Me)C(Me)=C(Me)N(Me)}], 13a	82
3.2.2.2 [Au(C ₆ F ₅) {S=CN(<i>i</i> -Pr)C(Me)=C(Me)N(<i>i</i> -Pr)}], 13b	84
3.2.2.3 [Au(C ₆ F ₅) {S=CNHCH ₂ CH ₂ NH}], 13c	85
3.2.2.4 [Cl ₃ Au {S=CN(Me)C(Me)=C(Me)N(Me)}], 14a and [Cl ₃ Au {S=CN(<i>i</i> -Pr)C(Me)=C(Me)N(<i>i</i> -Pr)}], 14b	86
3.2.3 Cationic sulphonium complexes of gold(I)	91
3.2.4 Spectroscopic characterisation of compounds 15a - 15c	93
3.2.4.1 (Cl)S—{AuP(Ph ₂)CH ₂ P(Ph) ₂ Au} ₂ —S(Cl)—{AuP(Ph ₂)CH ₂ P(Ph) ₂ Au}—S(Cl)— <u>{AuP(Ph₂)CH₂P(Ph)₂Au}₂—S(Cl)—{AuP(Ph₂)CH₂P(Ph)₂Au}</u> , 15a and di(1,3-dithian-2-yl)methanol	93

3.2.4.2	$(\text{Cl})\text{S}—\{\text{AuP}(\text{Ph}_2)(\text{CH}_2)_2\text{P}(\text{Ph})_2\text{Au}\}_2—\text{S}(\text{Cl})—\{\text{AuP}(\text{Ph}_2)(\text{CH}_2)_2\text{P}(\text{Ph})_2\text{Au}\}—$ $\text{S}(\text{Cl})—\{\text{AuP}(\text{Ph}_2)(\text{CH}_2)_2\text{P}(\text{Ph})_2\text{Au}\}_2—\text{S}(\text{Cl})—\{\text{AuP}(\text{Ph}_2)(\text{CH}_2)_2\text{P}(\text{Ph})_2\text{Au}\},$ 15b and di(1,3-dithian-2-yl)methanol	95
3.2.4.3	$[\text{S}(\text{AuP}(\text{Ph}_3))_2],$ 15c and di(1,3-dithian-2-yl)methanol	97
3.3	Crystal and molecular structure determinations by means of X-ray diffraction	99
3.3.1	The crystal and molecular structure of 13a	100
3.3.2	The crystal and molecular structure of 13b	103
3.3.3	The crystal and molecular structure of 14b	106
3.3.4	The crystal and molecular structure of 15a	109
3.4	Conclusions and future work.....	113
3.5	Experimental.....	114
3.5.1	Materials and methods	114
3.5.2	Preparations	115
3.5.2.1	Preparation of $[\text{Au}(\text{C}_6\text{F}_5)\{\text{S}=\text{CN}(i\text{-Pr})\text{C}(\text{Me})=\text{C}(\text{Me})\text{N}(i\text{-Pr})\}],$ 13b	115
3.5.2.2	Preparation of $[\text{Au}(\text{C}_6\text{F}_5)\{\text{S}=\text{CN}(\text{Me})\text{C}(\text{Me})=\text{C}(\text{Me})\text{N}(\text{Me})\}],$ 13a and $[\text{Au}(\text{C}_6\text{F}_5)\{\text{S}=\text{CNHCH}_2\text{CH}_2\text{NH}\}],$ 13c	115
3.5.2.3	Preparation of $[\text{Cl}_3\text{Au}\{\text{S}=\text{CN}(i\text{-Pr})\text{C}(\text{Me})=\text{C}(\text{Me})\text{N}(i\text{-Pr})\}],$ 14b	116
3.5.2.4	Preparation of $[\text{Cl}_3\text{Au}\{\text{S}=\text{CN}(\text{Me})\text{C}(\text{Me})=\text{C}(\text{Me})\text{N}(\text{Me})\}],$ 14a	116
3.5.2.5	Oxidation of the cyclic 1,3-dithiane-2-carbodithioate gold(I) complex to $(\text{Cl})\text{S}—\{\text{AuP}(\text{Ph}_2)\text{CH}_2\text{P}(\text{Ph})_2\text{Au}\}_2—\text{S}(\text{Cl})—\{\text{AuP}(\text{Ph}_2)\text{CH}_2\text{P}(\text{Ph})_2\text{Au}\}—\text{S}(\text{Cl})—$ $\{\text{AuP}(\text{Ph}_2)\text{CH}_2\text{P}(\text{Ph})_2\text{Au}\}_2—\text{S}(\text{Cl})—\{\text{AuP}(\text{Ph}_2)\text{CH}_2\text{P}(\text{Ph})_2\text{Au}\},$ 15a	116
3.5.2.6	Oxidation of the cyclic 1,3-dithiane-2-carbodithioate gold(I) complex to $(\text{Cl})\text{S}—\{\text{AuP}(\text{Ph}_2)(\text{CH}_2)_2\text{P}(\text{Ph})_2\text{Au}\}_2—\text{S}(\text{Cl})—\{\text{AuP}(\text{Ph}_2)(\text{CH}_2)_2\text{P}(\text{Ph})_2\text{Au}\}—$ $\text{S}(\text{Cl})—\{\text{AuP}(\text{Ph}_2)(\text{CH}_2)_2\text{P}(\text{Ph})_2\text{Au}\}_2—\text{S}(\text{Cl})—\{\text{AuP}(\text{Ph}_2)(\text{CH}_2)_2\text{P}(\text{Ph})_2\text{Au}\},$ 15b ...	117
3.5.2.7	Oxidation of the acyclic 1,3-dithiane-2-carbodithioate gold(I) complex to $[\text{S}(\text{AuP}(\text{Ph}_3))_2],$ 15c	117
3.5.3	X-ray structure determinations	117

Chapter – 4 New cationic and neutral imine complexes of gold(I) derived from HBBTM and HBBOM.....	121
4.1 Introduction and aims	121
4.1.1 General.....	121
4.1.2 Aims and objectives.....	126
4.2 Results and discussions	126
4.2.1 Synthesis of cationic and neutral heterocyclic complexes of gold(I)	126
4.2.2 Spectroscopic characterisation of compounds 16 - 20	130
4.2.2.1 [$\{(AuPPh_3)(BT-N)\}_2C=C\{(BT-N)(AuPPh_3)\}_2\}^{4+}4[BF_4]^-$ (BT = benzothiazolyl), 16	130
4.2.2.2 [$\{(PPh_3Au)(BT-N)\}_2CH_2\}^{2+}2[BF_4]^-$ (BT = benzothiazolyl), 17	132
4.2.2.3 [$(PPh_3)Au(BT-N)_2CH$] (BT = benzothiazolyl), 18	133
4.2.2.4 $\left\{ \begin{array}{l} (PPh_3)Au \overbrace{NC=CHCH=CHCH=C}^{SC} = \overbrace{CC=NC=CHCH=CHCH=CS}^{SC} \\ (PPh_3)Au \overbrace{NC=CHCH=CHCH=C}^{SC} = \overbrace{CC=NC=CHCH=CHCH=CS}^{SC} \end{array} \right\}$, 19	134
4.2.2.5 [$(PPh_3)Au(BO-N)_2CH$] (BO = Benzoxazolyl), 20	136
4.3 Crystal and molecular structure determinations by means of X-ray diffraction	140
4.3.1 The crystal and molecular structure of 16	140
4.3.2 The crystal and molecular structure of 17	144
4.3.3 The crystal and molecular structure of 19	147
4.3.4 The crystal and molecular structure of 20	151
4.4 Results and discussions for the oxidative dimerisation of HBBTM and HBBOM.....	154
4.4.1 Unexpected oxidative dimerisation of HBBTM and HBBOM.....	155
4.4.2 Spectroscopic characterisation of 2-(1,2,2-tri(benzo[<i>d</i>]thiazol-2-yl)vinyl)benzo[<i>d</i>]thiazole, $[S(AuP(Ph_3))_3]^+Cl^-$, 21 and 2-(1,2,2-tri(benzo[<i>d</i>]oxazol-2-yl)vinyl)benzo[<i>d</i>]oxazole, 22	157
4.4.2.1 $[(BT)_2C=C(BT)_2]$ (BT = benzothiazolyl), and $[S(AuP(Ph_3))_3]^+Cl^-$, 21	157
4.4.2.2 $\{BO\}_2C=C\{BO\}_2$ (BO = benzoxazolyl), 22 and $[S(Au(PPh_3))_3]^+Cl^-$	159

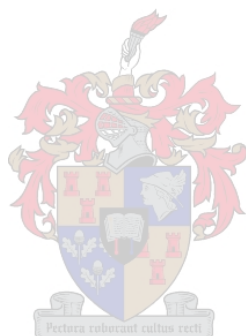
4.4.3 The crystal and molecular structures of 2-(1,2,2-tri(benzo[<i>d</i>]thiazol-2-yl)vinyl)benzo[<i>d</i>]thiazole, 11 and 2-(1,2,2-tri(benzo[<i>d</i>]oxazol-2-yl)vinyl)benzo[<i>d</i>]oxazole, 22	161
4.5 Conclusions and further work.....	165
4.6 Experimental.....	166
4.6.1 Materials and methods	166
4.6.2 Preparations	167
4.6.2.1 Preparation of	
$[\{\text{Ph}_3\text{PAu}(\text{BT}-N)\}_2\text{C}=\text{C}\{(\text{BT}-N)\text{AuPPh}_3\}_2]^{4+}4[\text{BF}_4]^-$, 16 and	
$[\{\text{Ph}_3\text{PAu}(\text{BT}-N,N)\}_2\text{CH}_2]^{2+}2[\text{BF}_4]^-$, 17	167
4.6.2.2 Preparation of $\text{PPh}_3\text{Au}(\text{BT}-N,N)_2\text{CH}$, 18	167
4.6.2.3 Preparation of $(\text{Ph}_3\text{P})\text{Au}-\overline{\text{NC}=\text{CHCH}=\text{CHCH}=\text{CSC}=\text{C}(\text{BT})-}$ $(\text{BT})\text{C}=\overline{\text{CSC}=\text{CHCH}=\text{CHCH}=\text{CN}}-\text{Au}(\text{PPh}_3)$, 19	168
4.6.2.4 Preparation of $[(\text{PPh}_3)\text{Au}\{\text{BO}\}_2\text{CH}]$, 20	168
4.6.2.5 $\{\text{BT}\}_2\text{C}=\text{C}\{\text{BT}\}_2$ and $[\text{S}(\text{AuP}(\text{Ph}_3))_3]^+\text{Cl}^-$, 21	168
4.6.2.6 $\{\text{BO}\}_2\text{C}=\text{C}\{\text{BO}\}_2$, 22 and $[\text{S}(\text{AuP}(\text{Ph}_3))_3]^+\text{Cl}^-$	169
4.6.3 X-ray structure determinations	169



Supplementary CD

The compact disk included in the back cover of this work contains:

- An electronic version (PDF) of this work.
- Crystallographic informations including hkl data, cif files and structure factors, of the X-ray crystal structures presented in this work.



Abbreviations

Å	Ångstrom (10^{-10} m)
acac	acetylacetonate
Bu	Butyl
FAB-MS	Fast Atom Bombardment Mass Spectrometry
HBBOM	bis(2-benzoxazolyl)methane
HBBTM	bis(2-benzothiazolyl)methane
<i>i</i> -Pr	Isopropyl
M ⁺	Molecular ion
M. p.	Melting point
M. W.	Molecular weight
Me	Methyl
MS	Mass Spectrometry
<i>m/z</i>	Mass/charge
NMR	Nuclear Magnetic Resonance
Ph	Phenyl
R	Alkyl group
<i>t</i> -Bu	Tertiary butyl
THF	Tetrahydrofuran
THT	Tetrahydrothiophene

NMR	b	Broad
	Δ	Difference between two values
	d	Doublet
	dd	Doublet of doublets
	dt	Doublet of triplets
	δ	Chemical shift (ppm)
	J	Coupling constant (Hz)
	m	Multiplet
	ppm	Parts per million
	q	Quartet
	s	Singlet
	t	Triplet
	tt	Triplet of triplets



Chapter 1

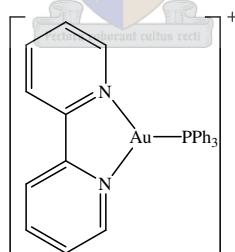
Introduction and Aims

1.1 Introduction

General

Gold, like copper and silver, has a single s electron outside a completed d shell with the electronic configuration $1s^2 2s^2 2p^6 3d^{10} 4s^2 4d^{10} 4f^{14} 5s^2 5p^6 5d^{10} 6s^1$. Gold chemistry is dominated by the oxidation states (I) and (III), with Au^+ and Au^{3+} having the electron configurations $[\text{Xe}]5d^{10}6s^06p^0$ and $[\text{Xe}]5d^86s^06p^0$, respectively.¹

Gold(I) complexes usually have coordination number of two with linear stereochemistry, and thus are coordinatively unsaturated 14-electron complexes. This is considered due to the relatively small energy difference between the filled d orbitals and the unfilled s orbital, which permits extensive hybridisation of these orbitals.² The Higher coordination numbers three, such as **I** shown in Scheme 1.1 and four for gold(I) complexes are also known and show trigonal planar and tetrahedral geometries, respectively.



I

Scheme 1.1

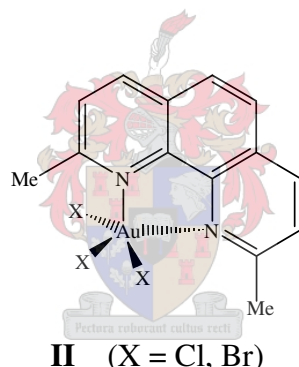
Gold(I) complexes that are three and four coordinated require the participation of the energetically high lying $6p_y$ and $6p_z$ orbitals thereby causing high promotion energy. Consequently, such coordination numbers are relatively rare and occur only with S- and/or P-donor atoms known to coordinate strongly with gold(I). It could be emphasised that

¹ B. F. G. Johnson and R. Davis, in: *Comprehensive Inorganic Chemistry*, eds. J. C. Bailar, H. J. Emeléus, R. Nyholm and A. F. Trotman-Dickenson, Pergamon, Oxford, 1973, p. 129.

² J. Strähle, in *Gold: Progress in Chemistry, Biochemistry and Technology*, ed. H. Schmidbaur, John Wiley & Sons, Chichester, 1999, p. 311.

only the four coordinate gold(I) complexes are coordinatively saturated with the gold having an 18-electron configuration.

On the other hand, gold(III) complexes have a strong preference for four coordination with square planar stereochemistry predominant and are discussed in more detail in Chapter 2. In these complexes gold has a 16-electron configuration and the $6p_z$ orbital remains vacant. Gold(III) is isoelectronic with platinum(II) which is well-known for its square-planar configuration (and *trans* effects experienced). This similarity opens the possibility that gold(III) complexes might have biological activity parallel to cisplatin and its homologues.^{1,2} Rare cases of five-coordination with the gold(III) centre, having square pyramidal or trigonalbipyramidal geometries, have been documented. The tetraphenylporphyrin complex AuCl(TPP), Au(dimphen)(X)₃ (X = Cl, Br), (2,9-dimethylphenanthroline), **II** and AuBr(CN)₂(terpy) (terpy = terpyridyl) are typical examples of square pyramidal gold(III) complexes.³



Scheme 1.2

Biological Activity of Gold

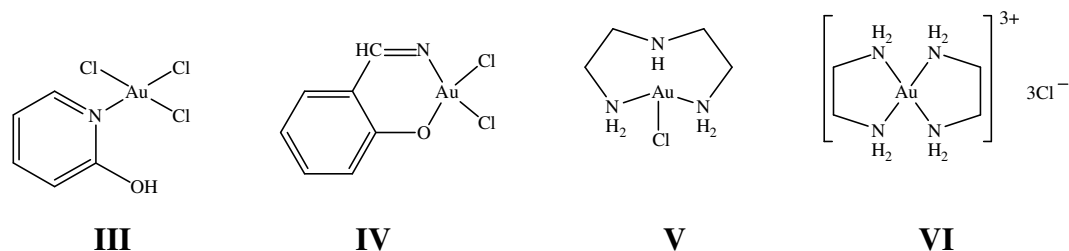
Gold and gold compounds were used in the past in the treatment of tuberculosis and are used at present in the treatment of arthritis. As mentioned, gold(III) complexes are isoelectronic and isostructural with those of platinum(II), whose anti-tumour activity is well recognised.⁴ Reactivity studies of gold(III) complexes have indicated that trichloropyridinegold(III) also reacts with DNA.⁵ Investigation of cytotoxic properties of certain gold(III) complexes such as trichloro(pyridylmethanol)gold(III), [AuCl₃(Hpm)] (**III**), dichloro(*N*-ethylsalicylaldiminato)gold(III), [AuCl₂(esal)] (**IV**),

³ S. A. Cotton, in: *Chemistry of Precious Metals*, 1st ed., 1997, Chapman and Hall, London, p. 305.

⁴ B. Bruni, A. Guerri, G. Marcon, L. Messor and P. Orioli, *Croat. Chim. Acta*, 1999, 221.

⁵ P. J. Sadler, M. Sasr and V. L. Narayanan, in *Platinum coordination complexes in cancer chemotherapy*, eds. E. B. Douple and I. H. Krakhoff, Nijhoff Publishers, Boston, 1984, p. 290.

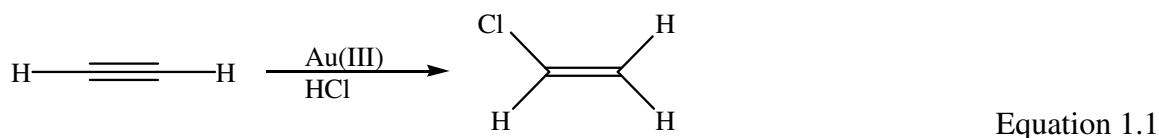
trichlorodiethylenediaminegold(III), $[\text{AuCl}(\text{dien})\text{Cl}_2]$ (V) and trichlorobisethylenediaminegold(III), $[\text{Au}(\text{en})_2\text{Cl}_3]$ (VI), revealed satisfactory results (Scheme 1.2).^{6,7,8,9} However, the toxic nature of these treatments is a setback and although partially excreted through the kidneys and the gastrointestinal tracts, it was reported that gold therapy causes pain, insomnia and anxiety. Such therapy can also affect bone marrow and produce stomatitis and histamine reactions.¹⁰



Scheme 1.3

Gold as Catalysts

Gold and its compounds are, in general, not catalytically efficient; however, a few discoveries involving gold(III) catalytic precursors have been made. AuCl_3 catalyses oxidation of trimethylamine to dimethylformamide, condensation of acetylene with aniline to obtain quinaldine and polymerisation of silacyclobutane reactions under mild conditions. $\text{H}[\text{AuCl}_4]$, which is easier to handle, catalyses the hydroxylation of olefins.¹¹ Hutching described that vinyl chloride, an important building block for vinyl polymers, can be obtained by activating alkynes using gold(III) for the addition of nucleophiles like Cl^- .¹²



⁶ A. Dar, K. Moss, S. M. Cottril, R. V. Parish, C. A. McAuliffe, R. G. Pritchard, B. Beagley and J. Sandbank, *J. Chem. Soc., Dalton Trans.*, 1992, 1907.

⁷ J. C. Bailar, *J. Am. Chem. Soc.*, 1951, **73**, 4722.

⁸ G. Nardin, L. Randaccio, G. Annibale, G. Natile and B. Pitteri, *J. Chem. Soc., Dalton Trans.*, 1979, 220.

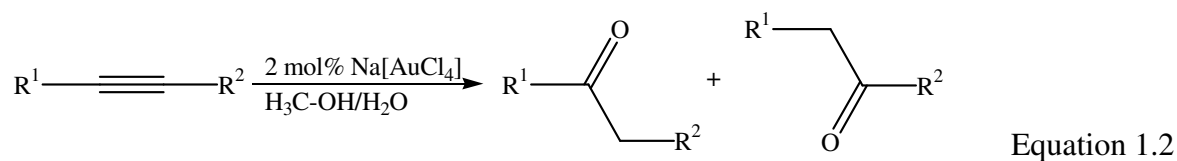
⁹ R. V. Parish, B. P. Howe, J. P. Wright, J. Mack, R. G. Pritchard, R. G. Buckley, A. M. Elsome and S. P. Fricker, *Inorg. Chem.*, 1996, **35**, 1659.

¹⁰ J. Strähle, in *Gold: Progress in Chemistry, Biochemistry and Technology*, ed. H. Schmidbaur, John Wiley & Sons, Chichester, 1999, p. 311.

¹¹ H. G. Raubenheimer and S. Cronje, in *Gold: Progress in Chemistry, Biochemistry and Technology*, ed. H. Schmidbaur, John Wiley & Sons, Chichester, 1999, p. 559.

¹² (a) A. S. K. Hashmi, *Gold Bulletin*, 2003, **36**, 3. (b) G. J. Hutching, *J. Catal.*, 1985, **96**, 292. (c) Y. Fukuda and Utimoto, *J. Org. Chem.*, 1991, **56**, 3729.

Utimoto *et al.* also described that several ketones could be obtained by the addition of weaker nucleophiles to alkynes in the presence of gold-catalysts.¹²



Aurophilicity

Aurophilicity is the tendency of closed-shell gold(I) atoms to aggregate at distances shorter than the sum of that van der Waals radii (2.884 - 3.60 Å) with an interaction energy that is comparable in strength to that of a hydrogen bond of 30 kJ mol⁻¹.¹³ Based on its position in the Periodic Table, relativistic effects are at a local maximum for the element gold. As a result (a) a stabilisation of the 6s orbitals and, to a lesser extent, of the 6p levels occur; (b) a radial expansion and energetic destabilisation of the 5d orbitals are taking place and this means that the closed shell 5d¹⁰ configuration in gold(I) compounds is no longer chemically inert and further interaction with other elements or other gold atoms is possible.¹⁴

N-Donor heterocyclic ligands and complexes of gold(I) and gold(III)

Heterocyclic ligands find numerous applications in C-C bond formation, asymmetric homogeneous and heterogeneous catalysis, DNA binding, the use as diagnostic agents and drugs, radio immunotherapy, and tumour targeting.¹⁵ A number of substituted thiazoles and thiazolidine ligands have low toxicity and radio protective activity. The inorganic coordination chemistry of azoles, purines and pyrimidines, which have ring systems that are also present in nucleic acids, vitamins, coenzymes and antibiotics, has been developed for gold(III).¹⁶ The thiazole skeleton (Scheme 1.3) dominates most of the work since it is an important constituent of many heterocyclic ligands such as benzothiazole, 4-

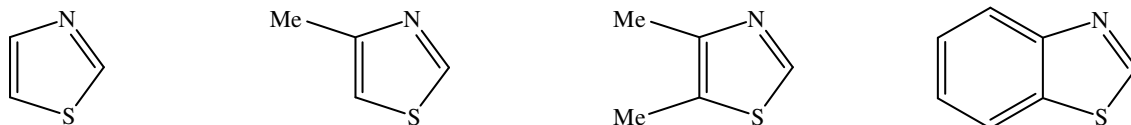
¹³ (a) A. Codina, E. J. Fernández, P. G. Jones, A. Laguna, J. M. López-de-Luzuriaga, M. Monge, M. E. Olmos, J. Pérez and M. A. Rodríguez, *J. Am. Chem. Soc.*, 2002, **124**, 6781. (b) H. Schmidbaur, W. Graf and G. Müller, *Angew. Chem. Int. Ed.*, 1988, **27**, 417. (c) P. Pyykkö, *Angew. Chem. Int. Ed.*, 2004, **43**, 4412.

¹⁴ A. Laguna, in *Gold: Progress in Chemistry, Biochemistry and Technology*, ed. H. Schmidbaur, John Wiley & Sons, Chichester, 1999, p. 349.

¹⁵ A. Abbotto, S. Bradamante, A. Facchetti and G. A. Pagani, *J. Org. Chem.*, 2002, **67**, 5753.

¹⁶ D. J. Radanović, Z. D. Matović, G. Ponticelli, P. Scano and I. A. Efimenko, *Trans. Met. Chem.*, 1994, **19**, 646.

methylthiazole, 4,5-dimethylthiazole and bis(2-benzothiazolyl)methane. Biomolecules including β -lactam antibiotics such as penicillin as well as natural products such as thiamine also, contain this ring system.



Scheme 1.4

The binding affinity of the donor atoms varies from one metal to another depending on the softness or hardness of the metal and the donor atom. Soft compounds (acid or base) are easily polarisable whereas hard compounds are less polarisable.¹⁷ Gold exhibits a moderate affinity to form bonds to nitrogen atoms. Nevertheless, a great number of gold(I) and gold(III) compounds with bonds between gold and nitrogen have been characterised in the last couple of years.¹⁸ An increasing *trans* influence of a ligand in a *trans* position effects an increasing tendency for *N*-coordination.¹⁹ Heterocyclic ligands such as thiazoles contain both S and N donor atoms. Normally *N*-coordination is preferred although one would intuitively expect the S donor atom.²⁰ Several such complexes with *N*-donor ligands have been reported.²¹ Heterocycles such as thiazoles are inherently polar and electronic distributions within the molecules are dominated by the more electronegative nitrogen atom. The heterocyclic nitrogen atom is consequently more nucleophilic than the heterocyclic sulfur atom and is expected to be the dominant donor.¹⁸ The coordination preferences of neutral heterocyclic molecules are primarily dependent on the relative positions of the N-C-S atoms in the heterocycle. When all the heteroatoms occupy heterocyclic positions, as in the 1,3-thiazoles and related molecules, the heterocyclic nitrogen is always the major donor. When the sulfur atom is exocyclic as in the thiones and their derivatives, thione-sulfur donation occurs (*vide-infra*).¹⁹

It has been reported that the equilibrium constants for the reaction

¹⁷ J. E. Huheey, in: *Inorganic chemistry, Principles of structure and reactivity*, 4th ed., Harper Collins College Publisher, New York, 1993, p. 344.

¹⁸ J. Strähle, in *Gold: Progress in Chemistry, Biochemistry and Technology*, ed. H. Schmidbaur, John Wiley & Sons, Chichester, 1999, p. 311.

¹⁹ J. B. Melpolder and J. L. Burmeister, *Inorg. Chim. Acta*, 1981, **45**, 115.

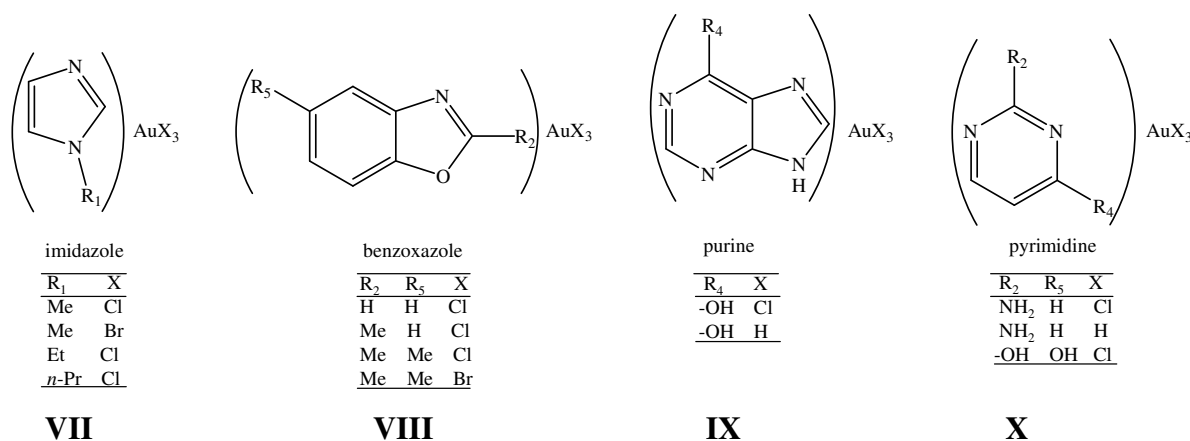
²⁰ E. S. Raper, *Coord. Chem. Rev.*, 1994, **129**, 91.

²¹ L. Canovese, L. Cattalini, M. Tomaselli and M. L. Tobe, *J. Chem. Soc., Dalton Trans.*, 1991, 307.



(where L includes thiazoles, oxazoles, pyridines or its derivatives, nitrile pyrimidine derivatives or imidazole) depend mainly on the basicity of the nitrogen in the ligand and steric requirement in its neighbourhood, irrespective of the ring size and further composition.²² In the case of thiazoles and oxazoles there is no significant systematic steric effect of the sort found for the more basic substituted pyridines.²¹ The enhanced reactivity of pyridine derivatives in nucleophilic substitution is due to stabilisation of the transition state by pyridines acting as stronger biphilic ligands than thiazoles and oxazoles.²¹

Reactions of $\text{H}[\text{AuCl}_4]$ with heterocyclic imine-containing ligands have been carried out and sometimes show diverse products such as metallated 6-(2'-thienyl)-2,2'-bipyridine ($\text{L}^{\wedge}\text{L}$).²³ Similarly, reaction of 2-phenylthiazole with $\text{H}[\text{AuCl}_4] \cdot x\text{H}_2\text{O}$ yields the immonium tetrachloroaurate(III) salt, $[\text{H}(\text{Hphtz})][\text{AuCl}_4]$ (Hphtz = 2-phenylthiazole).²⁴ However, the reaction of 2-phenylpyridine (L) with $\text{H}[\text{AuCl}_4]$ or $\text{Na}[\text{AuCl}_4]$ leads to the formation of square-planar *N*-bonded complexes $[\text{AuCl}_3(\text{L})]$. The gold(III) halides exhibit Lewis acidic behaviour and readily react with the *N*-donor ligand to afford adducts of the type $[\text{AuCl}_3(\text{L})]$, where L = *N*-methylimidazole, *N*-ethylimidazole, *N*-propylimidazole, benzoxazole (BO), 2-methylbenzoxazole, 2,5-dimethylbenzoxazole *etc.* (Scheme 1.5, VII – X).¹⁴



Scheme 1.5

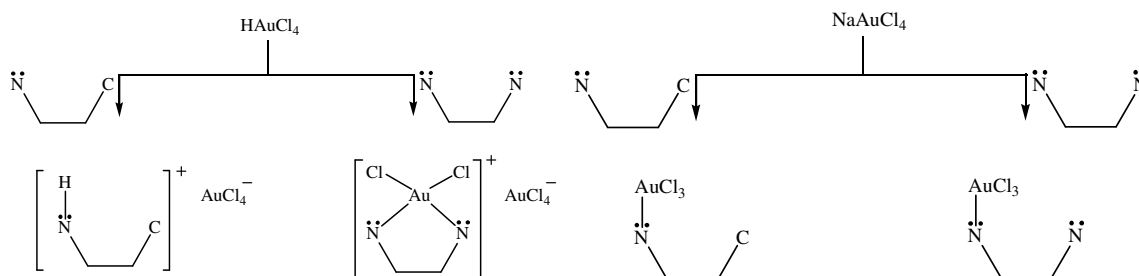
²² (a) L. Cattalini, R. J. H. Clark, A. Orio and C. K. Poon, *Inorg. Chim. Acta*, 1968, **6**, 62.

(b) J. Shamir, A. Givan, L. Canvese, L. Cattalini, P. Guagliati and M. L. Tobe, *J. Raman Spectrosc.*, 1993, **24**, 233.

²³ E. C. Constable and T. A. Leese, *J. Organomet. Chem.*, 1989, **363**, 419.

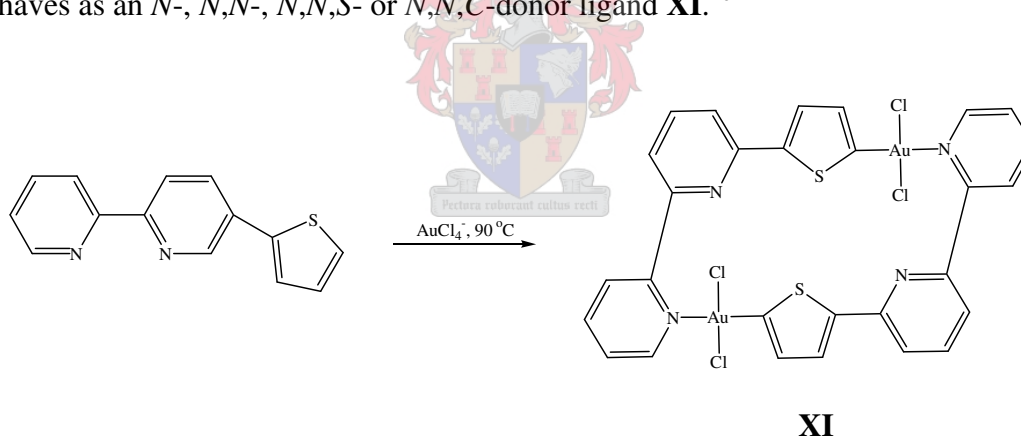
²⁴ H. Jeda, H. Fujiwara and Y. Fuchita, *Inorg. Chim. Acta*, 2001, **319**, 203.

There has been growing interest in the chemistry of cyclometallated compounds. Cyclometallated compounds contain exo-chelated ligands in which one of the donor sites is an anionic carbon centre (Scheme 1.6).²⁵



Scheme 1.6

Ligands such as 2-(2-thienyl)pyridine (Hthpy) (as discussed in Chapter 2) may act as a monodentate *N*-donor or could be cyclometallated at C³ to yield complexes of 6-(2''-thienyl)-2,2'-bipyridine. The ligand 6-(2-thienyl)-2,2'-pyridine forms complexes in which it behaves as an *N*-, *N,N*-, *N,N,S*- or *N,N,C*-donor ligand **XI**.²⁶



Scheme 1.7

Bipyridyl and 1,10-phenanthroline complexes of the type (L-L)Au₂Cl₆ are believed to consist of cationic complexes of the general formula [(L-L)AuCl₂][AuCl₄].²⁷ HAuCl₄ reacts with aminoalcohols in aqueous solution to give cationic complexes of the type

²⁵ M. Deetlefs, *Ph.D. Thesis*, University of Stellenbosch, 2001, p. 114.

²⁶ (a) E. C. Constable, R. P. G. Henney, P. R. Raithby and L. R. Sousa, *Angew. Chem. Int. Ed.*, 1991, **30**, 1363. (b) E. C. Constable, R. P. G. Henney and D. A. Tocher, *J. Chem. Soc., Dalton Trans.*, 1992, 2467. (c) E. C. Constable and L. R. Sousa, *J. Organomet. Chem.*, 1992, **427**, 125.

²⁷ (a) A. A. McConnel, D. H. Brown and W. E. Smith, *Spectrochim. Acta*, 1982, **38**, 265. (b) D. Belli, D. Amico and F. Calderazza, *Gazz. Chim. Ital.*, 1978, **108**, 11.

[AuL₂][AuCl₄] and with *t*-butylamine the complex AuCl₃(*t*-BuNH₂) has been isolated, whereas the reaction of Na[AuCl₄] with *n*-butylamine affords the imine gold(I) complex, [ClAu(NH=CH(CH₂)₂ Me)].²⁸

A member of our research group also recently reported unexpected but interesting cationic complexes of gold(III) with both monodentate (L = 1-methyl-2-(phenyl)imidazole), [AuCl₂(L)₂][AuCl₄] and bidentate ligands (L = 1-methyl-2-(2-pyridinyl)imidazole), [AuCl₂(L-L)][AuCl₄].²⁵ These reactions required further attention.

S-Donor heterocyclic ligands and complexes of gold(I) and gold(III)

The coordination chemistry of heterocyclic thiones has attracted attention for their potentially ambidentate or multi-functional donor capacity. Either the exocyclic S or heterocyclic N (or S) atoms are available for coordination to form complexes with transition metals and the possibility exists that coordination with harmful metal ions in an organism could occur.^{29,30} Apart from their biological activity, transition metal complexes containing sulfur-donor ligands are active catalysts in a considerable number of homogeneously catalysed reactions such as hydrogenation, isomerisation, hydroformylation, the Heck reaction and polymerisation.³¹ Thiourea and its derivatives find widespread use in the mining industry where they are employed as flotation aids for sulphidic ores and as complexing agents for the enrichment of metals through solid-liquid and liquid-liquid extraction processes. The high affinity of thioureas towards noble metals is underlined by the fact that thioureas are capable of dissolving gold or silver. In the solid state and in neutral solutions the thione sulfur atom is the favoured donor site. Thiones are generally classified according to their ring size, where the most common ones contain five- and six-membered heterocyclic rings (Schemes 1.8 and 1.9).³² Sulfur donor ligands such as thiones (or thioureas) have basic properties because of the presence of lone pairs of electrons on the nitrogen and sulfur atoms. These lone pairs of electrons have given them the ability to coordinate with transition metal ions such as gold.^{33,34,35,36}

²⁸ Y. Nagel and W. Beck, *Z. Anorg. Allg. Chem.*, 1985, **529**, 57.

²⁹ P. J. Cox, P. Aslanidis, P. Karagiannidis and S. Hadjikakou, *Inorg. Chim. Acta*, 2000, **310**, 268.

³⁰ R. Campo, J. Cardio, E. Garcia, M. Hermosa, A. Sanchez and J. Monzano, *J. Inorg. Bio. Chem.*, 2002, **89**, 74.

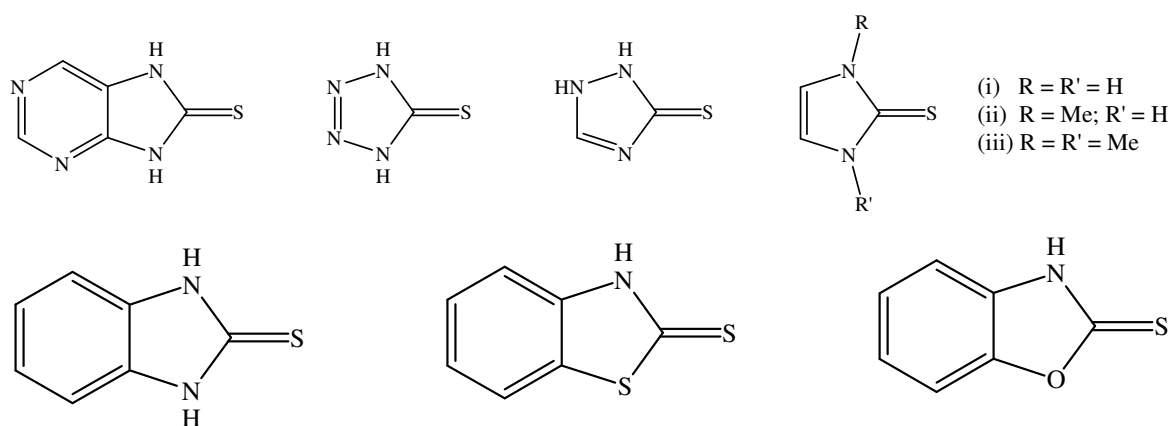
³¹ J. C. Bayón, C. Claver and A. M. Masdeu-Bultó, *Coord. Chem. Rev.*, 1999, **73**, 193.

³² P. D. Akrivos, *Coord. Chem. Rev.*, 2001, **213**, 181.

³³ J. S. Casas, A. Castiñeiras, M. C. Rodríguez-Argüelles, A. Sánchez, J. Sordo, A. Vázquez-López and E. M. Vázquez-López, *J. Chem. Soc., Dalton Trans.*, 2000, 2267.

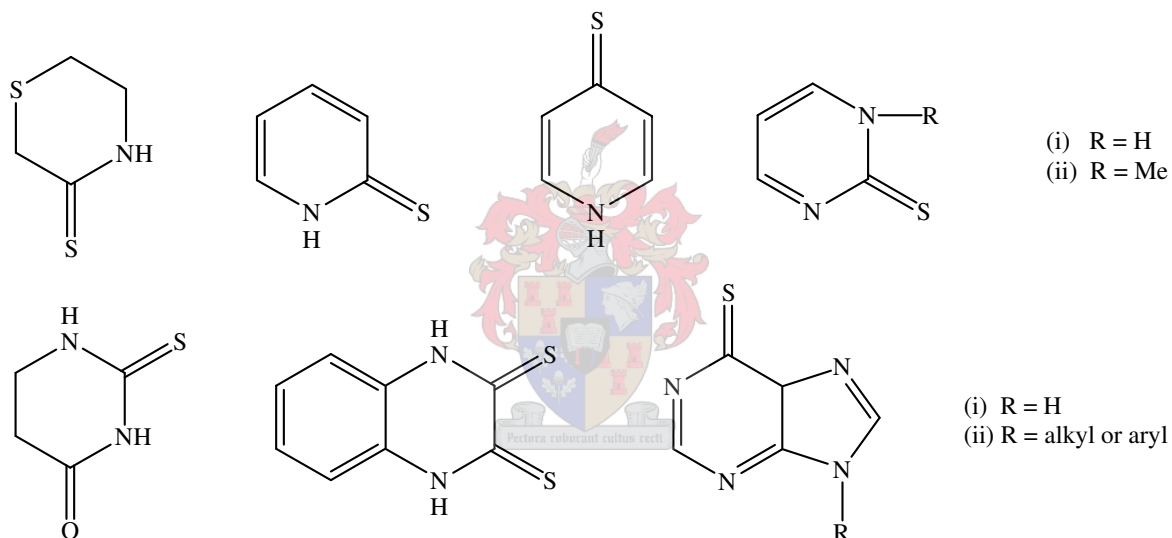
³⁴ E. Sanchez, P. Toro, O. Hernandez and L. Marin, *Spectrochim. Acta Part A*, 2002, **58**, 2281.

Five-membered thiones



Scheme 1.8

Six-membered thiones



Scheme 1.9

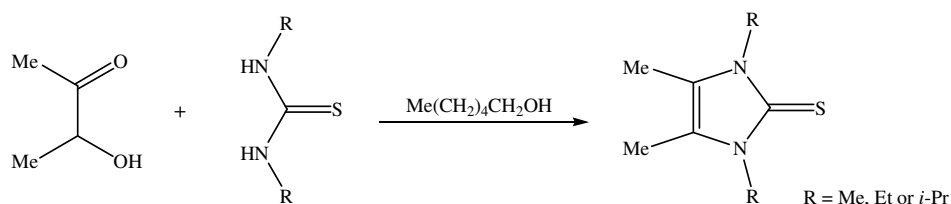
Dialkylimines are convenient starting materials for the rapid assembly of the 4,5-diacetylenyl imidazole core, since ring closure to the corresponding imidazole-2-thiones can be effected by quenching diimine dianions with CS_2 .³⁷ Some of the most important heterocyclic imidazole-2(3H)-thione ligands like 1,3,4,5-tetramethyl-1,3-dihydroimidazole-2-thione, 1,3-diethyl-4,5-dimethylimidazole-2(3H)-thione and 1,3-diisopropyl-4,5-dimethyl-1,3-dihydroimidazole-2-thione can be prepared by a condensation reaction

³⁵ K. R. Koch, C. Sacht and T. Grimmbacher, *S. Afri. J. Chem.*, 1995, **48**, 71.

³⁶ M. Gerrov, H. Kerdjaoudj, R. Mdinari and E. Drioli, *Sep. Purif. Technol.*, 2002, **28**, 235.

³⁷ R. Faust and B. Göbelt, *Chem. Comm.*, 2000, 919.

starting from thioureas and 3-hydroxy-2-butanone in boiling 1-hexanol as shown in Scheme 1.10.³⁸ Imidazole-2-thiones in turn are precursors for Arduengo-type carbenes,^{34,39}



Scheme 1.10

Recently, in our laboratory rhodium(I) thione complexes of 1,3,4,5-tetramethyl-1,3-dihydro-imidazole-2-thione and 1,3-diisopropyl-4,5-dimethyl-1,3-dihydro-imidazole-2-thione have been prepared successfully by addition of the thione ligand to a solution of the starting compound which has weakly coordinating ligands like cod or CO, e.g., $[\text{RhCl}(\text{cod})]_2$.⁴⁰ These products are active precatalysts for hydroformylation.

Room temperature irradiation of silver(I) complexes with heterocyclic thiones and tertiary phosphines as ligands in chloroform solution causes decomposition into two photoproducts.⁴¹ Compounds with the formula of $[\text{AuL}(\text{PMe}_3)]\text{Cl}$ (L = imidazolidine-2-thione (Imt)) has been reported. The coordination chemistry of the thioamide group in heterocyclic penta-, hexa- and hepta-atomic rings, such as imidazolidine-2-thione (Diaz), 1,3-diazepine-2-thione (Diap) and their derivatives with various metal ions such as gold(I), silver(I), copper(I), platinum(II) and zinc(II) indicated coordination *via* the thione sulfur.^{42,43}

Anhydrous gold(III) chloride and HAuCl_4 react readily with heterocyclic ligands and thiones.⁴⁴ Interestingly, Khan and Shahjahan synthesised bidentate 1-(2'-pyridyl)benzothiazole-2-thione, 2-(1-pyridine-2-thionato)benzoxazole (PTBOX) and 2-(1-pyridine-2-thionato)benzothiazole (PTBTH) (Scheme 1.11) complexes of Au(III) as well

³⁸ N. Kuhn and T. Kratz, *Synthesis*, 1993, 561.

³⁹ M. K. Denk, S. Gupta, J. Brownie, S. Tajammul and A. J. Lough, *Chem. Eur. J.*, 2001, **7**, 4477.

⁴⁰ A. Neveling, G. R. Julius, S. Cronje, C. Esterhuysen and H. G. Raubenheimer, *Dalton Trans.*, 2005, 181.

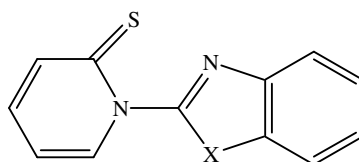
⁴¹ J. S. Coleman, L. P. Varga and S. H. Mastin, *Inorg. Chem.*, 1970, **9**, 1015.

⁴² M. N. Khtar, A. A. Isab, M. S. Hussain and A. R. Al-Arfaj., *Trans. Met. Chem.*, 1996, **21**, 553.

⁴³ P. Aslanidis, S. K. Hadjikakou, P. Karagiannidis, M. Gdaniec and Z. Kosturkiewicz, *Polyhedron*, 1993, **12**, 2221.

⁴⁴ H. G. Raubenheimer, R. Otte, L. Linford, W. E. Van Zyl, A. Lombard and G. J. Kruger, *Polyhedron*, 1992, **11**, 893.

as their complexes with other transition metal ions Cr(III), Mn(II), Fe(III), Co(II) Ni(II), Cu(II), Ru(III) and Rh(III).⁴⁵ The ligands behave as bidentate donors coordinating through the nitrogen atom of the benzoxazole or benzothiazole group and through the sulfur atom of the pyridine -2-thione moiety producing distorted square-based pyramidal coordination.

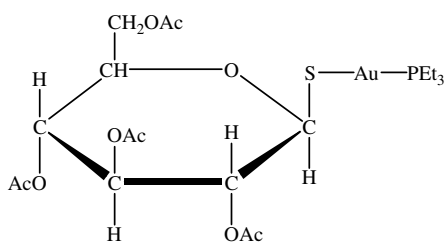


X = O, PTBOX
X = S, PTBTH

Scheme 1.11

In general, the Au(I)-S bond is kinetically labile with chemical exchange occurring readily. The value of (tetrahydrothiophene)gold(I) halide complexes, (tht)AuX, as precursors for other Au(I) substances depends on the chemical lability of the tht ligand.

To conclude, one has to mention the importance of gold drugs as anti-arthritis agents: Auranofin, **XII** (complex of gold(I) with 2,3,4,6-tetra-o-acetyl- β -1_D-thioglucose and triethylphosphine, Scheme 1.12) is one typical example in the market.⁴⁶



XII

Scheme 1.12

⁴⁵ T. A. Khan and Shahjahan, *Synth. React. Inorg. Met.-Org. Chem.*, 1998, **28**, 571.

⁴⁶ J. P. Fackler, W. E. van Zyl and B. A. Prihoda, in *Gold: Progress in Chemistry, Biochemistry and Technology*, ed. H. Schmidbaur, John Wiley & Sons, Chichester, 1999, p. 803.

1.2 Research goals and thesis outline

Imine nitrogens are known as excellent donor atoms and due to their nucleophilic nature they even coordinate with gold despite the fact that gold is classified as a soft metal. The growing interest in gold-containing heterocyclic compounds prompted us to investigate further the preparation of a series of gold(III) and gold(I) imine complexes to further establish the affinity of nitrogen for gold and to characterise the coordination mode by NMR studies and X-ray methods. Immonium tetrachloroaurate(III) salts, [LH][AuCl₄] and neutral complexes of the type [AuX₃(L)] are apparently obtained by reaction of aqueous solutions of HAuCl₄, AuCl₃ or NaAuCl₄ with imine ligands. Analogous reactions, independent of the employed reagent ratios, with chelating imines have also afforded mixed oxidation state gold(I) and gold(III) complexes thus leading to some uncertainty.^{47,48}

The versatility, activity and modes of coordination of S-donor ligands have stimulated our interest to investigate the interaction of selected thione ligands and other S-containing compounds with gold cationic centres.

The main aims and objectives of this work can be summarised as follows:

- to utilize nitrogen σ -donors in the preparation of gold(I) and gold(III) imine coordination complexes and establish the affinity of the soft metal for these harder ligands;
- to address ambiguities in the preparation of gold(III) imine coordinated complexes;
- to synthesise neutral and cationic gold(I) complexes of N- or C-donor heterocyclic ligands such as HBBTM and HBBOM and to establish their coordination modes;
- to further prepare new thione and thiolate complexes of gold(I) and gold(III) and to investigate their mode of coordination and molecular structures by using single crystal X-ray analysis and NMR techniques;
- to structurally characterise unusual and unexpected by-products in the above conversions.

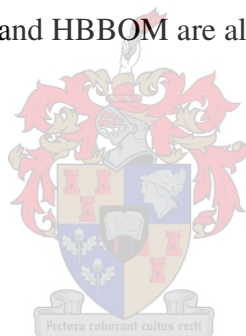
⁴⁷ R. J. Puddephatt, in: *Comprehensive Coordination Chemistry*, eds. G. Wilkinson, R. D. Gillard and J. A. McCleverty, Pergamon, Oxford, 1987, p. 862.

⁴⁸ R. J. Puddephatt, in: *The Chemistry of Gold*, Elsevier, Amsterdam, 1978, p. 98.

In **Chapter 2** the synthesis and characterisation of cationic complexes, immonium tetrachloroaurate(III) salts and neutral complexes of gold(III) are described. In this chapter several ligands with N,S-, N,O- and N,N-donor ligands are implemented to obtain the gold(III) compounds.

In **Chapter 3** the synthesis of new organosulfur complexes of gold(I) and gold(III) from industrially useful thione compounds are described. This chapter also highlights the problems and serendipitous discoveries associated with the reactions between dilithio-1,3-dithiane-2-carbodithioate and $(\text{AuCl})_2\text{dppm}$, $(\text{AuCl})_2\text{dppe}$ or $\text{AuCl}(\text{PPh}_3)$. Crystal structure determinations unequivocally allow the clarification of the unusual products obtained.

Chapter 4 encompasses a description of the synthesis and characterisation of new cationic and neutral complexes of gold(I) obtained from heterocyclic ligands like bis(2-benzothiazolyl)methane, HBBTM and bis(2-benzoxazolyl)methane, HBBOM. The oxidative dimerisation of HBBTM and HBBOM are also elaborated as an additional topic.



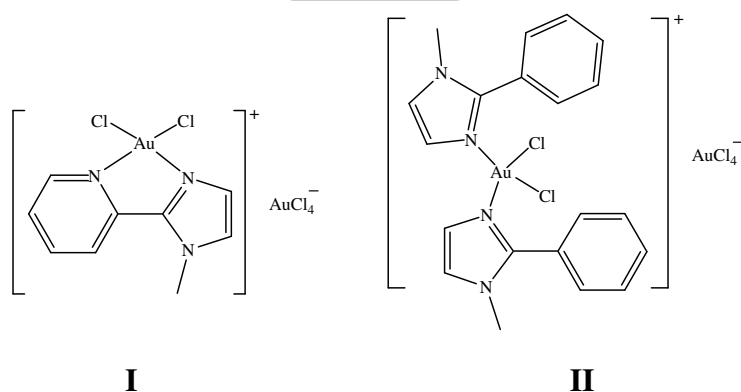
Chapter 2

Synthesis and characterisation of imine compounds of gold(III)

2.1 Introduction and aims

2.1.1 General

The interest in the synthesis of cationic gold(III) complexes and neutral adducts has been increasing since the last decade. Cationic complexes of the type $[\text{AuCl}_2(\text{L}^1\text{L}^2)]^+[\text{AuCl}_4]^-$ (L = bidentate ligand 1-methyl-2-(2-pyridinyl)imidazole), **I**, and $[\text{AuCl}_2(\text{L})_2]^+[\text{AuCl}_4]^-$ (L = monodentate ligand 1-methyl-2-(phenyl)imidazole), **II**, shown in Scheme 2.1, have been reported by a member of our research group.¹ Nitrogen donor ligands such as 4,4-dimethyl-2-(2'-thienyl)oxazole, 4,4-dimethyl-2-(phenyl)oxazole, 1-methyl-2-(2-pyridinyl)imidazole, 1-methyl-2-(phenyl)imidazole, thiazoles and oxazoles have been of particular interest. Even though the affinity of gold for nitrogen is poor, gold(I) and gold(III) imine complexes of these ligands were prepared by reaction of the ligand with $\text{NaAuCl}_4 \cdot 2\text{H}_2\text{O}$, $\text{HAuCl}_4 \cdot 4\text{H}_2\text{O}$ or $\text{AuCl}(\text{tht})$.¹



Scheme 2.1

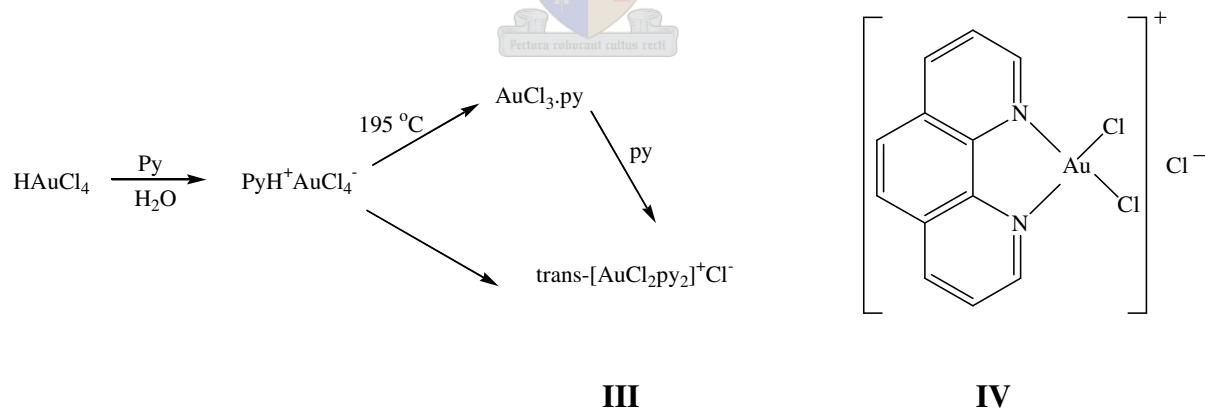
In the past few decades, several reactions of $\text{HAuCl}_4 \cdot 4\text{H}_2\text{O}$, $\text{NaAuCl}_4 \cdot 2\text{H}_2\text{O}$ and $\text{AuCl}_3 \cdot x\text{H}_2\text{O}$ with imine ligands have led to different classes of products, such as metallacycles, immonium tetrachloraurate(III) salts, neutral adducts and cationic gold(III)

¹ M. Deetlefs, *Ph.D. Thesis*, University of Stellenbosch, 2001, p. 114.

complexes.¹ The effects of solvent and temperature on the preparative methods for some of these products of gold(III) are well documented in most of the references quoted throughout this Chapter. However, certain factors such as basicity of the ligands, the presence of water molecules in the gold(III) precursors ($\text{HAuCl}_4 \cdot 4\text{H}_2\text{O}$, $\text{NaAuCl}_4 \cdot 2\text{H}_2\text{O}$ and $\text{AuCl}_3 \cdot x\text{H}_2\text{O}$) and stability of the salt products formed in the first step are also thought to play a role in the products obtained.

Cationic gold(III) complexes:

Cationic complexes of gold(III) are generally more difficult to prepare than gold(I) cationic complexes. Only limited numbers of these compounds are known thus far such as **I** and **II** mentioned above. Adams and Strahle used *N*-donor ligands such as pyridine to synthesise the cationic complex $[\text{AuCl}_2(\text{py})_2]^+\text{Cl}^-$ (py = pyridine), **III**. Addition of an excess of pyridine to the adduct leads to the cationic complex $[\text{AuCl}_2(\text{py})_2]\text{Cl}$. Scheme 2.2 shows that the mechanism involves a stepwise formation of the immonium tetrachloroaurate(III) salt, $[\text{pyH}][\text{AuCl}_4]$ and neutral complex, $[\text{AuCl}_3(\text{py})]$.² Moreover, the cytotoxic complex $[\text{AuCl}_2(\text{phen})]\text{Cl}$ (phen = phenanthroline), **IV** shown in Scheme 2.2, prepared from phenanthroline.HCl and HAuCl_4 , is similar to the cationic complex **I** in Scheme 2.1, except that the counter ion in the latter case is chloride.³

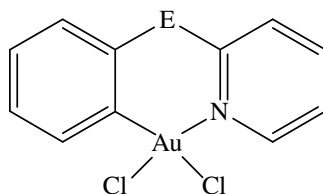


Scheme 2.2

² (a) S. A. Cotton, in: *Chemistry of Precious Metals*, 1st ed, Chapman and Hall, London, 1997, p. 302. (b) D. T. Hill, K. Burns, D. D. Titus, G. R. Girard, W. M. Reif and L. M. Mascavage, *Inorg. Chim. Acta*, 2003, **346**, 1.

³ F. Abbate, P. Orioli, B. Bruni, G. Marcon and L. Messori, *Inorg. Chim. Acta*, 2000, **311**, 1.

the mechanisms of the reactions are not clear. Hence, the same reactions afforded the corresponding adducts in a mixture of acetonitrile:water (1:1) at room temperature.¹²



VIII (E = NH, O, S)

Scheme 2.4

Neutral complexes of gold(III) and immonium tetrachloroaurate(III) salts:

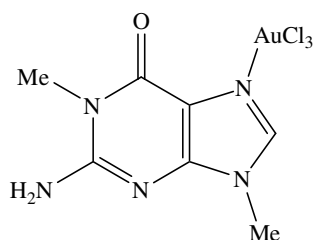
Immonium tetrachloroaurate(III) salts are very simple and easy to prepare under ambient conditions and are very important precursors in the preparations of neutral, cationic and metallacyclic complexes of gold(III). Gold(III) imine salts consist of protonated imine ligands, $[LH]^+$, and $AuCl_4^-$ as counter ion. Fuchita *et al.* reported the preparation of $[H(Hpi)][AuCl_4]$ and $[H(Hepi)][AuCl_4]$ from reaction of $AuCl_3 \cdot xH_2O$ and 2-phenyl-1H-imidazole (Hpi) or 1-ethyl-2-phenylimidazole (Hepi) in dichloromethane.¹³ Usually the tetrachloroauric(III) acid, $HAuCl_4 \cdot 4H_2O$, provides the proton for the formation of the imine salt.

Adducts and salts are the most widely known gold(III) imine compounds. Neutral complexes and salts of gold(III) imine compounds are prepared from several imine ligands and $HAuCl_4$, $AuCl_3$ or $NaAuCl_4$ depending on the reaction conditions (such as solvent and temperature). Adducts have the general formula $[AuCl_3(L)]$, where L can be any imine donor, such as thiazoles, oxazoles, imidazoles, purine and pyrimidine. Attempts at using some nucleobases such as 9-ethylguanine, 1-methylthymine and 1-methyluracil to obtain adducts of $AuCl_3$ resulted in salt compounds containing protonated nucleobases and $AuCl_4^-$ as counter ion. Adducts of general formula $[AuCl_3(L)]$ for several ligands such as thiazole ligands and nitrogen-donor bases such as imidazoles, purine and pyrimidine

¹² Y. Fuchita, H. Ieda, A. Kayama, J. Kinoshita-Nagaoka, H. Kawano, S. Kameda and M. Mikuriya, *J. Chem. Soc., Dalton Trans.*, 1998, 4095.

¹³ Y. Fuchita, H. Ieda and M. Yasutake, *J. Chem. Soc., Dalton Trans.*, 2000, 271.

derivatives have been studied analytically (IR and NMR spectroscopy)¹⁴ (Chapter 1, Scheme 1.5) but molecular structures are not widely reported. Shimanski *et al.* isolated and characterised the molecular structures of neutral complexes of the types $[\text{AuCl}_3(\text{L})]$, (**IX**), obtained by treatment of $\text{H}[\text{AuCl}_4]$ with various imine donor ligands such as cytosine and guanine.¹⁵ Adducts of AuCl_3 exhibit square planar coordination with monodentate ligands and slightly rigid square planar geometry with bidentate ligands.¹⁵



IX

Scheme 2.5

This chapter deals with the synthetic aspects and characterisation of new gold(III) compounds prepared by reaction of HAuCl_4 , AuCl_3 or NaAuCl_4 with a series of imine ligands such as thiazoles, imidazoles and oxazoles.

2.1.2 Aims and objectives

- Specifically, it was planned to again obtain products belonging to the family of cationic complexes **I** and **II** (Scheme 2.1). Furthermore, monodentate imine ligands such as thiazoles, oxazoles and one bidentate ligand bis(2-benzothiazolyl)methane HBBTM could be included in the study. In the process products belonging to the families discussed above could form and we planned to isolate and characterise them completely.
- Finally, it was also planned to determine structurally the coordination site of neutral gold(III) complexes of thiazole and its methyl- and benzo-derivative ligands.

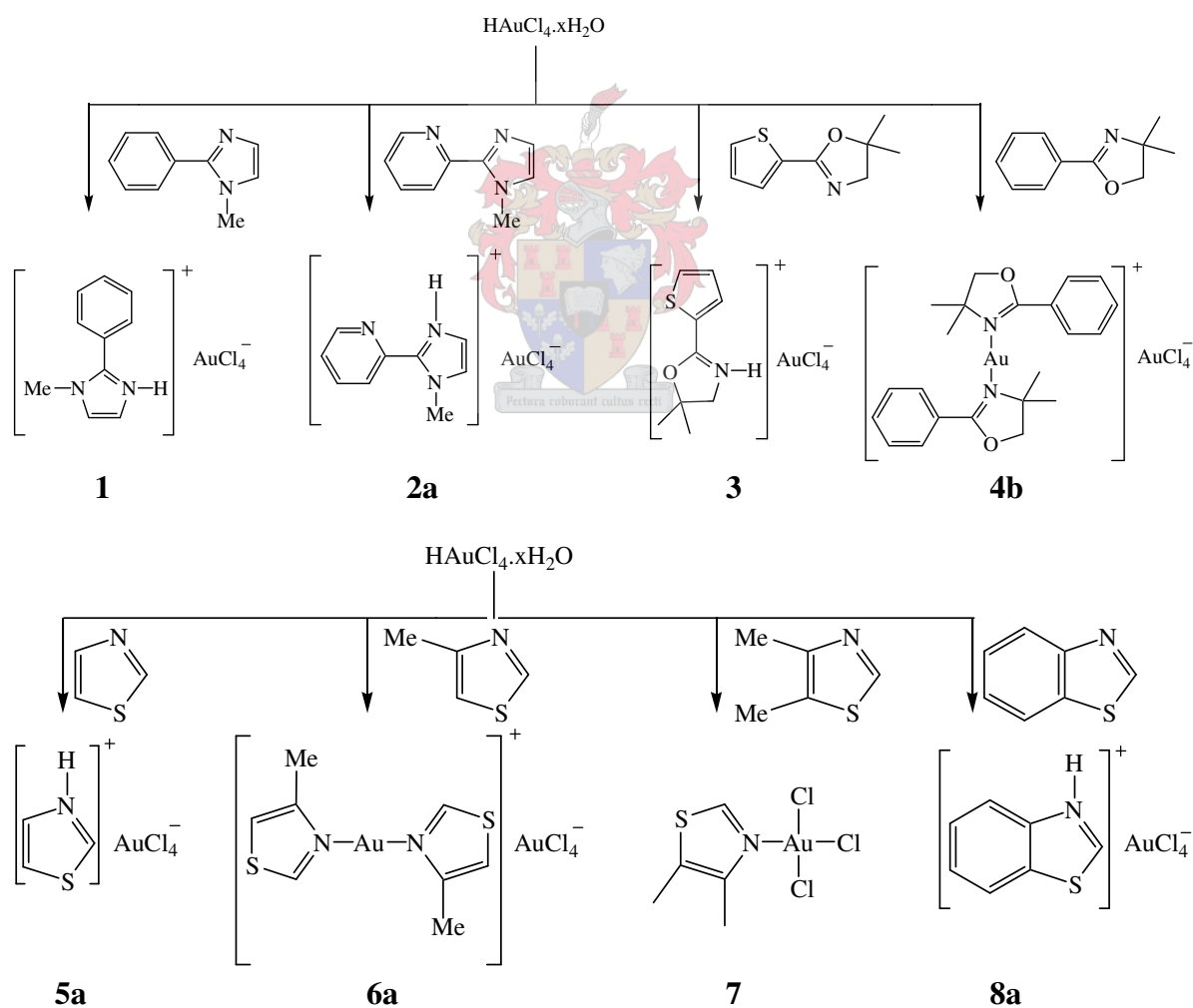
¹⁴ (a) D. J. Radanović, Z. D. Matović, G. Ponticelli, P. Scano and I. A. Efimenko, *Trans. Met. Chem.*, 1994, **19**, 646. (b) L. Canovese, L. Cattalini, M. Tomaselli and M. L. Tobe, *J. Chem. Soc., Dalton Trans.*, 1991, 309.

¹⁵ A. Shimanski, E. Fresinger, A. Erxleben and B. Lippert, *Inorg. Chim. Acta*, 1998, **283**, 223.

2.2 Results and discussions

2.2.1 Synthesis of immonium tetrachloroaurate(III) salts, neutral and cationic complexes

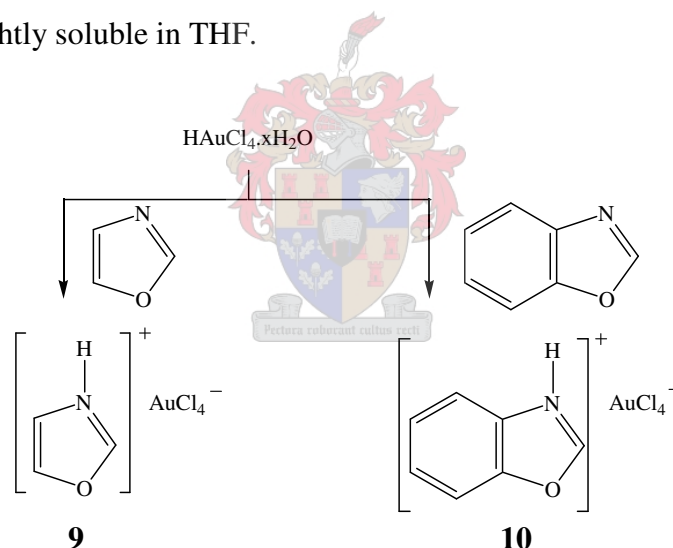
A series of *N*-heterocyclic compounds such as 1-methyl-2-(phenyl)imidazole, 1-methyl-2-(2-pyridinyl)imidazole, 4,4-dimethyl-2-(2'-thienyl)oxazole, 4,4-dimethyl-2-(phenyl)oxazole, thiazole and its benzo- and methyl-derivatives, oxazole and benzoxazole in acetonitrile were reacted with an aqueous solution of HAuCl_4 which led to the formation of immonium tetrachloroaurate(III) salts, $([\text{LH}][\text{AuCl}_4])$ (Scheme 2.6 and Scheme 2.7). The tetrachloroauric(III) acid, HAuCl_4 , is responsible for the protonation of the imines.



Scheme 2.6

During the reaction process all, except **1**, formed immediately yellow precipitates from the aqueous solution of HAuCl_4 and acetonitrile solution of the respective ligands. The final products were extracted with dichloromethane or THF depending on the solubility of the respective product. The extracts were dried over anhydrous magnesium sulphate. The orange precipitate which formed in reaction **10** (Scheme 2.7) existed only for a short period of time, and changed to a brown solid after 15 min of stirring at room temperature. This product could not be isolated in pure form.

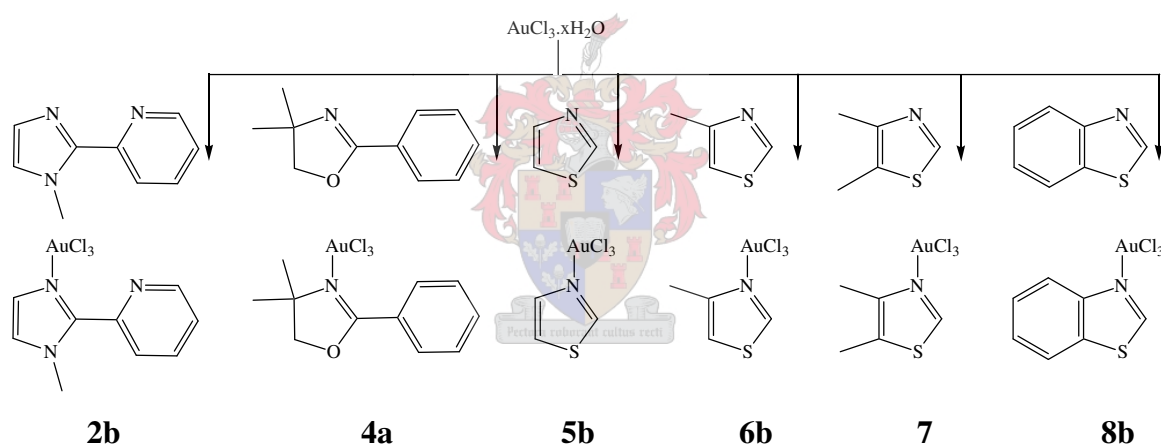
Immonium tetrachloroaurate(III) salts **1**, **3**, **9** and $[\text{LH}][\text{AuCl}_4]$, $\text{L} = 4,4\text{-dimethyl-2-(phenyl)oxazole}$, **4b'** were recrystallised from a dichloromethane solution layered with *n*-pentane at $-20\text{ }^\circ\text{C}$, whereas **8a** was recrystallised from a THF solution layered with *n*-pentane at $-20\text{ }^\circ\text{C}$. Most of these products were obtained in good yield and are air stable. Solubility tests have shown that most of the products are well soluble in non-polar solvents although insoluble in water; with exceptions **2a**, **8a** and **10** are well soluble only in DMSO and slightly soluble in THF.



Scheme 2.7

Cationic complexes $[\text{Au}\{\overline{\text{N}=\text{C}(\text{Ph})\text{OCH}_2\text{C}(\text{CH}_3)_2}\}_2][\text{AuCl}_4]$, **4b**, and $[\text{Au}\{\overline{\text{N}=\text{CHSCH}=\text{C}(\text{CH}_3)_2}\}_2][\text{AuCl}_4]$, **6a**, (Scheme 2.6) were isolated from reactions of acetonitrile solutions of 4,4-dimethyl-2-(phenyl)oxazole and 4-methylthiazole, respectively with aqueous solutions of similar mole quantities of HAuCl_4 at room temperature (Scheme 2.6). An immediate yellow precipitate of the products formed in good yield. The precipitates were extracted with dichloromethane and dried over anhydrous magnesium sulphate prior to solvent removal under vacuum. These products are air stable and generally soluble in non-polar solvents but practically insoluble in water.

The ^1H and ^{13}C NMR data of the crude products containing **4b** and **6a** revealed two sets of data indicating that there were two products in the mixture. Orange crystals of **4b** suitable for X-ray analyses were obtained from a dichloromethane solution layered with *n*-pentane and a concentrated chloroform-*d* solution at $-20\text{ }^\circ\text{C}$. Single crystal X-ray analysis enabled us to isolate and determine two different molecular structures, *i.e.*, the cationic complex $[\text{Au}\{\overline{\text{N}=\text{C}(\text{Ph})\text{OCH}_2\text{C}(\text{CH}_3)_2}\}_2][\text{AuCl}_4]$, **4b** and the immonium tetrachloroaurate(III) salt, $[\text{HN}=\overline{\text{C}(\text{Ph})\text{OCH}_2\text{C}(\text{CH}_3)_2}][\text{AuCl}_4]$, **4b'**. Similarly, orange crystals of **6a** suitable for X-ray analysis were obtained from concentrated chloroform-*d* solution at $-20\text{ }^\circ\text{C}$. However, only the molecular structure for the cationic complex $[\text{Au}\{\overline{\text{N}=\text{CHSCH}=\text{C}(\text{CH}_3)_2}\}_2][\text{AuCl}_4]$, **6a**, was isolated and determined structurally by single crystal X-ray analysis. The mechanism for the reduction of the cationic complexes to gold(I) is not clear, although $[\text{AuCl}_2(\text{L})_2]^+$ could probably be an intermediate, which is then reduced to $[\text{AuL}_2]^+$ by elimination of Cl_2 .

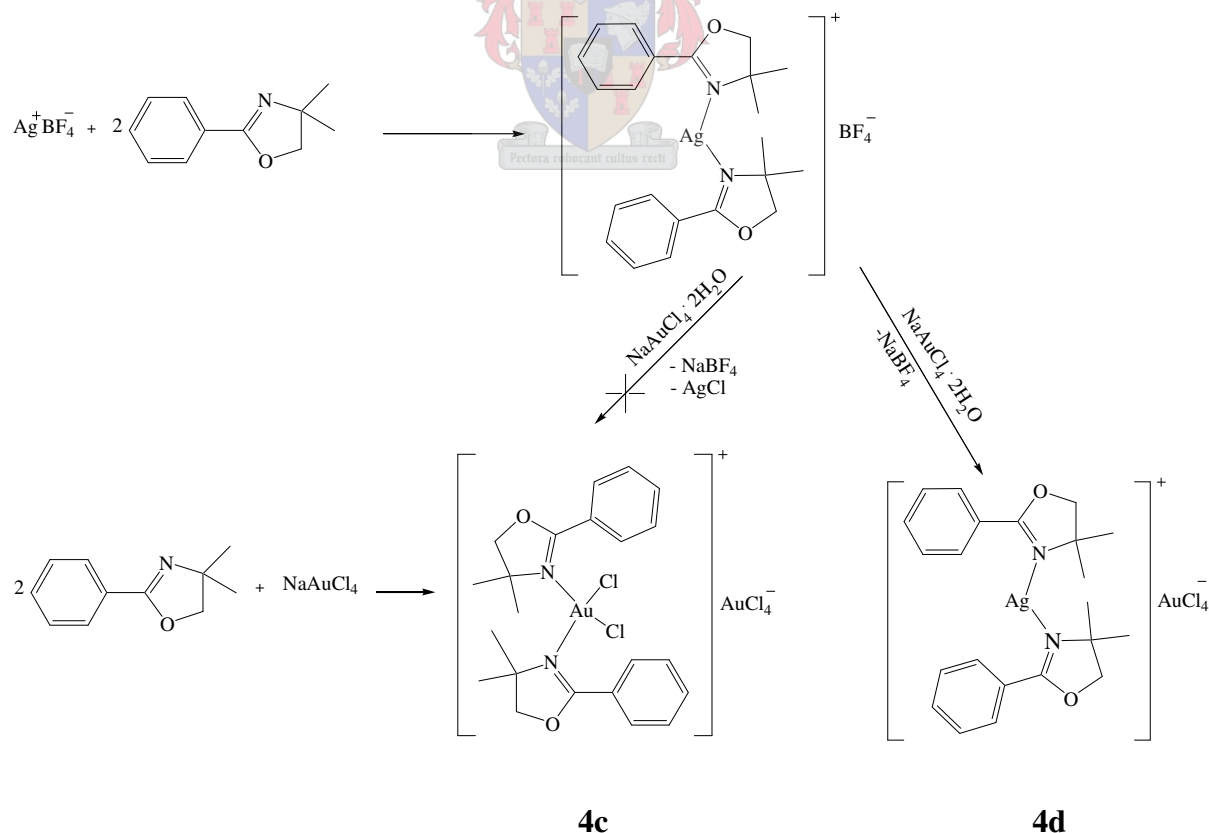


Scheme 2.8

Several neutral adducts of composition $[\text{AuCl}_3(\text{L})]$ (Scheme 2.8) were obtained by adding an acetonitrile solution of selected ligands such as thiazoles and their derivatives, 4,4-dimethyl-2-(phenyl)oxazole and 1-methyl-2-(phenyl)imidazole, to similar mole quantities of an aqueous solution of AuCl_3 (Scheme 2.8). The orange precipitates were extracted with dichloromethane or THF depending on the solubility of the precipitates and dried over magnesium sulphate prior to solvent removal under reduced pressure. These products are soluble in THF, acetone and dichloromethane, with the exception of **2b** and **8b** which dissolve only in DMSO and are only slightly soluble in THF. These products are stable in air. Suitable crystals for single crystal X-ray structure determination of **5b** and **7** were

obtained from dichloromethane solutions layered with *n*-pentane at -20 °C. The molecular structure of a neutral gold(III) complex **7**, [AuCl₃(L)] has been determined by X-ray analysis and is reported in Section 2.3.4.

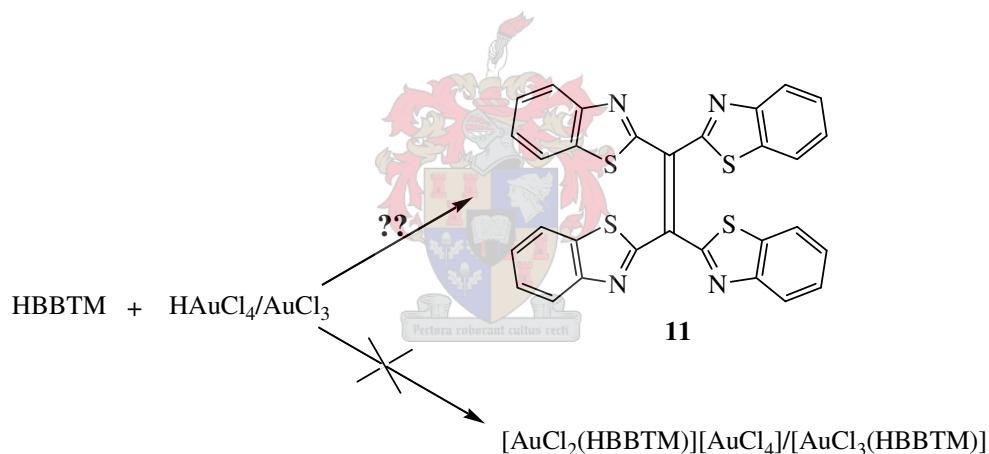
An attempt was made to prepare the ionic complex [AuCl₂(L₂)]⁺[AuCl₄]⁻, **4c** (Scheme 2.9), by treatment of two mole quantities of L = 4,4-dimethyl-2-(phenyl)imidazole or 1-methyl-2-(phenyl)imidazole) with an aqueous solution of one mole quantity of HAuCl₄ at room temperature. Products obtained from these two reactions appear to be soluble in most solvents except water and are stable in air. The products were extracted with dichloromethane, dried in anhydrous magnesium sulphate and evacuated under reduced pressure. The residues were crystallised from a dichloromethane solution by layering with *n*-pentane at -20 °C, however, due to weak crystal data sets the structures could not be solved. Another technique was attempted to obtain cationic complex **4c** by transmetallation of [AgL₂]⁺[BF₄]⁻ (originating from 4,4-dimethyl-2-(phenyl)oxazole and AgBF₄) up on reaction with NaAuCl₄ as shown in Scheme 2.9, but proper crystals could not be obtained for single crystal X-ray analysis.



Scheme 2.9

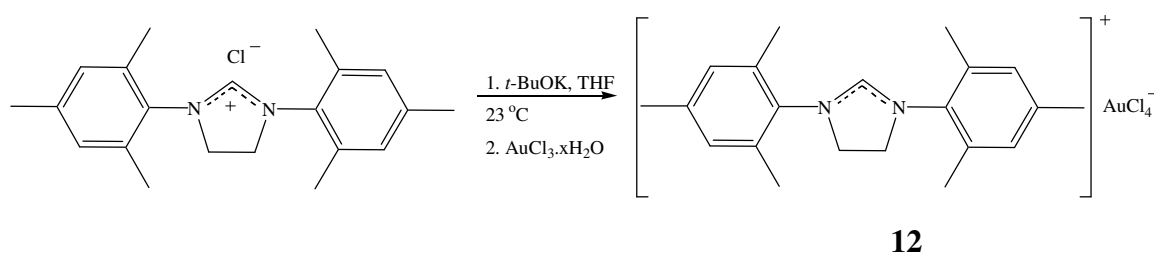
The ^1H and ^{13}C NMR investigations revealed similarity with the cationic complex **4b**. However, ESI MS data seemed to indicate a mixed complex of silver and gold of the type of $[\text{Ag}(\text{L})_2][\text{AuCl}_4]$.

The same procedure as mentioned for the reactions in Schemes 2.6 and 2.8 was repeated in an attempt to prepare ionic and neutral complexes of HBBTM with HAuCl_4 and AuCl_3 , respectively. Upon reaction a yellow precipitate formed immediately and slowly turned green. Extended hours of stirring at room temperature led to further reduction of the gold(III) to a gold film, $\text{Au}(0)$, and an oxidative dimerisation of the ligand to form 2-(1,2,2-tri(benzo[*d*]thiazol-2-yl)vinyl)benzo[*d*]thiazole (Scheme 2.10). The mechanism for this conversion is not known. The ^1H and ^{13}C NMR spectra show that the signals of the bridging methylene, CH_2 , group had disappeared. However, there is no evidence on whether the gold is coordinated or not. TLC or spot test (diethyl ether:*n*-hexane and ether as eluents) indicated that no movement of the gold containing compound.



Scheme 2.10

1,3-bis(2,4,6-trimethylphenyl)imidazolium chloride in THF was treated with *t*-BuOK at room temperature and then filtered through Celite into a solution of AuCl_3 in THF to obtain **12** (Scheme 2.11). The solvent was removed under reduced pressure.



Scheme 2.11

Orange crystals suitable for X-ray analysis were obtained from dichloromethane solution layered with *n*-pentane at -20 °C. The orange crystals are soluble in THF, dichloromethane and acetone but insoluble in *n*-pentane, *n*-hexane and ether.

Generally, ¹H and ¹³C NMR spectra for most of the obtained products, especially **1** – **9**, indicated the presence of inseparable by-products of low concentration.

2.2.2 Spectroscopic characterisation of compounds **1** – **4**

NMR spectroscopy

2.2.2.1 $[\text{HN}=\text{C}(\text{Ph})\text{NMeCH}=\text{CH}][\text{AuCl}_4]$, **1**

The ¹H and ¹³C NMR data of the free ligand and compound **1** are summarised in Table 2.1. The ¹H NMR spectrum of **1** shows slightly different chemical shifts with respect to those reported by Deetlefs.¹⁶ The doublet at 7.93 ppm is assigned to the *ortho*-protons H⁶ and H¹⁰ with downfield shift of Δδ 0.2 compared to the free ligand, with a coupling constant of 7.3 Hz. The broad signal observed at 7.89 ppm is assigned to the *meta*-protons H⁷ and H⁹ exhibiting a downfield shift of Δδ 0.44 compared to the free ligand. The multiplet at 7.83 - 7.73 ppm is assigned to protons H¹, H² and H⁸ based on spectral integration. The N-H appears as a broad signal at 3.11 ppm, which is in the range of amine-shifts.¹⁷ The methyl protons, H³, display a slight downfield change in chemical shift of Δδ 0.31 with respect to the free ligand. Generally, downfield shifts in ¹H NMR data are ascribed to an increase in positive charge.¹⁸ Thus L had formed a cation.

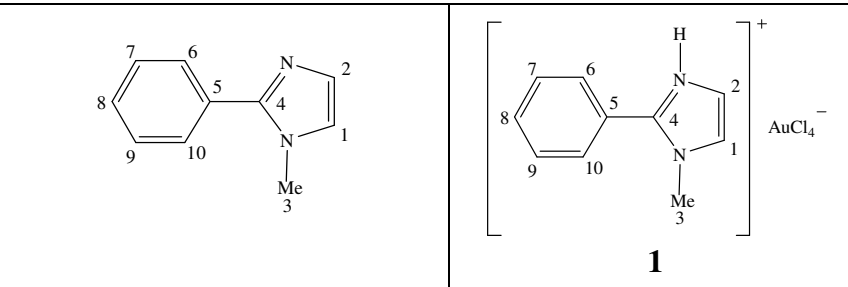
The ¹³C NMR data of **1** are discussed with respect to the corresponding signals for the free ligand. C⁵ and C¹ display upfield shifts of Δδ 5.6 and 7.9, respectively when compared to the ligand. C⁸ displays a slight downfield change in chemical shift of Δδ 3.5 with respect to the free ligand.

¹⁶ M. Deetlefs, *Ph.D. Thesis*, University of Stellenbosch, 2001, p. 147.

¹⁷ D. L. Pavia, G. M. Lampman and G. S. Kriz, *Introduction to Spectroscopy*, 3rd edition, Harcourt College Publishers, Fort Worth, 2001, p. 314.

¹⁸ M. Desmet, *Ph.D. Thesis*, Rand Afrikaans University, 1996, p. 52.

Table 2.1 ^1H and ^{13}C NMR data of the free ligand and compound **1** in acetone- d_6

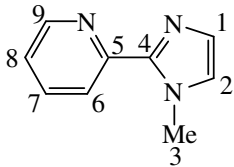
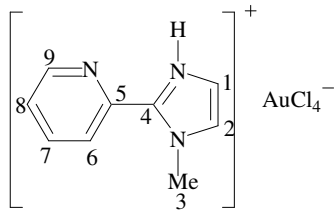
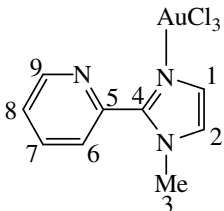
Assignment	$\delta(\text{ppm})$ (multiplicity, J(Hz))	$\delta(\text{ppm})$ (multiplicity, J(Hz))
		
^1H NMR		
H^6 and H^{10}	7.74 (2H, dt, $^3J_{\text{H}6,10-\text{H}7,9} = 7.6$ & $^4J_{\text{H}6,10-\text{H}8} = 1.6$)	7.93 (2H, d, $^3J_{\text{H}6-\text{H}7} = 7.3$ Hz)
H^7 and H^9	7.45 (2H, m)	7.89 (2H, bs)
H^8	7.45 (1H, m)	7.77 (1H, m)
H^1	7.15 (1H, d, $^3J_{\text{H}1-\text{H}2} = 1.1$ Hz)	7.77 (1H, m)
H^2	7.01 (1H, d, $^3J_{\text{H}2-\text{H}1} = 1.2$ Hz)	7.77 (1H, m)
H^3	3.80 (3H, s)	4.11 (3H, s)
N-H		3.11 (1H, bs)
^{13}C NMR		
C^4	148.3	146.3
C^5	131.6	126.0
C^8	130.0	133.5
C^7 and C^9	129.5	130.7
C^6 and C^{10}	129.2	130.6
C^1	128.3	120.4
C^2	123.9	123.5
C^3	34.8	36.5

2.2.2.2 $[\text{HN}=\text{C}(\text{py})\text{NMeCH}=\text{CH}][\text{AuCl}_4]$, **2a** and
 $[\text{Cl}_3\text{Au}\{\text{N}=\text{C}(\text{py})\text{NMeCH}=\text{CH}\}]$, **2b**

The ^1H and ^{13}C NMR data of the free ligand, compounds **2a** and **2b** are summarised in Table 2.2. All the signals are assigned unambiguously. Significant downfield change in chemical shifts of $\Delta\delta$ 0.83 and 0.61 are observed for protons H^1 and H^2 of compound **2a**, respectively compared to the free ligand. However, the same protons H^1 and H^2 in complex **2b** display even more noticeable downfield shifts of $\Delta\delta$ 0.80 and 0.58, respectively compared to the free ligand. The doublet signals observed at δ 8.89 and 8.85 are assigned to the proton H^9 of **2a** and **2b**, respectively. The proton H^9 of **2a** displayed a downfield shift of $\Delta\delta$ 0.27 comparable to the downfield shift of H^9 in **2b** ($\Delta\delta$ 0.23) when

compared to the free ligand. Protons H⁷ and H⁸ in **2a** also display downfield shifts of $\Delta\delta$ 0.31 and 0.37, respectively. The same protons H⁷ and H⁸ in **2b** display insignificant downfield shifts of $\Delta\delta$ 0.27 and 0.24, respectively compared to the free ligand. All coupling constants are listed in Table 2.2 and deviate slightly from the free ligand.

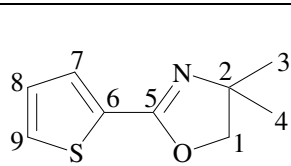
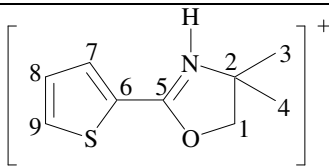
Table 2.2 ¹H and ¹³C NMR data of the free ligand, compounds **2a** and **2b** in DMSO-d₆

Assignment	δ (ppm) (multiplicity, J(Hz))	δ (ppm) (multiplicity, J(Hz))	δ (ppm) (multiplicity, J(Hz))
			
	2a	2b	
¹H NMR			
H ⁹	8.62 (1H, dq, ³ J _{H9-H8} = 4.9 & ⁴ J _{H9-H7} = 1.0)	8.89 (1H, d, ³ J _{H9-H8} = 4.9 Hz)	8.85 (1H, d, ³ J _{H9-H8} = 4.2 Hz)
H ⁶	8.10 (1H, dt, ³ J _{H6-H7} = 8.0 & ⁴ J _{H6-H8} = 1.1)	8.11 (1H, d, ³ J _{H6-H7} = 8.1 Hz)	8.07 (1H, d, ³ J _{H6-H7} = 8.1 Hz)
H ⁷	7.88 (1H, td, ³ J _{H7-H6,8} = 7.8 & ⁴ J _{H7-H9} = 1.8 Hz)	8.19 1H, td, ³ J _{H7-H6,8} = 7.8 & ⁴ J _{H7-H9} = 1.7 Hz)	8.15 (1H, td, ³ J _{H7-H6,8} = 8.3 & ⁴ J _{H7-H9} = 1.9 Hz)
H ⁸	7.35 (1H, dd, ³ J _{H8-H7,9} = 4.9 & ⁴ J _{H8-H6} = 1.4 Hz)	7.72 (1H, dd, ³ J _{H8-H7,9} = 4.9 & ⁴ J _{H8-H6} = 1.2 Hz)	7.69 (1H, dd, ³ J _{H8-H7,9} = 4.8 & ⁴ J _{H8-H6} = 1.1 Hz)
H ²	7.30 (1H, d, ³ J _{H2-H1} = 1.0 Hz)	7.91 (1H, d, ³ J _{H2-H1} = 1.8 Hz)	7.88 (1H, d, ³ J _{H2-H1} = 1.7 Hz)
H ¹	7.04 (1H, d, ³ J _{H1-H2} = 1.0 Hz)	7.87 (1H, d, ³ J _{H1-H2} = 1.9 Hz)	7.84 (1H, d, ³ J _{H1-H2} = 1.9 Hz)
H ³	4.05 (3H, s)	4.13 (3H, s)	4.11 (3H, s)
¹³C NMR			
C ⁴	150.8	150.4	150.1
C ⁵	148.7	142.8	142.4
C ⁹	144.2	141.7	141.4
C ⁶	137.2	138.4	138.1
C ⁷	128.0	124.6	124.5
C ⁸	125.4	119.7	119.5
C ²	122.7	126.5	126.2
C ¹	122.4	126.3	126.1
C ³	35.8	36.9	36.9

The ^{13}C NMR spectra of complexes **2a** and **2b** do not differ significantly from each other. Signals at δ 142.4, 124.6 and 119.5 are assigned to the carbons C^5 , C^7 and C^8 , respectively with upfield shifts of $\Delta\delta$ 6.0, 4.0 and 6.0, respectively compared to the free ligand. Signals at δ 126.2 and 126.1 are also, respectively assigned to C^1 and C^2 with downfield shifts of $\Delta\delta$ 3.9 and 3.8 compared to the free ligand.

2.2.2.3 $[\text{HN}=\text{C}(\text{C}=\text{CHCH}=\text{CHS})\text{OCH}_2\text{C}(\text{CH}_3)_2]_2[\text{AuCl}_4]$, **3**

Table 2.3 ^1H and ^{13}C NMR data of the free ligand¹⁹ and compound **3** in acetone- d_6

Assignment	$\delta(\text{ppm})$ (multiplicity, J(Hz))	$\delta(\text{ppm})$ (multiplicity, J(Hz))
		
^1H NMR		
H^7	7.69 (1H, dd, $J = 6.3$ Hz)	8.39 (1H, d, $^3J_{\text{H}^7-\text{H}^8} = 4.7$ Hz)
H^9	7.60 (1H, dd, $J = 6.3$ Hz)	8.35 (1H, d, $^3J_{\text{H}^9-\text{H}^8} = 3.7$ Hz)
H^8	7.17 (1H, dd, $J = 6.6$ Hz)	7.48 (1H, t, $^3J_{\text{H}^8-\text{H}^7,9} = 4.2$ Hz)
H^1	4.13 (2H, s)	5.07 (2H, s)
H^3 and H^4	1.31 (2H, s)	1.74 (6H, s)
^{13}C NMR		
C^5	158.1	165.7
C^6	133.1	140.3
C^7	131.0	138.9
C^8	130.8	130.1
C^9	128.3	121.2
C^1	78.2	83.9
C^2	68.3	63.8
C^3 and C^4	27.2	25.8

The ^1H and ^{13}C NMR data of the free ligand and compound **3** are summarised in Table 2.3. Based on spectral integration, the doublets at 8.39 and 8.35 ppm for compound **3** are assigned to the protons H^7 and H^9 with a coupling constant of 4.7 and 3.7 Hz, respectively. The triplet at 7.48 ppm is assigned to the thienyl proton, H^8 coupled by H^7 and H^9 (4.2 Hz). Generally, the thienyl protons H^7 , H^9 and H^8 display significant downfield shifts of

¹⁹ M. Deetlefs, *Ph.D. Thesis*, University of Stellenbosch, 2001, p. 121.

$\Delta\delta$ 0.70, 0.75 and 0.31, respectively compared to the free ligand. The signal at 5.07 ppm is characteristic of the methylene protons H^1 . These protons display significant downfield shift of $\Delta\delta$ 0.94 with respect to the free ligand and are chemically and magnetically equivalent. The N-H proton resonates at 3.28 ppm as a broad signal. The methyl protons, H^3 and H^4 , resonate at 1.74 ppm with a noticeable downfield shift of $\Delta\delta$ 0.43 compared to the free ligand.

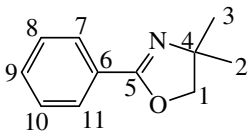
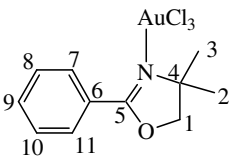
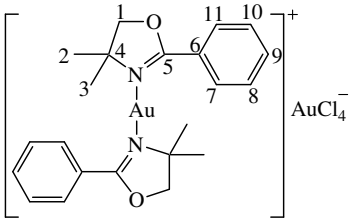
The ^{13}C NMR signals at δ 138.9, 130.1 and 121.2 are assigned to the thienyl carbons C^7 , C^8 and C^9 , respectively. The ^{13}C NMR spectrum indicates a significant upfield shift of $\Delta\delta$ 7.1 for the thienyl carbon C^9 with respect to the free ligand. On the other hand, C^7 of the thienyl group exhibits a significant downfield shift of $\Delta\delta$ 7.9 compared to the free ligand. The oxazole carbon C^5 and the thienyl carbon C^6 resonate at δ 165.7 and 140.3, respectively. Likewise, C^5 and C^6 also display significant downfield changes in chemical shift after coordination ($\Delta\delta$ 7.6 and 7.2), when compared to the free ligand. A signal at 68.3 ppm, assigned to the methylene carbon C^2 also displays an upfield change in chemical shift of $\Delta\delta$ 4.7 when compared to the free ligand.

2.2.2.4 $[\text{Cl}_3\text{Au}\{\text{N}=\text{C}(\text{Ph})\text{OCH}_2\text{C}(\text{CH}_3)_2\}]$, **4a** and $[\text{Au}\{\text{N}=\text{C}(\text{Ph})\text{OCH}_2\text{C}(\text{CH}_3)_2\}_2][\text{AuCl}_4]$, **4b**

The ^1H and ^{13}C NMR data of the free ligand, compounds **4a** and **4b** are shown in Table 2.4. The ^1H NMR spectra of **4a** and **4b**, as expected, indicate coordination of the oxazoline group to gold. Significant downfield changes in chemical shift of the signals in the ^1H and ^{13}C NMR spectra are diagnostic of coordination of the ligand. The degrees of downfield change in chemical shift in the ^1H NMR spectra of the compounds vary to some extent. Based on spectral integration the signals at 8.25 ppm and 7.71 ppm in **4a** are assigned to protons H^7/H^{11} and H^9 , respectively and show noticeable downfield shifts of $\Delta\delta$ 0.30 and 0.21 upon coordination. The coupling constants for these protons are 6.4 Hz and 7.6 Hz, respectively coupled to the respective neighbouring protons. Similarly, for **4a** the methylene protons H^1 and methyl protons H^2/H^3 display more significant downfield shifts of $\Delta\delta$ 0.46 and 0.41, respectively compared to the free ligand. In the ^1H NMR spectrum of **4b** signals at δ 4.87 and 1.78 are assigned to the oxazole protons H^1 and H^2/H^3 , respectively. These protons, H^1 and H^2/H^3 , display significant downfield shifts for **4b** of $\Delta\delta$ 0.76 and 0.48, respectively compared to the free ligand. The protons **4b** in the *ortho*-

para- and *meta*-positions, *i.e.*, H⁷/H¹¹, H⁹ and H⁸/H¹⁰ display downfield shift of $\Delta\delta$ 0.36, 0.36 and 0.25, respectively when compared to the free ligand. The methylene protons, CH₂, of the oxazole group in **3** are more deshielded compared to the methylene protons in 4,4-dimethyl-2-(phenyl)oxazole, in **4a** and **4b**. The ¹H NMR signals of the cationic complex **4b** are at a relatively lower field with respect to the neutral complex, **4a**.

Table 2.4 ¹H and ¹³C NMR data of the free ligand, compounds **4a** in CDCl₃ and **4b** in acetone-d₆

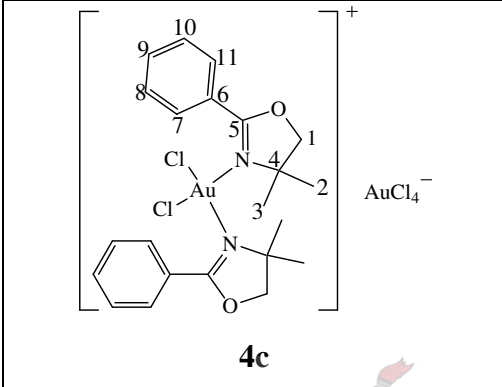
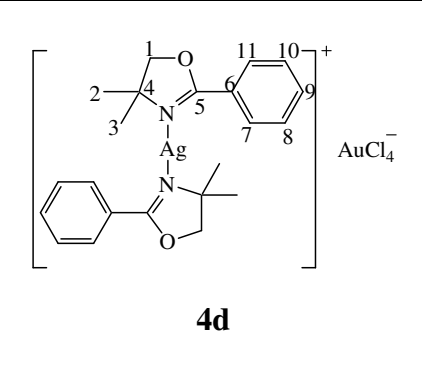
Assignment	δ (ppm) (multiplicity, J(Hz))	δ (ppm) (multiplicity, J(Hz))	δ (ppm) (multiplicity, J(Hz))
			
¹H NMR			
H ⁷ and H ¹¹	7.96 (2H, dt, ³ J _{H7,11-H8,10} = 6.5 & ⁴ J _{H7,11-H9} = 1.7 Hz)	8.25 (2H, dt, ³ J _{H7,11-H8,10} = 6.4 & ⁴ J _{H7,11-H9} = 1.7 Hz)	8.32 (2H, d, ³ J _{H7,11-H8,10} = 6.9 & ⁴ J _{H7,11-H9} = 1.5 Hz)
H ⁹	7.50 (1H, m)	7.71 (1H, tt, ³ J _{H9-H8,10} = 7.6 & ⁴ J _{H9-H7,11} = 1.2 Hz)	7.86 (1H, t, ³ J _{H9-H8,10} = 7.7 Hz)
H ⁸ and H ¹⁰	7.50 (2H, m)	7.57 (2H, t, ³ J _{H8-H7,9} = 6.9 Hz)	7.75 (2H, tm, ³ J _{H8-H7,9} = 7.5 Hz)
H ¹	4.11 (2H, s)	4.57 (2H, s)	4.87 (2H, s)
H ² and H ³	1.30 (6H, s)	1.71 (6H, s)	1.78 (6H, s)
¹³C NMR			
C ⁵	162.3	170.6	171.8
C ⁶	132.2	123.8	125.7
C ⁹	129.7	135.1	135.9
C ⁸ and C ¹⁰	129.5	129.7	130.6
C ⁷ and C ¹¹	129.2	129.6	130.4
C ¹	79.7	81.8	83.1
C ⁴	68.5	70.8	72.0
C ² and C ³	28.6	27.9	28.1

The ¹³C NMR signals corresponding to the carbon atom C⁵ in **4a** and **4b** display noticeable downfield shifts of $\Delta\delta$ 8.3 and 9.5, respectively compared to the free ligand. Similarly, after coordination of the ligand the ¹³C NMR resonance of C⁹ in **4a** and **4b**

displays a downfield shift of δ 5.4 and 6.2, respectively with respect to the free ligand. The *ipso*-carbon C⁶ of the phenyl ring in **4a** and **4b**, however, exhibits a significant upfield shift of $\Delta\delta$ 8.6 and 6.5, respectively after coordination.

2.2.2.5 $[\text{Cl}_2\text{Au}\{\text{N}=\text{C}(\text{Ph})\text{OCH}_2\text{C}(\text{CH}_3)_2\}_2][\text{AuCl}_4]$, **4c** and
 $[(\text{Ag}\{\text{N}=\text{C}(\text{Ph})\text{OCH}_2\text{C}(\text{CH}_3)_2\}_2)[\text{AuCl}_4]$, **4d**

Table 2.5 ¹H and ¹³C NMR data of compounds **4c** and **4d** in acetone-d₆

Assignment	δ (ppm) (multiplicity, J(Hz))	δ (ppm) (multiplicity, J(Hz))
<div style="display: flex; justify-content: space-around; align-items: center;"> <div style="text-align: center;">  <p>4c</p> </div> <div style="text-align: center;">  <p>4d</p> </div> </div>		
¹H NMR		
H ⁷ and H ¹¹	8.32 (2H, dm, ³ J _{H^{7,11}-H^{8,10}} = 7.4 Hz)	8.13 (2H, dm, ³ J _{H⁷-H⁸} = 7.7 Hz)
H ⁹	7.87 (1H, tt, ³ J _{H⁹-H^{8,9}} = 7.5 & ⁴ J _{H⁹-H^{7,11}} 1.6 Hz)	7.73 (1H, m)
H ⁸ and H ¹⁰	7.75 (2H, tt, ³ J _{H⁸-H^{7,9}} = 7.6 Hz & ⁴ J _{H⁸-H¹⁰} = 1.5 Hz)	7.73 (2H, m)
H ¹	4.87 (2H, s)	4.96 (2H, s)
H ² and H ³	1.78 (6H, s)	1.68 (6H, s)
¹³C NMR		
C ⁵	171.8	170.4
C ⁶	125.7	130.1
C ⁹	139.0	136.7
C ⁸ and C ¹⁰	130.5	130.4
C ⁷ and C ¹¹	130.6	130.3
C ¹	83.2	83.8
C ⁴	72.1	65.2
C ² and C ³	28.2	26.4

The ¹H and ¹³C NMR data of compounds **4c** and **4d** are presented in Table 2.5. The proton NMR signals of **4d** corresponding to the phenyl protons H⁷/H¹¹, H^{8,10} and H⁹ show a small downfield shift of $\Delta\delta$ 0.17, 0.23 and 0.23, respectively upon coordination. The signals at δ

4.96 and 1.68 are assigned to the methylene, H¹, and methyl, H²/H³, protons of the oxazole with downfield shift of Δδ 0.85 and 0.38, respectively when compared to the free ligand. The chemical and magnetic equivalence of the methyl protons H²/H³ is evident. The signal corresponding to the methylene protons, H¹, in **4d** appears at a lower field when compared to proton H¹ in **4a**, **4b** and **4c**, whereas, the methyl protons, H²/H³, appear at higher field compared to those of **4a**, **4b** and **4c**. The ¹H NMR signals of H⁷/H¹¹, H⁹, H⁸/H¹⁰, H¹ and H²/H³ of **4c** are comparable to those of **4b** (Table 2.4).

The ¹³C NMR signals of **4c** are assigned in a similar fashion as for **4b**. The ¹³C NMR signals at δ 171.8 and 139.0 are assigned to C⁵ and C⁹, respectively with significant downfield shifts of Δδ 9.5 and 9.3 when compared to the free ligand (Table 2.4). The methyl carbons, C²/C³, are assigned at 28.2 ppm and are chemically equivalent. The *ipso*-position carbon, C⁶, also resonates upfield by 6.5 after coordination. All these changes in chemical shifts are indicative of coordination of the ligand.

The signal of the oxazole carbon C⁵ and the phenyl carbon in *para*-position, C⁹ in **4d** displayed significant downfield shifts of Δδ 8.1 and 7.0, respectively upon coordination. The methyl carbons resonate at 26.4 ppm and are shifted slightly upfield after coordination compared to the free ligand. The ¹³C NMR signal of **4d** at 130.1 ppm is assigned to C⁶. Comparison of this chemical shift to the signal for the same carbon in **4a**, **4b** and **4c** shows that the signal for **4c** has the lowest chemical shift. The signal at 65.2 ppm is assigned to C⁴ and appears upfield by Δδ 3.2 when compared to compounds **4a**, **4b** and **4c**.

Mass Spectrometry

Table 2.6 Mass spectrometric data of compound **1**

<i>m/z</i>	Intensity (%)	Fragment ion
585	6	[{Cl ₂ Au}{N=C(Ph)N(Me)CH=CH} ₂] ⁺
515	3	[Au{N=C(Ph)N(Me)CH=CH} ₂] ⁺
499	2	[{Cl ₄ Au}{HN=C(Ph)N(Me)CH=CH}] ⁺
427	3	[{Cl ₂ Au}{N=C(Ph)N(Me)CH=CH}] ⁺
159	100	[HN=C(Ph)N(Me)CH=CH] ⁺
77	10	[Ph] ⁺

The FAB MS data of complex **1**, summarised in Table 2.6, does not show the molecular ion peak. However, peaks for the respective cationic fragments are observed at m/z 585, 515, and 427, indicating the presence of the proposed cationic complex, $[\text{AuCl}_2\{\overline{\text{N}=\text{C}(\text{Ph})\text{N}(\text{Me})\text{CH}=\text{CH}}\}_2]^+$ or its formation after rearrangement of the fragmented species. A weak signal detected at m/z 499 also indicates the anticipated cation $[\{\text{Cl}_4\text{Au}\}\{\overline{\text{HN}=\text{C}(\text{Ph})\text{N}(\text{Me})\text{CH}=\text{CH}}\}]^+$. The base peak (100%) at m/z 159 indicate the presence of cation $[\overline{\text{HN}=\text{C}(\text{Ph})\text{N}(\text{Me})\text{CH}=\text{CH}}]^+$.

Table 2.7 Mass spectrometric data of compound **2a** and **2b**

m/z	Intensity (%)	Fragment ion
160	37	$[\overline{\text{N}=\text{C}(\text{py})\text{NMeCH}=\text{CH}}]^+$
154	19	$[\overline{\text{N}=\text{C}(\text{py})\text{NMeCH}=\text{CH}}]^+$
81	6	$[\overline{\text{N}=\text{CNMeCH}=\text{CH}}]^+$

The molecular ions of the proposed compounds **2a** and **2b** could not be observed. However, a typical pattern of the ligand fragments are shown in Table 2.7.

Table 2.8 Mass spectrometric data of compound **3**

m/z	Intensity (%)	Fragment ion
640	25	$[\text{Cl}_2\text{Au}\{\overline{\text{N}=\text{C}(\text{C}=\text{CHCH}=\text{CHS})\text{OCH}_2\text{C}(\text{CH}_3)_2}\}_2]^+$
559	50	$[\text{Au}\{\overline{\text{N}=\text{C}(\text{C}=\text{CHCH}=\text{CHS})\text{OCH}_2\text{C}(\text{CH}_3)_2}\}_2]^+$
449	3	$[\text{Cl}_2\text{Au}\{\overline{\text{N}=\text{C}(\text{C}=\text{CHCH}=\text{CHS})\text{OCH}_2\text{C}(\text{CH}_3)_2}\}]^+$
378	6	$[\text{Au}\{\overline{\text{N}=\text{C}(\text{C}=\text{CHCH}=\text{CHS})\text{OCH}_2\text{C}(\text{CH}_3)_2}\}]^+$
182	100	$[\overline{\text{N}=\text{C}(\text{C}=\text{CHCH}=\text{CHS})\text{OCH}_2\text{C}(\text{CH}_3)_2}]^+$

ESI MS data of **3** are summarised in Table 2.8. The molecular ion is not observed but the peak at m/z 640 indicates of the cation of the presence of the proposed structure $[\text{Cl}_2\text{Au}\{4,4\text{-dimethyl-2-(2'-thienyl)oxazole}\}_2]^+$. There are two daughter fragmentation peaks of the cation at m/z 559 and 449. The first signal at m/z 559 shows a loss of Cl_2 to yield $[\text{Au}\{4,4\text{-dimethyl-2-(2'-thienyl)oxazole}\}_2]^+$ and the second signal at m/z 449 indicates a loss of one of the ligand entities to form $[\text{Cl}_2\text{Au}\{4,4\text{-dimethyl-2-(2'-thienyl)oxazole}\}]^+$. A further peak at m/z 378, with a loss of either Cl_2 or one of the

ligands from the daughter fragments, represents $[\text{Au}\{4,4\text{-dimethyl-}2\text{-(}2'\text{-thienyl)oxazole}\}]^+$. The base peak at m/z 176 represents the ligand.

Table 2.9 Mass spectrometric data of compounds **4b** and **4c**

m/z	Intensity (%)	Fragment ion
620	4	$[\text{Cl}_2\text{Au}\{\overline{\text{N}=\text{C}(\text{Ph})\text{OCH}_2\text{C}(\text{CH}_3)_2}\}_2]^+$
443	20	$[\text{Cl}_2\text{Au}\{\overline{\text{N}=\text{C}(\text{Ph})\text{OCH}_2\text{C}(\text{CH}_3)_2}\}]^+$
409	4	$[\text{ClAu}\overline{\text{N}=\text{C}(\text{Ph})\text{OCH}_2\text{C}(\text{CH}_3)_2}]^+$
176	100	$[\overline{\text{N}=\text{C}(\text{Ph})\text{OCH}_2\text{C}(\text{CH}_3)_2}]^+$
109	8	$[\text{PhCO}]^+$
77	10	$[\text{Ph}]^+$

The molecular ion peak of the proposed compounds **4b** and **4c** could not be observed, however, peaks in the spectra appear to be similar as shown in Table 2.9. The peak at m/z 620 indicates presence of the cation of the proposed compound $[\{\text{Cl}_2\text{Au}\}\{\overline{\text{N}=\text{C}(\text{Ph})\text{OCH}_2\text{C}(\text{CH}_3)_2}\}_2]^+$ and the peak at m/z 443 is due to the loss of one ligand from the cationic complex. The peak at m/z 409 also indicates the loss of Cl, yielding $[\{\text{ClAu}\}\overline{\text{N}=\text{C}(\text{Ph})\text{OCH}_2\text{C}(\text{CH}_3)_2}]^+$. The peak representing the ligand appears as displayed the base peak at m/z 176. The fragmentation pattern of adduct **4a** showed of only a peak representing the free ligand at m/z 176. Hence, MS data of **4a** is not reported.

Table 2.10 Mass spectrometry data of compound **4d**

m/z	Intensity (%)	Fragment ion
723	22	$[(\text{Ag}\{\overline{\text{N}=\text{C}(\text{Ph})\text{OCH}_2\text{C}(\text{CH}_3)_2}\}_2)(\text{AuCl}_4)]^+$
460	33	$[\text{Ag}\{\overline{\text{N}=\text{C}(\text{Ph})\text{OCH}_2\text{C}(\text{CH}_3)_2}\}_2]^+$
280	27	$[\text{Ag}\{\overline{\text{N}=\text{C}(\text{Ph})\text{OCH}_2\text{C}(\text{CH}_3)_2}\}]^+$
176	9	$[\overline{\text{N}=\text{C}(\text{Ph})\text{OCH}_2\text{C}(\text{CH}_3)_2}]^+$
107	25	$[\text{PhCO}]^+$

The FAB MS data of compound **4d** are summarised in Table 2.10. The molecular ion is observed at m/z 723. After a loss of the counter ion, AuCl_4^- , a base peak at m/z 460 could be assigned to the cationic complex, $[\text{Ag}\{\overline{\text{N}=\text{C}(\text{Ph})\text{OCH}_2\text{C}(\text{CH}_3)_2}\}_2]^+$. The peak for the

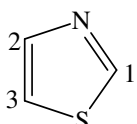
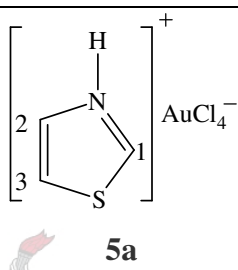
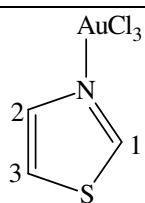
fragment observed at m/z 280 indicates the loss of one ligand. A peak corresponding to the ligand is observed at m/z 176.

2.2.3 Spectroscopic characterisation of compounds **5** - **12**

NMR spectroscopy

2.2.3.1 $[\text{HN}=\text{CHSCH}=\text{CH}][\text{AuCl}_4]$, **5a** and $[\text{Cl}_3\text{Au}\{\text{N}=\text{CHSCH}=\text{CH}\}]$, **5b**

Table 2.11 ^1H and ^{13}C NMR data of the free ligand, compounds **5a** and **5b** in acetone- d_6

Assignment	$\delta(\text{ppm})$ (multiplicity, J(Hz))	$\delta(\text{ppm})$ (multiplicity, J(Hz))	$\delta(\text{ppm})$ (multiplicity, J(Hz))
			
		5a	5b
$^1\text{H NMR}$			
H ¹	9.07 (1H, d, $^4J_{\text{H}1-\text{H}4} = 1.5$ Hz)	10.06 (1H, dm, $^4J_{\text{H}1-\text{H}2,3} = 2.2$ Hz)	10.06 (1H, dm, $^4J_{\text{H}1-\text{H}4} = 2.2$ Hz)
H ³	7.99 (1H, d, $^3J_{\text{H}3-\text{H}2} = 3.1$ Hz)	8.54 (1H, d, $^3J_{\text{H}3-\text{H}2} = 3.5$ Hz)	8.54 (1H, d, $^3J_{\text{H}3-\text{H}2} = 3.4$ Hz)
H ²	7.68 (1H, dd, $^3J_{\text{H}2-\text{H}3} = 3.1$ & $^4J_{\text{H}2-\text{H}1} = 1.7$ Hz)	8.34 (1H, dd, $^3J_{\text{H}2-\text{H}3} = 3.5$ & $^4J_{\text{H}2-\text{H}1} = 2.1$ Hz)	8.34 (1H, dd, $^3J_{\text{H}2-\text{H}3} = 2.4$ & $^4J_{\text{H}2-\text{H}1} = 2.3$ Hz)
$^{13}\text{C NMR}$			
C ¹	154.2	161.5	161.5
C ²	144.6	142.4	142.4
C ³	120.1	124.6	124.6

The ^1H and ^{13}C NMR data of the free ligand, compounds **5a** and **5b** are summarised in Table 2.11. The ^1H NMR spectra for compounds **5a** and **5b** displayed three broad signals and the resonances of both compounds compare well. All signals appear at lower field compared to the free ligand. The doublet of multiplets at 10.06 ppm is assigned to the acidic proton H¹ in **5a** and **5b**. This proton displayed the most significant downfield shift of $\Delta\delta$ 1.0 with respect to the free ligand upon coordination. Similarly, the two signals at δ

8.54 and 8.34 are assigned to H³ and H², respectively. Protons H² and H³ also experience noticeable downfield shifts of $\Delta\delta$ 0.66 and 0.55, respectively upon coordination when compared the free ligand. Such a downfield change in chemical shifts is indicative of coordination. The deshielding effect of the protons is attributed to the delocalisation of the electron density to the gold(III) centre. The coupling constants determined for the protons H¹ ($^4J_{H1-H2,3} = 2.2$ Hz), H² ($^3J_{H2-H3} = 3.5$ Hz) and H³ ($^3J_{H3-H2} = 2.8$ Hz) do not show significant difference when compared to the free ligand (Table 2.11).

The ¹³C NMR spectrum shows three sharp signals at δ 161.5, 142.4 and 124.6 corresponding to C¹, C² and C³, respectively. The C¹ carbon specifically shows a considerable downfield shift of $\Delta\delta$ 7.3 upon coordination. Whereas, C³ displayed a small downfield shift of $\Delta\delta$ 4.5. The smallest change in chemical shift is noticed for C² with a downfield shift of $\Delta\delta$ 2.2 for both, **5a** and **5b**, when compared with the free ligand.

2.2.3.2 $[\text{Au}\{\text{N}=\text{CHSCH}=\text{C}(\text{CH}_3)\}_2][\text{AuCl}_4]$, **6a** and $[\text{Cl}_3\text{Au}\{\text{N}=\text{CHSCH}=\text{C}(\text{CH}_3)\}]$, **6b**

The ¹H and ¹³C NMR spectra of the free ligand, **6a** and **6b** are summarised in Table 2.12. The ¹H NMR spectra of the compounds show broad singlets and have similar chemical shifts. The proton NMR signals for H¹, H² and H⁴ resonate downfield from their signals for the free ligand, $\Delta\delta$ 1.16, 0.82 and 0.34, respectively. The two ligands in the cationic complex **6a** are chemically equivalent thus only one set of signals is observed. The coupling constants are difficult to determine due to broadening of the signals. The ¹H NMR signals of **6a** and **6b** show a considerable downfield change in chemical shift with respect to the corresponding signals of the gold(I)(4-methylthiazole)(C₆F₅) complex.^{20,21}

Both compounds **6a** and **6b** have similar ¹³C NMR chemical shifts. C¹ and C² appear at δ 160.5 and 120.8, respectively and are significantly deshielded after coordination ($\Delta\delta$ 6.0 and 6.8) compared to the free ligand. These chemical shifts have some similarities with the signals observed for the gold(I) imine complex reported for the same ligand.

²⁰ H. G. Raubenheimer, P. J. Olivier, L. Lindeque, M. Desmet, J. Hrusak, G. J. Kruger, *J. Organomet. Chem.*, 1997, **544**, 91.

²¹ S. Cronje, H. G. Raubenheimer, H. S. C. Spies, C. Esterhuysen, H. Schmidbaur, A. Schier and G. J. Kruger, *Dalton Trans.*, 2003, 2859.

Table 2.12 ^1H and ^{13}C NMR data of the free ligand, compounds **6a** and **6b** in CDCl_3

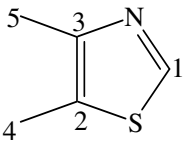
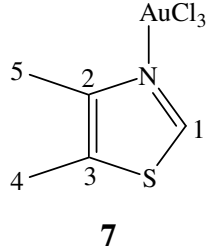
Assignment	$\delta(\text{ppm})$ (multiplicity, J(Hz))	$\delta(\text{ppm})$ (multiplicity, J(Hz))	$\delta(\text{ppm})$ (multiplicity, J(Hz))
^1H NMR			
H^1	8.90 (1H, d, $^4J_{\text{H}^1-\text{H}^2} = 1.8$ Hz)	10.06 (1H, s)	10.07 (1H, s)
H^2	7.18 (1H, m)	8.00 (1H, s)	8.01 (1H, s)
H^4	2.43 (1H, dm, $^4J_{\text{H}^4-\text{H}^2} = 1.0$ Hz)	2.77 (3H, s)	2.77 (3H, s)
^{13}C NMR			
C^1	154.6	160.5	160.5
C^3	153.5	150.8	150.8
C^2	114.2	120.8	120.8
C^4	16.8	17.0	16.9

2.2.3.3 $[\text{Cl}_3\text{Au}\{\text{N}=\text{CHSC}(\text{CH}_3)=\text{C}(\text{CH}_3)\}], \mathbf{7}$

The ^1H and ^{13}C NMR spectra of the free ligand and compound **7** are summarised in Table 2.13. The data reported in Table 2.13 are for the products obtained from the reaction between 4,5-dimethylthiazole and HAuCl_4 or AuCl_3 . The acidic proton H^1 resonates at 8.99 ppm with a downfield shift of $\Delta\delta$ 0.53 after coordination. The signals of the methyl protons, H^4 and H^5 of the free ligand appear as a singlet, despite the fact that they are not chemically equivalent. However, in the ^{13}C NMR spectrum these methyl groups, C^4 and C^5 , appear as two independent signals at δ 14.3 and 10.8, respectively indicating that they are not chemically equivalent. The methyl protons, H^4 and H^5 , in complex **7** appear as two independent doublet signals at δ 2.50 and 2.65, respectively. These signals exhibit a downfield shift of $\Delta\delta$ 0.20 and 0.35 compared to the free ligand. These two protons experience very weak coupling constant of 0.7 Hz. The methyl protons, H^5 that resonate at

2.65 ppm are more deshielded compared to the methyl protons H⁴ after coordination, which resonate at 2.50 ppm.

Table 2.13 ¹H and ¹³C NMR data of the free ligand and compound **7** in CDCl₃

		
Assignment	δ(ppm) (multiplicity, J(Hz))	δ(ppm) (multiplicity, J(Hz))
¹H NMR		
H ¹	8.46 (1H, s)	8.99 (1H, s)
H ⁴	2.30 (3H, s)	2.50 (3H, d, ⁵ J _{H4-H5} = 0.7 Hz)
H ⁵	2.30 (3H, s)	2.65 (3H, d, ⁵ J _{H5-H4} = 0.7 Hz)
¹³C NMR		
C ¹	149.1	154.6
C ³	148.6	153.3
C ²	125.9	131.2
C ⁴	14.3	15.4
C ⁵	10.8	12.3

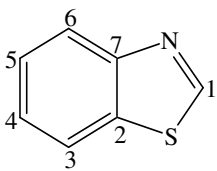
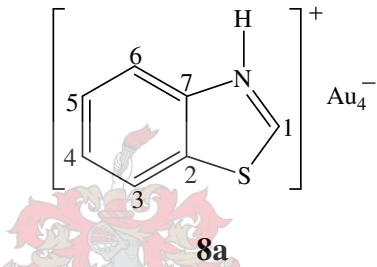
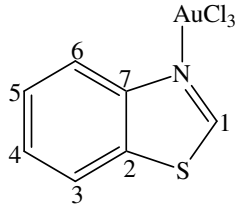
The ¹³C NMR signal at 154.6 ppm is assigned to C¹. It exhibits a downfield change in chemical shift of Δδ 5.5 after coordination with respect to the free ligand. The methyl carbons C⁴ and C⁵ appear at δ 15.4 and 12.3, respectively exhibiting an small changes in chemical shift upon coordination.

2.2.3.4 $[\text{HN}=\text{CHSC}=\text{CHCH}=\text{CHCH}=\text{C}][\text{AuCl}_4]$, **8a** and
 $[\text{Cl}_3\text{Au}\{\text{N}=\text{CHSC}=\text{CHCH}=\text{CHCH}=\text{C}\}]$, **8b**

The ¹H and ¹³C NMR data of the free ligand, compounds **8a** and **8b** are summarised in Table 2.14. The ¹H NMR spectra for **8a** and **8b** are slightly different from each other. The ¹H NMR signals of compound **8a** appear slightly upfield from the free ligand. The doublet of doublets at 7.98 ppm is assigned to the thiazole proton H³, which is coupled to proton H⁴. The proton H³ in the spectrum appears slightly upfield (Δδ 0.15) when compared to

the free ligand. The signal for H¹ has shifted upfield by $\Delta\delta$ 0.38. The most deshielded broad signal at 9.54 ppm is assigned to the N-H proton. This indicates formation of the immonium tetrachloroaurate(III) salt of the benzothiazole. The coupling constants between the protons of **8a**; H⁶ ($^3J_{H6-H5} = 8.6$ Hz), H³ ($^3J_{H3-H4} = 8.7$ Hz), H⁵ ($^3J_{H5-H4,6} = 7.7$ Hz) and H⁴ ($^3J_{H4-H3,5} = 7.7$ Hz) are comparable to those of the free ligand (Table 2.14). The ¹H NMR spectrum of the proposed adduct of **8b** shows no significant change in chemical shift in DMSO-d when compared to the free ligand. Since DMSO is a known donor solvent the ligand might have dissociated.

Table 2.14 ¹H and ¹³C NMR data of the free ligand²² in DMSO, compounds **8a** in chloroform and **8b** in DMSO-d₆

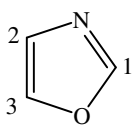
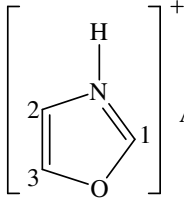
			
Assignment	δ (ppm) (multiplicity, J(Hz))	δ (ppm) (multiplicity, J(Hz))	δ (ppm) (multiplicity, J(Hz))
¹H NMR			
H ¹	9.43 (1H, s)	9.05 (1H, s)	9.44 (1H, s)
H ⁶	8.19 (1H, dm, $^3J_{H6-H5} = 7.8$ Hz)	8.16 (1H, dm, $^3J_{H6-H5} = 8.6$ Hz)	8.20 (1H, dm, $^3J_{H6-H5} = 7.8$ Hz)
H ³	8.13 (1H, dm, $^3J_{H3-H4} = 8.0$ Hz)	7.98 (1H, dm, $^3J_{H3-H4} = 8.7$ Hz)	8.12 (1H, dm, $^3J_{H3-H4} = 7.4$ Hz)
H ⁴	7.56 (1H, t, $^3J_{H4-H3,5} = 7.6$ Hz)	7.51 (1H, tm, $^3J_{H4-H3,5} = 7.7$ Hz)	7.57 (1H, tm, $^3J_{H4-H3,5} = 7.6$ Hz)
H ⁵	7.49 (1H, t, $^3J_{H5-H4,6} = 7.5$ Hz)	7.46 (1H, tm, $^3J_{H5-H4,6} = 7.7$ Hz)	7.50 (1H, tm, $^3J_{H5-H4,6} = 7.5$ Hz)
N-H		9.54 (1H, s)	
¹³C NMR			
C ¹	156.3	156.4	156.6
C ⁷	153.4	153.2	153.1
C ²	133.8	133.8	133.8
C ⁵	126.4	126.8	126.6
C ⁴	125.7	125.9	125.8
C ⁶	123.3	123.7	123.2
C ³	122.7	122.1	122.8

²² SDBS web: <http://www.aist.go.jp/RIODBS/SDBS> (National Institute of Advanced Industrial Science and Technology, 03 May 2005).

The ^{13}C NMR data of both compounds **8a** and **8b** are very similar to the data of the free ligand. **8a** and **8b** are poorly soluble in acetone, dichloromethane and chloroform. Despite the fact that DMSO- d_6 is a much better solvent for **8a** and **8b**, its donor property dissociates complex **8b**.

2.2.3.5 $[\text{HN}=\overline{\text{CHOCH}=\text{CH}}][\text{AuCl}_4]$, **9** and
 $[\text{HN}=\overline{\text{CHOC}=\text{CHCH}=\text{CHCH}=\text{C}}][\text{AuCl}_4]$, **10**

Table 2.15 ^1H and ^{13}C NMR data of the free ligand and compound **9** in CD_2Cl_2

		
Assignment	$\delta(\text{ppm})$ (multiplicity, J(Hz))	$\delta(\text{ppm})$ (multiplicity, J(Hz))
^1H NMR		
H ¹	7.93 (1H, s)	9.27 (1H, s)
H ³	7.73 (1H, s)	8.15 (1H, s)
H ²	7.15 (1H, s)	7.85 (1H, s)
^{13}C NMR		
C ¹	151.8	155.4
C ³	139.5	142.1
C ²	127.1	124.8

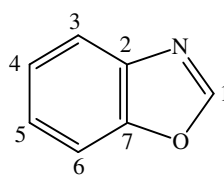
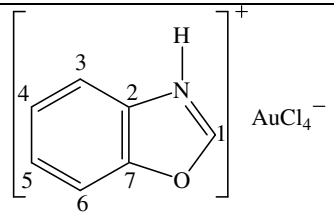
The ^1H and ^{13}C NMR data of compound **9** are summarised in Table 2.15. The ^1H NMR spectrum for **9** displays three sharp and strong signals with significant downfield change in chemical shift when compared to the free ligand. The protons H¹, H³ and H² exhibit a noticeable downfield shift of $\Delta\delta$ 1.34, 0.42 and 0.70, respectively upon coordination. No coupling is observed for the protons H³ and H² before coordination.

In the ^{13}C NMR spectrum of **9** the signals for C¹ and C³ appear slightly downfield ($\Delta\delta$ 3.6 and 2.6, respectively) while C² appears upfield ($\Delta\delta$ 2.3).

The ^1H and ^{13}C NMR data of the free ligand and compound **10** are summarised in Table 2.16. The phenyl protons H⁴ and H⁵ appear as a multiplet of signals at 6.97 ppm, showing

an upfield shift of $\Delta\delta$ 0.6 compared to the free ligand. The doublet signal at 7.52 ppm is assigned to the proton H^3 upfield by $\Delta\delta$ 0.2 relative to the free ligand, with a coupling constant of 8.8 Hz. Similarly, the doublet at 7.87 ppm is assigned to proton H^6 with the coupling constant of 9.4 Hz. The most deshielded broad signal at 9.22 ppm is assigned to the N-H proton indicating the formation of an immonium tetrachloroaurate(III) salt.

Table 2.16 1H and ^{13}C NMR data of the ligand and compound **10** in acetone- d_6

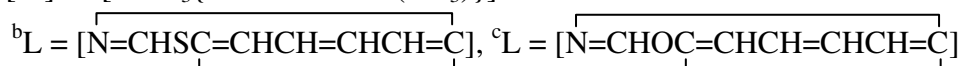
		
Assignment	δ (ppm) (multiplicity, J(Hz))	δ (ppm) (multiplicity, J(Hz))
1H NMR		
H^1	8.49 (1H, s)	8.41 (1H, s)
H^6	7.80 (1H, dm, $^3J_{H^6-H^5} = 8.8$ Hz)	7.87 (1H, d, $^3J_{H^6-H^5} = 9.4$ Hz)
H^3	7.70 (1H, dm, $^3J_{H^3-H^4} = 7.8$ Hz)	7.52 (1H, m)
H^4 and H^5	7.43 (2H, m)	6.97 (2H, m)
N-H		9.22 (1H, bs)
^{13}C NMR		
C^1	154.6	161.3
C^7	151.2	150.8
C^2	141.5	144.0
C^4	126.6	126.7
C^5	125.6	126.2
C^3	121.4	120.9
C^6	111.9	104.6

In the ^{13}C NMR spectrum, C^1 is evident at 161.3 ppm and exhibits a noticeable downfield shift of $\Delta\delta$ 6.7. The signal at 104.6 ppm is assigned to C^6 and shows an upfield shift of $\Delta\delta$ 7.4 compared to the free ligand. The chemical shift of C^1 is comparable with the analogous carbon of the thiazole gold(III) compounds **5** - **8**.

Mass Spectrometry

Table 2.17 FAB Mass spectrometric data of compounds 5 - 10

<i>m/z</i>	Intensity (%)	Fragment ion	<i>m/z</i>	Intensity (%)	Fragment ion
5a			114	50	$[\overline{\text{N}=\text{CHSC}(\text{CH}_3)=\text{C}(\text{CH}_3)}]^+$
371	2	$[\text{Au}(\overline{\text{N}=\text{CHSCH}=\text{CH}})_2]^+$			
86	10	$[\overline{\text{HN}=\text{CHSCH}=\text{CH}}]^+$	8a		
5b			136	17	$[\overline{\text{HN}=\text{CHSC}=\text{CHCH}=\text{CHCH}=\text{C}}]^+$
353	2	$[\text{Au}(\text{Cl})(\overline{\text{N}=\text{CHSCH}=\text{CH}})]^+$	8b		
281	10	$[\text{Au}(\overline{\text{N}=\text{CHSCH}=\text{CH}})]^+$	468	2	$[\text{Au}({}^b\text{L})_2]^+$
85	9	$[\overline{\text{N}=\text{CHSCH}=\text{CH}}]^+$	329	9	$[\text{Au}({}^b\text{L})]^+$
6a			136	13	$[\overline{\text{HN}=\text{CHSC}=\text{CHCH}=\text{CHCH}=\text{C}}]^+$
100	27	$[\overline{\text{HN}=\text{CHSCH}=\text{C}(\text{CH}_3)}]^+$	9		
6b			136	14	$[\overline{\text{OCHCHN}=\text{C}-\text{C}=\text{NCHCHO}}]^+$
401	5	${}^a[\text{M}]^+$	70	4	$[\overline{\text{HN}=\text{CHOCH}=\text{CH}}]^+$
296	3	$[\text{M}]^+-\text{Cl}_3$	10		
100	26	$[\overline{\text{HN}=\text{CHSCH}=\text{C}(\text{CH}_3)}]^+$	577	3	$[\text{AuCl}_2({}^c\text{L})_2(\text{thf})]^+$
7			119	0.5	$[\overline{\text{HN}=\text{CHOC}=\text{CHCH}=\text{CHCH}=\text{C}}]^+$
425	3	$[\text{Au}\{\overline{\text{N}=\text{CHSC}(\text{CH}_3)=\text{C}(\text{CH}_3)}\}_2]^+$			



The FAB MS data of compounds 5 - 10 are summarised in Table 2.17. The majority of the proposed molecular ions were not observed. Although, the molecular ion peak for adduct **6b** appears at *m/z* 401. Most of the peaks could be assigned to the respective free ligands. Compound **8a** shows a peak at *m/z* 136, indicating the presence of protonated

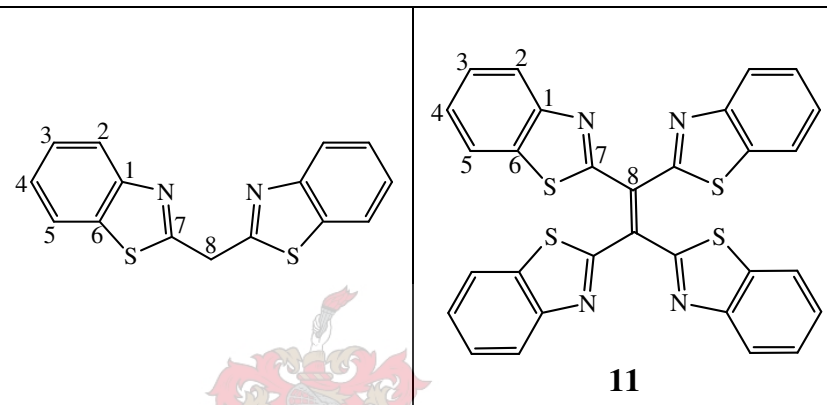
benzothiazole, *i.e.*, [^bLH]⁺. Compound **10** also shows a peak at *m/z* 578 indicating the presence of $[\text{Au}(\text{N}=\text{CHOC}=\text{CHCH}=\text{CHCH}=\text{C})_2^+\text{Cl}_2(\text{THF})]^+$.

2.2.4 Spectroscopic characterisation of compounds 11 - 12

NMR spectroscopy

2.2.4.1 (BT)₂C=C(BT)₂, BT = benzothiazolyl, **11**

Table 2.18 ¹H and ¹³C NMR data of the free ligand and compound **11** in CDCl₃

Assignment	δ(ppm) (multiplicity, J(Hz))	δ(ppm) (multiplicity, J(Hz))
		
¹H NMR		
H ²	8.03 (2H, d, ³ J _{H2-H3} = 8.1 Hz)	8.06 (4H, m)
H ⁵	7.80 (2H, d, ³ J _{H5-H4} = 7.8 Hz)	7.92 (4H, m)
H ³	7.45 (2H, t, ³ J _{H3-H2,4} = 7.7 Hz)	7.47 (4H, m)
H ⁴	7.34 (2H, t, ³ J _{H4-H3,5} = 7.6 Hz)	7.42 (4H, m)
H ⁸	4.92 (2H, s)	
¹³C NMR		
C ⁷	165.9	167.8
C ¹	153.3	152.4
C ⁶	136.0	136.8
C ²	126.4	126.3
C ⁵	125.5	126.1
C ³	123.3	124.1
C ⁴	121.8	121.2
C ⁸	38.7	135.1

The ¹H and ¹³C NMR data of the free ligand and compound **11** are summarised in Table 2.18. The ¹H and ¹³C NMR investigations of the reaction products obtained from the

reaction of HBBTM and $\text{HAuCl}_4/\text{AuCl}_3$ do not give conclusive evidence on the coordination (cationic or neutral complex) of the gold(III) to the ligand. However, a thorough investigation of the methylene carbon, CH_2 , helped us propose the oxidative dimerisation of the ligand to 2-(1,2,2-tri(benzo[*d*]thiazol-2-yl)vinyl)benzo[*d*]thiazole. Thus, further clarifications would be required by X-ray analysis. The molecular structure of 2-(1,2,2-tri(benzo[*d*]thiazol-2-yl)vinyl)benzo[*d*]thiazole is also discussed in detail in Chapter 4, Section 4.4.3. The ^1H NMR signals representing the phenyl rings appeared as multiplets and most of the signals resonate slightly downfield when compared to the free ligand. The multiplet of signals displayed at 7.73 - 7.44 ppm are assigned to the protons H^3 and H^4 . A signal at 4.93 ppm (characteristic chemical shift of the bridging methylene CH_2 protons) is expected to shift upon coordination; however, signals related to these protons completely disappear from the ^1H NMR spectrum of **11**. This is diagnostic of an oxidative dimerisation of the ligand to 2-(1,2,2-tri(benzo[*d*]thiazol-2-yl)vinyl)benzo[*d*]thiazole.²³

The ^{13}C NMR resonance at 167.8 ppm is assigned to C^7 showing an insignificant downfield shift. The low field signals at δ 152.4 and 136.8 are assigned to the azoly carbons C^1 and C^6 , respectively. The chemical shift of C^8 is very crucial in determining the structural background of the compound (although it may not be possible to determine the structure completely by ^1H and ^{13}C NMR alone, especially in regard to the coordination of the metal). C^8 displayed a significant downfield change in chemical shift at 135.1 ppm. This chemical shift is characteristic for a sp^2 carbon. This reveals the formation of 2-(1,2,2-tri(benzo[*d*]thiazol-2-yl)vinyl)benzo[*d*]thiazole due to oxidative dimerisation. Because of the poor solubility of the crude product an attempt to correct the ^{15}N NMR spectrum to investigate the imine-*N* coordination was not successful.

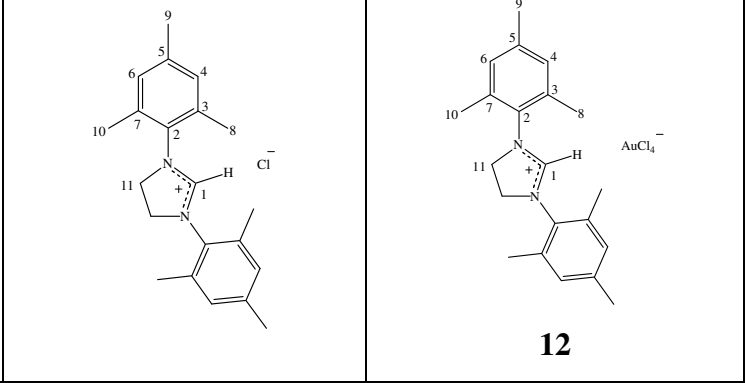
2.2.4.2 $[\text{N}(\text{mes})\text{CHN}(\text{mes})\text{CH}_2\text{CH}_2][\text{AuCl}_4]$ (mes = 2,4,6-trimethylphenyl), **12**

The ^1H and ^{13}C NMR data of the free ligand and compound **12** are summarised in Table 2.19. The proton NMR signals of the gold(III) 1,3-bis-(2,4,6-trimethylphenyl)imidazolinium salt do not show any change in chemical shift with respect to the free ligand 1,3-bis-(2,4,6-trimethylphenyl)imidazolinium chloride. The ^1H NMR signal at 9.24

²³ D. B. Dell'amico and F. Calderazzo, *Gazz. Chim. Ital.*, 1973, **103**, 1099.

ppm is assigned to H¹ and indicates that the proposed imidazolium gold(III) carbene complex does not form.

Table 2.19 ¹H and ¹³C NMR data of the free ligand²⁴ and compound **12** in CDCl₃

Assignment	δ(ppm) (multiplicity, J(Hz))	δ(ppm) (multiplicity, J(Hz))
		
¹H NMR		
H ¹	9.22	9.24 (1H, s)
H ⁴ and H ⁶	7.08	6.93 (4H, s)
H ¹¹	4.48	4.55 (4H, s)
H ⁸ and H ¹⁰	2.36	2.34 (12H, s)
H ⁹	2.28	2.24 (6H, s)
¹³C NMR		
C ¹	160.2	164.0
C ²	130.8	130.3
C ³ and C ⁷	135.3	135.1
C ⁵	139.5	140.8
C ⁴ and C ⁶	129.3	130.2
C ¹¹	50.9	51.9
C ⁸ and C ¹⁰	17.2	17.8
C ⁹	20.5	20.8

The ¹³C NMR spectrum of the compound also exhibits similar chemical shifts to 1,3-bis-(2,4,6-trimethylphenyl)imidazolium chloride.²⁴ The signal displayed at 160.1 ppm is characteristic for the precursor imidazoline carbon, C¹. The free ligand carbene carbon usually appears at low chemical shift of 243.8 ppm.²³

²⁴ A. J. Arduengo, III, R. Krafczyk and R. Schmutzler, *Tetrahedron*, 1999, **55**, 14523.

Mass Spectrometry

Table 2.20 Mass spectrometry data of compound **11** and **12**

m/z	Intensity (%)	Fragment ion
11		
560	75 (EI MS, FAB MS, ESI MS)	[(BBTM)=(BBTM)] ⁺
428	40 (EI MS, FAB MS, ESI MS)	[{(BBTM)=(BBTM)}-benzothiazole] ⁺
317	5 (FAB MS, ESI MS)	[HBBTMCl] ⁺
282	90 (EI MS, FAB MS, ESI MS)	[HBBTM] ⁺
148	10 (EI MS, FAB MS)	[HBBTM-benzothiazole] ⁺
136	5 (EI MS, FAB MS)	[benzothiazole] ⁺
12		
307	100 (FAB MS)	[N(mes)CHN(mes)CH ₂ CH ₂] ⁺
119	4 (FAB MS)	[2,4,6-trimethylphenyl] ⁺

The MS data of **11** and **12** are summarised in Table 2.20. The MS data for **11** are reported based on results obtained from FAB MS, ESI MS and EI MS. The signal exhibited at *m/z* 560 is characteristic of the dimeric product 2-(1,2,2-tri(benzo[*d*]thiazol-2-yl)vinyl)benzo[*d*]thiazole. The subsequent fragment ion at *m/z* 428 reveals the loss of one of the benzothiazolyl groups from the dimer. The base peak at *m/z* 282 indicates the presence of the free ligand. The proposed molecular ion fragment of the imidazolium gold(III) salt compound **12** could not be observed, however, a base peak characteristic of the 1,3-bis-(2,4,6-trimethylphenyl)imidazolium cation was evident at *m/z* 307.

2.3 Crystal and molecular structure determinations by means of X-ray diffraction

The crystal and molecular structures of **4b**, **4b'**, **6a**, **7**, **8a** and **12** are discussed in the following subsections 2.3.1 – 2.3.6. In the molecular structures of **4b'** and **12** only selected hydrogen atoms are shown in the diagrams (Figures 2.4 and 2.16). Hydrogen atoms are

omitted in the unit cell packing diagrams for clarity. Selected molecular interactions accompanied by diagrams are also reported for each structure.

It has been mentioned previously that the ^1H and ^{13}C NMR studies indicated the presence of more than one product as extra sets of signals in the spectra were observed. As a result crystals of the cationic complex, **4b** and the immonium tetrachloroaurate(III) salt, **4b'** were isolated and characterised from the same reaction mixture in Sections 2.3.1 and 2.3.2.

2.3.1 The crystal and molecular structure of **4b**

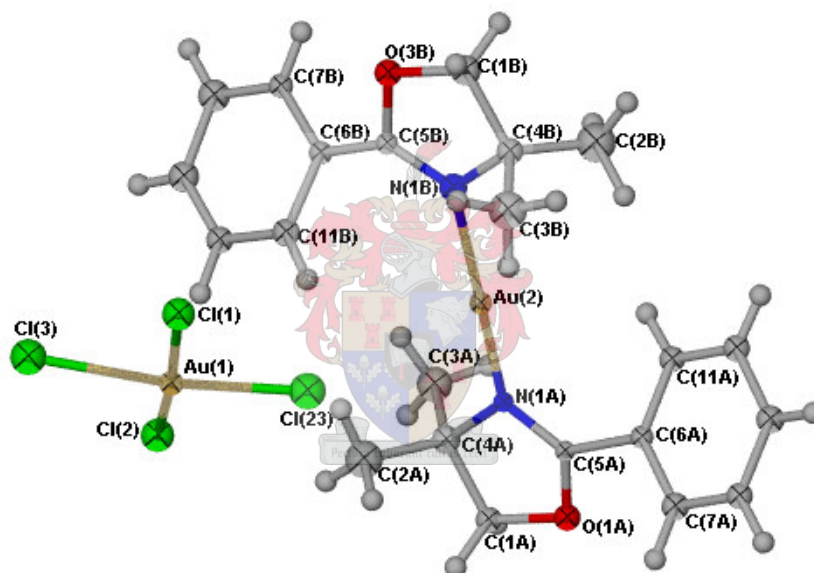


Figure 2.1 Molecular structure of **4b**.

The compound was crystallised from a concentrated chloroform- d solution in the triclinic space group $P\bar{1}$ as orange crystals. Selected bond lengths and angles are listed in Table 2.21. The molecular structure of the cationic complex **4b** is shown in Figure 2.1. The structure shows that Au(I) is coordinated linearly with a pair of 4,4-dimethyl-2-phenyl oxazole ligands *via* the imine- N atoms. The compound contains both gold(I) and gold(III) oxidation states with the latter acting as the anionic counter ion. The mean Au(2)–N(1A) and Au(2)–N(1B) bond length of [2.010 Å] is comparable to the Au–N bond lengths in dichloro-(2-(4,5-dihydro-4,4-dimethyloxazol-2-yl)phenyl- N)gold(III) [2.039 Å] and (4–

methylthiazole-*N*)-pentafluorophenyl-gold(I) [2.08 Å].²⁵ The deviation of the plane defined by the five membered oxazoline groups and the metal centre, *i.e.* C(5B), O(3B), C(1B), C(4B), N(1B), Au(2), C(5A), O(1A), C(1A), C(4A) and N(1A) from the least square plane is [0.0296 Å].

The geometry at the AuCl₄⁻ counter ion is as expected square planar with bond angles of 89.48(16) and 90.47(16)°. The Au(1)–Cl(3) and Au(1)–Cl(2) bond lengths [2.264 Å] are slightly shorter compared to the Au(1)–Cl(23) and Au(1)–Cl(1) bond lengths [2.294(4) and 2.297(4) Å], respectively. The geometry at the coordination centre N(1A)–Au(2)–N(1B) [179.4(5)°] indicates the perfect linearity of the cationic complex. The torsion angles Au(2)–N(1B)–C(4B)–C(2B) [57.9(11)°] and Au(2)–N(1A)–C(4A)–C(2A) [63.3(13)°] show that the methyl groups lie outside the coordination plane. The two bicyclic ligands of the cationic complex **4b** are not co-planar and they are related to each other by a centre of inversion lying at Au(2). Torsion angles C(11B)–C(6B)–C(5B)–N(1B) [39.9(18)°] and C(7B)–C(6B)–C(5B)–N(1B) [-140.9(12)°], illustrate the deviation of the phenyl group from the oxazole plane due to rotation around the C(6B)–C(5B) bonds [1.424(16) Å]. No intermolecular and intramolecular gold-gold interactions occur probably due to the steric demand by the methyl substituents.

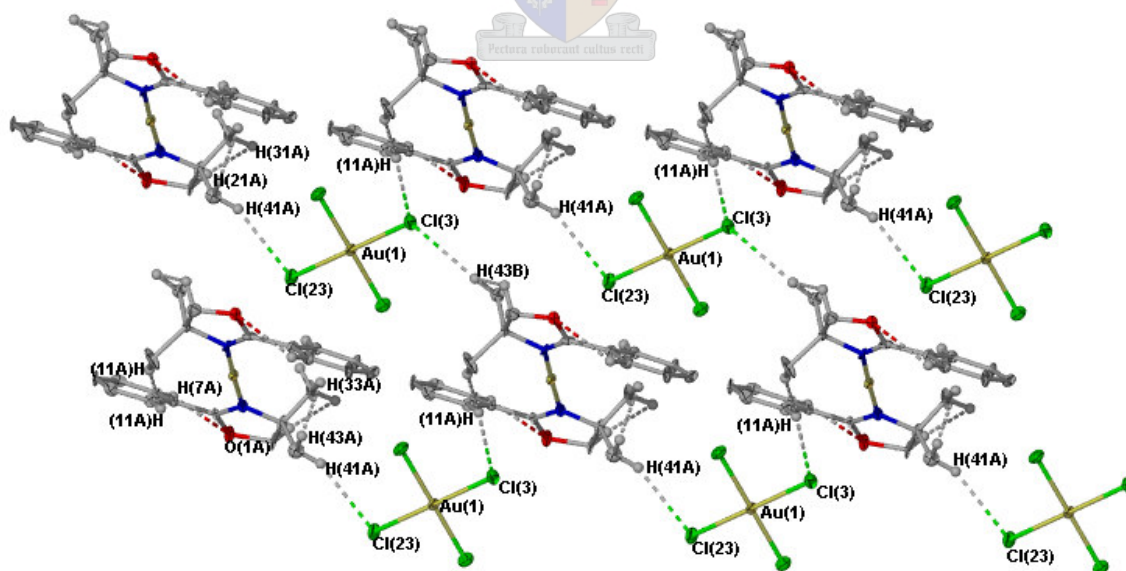


Figure 2.2 Diagram of **4b** showing intermolecular and intramolecular interactions.

²⁵ P. A. Bonnardel, R. V. Parish and R. G. Pritchard, *J. Chem. Soc., Dalton. Trans.*, 1996, 3185.

Molecules of the cationic complex are assembled in an alternating fashion connected by intermolecular and intramolecular hydrogen bond as shown in Figure 2.2. The only intramolecular interaction observed between H(7A)---O(1A) [2.517 Å] lies within the range of hydrogen bonding. The counter ions, AuCl₄⁻, act as bridging units between the cations: Cl(23)---H(41A) [2.908 Å], H(43B)---Cl(3) [2.863 Å] and Cl(3)---H(11A) [2.965 Å].

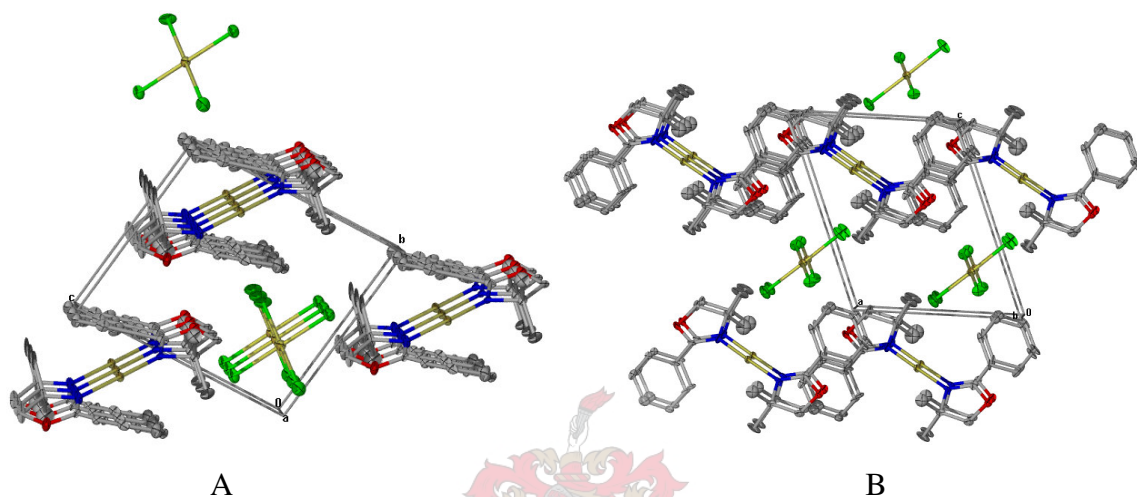


Figure 2.3 Packing diagram of the molecules of **4b** along the a-axis (A) and b-axis (B).

Molecular packing along the crystallographic a-axis (A) and b-axis (B) are shown in Figure 2.3. The cations as well as the AuCl₄⁻ counter ions are independently stacked on top of each other when viewed down the crystallographic a-axis. The packing along the crystallographic b-axis also shows that the cations are stacked on top of each other alternately, where cations in one layer are oriented in opposite direction to the cations in the next layer.

Table 2.21 Selected bond lengths (Å) and angles (°) for **4b**

Au(2)–N(1B)	2.009(9)	O(3B)–C(5B)	1.382(13)
Au(2)–N(1A)	2.010(9)	O(3B)–C(1B)	1.420(13)
Au(1)–Cl(3)	2.264(4)	C(6B)–C(5B)	1.424(16)
Au(1)–Cl(2)	2.264(4)	C(1A)–C(4A)	1.573(14)
Au(1)–Cl(23)	2.294(4)	N(1A)–C(5A)	1.267(14)
Au(1)–Cl(1)	2.297(4)	N(1A)–C(4A)	1.509(15)
O(1A)–C(5A)	1.301(12)	C(5A)–C(6A)	1.505(14)

(continued...)

O(1A)–C(1A)	1.490(12)	C(4B)–C(1B)	1.491(15)
C(5A)–C(6A)	1.505(14)		
N(1B)–Au(2)–N(1A)	179.4(5)	O(1A)–C(1A)–C(4A)	104.6(8)
Cl(3)–Au(1)–Cl(2)	90.47(16)	C(5A)–N(1A)–C(4A)	109.8(8)
Cl(3)–Au(1)–Cl(23)	178.5(3)	C(5A)–N(1A)–Au(2)	130.7(8)
Cl(2)–Au(1)–Cl(23)	89.48(16)	C(4A)–N(1A)–Au(2)	119.6(6)
Cl(3)–Au(1)–Cl(1)	89.79(16)	N(1A)–C(5A)–O(1A)	118.9(10)
Cl(2)–Au(1)–Cl(1)	179.6(2)	N(1A)–C(5A)–C(6A)	128.1(9)
Cl(23)–Au(1)–Cl(1)	90.26(15)	O(1A)–C(5A)–C(6A)	113.0(9)
C(5A)–O(1A)–C(1A)	106.5(8)	N(1B)–C(5B)–O(3B)	113.3(10)
C(5B)–O(3B)–C(1B)	107.7(8)	O(3B)–C(5B)–C(6B)	118.2(9)
C(7A)–C(6A)–C(1A)	122.8(10)	C(2A)–C(4A)–N(1A)	109.4(10)
C(11A)–C(6A)–C(5A)	119.5(9)	C(3A)–C(4A)–N(1A)	107.8(10)
C(7A)–C(6A)–C(5A)	117.7(9)	N(1A)–C(4A)–C(1A)	99.9(8)

2.3.2 The crystal and molecular structures of 4,4-dimethyl-2-phenyl-oxazoline tetrachloroaurate(III) salt, 4b'

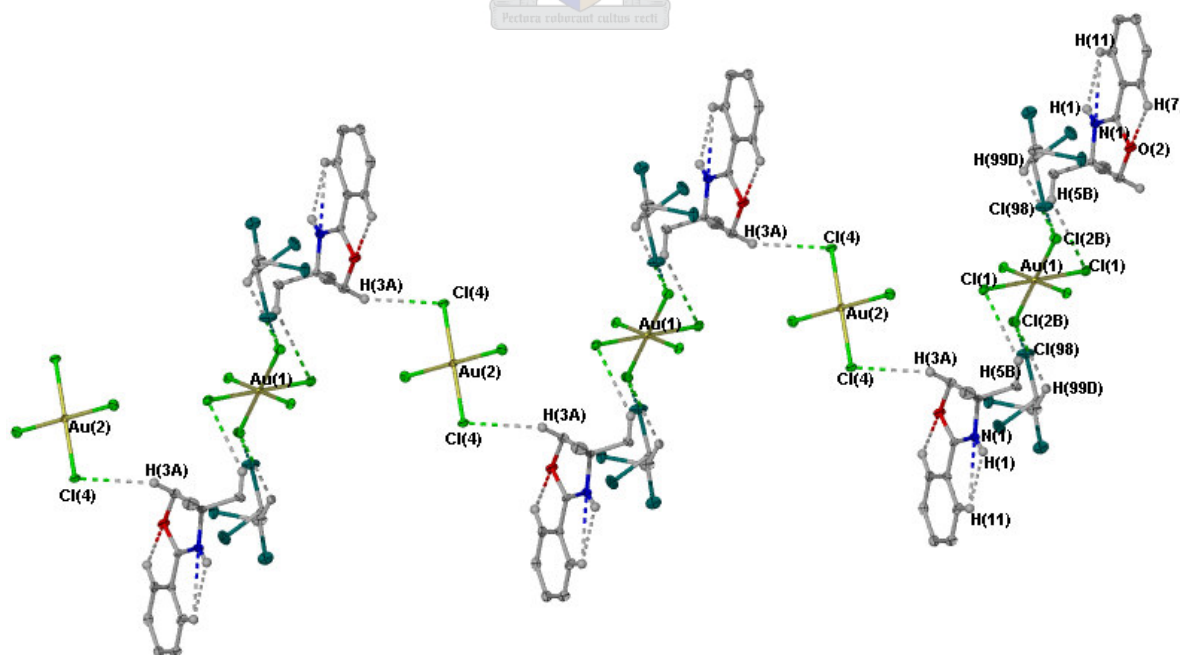


Figure 2.4 Molecular structure of 4,4-dimethyl-2-phenyl-oxazolinium tetrachloroaurate(III) salt, 4b'.

The compound crystallised from a dichloromethane solution layered with *n*-pentane in the triclinic space group $P\bar{1}$ as orange crystals in mixture with the cationic complex **4b**. Selected bond lengths and angles are listed in Table 2.22. The crystal and molecular structure of 4,4-dimethyl-2-phenyl-oxazolinium tetrachloroauric(III) salt is shown in Figure 2.4. The chlorine atoms of the solvent molecules are represented by a different colour (deep green) for distinction from the counter ions, AuCl_4^- . The imine-*N* of the oxazoline is protonated by the tetrachloroauric(III) acid, $\text{H}[\text{AuCl}_4]$. Two independent counter ions, AuCl_4^- , occur in the structure. The first, $\text{Au}(1)\text{Cl}_4^-$, is disordered. As for d^8 electronic configuration metals such as Pt(II) and Pd(II), the, AuCl_4^- ion has essentially square planar geometry. All the Au–Cl bond lengths shown in Table 2.22 are comparable to the Au–Cl bond lengths observed for the cationic and neutral gold(III) complexes reported in this Chapter.

The O(2)---H(10) separation [2.694 Å] shows the intermolecular interactions between two cations (Figure 2.4). Intramolecular interactions are also observed between the cations: H(7)---O(2) [2.478 Å] and N(1)---H(11) [2.680 Å]. The cations act as bridges between the AuCl_4^- counter ions. The H(5B)---Cl(1) and H(3A)---Cl(4) separations of 2.984 and 2.948 Å, respectively indicate the presence of weak intermolecular interactions between the atoms of the cations and the counter ions, AuCl_4^- .

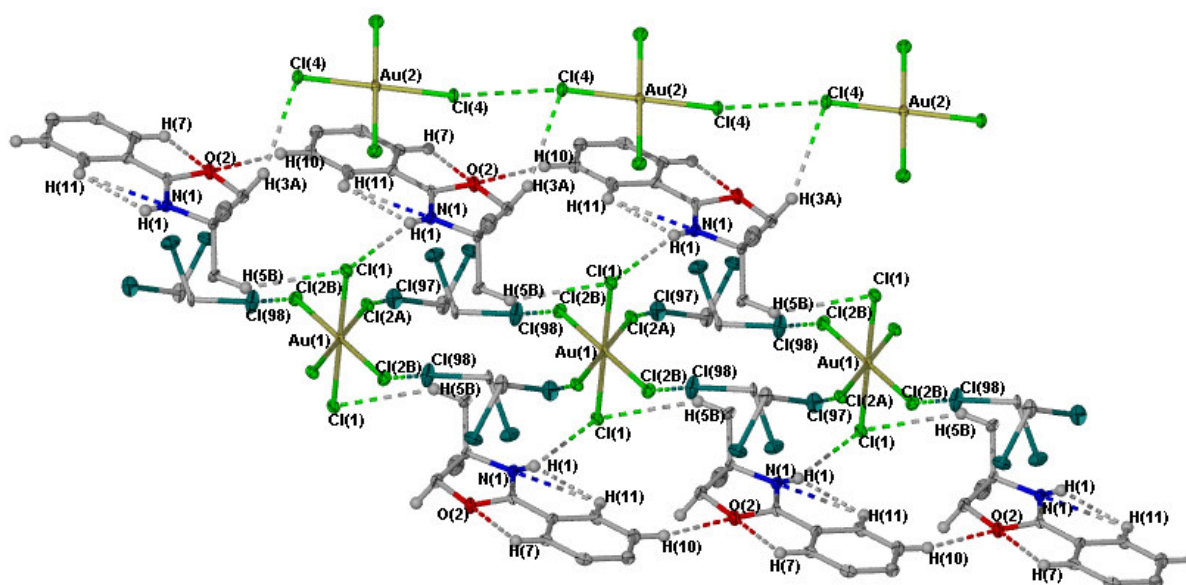


Figure 2.5 Molecular structure of 4,4-dimethyl-2-phenyl-oxazolinium tetrachloroauric(III) salt, **4b'**, showing the intermolecular and intramolecular interactions.

The molecular structure in Figure 2.5 shows that the cations and the counter ions are interlinked both by intermolecular and intramolecular interactions. The counter ions, $\text{Au}(1)\text{Cl}_4^-$ and $\text{Au}(2)\text{Cl}_4^-$, are separated by the cations. The $\text{N}(1)\text{---H}(1\text{N})$ bond length [0.734 Å] is slightly shorter than the bond length observed for **8a** (Figure 2.5). The $\text{Cl}(2\text{B})\text{---Cl}(98)$ and $\text{Cl}(2\text{A})\text{---Cl}(98)$ separations [1.542 and 3.453 Å], respectively depict that the solvent molecules act as bridging units to the counter ions, $\text{Au}(1)\text{Cl}_4^-$. The $\text{Cl}(4)\text{---Cl}(4)$ and $\text{H}(3\text{A})\text{---Cl}(4)$ distances [3.304 and 2.948 Å], respectively indicate the counter ions, $\text{Au}(2)\text{Cl}_4^-$, are interlinked hand-to-hand and at the same time they are connected with the cations.

Molecular packing of the unit cell along the crystallographic a-axis (A) and b-axis (B) is shown in Figure 2.6. When the unit cell is viewed down the crystallographic a-axis, a tunnel through the middle of the unit cell occupied by the solvent molecules is observed. The corners of the unit cell are occupied by the counter ions $\text{Au}(2)$ atoms. The cations and counter ions, $\text{Au}(2)\text{Cl}_4^-$, lie parallel to the crystallographic a-axis along two parallel sides of the unit cell, while the first counter ions, $\text{Au}(1)\text{Cl}_4^-$, are stacked on top of each other. The molecular packing along the crystallographic b-axis also shows the cations and the counter ions are stacked on top of each other.

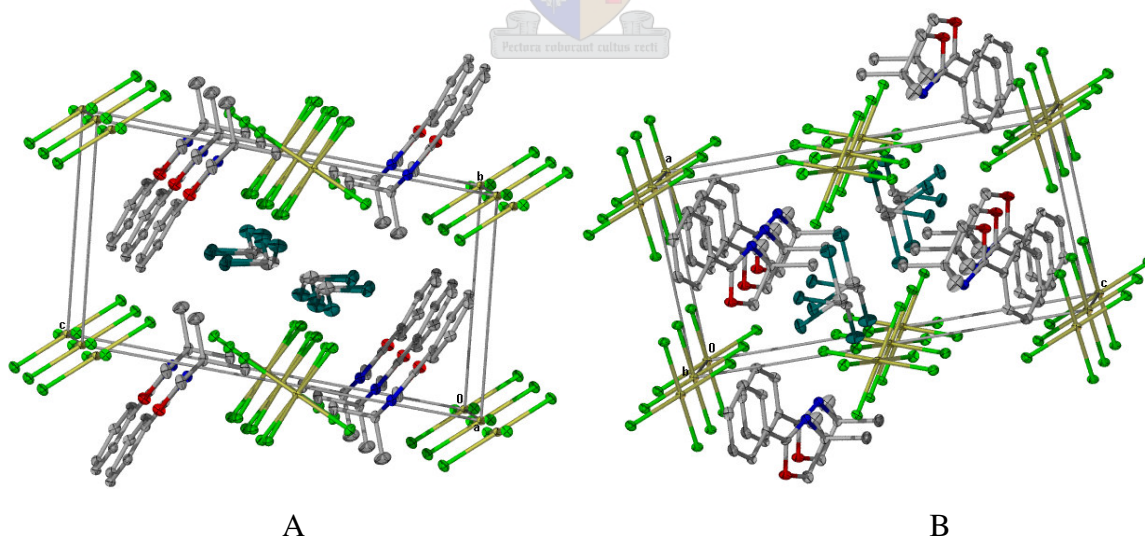


Figure 2.6 Packing diagram of 4,4-dimethyl-2-phenyl-oxazolinium tetrachloroauric(III) salt, $[\text{LH}][\text{AuCl}_4]$, along the a-axis (A) and b-axis (B).

Table 2.22 Selected bond lengths (Å) and angles (°) for 4,4-dimethyl-2-phenyl-oxazolinium tetrachloroauric(III) salt, **4b'**

Au(1)–Cl(2B)	2.278(2)	N(1)–C(2)	1.489(6)
Au(1)–Cl(1)	2.2800(11)	N(1)–H(1)	0.73(7)
Au(1)–Cl(2A)	2.281(2)	O(2)–C(1)	1.315(5)
Au(2)–Cl(4)	2.2833(11)	O(2)–C(3)	1.475(6)
Au(2)–Cl(3)	2.2866(11)	C(1)–C(6)	1.459(6)
N(1)–C(1)	1.291(6)		
<hr/>			
Cl(2B)–Au(1)–Cl(2B)	180.00(6)	C(1)–N(1)–H(1)	124(5)
Cl(2B)–Au(1)–Cl(1)	92.72(7)	C(2)–N(1)–H(1)	123(5)
Cl(2B)–Au(1)–Cl(2A)	55.17(8)	C(1)–O(2)–C(3)	108.4(4)
Cl(2B)–Au(1)–Cl(2A)	124.83(8)	N(1)–C(1)–O(2)	113.2(4)
Cl(2B)–Au(1)–Cl(2A)	124.83(8)	N(1)–C(1)–C(6)	127.3(4)
Cl(2B)–Au(1)–Cl(2A)	55.17(8)	O(2)–C(1)–C(6)	119.4(4)
Cl(4)–Au(2)–Cl(4)	180.00(6)	N(1)–C(2)–C(3)	98.8(4)
Cl(4)–Au(2)–Cl(3)	90.44(4)	O(2)–C(3)–C(2)	105.9(4)
C(1)–N(1)–C(2)	113.3(4)		

2.3.3 The crystal and molecular structure of **6a**

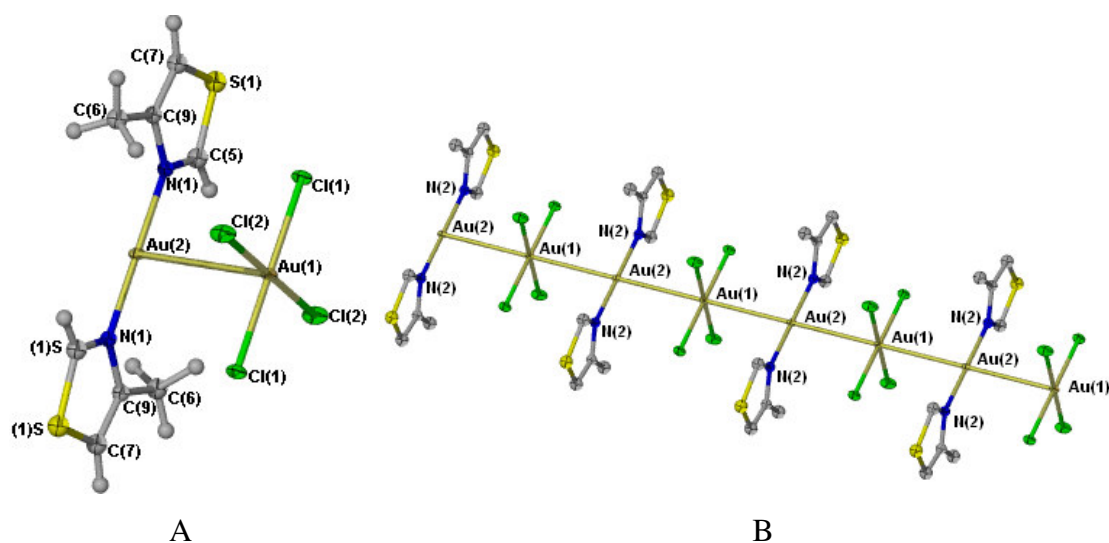


Figure 2.7 Molecular structure of **6a**.

Compound **6a** crystallised in the orthorhombic space group *Cmca* as orange crystals. Selected bond lengths and angles are listed in Table 2.23. The structure of **6a** is shown in Figure 2.7. Figure 2.7 (B) shows an unprecedented linear interaction between the Au(I) and Au(III) centre. The separation is measured as 3.3626(4) Å somewhat extended from the normal aurophilic interaction distance of *ca.* [3.1 Å].²⁶ Similar features to those in complex **4b** are present: similar Au–Cl distances as well as imine N–Au bond lengths of *ca.* [2.01 Å] are present in both compounds. In the present compound, however, the gold(I) ions are positioned perfectly perpendicular to the square planar geometry of the counter ion, AuCl₄[−], a situation absent in **4b**. The geometry about the coordination centre, Au(I), is perfectly linear with bond angle a N(1)–Au(2)–N(1) of 180.0(3)° which is comparable to the cationic complex **4b**. The Cl(1)–Au(1)–Cl(2) angle [89.67(6)°] lies within the range of the right-angle [90°]. Presently it is not possible to say whether the interaction between the two gold centres is purely electrostatic or also due to aurophilicity. The bond lengths Au(1)–Cl(2) [2.2886(17) Å] and Au(1)–Cl(1) [2.2893(16) Å] of the counter ion, AuCl₄[−], are comparable to **1** and **4b**. However, slight deviations have been observed from the Au–Cl bond lengths [2.260 - 2.283 Å] reported for bis(3-phenyl-5-diethylamino-1,2,4-thiadiazolium)chloride tetrachlorogold(III) and 9-ethylguaninium tetrachlorogold(III) monohydrate.¹⁴ The molecular structure shows a normal Au(2)–N(1) bond length [2.005(5) Å], comparable to imine-gold complexes such as **4b**, tris(*μ*-chloro-3,5-dimethylpyrozolate)hexachloro-tri-gold(III) and (4-methylthiazole)pentafluorophenyl gold(I)²¹ with an Au–N bond length of [2.008 Å]. The bond lengths N(1)–C(5) [1.292(9) Å] and N(1)–C(9) [1.403(9) Å] are characteristic of N–C double and single bonds, respectively and are comparable to the bond lengths reported for **4b**.

Figure 2.8 shows intermolecular interactions between two linear chains of **6a**. The H(7)---Cl(1) separation [2.687 Å], indicating that the molecules are connected to each other via hydrogen bonding.

²⁶ (a) M. Desmet, H. G. Raubenheimer and G. J. Kruger, *Organometallics*, 1997, **16**, 3324. (b) P. G. Jones, G. M. Sheldrick, E. Hädicke, *Acta. Crystallogr. Sect. B*, 1986, **36**, 2777.

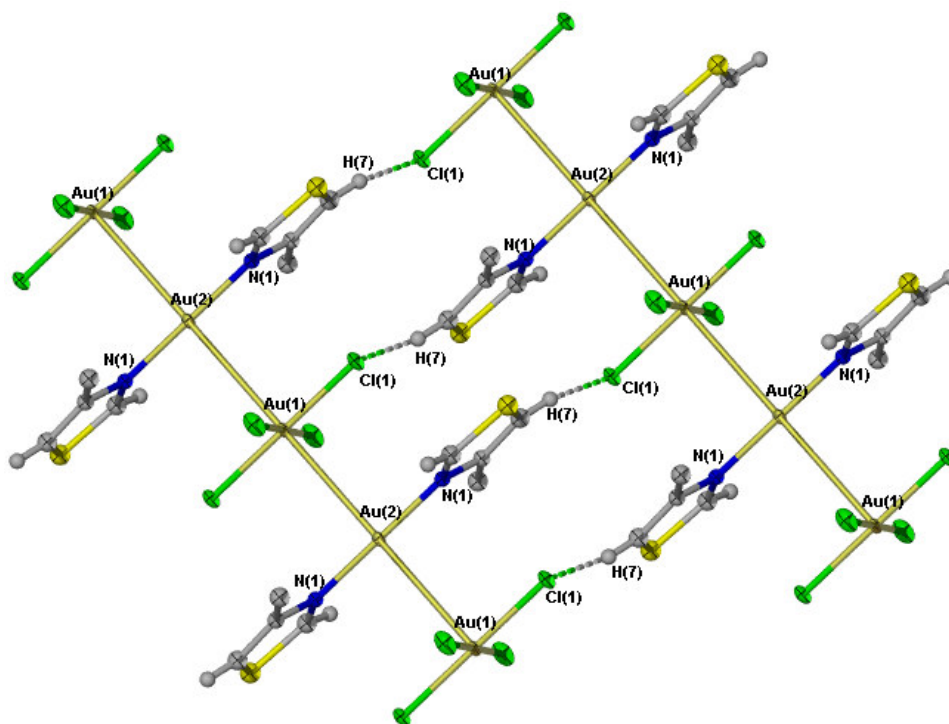


Figure 2.8 Diagram of **6a** showing intermolecular interactions *via* hydrogen bonding.

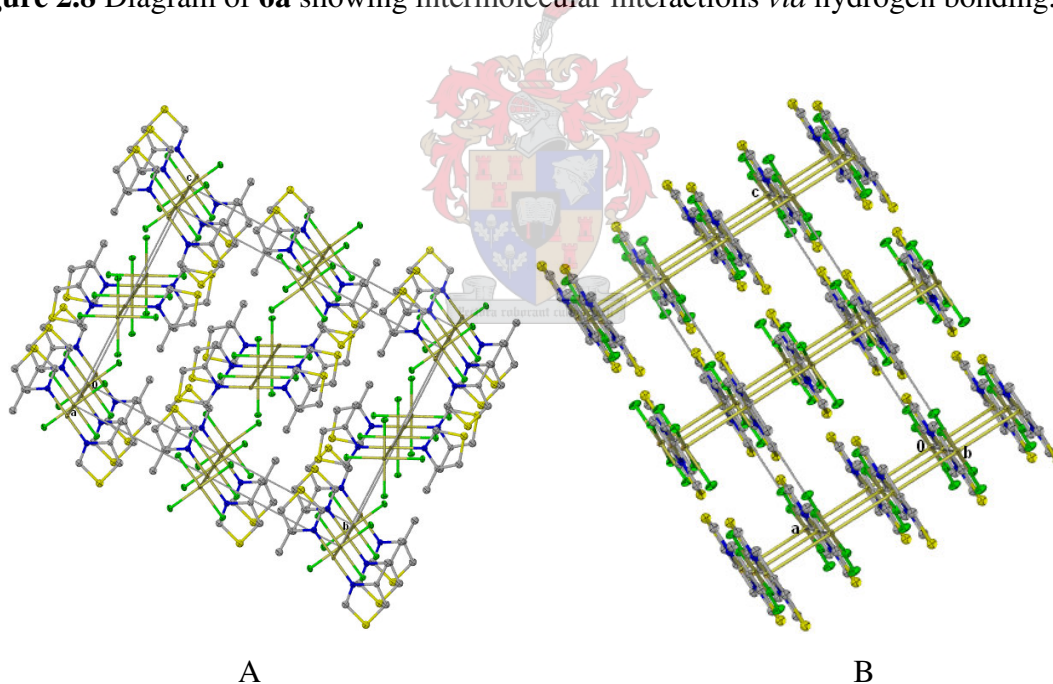


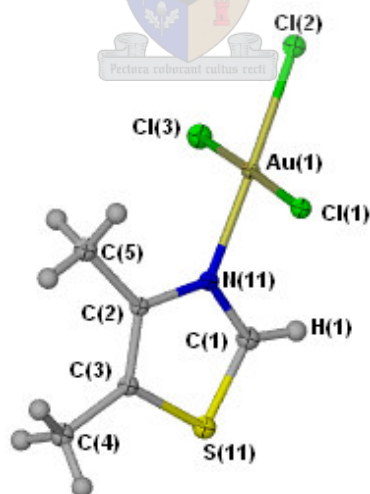
Figure 2.9 Packing diagram of the molecules of **6a** along the a-axis (A) and b-axis (B).

Molecular packing along the crystallographic a-axis (A) and b-axis (B) are shown in Figure 2.9. The cations and the AuCl_4^- counter ions are stacked alternately in asymmetric fashion on top of each other along the crystallographic a-axis. Similarly, the cations and the AuCl_4^- counter ions along the crystallographic b-axis and c-axis form a layer parallel to the axes.

Table 2.23 Selected bond lengths (Å) and angles (°) for **6a**

Au(1)–Cl(2)	2.2886(17)	Au(2)–N(1)	2.005(5)
Au(1)–Cl(2)	2.2886(17)	Au(2)–Au(1)	3.3626(4)
Au(1)–Cl(1)	2.2893(16)	N(1)–C(5)	1.292(9)
Au(1)–Cl(1)	2.2893(16)	N(1)–C(9)	1.403(9)
Au(1)–Au(2)	3.3626(4)	S(1)–C(5)	1.699(8)
Au(1)–Au(2)	3.3626(4)	S(1)–C(7)	1.721(8)
Au(2)–N(1)	2.005(5)	C(7)–C(9)	1.348(10)
Cl(2)–Au(1)–Cl(2)	180.00(8)	Au(2)–Au(1)–Au(2)	180.0
Cl(2)–Au(1)–Cl(1)	89.67(6)	N(1)–Au(2)–N(1)	180.0(3)
Cl(2)–Au(1)–Cl(1)	90.33(6)	N(1)–Au(2)–Au(1)	90.0
Cl(1)–Au(1)–Cl(1)	180.00(4)	Au(1)–Au(2)–Au(1)	180.0
Cl(2)–Au(1)–Au(2)	90.0	C(5)–N(1)–Au(2)	123.5(5)
Cl(1)–Au(1)–Au(2)	90.0	C(9)–N(1)–Au(2)	123.5(4)

2.3.4 The crystal and molecular structure of **7**

**Figure 2.10** Molecular structure of **7**.

The compound crystallised in the monoclinic space group $P2_1/c$ as orange crystals. Selected bond lengths and angles are shown in Table 2.24. The crystal and molecular structure of adduct **7a** is shown in Figure 2.10. The structure shows the 4,5-dimethylthiazole ligand coordinated to the gold(III) trichloride *via* the imine-*N* atom regardless of the HSAB

principle, where sulfur is more suitable donor for Au due to its soft character. The bond length Au(1)–Cl(1) [2.287(2) Å] is slightly longer than Au(1)–Cl(2) [2.270(2) Å] indicating that a higher *trans*-influence is being exerted by Cl(3) when compared with the N(11). The Au(1)–N(11) bond length [2.037(9) Å] is comparable with the cationic complexes **4b**, **6a** and trichloro-(7-chloro-1-chlorophenylmethyl)-1,3-dihydro-5-phenyl-2*H*-1,4-benzodiazepin-2-one gold(III) [2.030(15) Å].²⁷ The deviation from the least square plane defined by Au(1) Cl(1) Cl(2) Cl(3) N(11) is 0.0240 Å.

The geometry of the complex at the coordination centre is essentially square planar. The bond angles N(11)–Au(1)–Cl(2) and Cl(3)–Au(1)–Cl(1) [176.8(2)° and 178.46(9)°], respectively deviate slightly from linearity indicating that the geometry of the coordination centre is distorted. Nevertheless, the bond angles N(11)–Au(1)–Cl(3) [90.0(2)°], Cl(2)–Au(1)–Cl(3) [91.78(10)°], N(11)–Au(1)–Cl(1) [88.4(2)°] and Cl(2)–Au(1)–Cl(1) [89.76(9)°] illustrate the square planarity of the geometry as typical for the d⁸ electronic configuration metals such as Pt(II) and Pd(II). The torsion angles Cl(3)–Au(1)–N(11)–(C1) [89.9(9)°], Cl(2)–Au(1)–N(11)–C(1) [-146(4)°], Cl(1)–Au(1)–N(11)–C(1), [-90.1(9)°] and Cl(2)–Au(1)–N(11)–C(2) [100.3(10)°] show deviation of the coordination plane from the plane of the thiazole group. The dihedral angle [83.76°] indicates the deviation angle between planes defined by the thiazole ring N(11), C(1), C(2), C(3) and S(11) and the plane containing the coordination centre, N(11), Au(1), Cl(1), Cl(2) and Cl(3).

The intermolecular and intramolecular interactions between molecules of **7** are shown in Figure 2.11: H(1)---Cl(1) [2.644 Å] and Cl(3)---H(4B) [2.866 Å]. The separations observed between two adjacent Cl atoms Cl(1)---Cl(3) [3.270 Å] are within the range of van der Waals interaction.

²⁷ G. Minghetti, M. Ganadu, C. Foddai, M. A. Cinellu, F. Cariati, F. Demartin and M. Manassero, *Inorg. Chim. Acta*, 1984, **86**, 101.

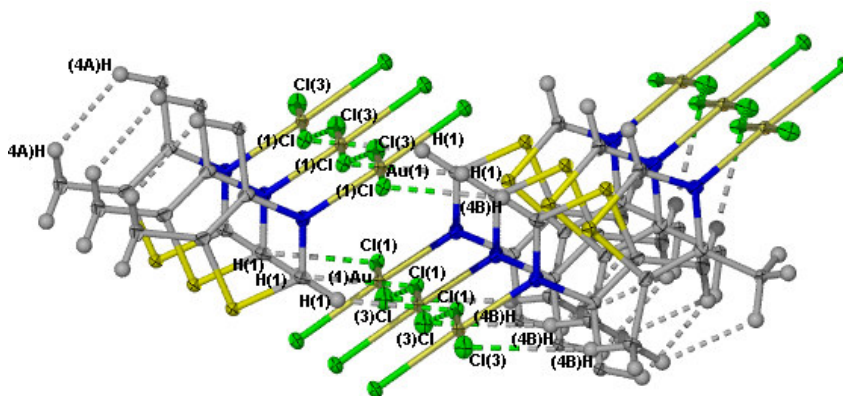


Figure 2.11 Diagram of **7** showing intermolecular and intramolecular interactions.

The molecular packing of molecules of **7** along the crystallographic a-axis (A) and b-axis (B) is shown in Figure 2.12. When the molecules in the unit cell are viewed down the crystallographic a-axis the AuCl₃ groups are stacked on top of each other, while the 4,5-dimethylthiazoles are oriented parallel to a-b-plane in such a way that the ligand entities in one layer are pointing to the same direction, whereas, molecules in the next layer point in the opposite direction. Packing of the molecules along the crystallographic b-axis also shows similar features.

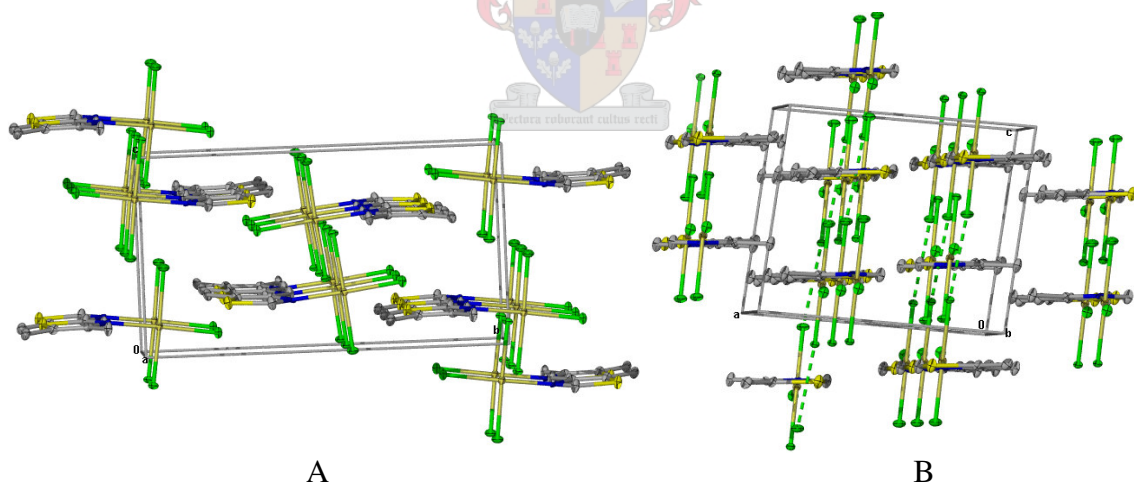
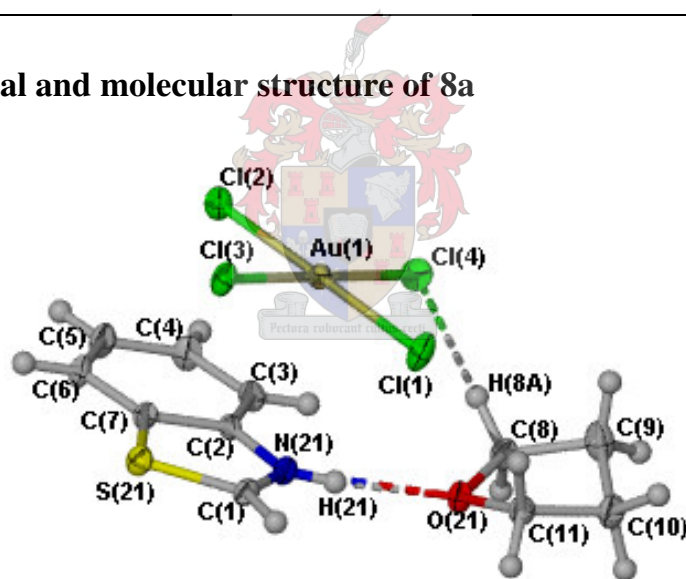


Figure 2.12 Packing diagram of the molecules of **7** along the a-axis (A) and b-axis (B).

Table 2.24 Selected bond lengths (Å) and angles (°) for **7**

Au(1)–N(11)	2.037(9)	N(11)–C(2)	1.398(12)
Au(1)–Cl(2)	2.270(2)	C(2)–C(3)	1.355(14)
Au(1)–Cl(3)	2.274(3)	C(1)–S(11)	1.686(11)
Au(1)–Cl(1)	2.287(2)	S(11)–C(3)	1.734(10)
N(11)–C(1)	1.306(13)		
<hr/>			
N(11)–Au(1)–Cl(2)	176.8(2)	C(1)–N(11)–Au(1)	123.8(7)
N(11)–Au(1)–Cl(3)	90.0(2)	C(2)–N(11)–Au(1)	121.6(6)
Cl(2)–Au(1)–Cl(3)	91.78(10)	N(11)–C(2)–C(5)	120.6(8)
N(11)–Au(1)–Cl(1)	88.4(2)	N(11)–C(1)–S(11)	113.1(8)
Cl(2)–Au(1)–Cl(1)	89.76(9)	C(1)–S(11)–C(3)	90.8(5)
Cl(3)–Au(1)–Cl(1)	178.46(9)	C(2)–C(3)–S(11)	110.3(8)
C(1)–N(11)–C(2)	113.8(9)		

2.3.5 The crystal and molecular structure of **8a**

**Figure 2.13** Molecular structure of **8a**.

The compound crystallised in the triclinic space group $P\bar{1}$ as orange crystals. Selected bond lengths and angles are listed in Table 2.25. The crystal and molecular structure of **8a** is shown in Figure 2.13. The structure shows that the immonium tetrachloroaurate(III) salt of the benzothiazolyl ligand is connected to a solvent molecule, THF, *via* hydrogen bonding N–H...O [1.91 Å]. The ligand is protonated at the N(21) position. The N(21)–H(21) bond length [1.0160 Å] is slightly longer than that in **4b'** [0.73(7) Å]. The N(21)–C(1) bond length [1.310(7) Å] is characteristic of an N–C double bond [1.340 Å] in

comparison to bis(2-aminobenzothiazolinium) tetrachlorocopper(II).²⁸ The geometry about the anion, AuCl_4^- , is as expected square planar and all the bond lengths and angles are normal and comparable to those in **4b** and **6a**.

Figure 2.14 shows several intermolecular interactions of **8a** at a distance less than [3.000 Å]: H(2)---Cl(3) [2.669 Å], Cl(2)---H(6) [2.782 Å], Cl(3)---H(6) [2.906 Å], Cl(3)---H(5) [2.964 Å] and Cl(4)---H(8A) [2.921 Å]. The Cl(4)---H(8A) separation [2.921 Å] indicates a THF-counter ion interaction. Each counter ion is also connected to the cations: H(6)---Cl(2) [2.782 Å], H(6)---Cl(3) [2.906 Å], H(5)---Cl(3) [1.964 Å] and Cl(3)---H(2) [2.669 Å].

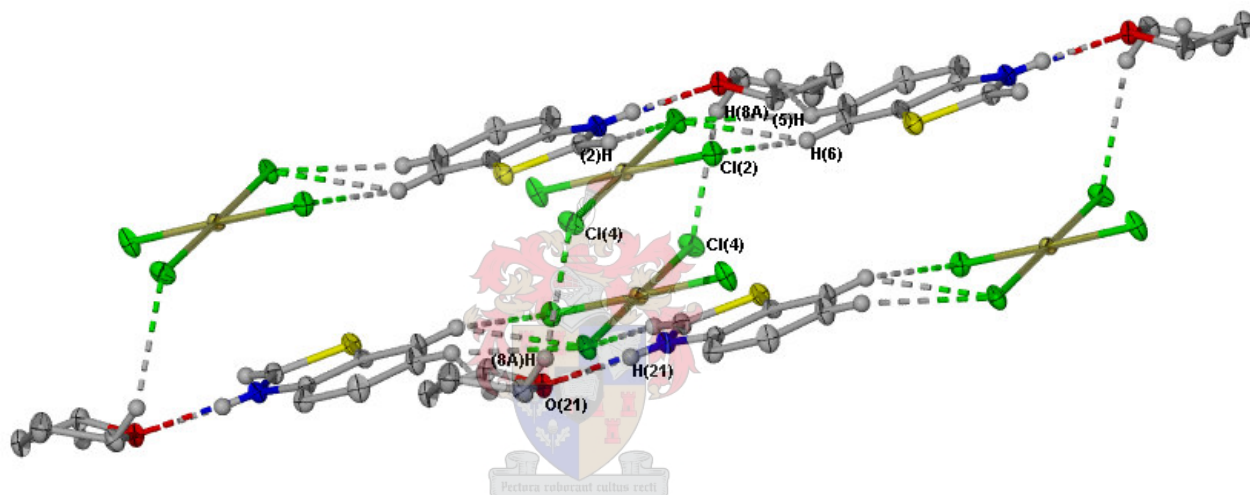


Figure 2.14 Diagram of **8a** showing intermolecular and intramolecular interactions

The molecular packing of **8a** when viewed down the crystallographic a-axis (A) and c-axis (B) is shown in Figure 2.15. The packing along the crystallographic a-axis shows that the counter ions, AuCl_4^- , are stacked on top of each other. Similarly, when the packing of the unit cell is viewed down the crystallographic c-axis the cations are stacked on top of each other in an alternating fashion.

²⁸ L. Antolini, A. Benedetti, A. C. Farbetti and A. Giusti, *Inorg. Chem.*, 1988, **27**, 2192.

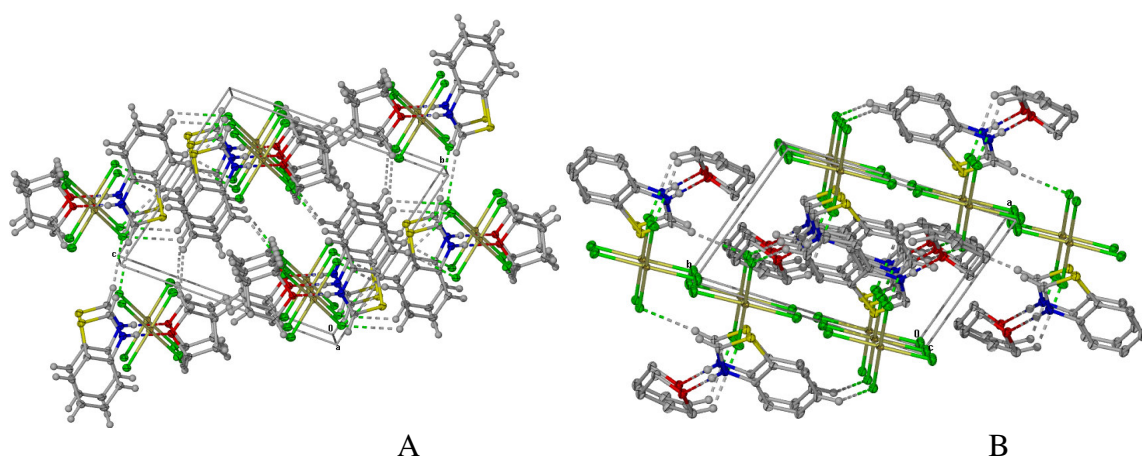


Figure 2.15 Packing diagram of the molecules of **8a** along the a-axis (A) and c-axis (B).

Table 2.25 Selected bond lengths (Å) and angles (°) for **8a**

Au(1)–Cl(4)	2.2738(13)	O(21)–C(11)	1.442(6)
Au(1)–Cl(1)	2.2834(13)	O(21)–C(8)	1.450(6)
Au(1)–Cl(3)	2.2847(12)	N(21)–C(1)	1.310(7)
Au(1)–Cl(2)	2.2866(13)	N(21)–C(2)	1.393(6)
S(21)–C(1)	1.689(5)	N(21)–H(21)	1.0160
S(21)–C(7)	1.744(5)		
Cl(4)–Au(1)–Cl(1)	90.13(5)	C(2)–N(21)–H(21)	122.9
Cl(4)–Au(1)–Cl(3)	179.28(5)	N(21)–C(1)–S(21)	114.3(4)
Cl(1)–Au(1)–Cl(3)	89.19(5)	N(21)–C(1)–H(2)	122.8
Cl(4)–Au(1)–Cl(2)	89.41(5)	S(21)–C(1)–H(2)	122.8
Cl(1)–Au(1)–Cl(2)	179.07(5)	C(3)–C(2)–N(21)	127.5(5)
Cl(3)–Au(1)–Cl(2)	91.27(4)	N(21)–C(2)–C(7)	110.9(4)
C(1)–S(21)–C(7)	90.1(2)	C(6)–C(7)–S(21)	128.6(4)
C(11)–O(21)–C(8)	109.0(4)	C(2)–C(7)–S(21)	110.5(4)
C(1)–N(21)–C(2)	114.1(4)	O(21)–C(8)–C(9)	106.4(4)
C(1)–N(21)–H(21)	122.9		

2.3.6 The crystal and molecular structure of **12**

The compound crystallised in the monoclinic space group $P2_1/c$ as orange crystals. Selected bond lengths and angles are listed in Table 2.26. The crystal and molecular structure of **12** is shown in Figure 2.16. The molecular structure shows the compound

isolated is 1,3-bis(2,4,6-trimethylphenyl)imidazolium tetrachloroaurate(III) salt, **12**. The solvent molecule and the hydrogen atoms in the crystal structure are omitted for clarity except H(1) (to illustrate that the intended Au(III) carbene complex was not formed).

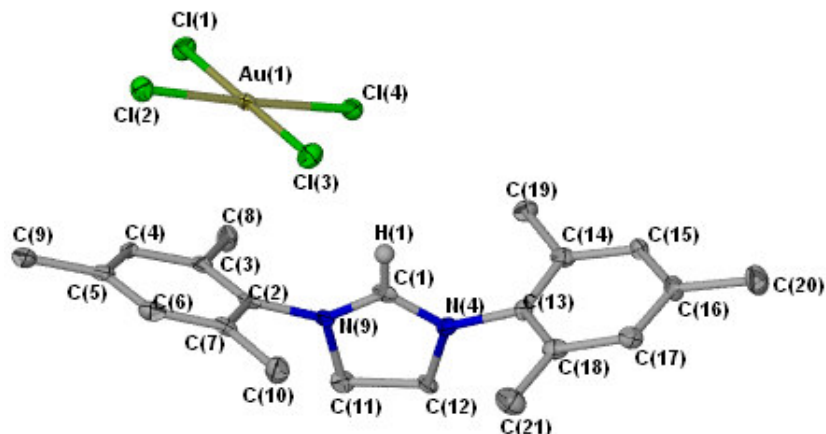


Figure 2.16 Molecular structure of **12**.

The bond lengths for N(9)–C(1) and N(4)–C(1) are 1.294(8) and 1.315(8) Å, respectively. The corresponding N(4)–C(13) and C(2)–N(9) bond lengths [1.446(8) and 1.446(8) Å] are typical for single bonds. The geometry of the AuCl₄⁻ counter ion is square planar as expected for metal ions d⁸ electronic configurations.

The N(9)–C(1)–N(4) angle [114.2(6)°] is comparable to the free ligand. The bond angles C(1)–N(4)–C(13) and C(1)–N(9)–C(2) [128.7(5) and 124.8(5)°] are as expected with respect to the free ligand. The torsion angles for C(1)–N(9)–C(2)–C(3) [118.8(7)°] and C(1)–N(9)–C(2)–C(7) [-65.4(8)°] show that the plane of the trimethylphenyl group is twisted with respect to the central imidazole ring. Analogous torsion angles for C(1)–N(4)–C(13)–C(18) [94.0(8)°] and C(1)–N(4)–C(13)–C(14) [-88.8(8)°] also show that the two planes are perpendicular with respect to the imidazole ligand.

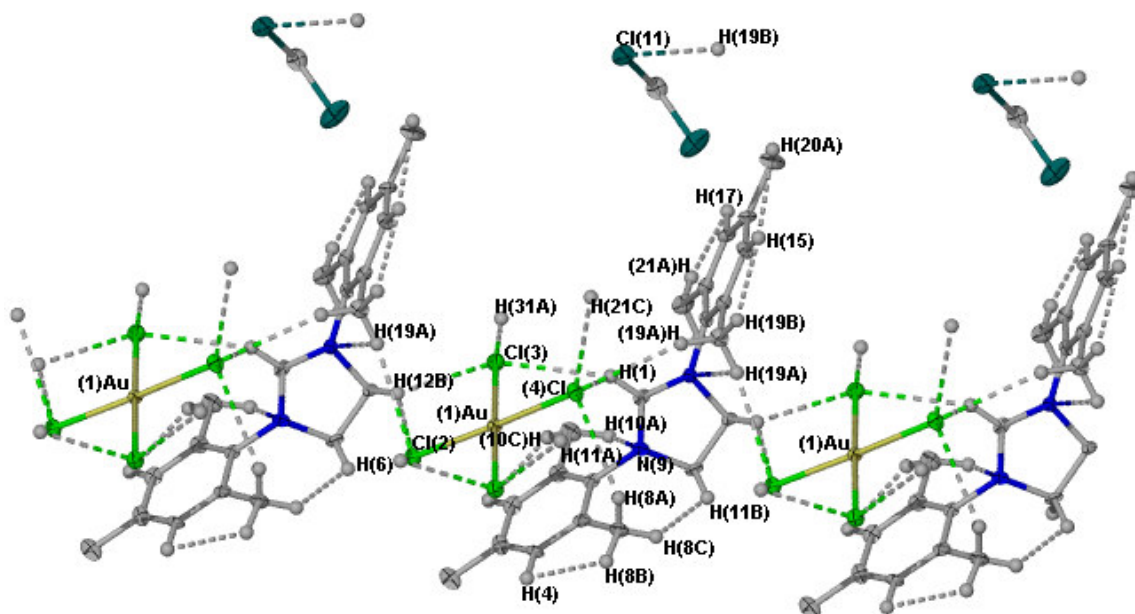


Figure 2.17 Diagram of **12** showing intermolecular and intramolecular interactions.

The molecular packing for **12** along the crystallographic a-axis (A) and b-axis (B) is shown in Figure 2.18. Solvent molecules are omitted from diagram 2.18 (B). The cations when viewed down the crystallographic a-axis are stacked on top of each other in an alternating fashion. Similarly, the molecules when viewed down the crystallographic b-axis are stacked on top of each other.

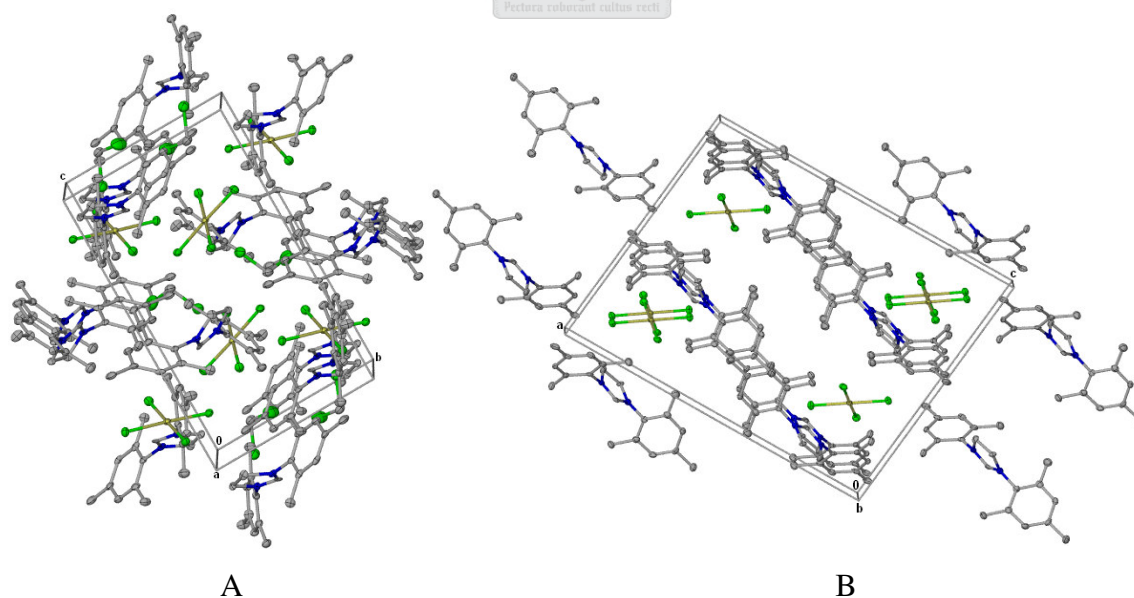


Figure 2.18 Packing diagram of the molecules of **12** along the a-axis (A) and b-axis (B).

Table 2.26 Selected bond lengths (Å) and angles (°) for **12**

Au(1)–Cl(1)	2.2734(17)	N(4)–C(12)	1.486(7)
Au(1)–Cl(2)	2.2756(16)	C(2)–N(9)	1.446(8)
Au(1)–Cl(3)	2.2871(17)	N(9)–C(1)	1.294(8)
Au(1)–Cl(4)	2.2879(16)	N(9)–C(11)	1.475(8)
N(4)–C(1)	1.315(8)	C(11)–C(12)	1.522(8)
N(4)–C(13)	1.446(8)		
Cl(1)–Au(1)–Cl(2)	89.84(6)	C(13)–N(4)–C(12)	122.1(5)
Cl(1)–Au(1)–Cl(3)	179.12(6)	C(7)–C(2)–N(9)	118.7(6)
Cl(2)–Au(1)–Cl(3)	90.99(6)	C(1)–N(9)–C(2)	124.8(5)
Cl(1)–Au(1)–Cl(4)	89.75(6)	C(1)–N(9)–C(11)	110.6(5)
Cl(2)–Au(1)–Cl(4)	177.56(6)	C(2)–N(9)–C(11)	122.8(5)
Cl(3)–Au(1)–Cl(4)	89.43(6)	N(9)–C(1)–N(4)	114.2(6)
C(1)–N(4)–C(13)	128.7(5)	N(9)–C(11)–C(12)	102.6(5)
C(1)–N(4)–C(12)	109.0(5)	N(4)–C(12)–C(11)	103.3(5)
C(3)–C(2)–N(9)	118.6(6)		

2.4 Conclusions and future work

The reactions of most of the heterocyclic imine ligands that were studied appear to be more complex than originally expected due to the formation of products which could not be separated. Aqueous solutions of HAuCl_4 treated with heterocyclic ligands yielded different types of products including cationic complexes, $[\text{AuL}_2][\text{AuCl}_4]$, immonium tetrachloroaurate(III) salts, $[(\text{HL})][\text{AuCl}_4]$ and adducts, $[\text{AuCl}_3(\text{L})]$. The molecular structures of immonium tetrachloroaurate(III) salts $[\text{HN}=\text{C}(\text{Ph})\text{OCH}_2\text{C}(\text{CH}_3)_2][\text{AuCl}_4]$, **4b'**, and $[\text{HN}=\text{CHSC}=\text{CHCH}=\text{CHCH}=\text{C}][\text{AuCl}_4]$, **8a** were determined by X-ray analysis. The reaction of HAuCl_4 with 4,4-dimethyl-2-(phenyl)oxazole and 4-methylthiazole generated cationic gold(I) complexes of $[\text{Au}\{\text{N}=\text{C}(\text{Ph})\text{OCH}_2\text{C}(\text{CH}_3)_2\}_2][\text{AuCl}_4]$, **4b**, and $[\text{Au}\{\text{N}=\text{CHSCH}=\text{C}(\text{CH}_3)_2\}_2][\text{AuCl}_4]$, **6a**, respectively. The molecular structure of **6a**, a unique example of a compound with Au(I)-Au(III) interactions, revealed weak intermolecular and intramolecular aurophilic interactions in an alternating fashion Au(I)---Au(III), [3.34 Å]. No aurophilic interaction occurs in the cationic complex **4b** due to the

steric bulkiness of the methyl substituents. The low concentration product present in the reaction mixture with **4b** was isolated and its molecular structure indicated it to be $[\overline{\text{HN}=\text{C}(\text{Ph})\text{OCH}_2\text{C}(\text{CH}_3)_2}][\text{AuCl}_4]$, **4b'**.

Reactions with an aqueous solution of AuCl_3 and selected ligands such as 1-methyl-2-phenyl-imidazole, 4,4-methyl-2-phenyl oxazole, thiazole and their benzo- and methyl-substituted also afforded neutral complexes of the type $[\text{AuCl}_3(\text{L})]$. The crystal and molecular structures of **5b** and **7b** revealed square planar geometry where the heterocyclic imine-*N* donors coordinate with the gold. The molecular structure of **5b** is not reported due to the poor crystal data.

An attempt to obtain the cationic complex $[\text{Cl}_2\text{Au}\{\overline{\text{N}=\text{C}(\text{Ph})\text{OCH}_2\text{C}(\text{CH}_3)_2}\}_2][\text{AuCl}_4]$, **4c** by a metal exchange reaction between $[\text{Ag}\{\overline{\text{N}=\text{C}(\text{Ph})\text{OCH}_2\text{C}(\text{CH}_3)_2}\}_2]\text{BF}_4$ and NaAuCl_4 led to the formation of a mixed metal complex, $[\text{Ag}\{\overline{\text{N}=\text{C}(\text{Ph})\text{OCH}_2\text{C}(\text{CH}_3)_2}\}_2][\text{AuCl}_4]$, **4d**. The ^1H and ^{13}C NMR data are similar to that of $[\text{Au}\{\overline{\text{N}=\text{C}(\text{Ph})\text{OCH}_2\text{C}(\text{CH}_3)_2}\}_2][\text{AuCl}_4]$, **4b**. Hence, further clarification of the structure is required.

The ^1H and ^{13}C NMR spectra of **2a**, **2b**, **8a** and **8b** in DMSO-d_6 exhibited similar chemical shifts as the respective free ligands indicating that the coordinated ligands dissociate in this donor-solvent. In reactions between HAuCl_4 and AuCl_3 with HBBTM, **11**, led to the reduction of gold(III) to gold(0) and an oxidative dimerisation reaction of the ligand to 2-(1,2,2-tri(benzo[*d*]thiazol-2-yl)vinyl)benzo[*d*]thiazole. Hence, further investigation will be required to understand the mechanism by which the reduction of Au(III) to Au(0) and the oxidative dimerisation of the ligand takes place.

An effort to prepare a 1,3-bis-(2,4,6-trimethylphenyl)imidazolidine gold(III) complex from 1,3-bis(2,4,6-trimethylphenyl)imidazolium chloride, *t*-BOK and AuCl_3 , led to the formation of 1,3-bis(2,4,6-trimethylphenyl)imidazolium tetrachloroaurate(III).

New compounds should in the future be tested for biological activity. It is, unfortunately, still not clear how compounds **I** and **II** (characterised by structure determination) (Scheme 2.1) were obtained.

2.5 Experimental

2.5.1 Materials and methods

All reactions were performed in a dry, deoxygenated nitrogen or argon atmosphere, using standard vacuum-line and Schlenk techniques. All glassware was dried at $>100\text{ }^{\circ}\text{C}$ prior to use.

All solvents were dried by conventional methods and freshly distilled from sodium wire, except dichloromethane and acetonitrile, which were distilled from CaH_2 , under nitrogen, shortly before use. All solvents were pre-dried on either 4 \AA molecular sieves (acetonitrile, dichloromethane, *n*-pentane and *n*-hexane) or KOH (THF and diethyl ether) before distillation.

NMR spectra were recorded on a Varian VXR 300 (300 MHz for ^1H and 75 MHz for ^{13}C), a VARIAN UNITY INOVA (400 MHz for ^1H and 101 MHz for ^{13}C) or on a INOVA (600 MHz for ^1H and 151 MHz for ^{13}C) NMR spectrometer. ^1H and ^{13}C NMR chemical shifts are reported in ppm. The ^1H and ^{13}C NMR spectra were referenced to the deuterated solvents. Mass spectra were recorded on a VG Quattron (ESI, 70 eV), AMD 604 (EI, 70eV) or VG 70 SEQ (FAB, 70 eV, 3-nitrobenzylalcohol) instrument.

The following compounds: oxazole, benzoxazole, thiazole, 4-methylthiazole, 4,5-dimethylthiazole, benzothiazole, $\text{NaAuCl}_4 \cdot 2\text{H}_2\text{O}$ and AgBF_4 were commercially obtained from Aldrich and used without further purification. Ligands such as HBBTM,²⁹ 1,3-bis(2,4,6-trimethylphenyl)imidazolium chloride,²⁴ 1-methyl-2-(phenyl)imidazole,³⁰ 1-methyl-2-(2-pyridinyl)imidazole,³⁰ 4,4-dimethyl-2-(2-thienyl)oxazole,³¹ 4,4-dimethyl-2-(phenyl)oxazole,³⁰ AuCl_3 ²³ and $\text{HAuCl}_4 \cdot 4\text{H}_2\text{O}$ ³² were prepared according to methods described in the literature. The drying agent anhydrous magnesium sulphate was obtained from Aldrich.

²⁹ C. Rai and J. B. Braunwarth, *J. Org. Chem.*, 1961, **25**, 3434.

³⁰ A. S. Bell, D. A. Roberts and K. S. Ruddock, *Tetrahedron Lett.*, 1988, **29**, 5013.

³¹ A. I. Meyer, D. L. Temple, R. L. Nolen and E. D. Mihelich, *J. Org. Chem.*, 1974, **39**, 2778.

³² G. Brauer, *Handbuch der Präparativen Anorganischen Chemie.*, 3rd ed., Verlag, Stuttgart, 1978, p. 1014.

Note: Due to impurities present in the final product mixtures, melting points and yields are not reported.

2.5.2 Preparations

2.5.2.1 Preparation of tetrachloroaurate(III) imine salts [LH][AuCl₄], **1**, **2a** and **3** and cationic complex [AuL₂][AuCl₄], **4b**



An acetonitrile solution (5.0 cm³) of 1-methyl-2-(phenyl)imidazole (0.11 g, 0.68 mmol) was added to a similar mole quantity of HAuCl₄.4H₂O (0.28 g, 0.68 mmol) in an aqueous solution (5.0 cm³). The solution was stirred for 2.5 h at room temperature. The mixture was then extracted with THF (5 x 5.0 cm³). The combined organic layers were filtered, dried over anhydrous magnesium sulphate followed by solvent removal under high vacuum. The orange residue was washed with *n*-pentane.



Tetrachloroaurate(III) imine salt **2a** was prepared in a similar way as described for **1** by reacting 1-methyl-2-(2-pyridinyl)imidazole (0.20 g, 1.2 mmol) in acetonitrile (5.0 cm³) with a similar mole quantity of HAuCl₄.4H₂O (0.49 g, 1.2 mmol) in aqueous solution. An orange precipitate was formed immediately. The product was extracted with dichloromethane (5 x 5.0 cm³). The solvent was removed in *vacuo* to give an orange residue. The residue was recrystallised by diffusion from dichloromethane solution layered with *n*-pentane at -20 °C.



Tetrachloroaurate(III) imine salt **3** was prepared in a similar manner to **1** by reacting 4,4-dimethyl-2-(2-thienyl)oxazole (0.12 g, 0.64 mmol) with a similar mole quantity of HAuCl₄.4H₂O (0.29 g, 0.72 mmol). The product was extracted with dichloromethane (5 x 5.0 cm³). The solvent was removed under vacuum yielding a yellow residue. The residue

was recrystallised by diffusion from dichloromethane solution layered with *n*-pentane at -20 °C.



Cationic gold(I) imine complex, **4b** was prepared similarly as described for **1** by reacting 4,4-dimethyl-2-(phenyl)oxazole (0.083 g, 0.48 mmol) with similar mole quantity of HAuCl₄.4H₂O (0.20 g, 0.48 mmol). The yellow precipitate formed was extracted with dichloromethane (5 x 5.0 cm³). The residue was recrystallised from a concentrated acetone-d₆ solution and by diffusion from dichloromethane solution layered with *n*-pentane at -20 °C.

2.5.2.2 Preparation of adducts [AuCl₃(L)], **2b** and **4a**



2b was prepared by transferring 1-methyl-2-(2-pyridinyl)imidazole in acetonitrile solution to an aqueous solution of similar mole quantity of AuCl₃ (0.49 g, 1.2 mmol). An insoluble orange residue was separated from the solution by filtration and washed with diethyl ether (3 x 50 cm³). The mother liquor was extracted with a mixture of THF and dichloromethane (1:1, 150 cm³). The extract was filtered over anhydrous magnesium sulphate, followed by the solvent removal. The obtained product was only soluble in DMSO.



Complex **4a** was prepared in the same way as **2b** by reaction of AuCl₃ (0.15 g, 0.57 mmol) with a similar mole quantity of 4,4-dimethyl-2-(phenyl)oxazole (0.10 g, 0.57 mmol). The yellow residue was extracted with dichloromethane (5 x 10 cm³). The solvent was removed under vacuum. Crystallisation of the residue from dichloromethane solution layered with *n*-pentane at -20 °C yielded yellow crystals of **4a**.

2.5.2.3 Preparation of cationic complex [AuCl₂(L₂)]⁺[AuCl₄]⁻



A solution of 4,4-dimethyl-2-phenyl-4,5-dihydro-oxazole (0.36 g, 2.1 mmol) in acetonitrile was added to an aqueous solution of NaAuCl₄.2H₂O (0.41 g, 1.0 mmol). A yellow precipitate was formed after 5 h of stirring at room temperature. The reaction mixture was then stirred overnight, followed by extraction with dichloromethane (3 x 10 cm³) and filtration over anhydrous magnesium sulphate. The solvent was removed under vacuum and the remaining residue was washed with diethyl ether. Crystallisation from a dichloromethane solution layered with *n*-pentane solution at -20 °C afforded yellow crystals of **4c**.



A solution of 4,4-dimethyl-2-phenyl-4,5-dihydro-oxazole (0.40 g, 2.3 mmol) in THF was added to a solution of AgBF₄ (0.22 g, 1.2 mmol) in THF. The colourless mixture was stirred for 2 h at room temperature. A solution of NaAuCl₄.2H₂O (0.46 g, 1.2 mol) in acetonitrile was transferred to the brown reaction mixture and stirred at room temperature. An immediate precipitate (formation of NaBF₄ and/or AgCl) was observed during the addition. The reaction mixture was stirred overnight at room temperature. The solvent was stripped under vacuum, the residue re-dissolved in dichloromethane (20 cm³) and filtered through anhydrous MgSO₄. The solvent was removed in *vacuo* and a yellow crude product was collected. Crystallisation of **4d** from a dichloromethane solution layered with *n*-pentane solution at -20 °C afforded yellow crystals.

2.5.2.4 Preparation of tetrachloroaurate(III) imine salts **5a** and **8a**, adduct, **7a** and cationic complex, **6a**



5a was prepared with a similar approach to compounds **1** - **4b** by reacting a solution of thiazole (0.068 g, 0.80 mmol) in acetonitrile with a similar mole amount of aqueous solution of H[AuCl₄].4H₂O (0.38 g, 0.80 mmol) at room temperature. The yellow precipitate was extracted with dichloromethane and then the solvent was removed by

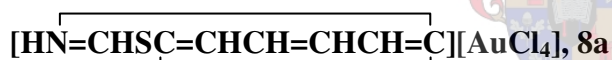
vacuo. Yellow crystals were obtained by slow evaporation from a dichloromethane solution.



The cationic gold(I) complex **6a** was prepared in a similar fashion as **1** - **4b** from 4-methylthiazole (0.071g, 0.11 mmol) and similar mole quantities of H₂AuCl₄·4H₂O (0.29 g, 0.71 mmol). Crystallisation of **6a** from a concentrated solution of chloroform-d at -20 °C and by slow evaporation afforded yellow crystals suitable for single crystal X-ray determination.



Neutral complex **7** was prepared in a similar fashion as **1** - **4b** from 4,5-dimethylthiazole (0.086 g, 0.76 mmol) and similar mole quantities of H₂AuCl₄·4H₂O (0.31 g, 0.76 mmol). Yellow crystals of **7** suitable for X-ray analysis were obtained from a concentrated chloroform-d solution at -20 °C and by slow evaporation of a solution of dichloromethane.



The tetrachloroaurate(III) salt of benzothiazole, **8a**, was prepared from benzothiazole (0.10 g, 0.76 mmol) and a similar mole amount of H₂AuCl₄·4H₂O (0.31 g, 0.76 mmol). The product was extracted with a mixture of dichloromethane/THF (1:1, 150 cm³) to yield a yellow residue after solvent removal under vacuum. Crystallisation of **8a** was obtained by diffusion from THF solution layered with *n*-pentane at -20 °C.

2.5.2.5 Preparation of adducts of [AuCl₃(L)], **5b**, **6b**, **7** and **8b**



The procedure used in Section 2.4.2.3a was repeated by substituting H₂AuCl₄·4H₂O with similar mole quantities of AuCl₃ (0.31 g, 1.0 mmol) and reacting with the ligand thiazole (0.086 g, 1.0 mmol) in acetonitrile. Crystallisation from a concentrated dichloromethane solution layered with *n*-pentane at -20 °C afforded yellow crystals of adduct **5b** suitable for single crystal X-ray structure determination.



Adduct **6b** was prepared in similar fashion as **5b** using 4-methylthiazole (0.14 g, 1.4 mmol) ligand and similar mole quantities of $\text{AuCl}_3 \cdot x\text{H}_2\text{O}$ (0.42 g, 1.4 mmol).

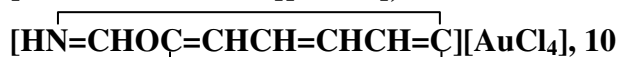


The procedure followed for complex **5b** was used to prepare adduct **7** from 4,5-dimethylthiazole (0.13 g, 1.2 mmol) and similar mole quantities of $\text{AuCl}_3 \cdot x\text{H}_2\text{O}$ (0.35 g, 1.1 mmol). Crystallisation of **7** was obtained from concentrated a chloroform-d solution at $-20\text{ }^\circ\text{C}$.



Neutral adduct **8a** was prepared by a similar method as described for **5b** using benzothiazole (0.13 g, 0.94 mmol) and similar mole quantities of AuCl_3 (0.28 g, 0.94 mmol). Yellow crystals suitable for X-ray diffraction were obtained by diffusion from dichloromethane solution layered with *n*-pentane at $-20\text{ }^\circ\text{C}$.

2.5.2.6 Preparation of tetrachloroaurate(III) imine salts, **9** or **10**

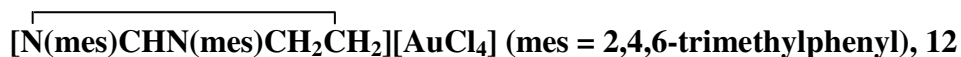


Compounds **9** or **10** were prepared following a method similar to that described in Section 2.4.2.3a by using oxazole (0.060 g, 0.93 mmol) or benzoxazole (0.11 g, 0.92 mmol) and $\text{HAuCl}_4 \cdot 4\text{H}_2\text{O}$ (0.38 g, 0.93 mmol) for compound **9** or (0.25 g, 0.61 mmol) for compound **10**, respectively. The yellow precipitate in reaction **10** turned brown in 15 min at room temperature. Extraction with dichloromethane/THF mixtures (1:1) afforded **9** or **10**. Yellow crystals of **9** suitable for single crystal X-ray diffraction were obtained from dichloromethane solution layered with *n*-pentane at $-20\text{ }^\circ\text{C}$.

2.5.2.7 (BT)₂C=C(BT)₂, **11**

The same method of reaction applied in the above reactions was repeated between HBBTM solution (0.10 g, 0.36 mmol) in acetonitrile and two equivalent quantities of HAuCl₄·4H₂O (0.30 g, 0.73 mmol) in aqueous solution. A yellow precipitate formed which slowly turned green during the reaction process. Reduction of Au(III) to Au(0), in the form of a thin gold film, was observed in an extended period of time (up to 24 h). The compound was extracted with THF. The same observation was also made when the precursor HAuCl₄·4H₂O was substituted with AuCl₃ (0.25 g, 0.82 mmol)

2.5.2.8 Preparation of 1,3-bis(2,4,6-trimethylphenyl)-imidazolinium tetrachloroaurate(III) salt, **12**



A suspension of t-BuOK (0.13 g, 1.2 mmol) in THF was added to a suspension of 1,3-bis(2,4,6-trimethylphenyl)imidazolinium chloride (0.40 g, 1.2 mmol) in THF at room temperature. A moderate evolution of gas (probably CH(CH₃)₃) was observed. The mixture was stirred for 3 h at room temperature until the evolution of gas ceased completely. The solution was filtered through Celite directly onto a solution of AuCl₃ (0.35 g, 1.2 mmol) in THF. The reaction mixture was stirred for 2 h at ambient temperature. The solvent was stripped under high vacuum. The crude product **12** was recrystallised by diffusion from dichloromethane solution layered with *n*-hexane at -20 °C and orange crystals were obtained.

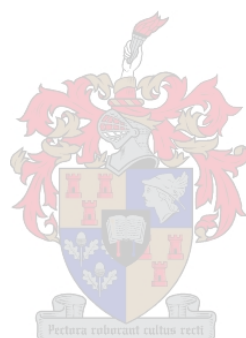
N.B. All the melting points and percentage yields are not corrected since by-products are also present in mixture with the main product.

2.5.3 X-ray structure determinations

The crystal data collection and refinement details for complexes **4b**, **4b'**, **6a**, **7**, **8a** and **12** are summarised in Table 2.28 and Table 2.29. All data sets were collected on a Bruker SMART-Apex diffractometer using graphite monochromated Mo-K α radiation ($\lambda =$

0.71073 Å).³³ Except for **8a**, which was measured at 273 K, all measurements were made at 100 K. Data reduction was carried out with standard methods from the software package Bruker SAINT.³⁴ Empirical corrections were performed using SCALEPACK and SMART.³⁵ For adsorption corrections the data were treated with SADABS.^{36,37} The program X-Seed³⁸ was used as a graphical interface for structure solution and refinement with direct methods using SHELX. All non-hydrogen atoms were refined anisotropically by full-matrix least squares calculations on F² using SHELXL-97. The hydrogen atoms were fixed in calculated positions. POV-Ray for Windows was used to generate the various figures of the six compounds at the 50% probability level.

Additional information concerning the X-ray work is available from Prof H. G. Raubenheimer, Department of Chemistry, University of Stellenbosch.



³³ SMART Data collection software (version 5.629), Bruker AXS Inc., Madison, WI, 2003.

³⁴ SAINT, Data reduction software (version 6.45) Bruker AXS Inc., Madison, WI, 2003.

³⁵ L.J. Ferrugia, *J. Appl. Crystallogr.*, 1999, **32**, 837.

³⁶ R.H. Blessing, *Acta Crystallogr., Sect. A*, 1995, **51**, 33.

³⁷ SADABS (version 2.05) Bruker AXS Inc., Madison, WI, 2002.

³⁸ (a) L. J. Barbour, *J. Supramol. Chem.*, 2001, **1**, 189. (b) J. L. Atwood and L. J. Barbour, *Cryst. Growth Des.*, 2003, **3**, 3.

Table 2.28 Crystallographic data for complexes **4b**, **4b'** and **6a**

	4b	4b'	6a
Empirical formula	C ₈ H ₁₀ Au ₂ Cl ₄ N ₂ S ₂	C ₁₂ H ₁₆ AuCl ₆ NO	C ₈ H ₁₀ Au ₂ Cl ₄ N ₂ S ₂
Formula weight (g.mol ⁻¹)	734.03	599.92	734.03
Crystal system	Orthorhombic	Triclinic	Orthorhombic
Space group	<i>Cmca</i>	<i>P</i> $\bar{1}$	<i>Cmca</i>
a (Å)	6.7252(7)	7.8168(10)	6.7252(7)
b (Å)	18.000(2)	8.9538(12)	18.000(2)
c (Å)	13.5553(15)	14.7156(19)	13.5553(15)
α (°)	90.00	80.385(2)	90.00
β (°)	90.00	86.244(2)	90.00
γ (°)	90.00	66.876(2)	90.00
Volume (Å ³)	1640.9(3)	933.9(2)	1640.9(3)
Z	4	2	4
Calculated density (g.cm ⁻³)	2.971	2.133	2.971
Wave length (Å)	0.71073	0.71073	0.71073
Temperature (K)	100(2)	100(2)	100(2)
Absorption coefficient (μ mm ⁻¹)	18.749	8.731	18.749
Crystal size (mm ³)	0.40 x 0.30 x 0.20	0.20 x 0.10 x 0.10	0.40 x 0.30 x 0.20
$2\theta_{\max}$ (°)	56.5	53.4	56.5
Index range, <i>hkl</i>	-8 ≤ <i>h</i> ≤ 8 -21 ≤ <i>k</i> ≤ 22 -13 ≤ <i>l</i> ≤ 17	-9 ≤ <i>h</i> ≤ 9 -11 ≤ <i>k</i> ≤ 9 -18 ≤ <i>l</i> ≤ 15	-8 ≤ <i>h</i> ≤ 8 -21 ≤ <i>k</i> ≤ 22 -13 ≤ <i>l</i> ≤ 17
Reflections collected	4927	5501	4927
No. of independent reflections	1048 (R _{int} = 0.0258)	3830 (R _{int} = 0.0146)	1048 (R _{int} = 0.0258)
Parameters	40	236	40
Goodness of fit	1.283	1.049	1.283
Largest peak	1.55	1.58	2.32
Deepest hole	-1.03	-1.33	-1.92
R ₁ (F _o > 2σF _o)	0.0279	0.0255	0.0279
wR ₂	0.1521	0.0578	0.1521

Table 2.29 Crystallographic data for complexes **7**, **8a** and **12**

	7	8a	12
Empirical formula	C ₅ H ₇ AuCl ₃ NS	C ₁₁ H ₁₄ AuCl ₄ NOS	C ₅ H ₇ AuCl ₃ NS
Formula weight (g.mol ⁻¹)	416.35	547.06	645.8
Crystal system	Monoclinic	Triclinic	Monoclinic
Space group	<i>P2₁/c</i>	<i>P</i> $\bar{1}$	<i>P2₁/c</i>
a (Å)	9.144(3)	7.3213(7)	19.590(3)
b (Å)	13.962(4)	10.3498(10)	8.9986(13)
c (Å)	7.735(2)	11.8783(12)	15.306(2)
α (°)	90.00	99.3310(10)	90.00
β (°)	93.591(5)	107.5790(10)	96.602(2)
γ (°)	90.00	104.483(2)	90.00
Volume (Å ³)	985.5(5)	802.75(14)	2680.4(7)
Z	2	2	4
Calculated density (g.cm ⁻³)	2.807	2.263	1.812
Wave length (Å)	0.71073	0.71073	0.71073
Temperature (K)	100(2)	273	100(2)
Absorption coefficient (μ mm ⁻¹)	15.889	9.949	6.100
Crystal size (mm ³)	0.34 x 0.26 x 0.12	0.30 x 0.20 x 0.10	0.30 x 0.25 x 0.10
$2\theta_{\max}$ (°)	56.7	56.6	56.6
Index range, <i>hkl</i>	-9 \leq <i>h</i> \leq 12 -18 \leq <i>k</i> \leq 17 -9 \leq <i>l</i> \leq 7	-9 \leq <i>h</i> \leq 9 -13 \leq <i>k</i> \leq 13 -14 \leq <i>l</i> \leq 15	-21 \leq <i>h</i> \leq 25 -9 \leq <i>k</i> \leq 9 -19 \leq <i>l</i> \leq -19
Reflections collected	10893	4962	15566
No. of independent reflections	2324 ($R_{\text{int}} = 0.0427$)	3508(0.0126)	6093 ($R_{\text{int}} = 0.0939$)
Parameters	102	174	287
Goodness of fit	1.106	1.201	0.918
Largest peak	7.57	2.24	2.18
Deepest hole	-2.46	-1.06	-2.22
R_1 ($F_o > 2\sigma F_o$)	0.0486	0.0267	0.0448
w R_2	0.1404	0.0631	0.0855

Chapter 3

Thione complexes of gold(I) and gold(III) and; cationic sulphonium complexes of gold(I)

3.1 Introduction and aims

3.1.1 General

Investigations involving sulfur-donor-ligand complexes of gold(I) have inspired researchers in the past by their potential medicinal application as anti-arthritic drugs. Thione gold(I) complexes are believed to be biologically active.¹

Thioethers form important precursor complexes of the type $\text{AuCl}(\text{SR}_2)$. Various thione complexes of gold(I) are obtained by replacement of the weakly coordinated thioether ligands like tht or SMe_2 leading to stable and linear gold(I) complexes. The coordination chemistry of thioamide ligands is also broadly established with several transition metals due to the versatility of the ligands in adopting monodentate, bridging and chelating modes of coordination.¹

Gold(I) complexes with thiones have two stoichiometries, these categories include neutral and cationic complexes such as $[\text{AuXL}]$ ($X = \text{Cl}, \text{C}_6\text{F}_5$) and $[\text{AuL}_2]^+$, respectively.²

The neutral gold(I) complexes of the type $\text{AuX}(\text{L})$ have been obtained by displacement of the weakly coordinating ligand tetrahydrothiophene, tht, in $\text{AuX}(\text{tht})$, ($X = \text{C}_6\text{F}_5, \text{Cl}$) with heterocyclic thione ligands such as ($\text{L} = 1,3\text{-thiazolidine-2-thione}, 1\text{H-pyrimidine-2-thione}, \text{pyridine-2-thione}, \text{benzothiazolidine-2-thione}$ or $\text{benzimidazol-2-thione}$).³

The cationic monomeric gold(I) complexes $[\text{Au}(\text{L})_2]\text{ClO}_4$ or $[\text{Au}(\text{PPh}_3)(\text{L})]\text{ClO}_4$ have also been obtained in a similar fashion to the neutral complexes by displacement of the weakly

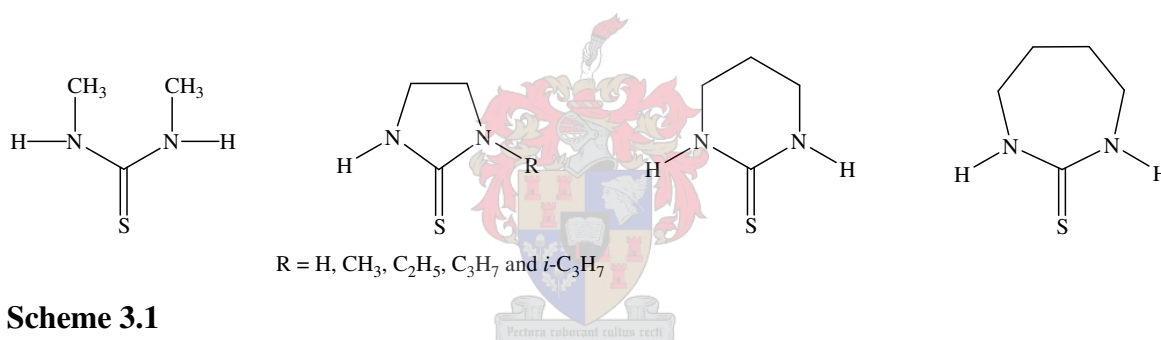
¹ P. D. Akrivos, *Coord. Chem. Rev.*, 2001, **213**, 181.

² M. C. Gimeno and A. Laguna, in: *Silver and Gold, Comprehensive Coordination Chemistry II*, 1st ed, Editors in Chief J. A. McCleverty and T. J. Meyer, Volume Editor D. E. Fenton, Elsevier Ltd./Elsevier Inc., Oxford/San Diego, 2004, p. 1034.

³ R. Usón, A. Laguna, M. Laguna, J. Jiménez, M. P. Gómez, A. Sainz and G. P. Jones, *J. Chem.Soc., Dalton Trans.*, 1990, 3457.

coordinating thioether ligand tht in $[\text{Au}(\text{tht})_2]\text{ClO}_4$ or $[\text{Au}(\text{PPh}_3)(\text{tht})]\text{ClO}_4$, respectively with heterocyclic thiones (HL = 1,3-thiazolidine-2-thione, 1H-pyrimidine-2-thione, pyridine-2-thione, benzothiazolidine-2-thione or benzimidazol-2-thione) as ligands.¹ Similarly, homoleptic rearrangement of neutral gold(I) complexes also afford cationic complexes, $[\text{AuL}_2]^+$ with the heterocyclic thione ligands such as [L = imidazoline-2-thione, N-R-1,3-imidazoline-2-thione (R = Pr, Et)].²

Ligand scrambling reactions in cyano(thione)gold(I) complexes [$>\text{C}=\text{S}-\text{Au}-\text{CN}$] to form $[\text{Au}(>\text{C}=\text{S})_2]^+$ and $[\text{Au}(\text{CN})_2]^-$ have also been investigated for a series of thiones (Equation 3.1) in DMSO.⁴ Thiones are generally classified according to their ring size; the most common ones are five-, six- and higher-membered heterocyclic rings (Scheme 3.1).



Scheme 3.1

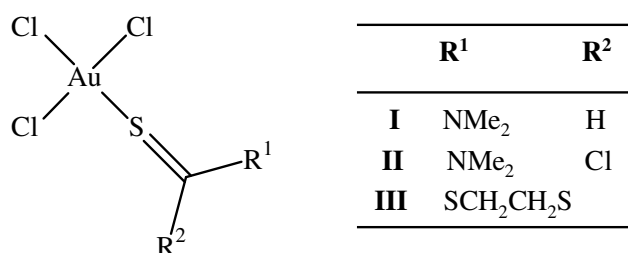
Sulfur insertion into Au-C bond of aurates $\text{Li}[\text{Au}(\overline{\text{C}=\text{NCX}_1=\text{CX}_2\text{S}})_2]$ ($\text{X}_1\text{X}_2 = \text{C}_4\text{H}_4$; $\text{X}_1 = \text{Me}$, $\text{X}_2 = \text{H}$) leads to anionic complexes $\text{Li}[\text{Au}(\overline{\text{C}=\text{NCX}_1=\text{CX}_2\text{S}})(\overline{\text{SC}=\text{NCX}_1=\text{CX}_2\text{S}})]$, which can readily be protonated, to give thiazoles and the polymeric Au sulfides $[\text{AuSC}=\overline{\text{NCX}_1=\text{CX}_2\text{S}}]_x$.⁵ Essentially linear coordination is found in thiourea complexes $\text{AuBr}[\text{S}=\text{C}(\text{NR}_2)_2]$ (R = H, Me) and $[\text{Au}(\overline{\text{S}=\text{CNHCH}_2\text{CH}_2\text{NH}})_2]^+\text{Cl}^-$.

Existing reports on thione complexes of gold(I) and gold(III) derived from thiourea or thioamides describe stable complexes. Only a few gold(III) thione adducts (**I** – **III**) are reported in the literature (Scheme 3.2).⁶

⁴ S. Ahmad, A. A. Isab and H. P. Perzanowski, *Can. J. Chem.*, 2002, **80**, 1279.

⁵ H. G. Raubenheimer, P. J. Olivier and J. G. Toerien, *S. Afr. J. Chem.*, 1995, **48**, 60.

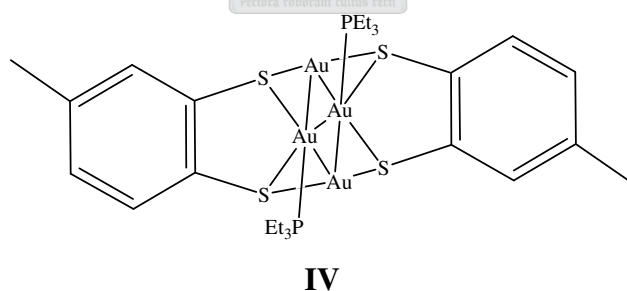
⁶ H. G. Raubenheimer, R. Otte, L. Linford, W. E. Van Zyl, A. Lombard and G. J. Kruger, *Polyhedron*, 1992, **11**, 893.



Scheme 3.2

Trigonal bipyramidal Au(L)Cl₃ complexes with 2-(2-thiono-1-pyridyl)benzoxazole (PTBOX) and 2-(2-thiono-1-pyridyl)benzothiazole (PTBTH) (Chapter 1, Scheme 1.11) behaving as bidentate donors while coordinating through the N and thione S atoms of the moiety, have been reported by Khan and Shahjahan.⁷

High nuclearity gold(I) sulphide complexes with bridging diphosphine ligands have been synthesised by bubbling H₂S through ethanol/pyridine solutions of [Au₂Cl₂(μ-P-P)]. These complexes have the general formula [Au₁₀(μ₃-S)₄{μ-(PPh₂)₂NR₂}₄]X₂ (R = alkyl or aryl, X = PF₆ or ClO₄), [Au₁₂(μ₃-S)₄(μ-dppm)₆]X₄ or [Au₆(μ-S)₂{μ-(PPh₂)₂NR₂}₃]X₂ (R = alkyl or aryl; X = PF₆ or ClO₄) and display rich luminescence upon excitation at λ > 350 nm. Similarly, an unusual tetranuclear complex [{Au₂(1,2-S₂C₆H₄)(PEt₃)}]₂, **IV**, is known in which the gold(I) atoms are in a square arrangement with a short contact of ca. 3.1 Å (Scheme 3.3).⁸



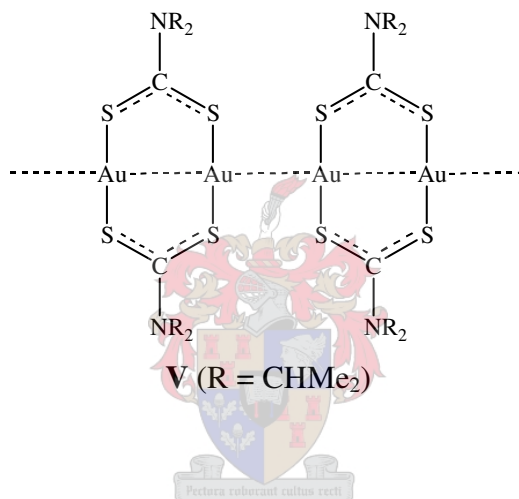
Scheme 3.3

Aggregation of gold atoms around the thiolate group of the stoichiometric [RS(AuPR₃)₂]⁺ or the four-coordinated [MeS(AuPMe₃)₃]²⁺ have also been obtained. Similar species such

⁷ T. A. Khan and Shahjahan, *Synth. React. Inorg. Met.-Org. Chem.*, 1998, **28**, 571.

⁸ H. G. Raubenheimer and S. Cronje, in *Gold: Progress in Chemistry, Biochemistry and Technology*, ed. H. Schmidbaur, John Wiley & Sons, Chichester, 1999, p. 307.

as $[S(AuL)_3]^+$, have also been characterised structurally.⁹ Theoretical studies suggest that gold-gold interactions are strong in S-Au-PR₃ compounds in which the gold atoms are separated by about 3.1 Å. The chemistry of gold dithiolates and related ligands also feature in this active research field.¹⁰ The existence of cations such as $[(R_3PAu)_3S]^+$ (R = alkyl or aryl) indicate the thiophilicity of gold. The most important complexes of S-donors are thiolates, simply regarded as $[Au(SR)]_n$. Sulphate and thiosulphate bound through sulfur have linear coordination. Bidentate dithiolate ligands afford complexes like $Au(S_2CNR_2)$ (R = Et, Pr, Bu) and $Au(S_2PR_2)$ (R = Pr), with dimeric 8-membered gold-containing rings (**V**) with linear S-Au-S coordination and short (3.012 Å) Au-Au distances (Scheme 3.4).¹¹



Scheme 3.4

The tendency to form linear complexes and 2-coordinate complexes that may experience additional (weaker) gold-gold attractions have been reported for products from $(ClAuPPh_2)_2(CH)_n$ precursors.¹² The nine-membered diauracycle, **VI**, has structurally been assembled from $NBu_4[Au_2(\mu-CH_2PPh_2CH_2PPh_2)Br_2]$ and $Na_2[C_3S_5]$ and the molecular structure features intramolecular aurophilic interactions at a distance of 3.048 Å (Scheme 3.5).¹³

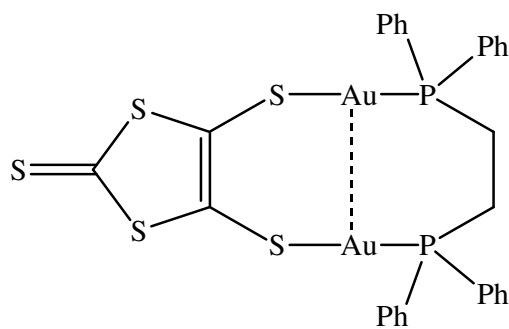
⁹ (a) V. G. Albano, C. Castellari, C. Femoni, M. C. Iapalucci, G. Longoni, M. Monari, M. Rauccio and S. Zacchini, *Inorg. Chim. Acta*, 1999, **291**, 372. (b) E. W. Abel, and C. R. Jenkins, *J. Organomet. Chem.*, 1968, **14**, 285. (c) C. Lensch, P. G. Jones and G. M. Sheldrick, *Z. Naturforsch.*, 1982, **37B**, 944.

¹⁰ J. Vicente, P. G-Herrero and Y. G-Sánchez, *Inorg. Chem.*, 2004, **43**, 7516.

¹¹ S. A. Cotton, in: *Chemistry of Precious Metals*, 1st ed, Chapman and Hall, London, 1997, p. 296.

¹² M.-C. Brandys, M. C. Jennings and R. J. Puddephatt, *J. Chem. Soc., Dalton Trans.*, 2000, 4601.

¹³ E. Cerrada, P. G. Jones, A. Laguna and M. Laguna, *Inorg. Chim. Acta*, 1996, **249**, 163.



VI

Scheme 3.5

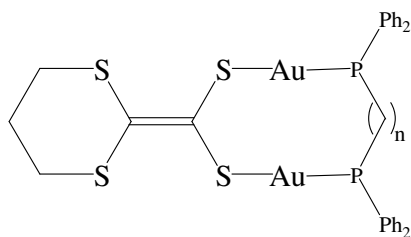
A series of neutral dinuclear gold(I) complexes containing phosphine and thiolate ligands have been prepared by ligand substitution reactions of the corresponding gold(I) phosphine chloride complexes with alkanes or arene thiolates.¹⁴ The luminescent character of the gold(I)-gold(I) bonding interaction has been demonstrated by diphosphine digold(I) pyridine-2-thiolate complexes [(AuSN)₂dppm] and [(AuSN)₂dpph].¹⁵

3.1.2 Aims and objectives

- The interest in organosulfur compounds of gold for pharmaceutical applications inspired us to prepare a series of gold(I) and gold(III) thione compounds and to characterise and establish their coordination modes by structural and NMR studies.
- Second, we planned to use an alkene dithiolate in attempts to prepare the cyclic gold(I) compounds **VII** and **VIII** (Scheme 3.6) from dilithio-1,3-dithiane-2-carbodithioate and AuCl(PPh₃), (AuCl)₂(dppm) or (AuCl)₂(dppe) and investigate possible aurophilic interactions. Some of the compounds finally obtained were not analytically pure but sufficient crystals for single crystal X-ray analysis could be grown in order to determine their molecular structures.

¹⁴ R. Narayanaswamy, M. A. Young, E. Parkhurst, M. Ouellette, M. E. Kerr, D. M. Ho, R. C. Elder, A. E. Bruce and M. R. M. Bruce, *Inorg. Chem.*, 1993, **32**, 2506.

¹⁵ B.-C. Jzeng, J.-H. Liao, G.-H. Lee and S.-M. Peng, *Inorg. Chim. Acta*, 2004, **357**, 1405.



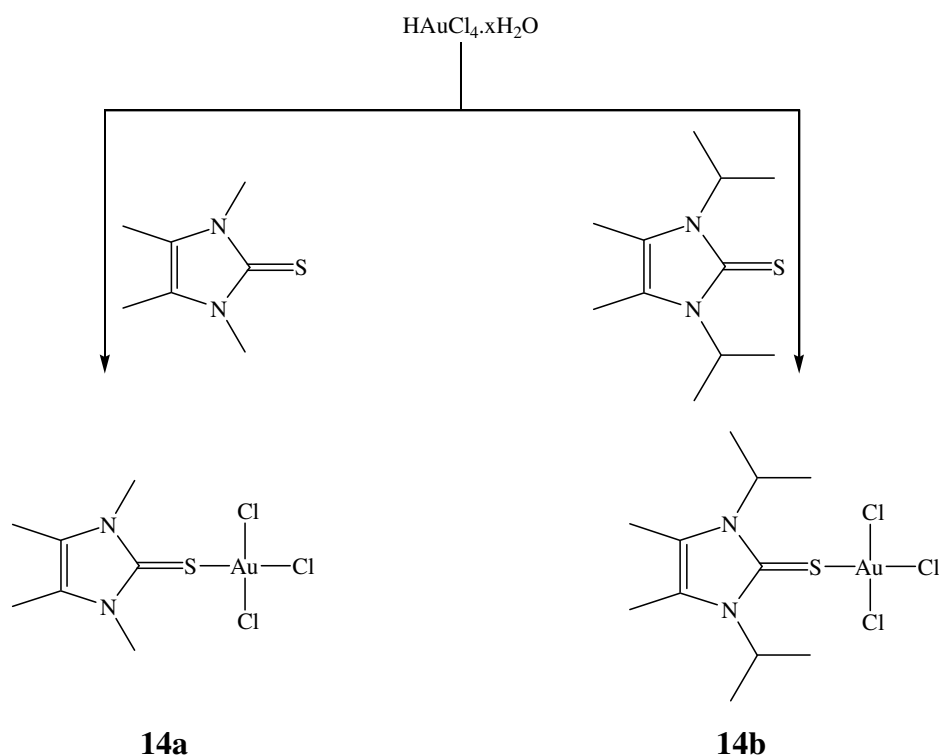
VII (n = 1); VIII (n = 2)

Scheme 3.6

3.2 Results and discussions

3.2.1 Preparation of thione complexes of gold(I) and gold(III)

[Au(C₆F₅)(thione)] complexes were prepared by substitution of the weakly coordinated thioether tht in Au(tht)(C₆F₅) with similar mole quantities of a series of thiones like 1,3,4,5-tetramethyl-1,3-dihydro-imidazole-2-thione, 1,3-diisopropyl-4,5-dimethyl-1,3-dihydro-imidazole-2-thione or 2-imidazolidinethione to yield [Au(C₆F₅){S=CN(Me)C(Me)=C(Me)N(Me)}], **13a**, [Au(C₆F₅){S=CN(*i*-Pr)C(Me)=C(Me)N(*i*-Pr)}], **13b** or [Au(C₆F₅){S=CNHCH₂CH₂NH}], **13c**, respectively (Scheme 3.7) under ambient conditions in dichloromethane and/or diethyl ether. These compounds are obtained as colourless and air-stable crude products, however, in solution complexes **13a** and **13b** slowly turn yellow upon exposure to air. High yields of the complexes were obtained. They are all well-soluble in THF, dichloromethane and acetone, and are slightly soluble in diethyl ether but insoluble in *n*-hexane and *n*-pentane. Colourless crystals suitable for single crystal X-ray molecular structure determination were obtained for the gold(I) complexes of **13a** and **13b** from dichloromethane solutions layered with diethyl ether or *n*-hexane at -20 °C. Comparison of the proton NMR spectra of the free ligands to the products obtained, confirmed that bonding occurs *via* the thione sulfur. Molecular structures of **13a** and **13b** were also obtained from single crystal X-ray analysis and are reported in Section 3.3.



Scheme 3.8

3.2.2 Spectroscopic characterisation of the new thione-coordinated gold(I) and gold(III) compounds **13a** - **14b**

NMR spectroscopy

3.2.2.1 [Au(C₆F₅){S=CN(Me)C(Me)=C(Me)N(Me)}], **13a**

The ¹H and ¹³C NMR data of compound **13a** are summarised in Table 3.1. Two broad signals for the methyl protons are observed in the ¹H NMR spectra. The signal appearing at 3.78 ppm is assigned to the methyl protons H⁵ and H⁶. The second group of methyl protons H¹ and H⁴ also appear as a broad signal at 2.16 ppm. The methyl protons H¹ and H⁴ are chemically and magnetically equivalent. The ¹H NMR signals of **13a** with respect to the free ligand⁷ and Rh complexes¹⁶ do not show significant changes in chemical shifts. The ¹H NMR signals of the ligand tht in the precursor [Au(C₆F₅)(tht)], are not observed indicating that the ligand has been quantitatively substituted by the thione ligand.

¹⁶ A. Neveling, G. R. Julius, S. Cronje, C. Esterhuysen and H. G. Raubenheimer, *Dalton Trans.*, 2005, **1**, 181.

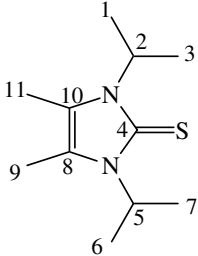
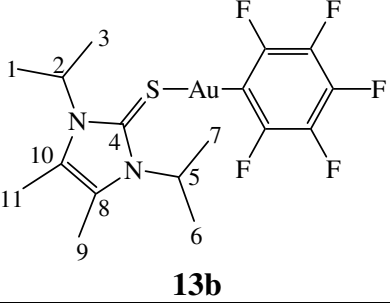
Table 3.1 ^1H and ^{13}C NMR data of compound **13a** and the free ligand in CD_2Cl_2

Assignment	$\delta(\text{ppm})$ (multiplicity, J(Hz))	$\delta(\text{ppm})$ (multiplicity, J(Hz))
$^1\text{H NMR}$		
H^5 and H^6	3.48 (6H, s)	3.78 (6H, bs)
H^1 and H^4	2.06 (6H, s)	2.16 (6H, bs)
$^{13}\text{C NMR}$		
C^7	161.1	203.4
C^2 and C^3	120.7	125.0 (m)
C^5 and C^6	31.7	33.3
C^1 and C^4	9.1	9.3
C^{ortho}		148.8 (m, $J_{\text{C-F}} = 220.8$ Hz)
C^{para}		125.0 (m, $J_{\text{C-F}} = 244.6$ Hz)
C^{meta}		137.2 (m, $J_{\text{C-F}} = 252.8$ Hz)
C^{ipso}		138.5 (m, $J_{\text{C-F}} = 245.2$ Hz)

The ^{13}C NMR signal of the thione-carbon C^7 appears at 203.4 ppm, with a significant downfield shift of $\Delta\delta$ 42.3 compared to the free ligand. The chemical shift of the same thione carbon in rhodium complexes,¹⁶ however, does not show noticeable shift compared to the free ligand. The chemical shift change for C^2 and C^3 upon coordination is $\Delta\delta$ 4.3 with respect to the free ligand. The chemical shifts observed for C^5/C^6 and C^1/C^4 , and the pentafluorophenyl carbon atoms do not change significantly when compared to the free ligand and the precursor respectively. The coupling constants of the pentafluorophenyl carbons are comparable to those of the precursor, $\text{Au}(\text{C}_6\text{F}_5)(\text{tht})$.¹⁰ The signals corresponding to the tht ligand in the precursor $\text{Au}(\text{C}_6\text{F}_5)(\text{tht})$ disappeared from the ^{13}C NMR spectrum confirming the coordination of the thione.

3.2.2.2 $[\text{Au}(\text{C}_6\text{F}_5)\{\text{S}=\text{CN}(i\text{-Pr})\text{C}(\text{Me})=\text{C}(\text{Me})\text{N}(i\text{-Pr})\}], \mathbf{13b}$

Table 3.2 ^1H and ^{13}C NMR data of compound **13b** in CDCl_3 and the free ligand¹⁷ in CD_2Cl_2

Assignment	δ (ppm) (multiplicity, J(Hz))	δ (ppm) (multiplicity, J(Hz))
		 <p style="text-align: center;">13b</p>
^1H NMR		
H^2 and H^5	5.57 (2H, bs)	5.77 (2H, s)
H^9 and H^{11}	2.14 (6H, s)	2.28 (6H, s)
$\text{H}^1, \text{H}^3, \text{H}^6$ and H^7	1.39 (12H, d, $^3J_{\text{H}1,3-\text{H}2} = 7.2$ Hz)	1.57 (12H, d, $^3J_{\text{H}1,3-\text{H}2} = 7.2$ Hz)
^{13}C NMR		
C^4	160.7	not observed
C^8 and C^{10}	121.5	125.1
C^2 , and C^5	49.3	51.2
$\text{C}^1, \text{C}^3, \text{C}^6$ and C^7	20.7	20.9
C^9 and C^{11}	10.4	10.4
C^{ortho}		136.9 (dm, $J_{\text{C-F}} = 250.8$ Hz)
C^{para}		138.2 (dm, $J_{\text{C-F}} = 244.8$ Hz)
C^{meta}		148.5 (dm, $J_{\text{C-F}} = 226.8$ Hz)
C^{ipso}		126.5 (m)

The ^1H and ^{13}C NMR spectra of complex **13b** are summarised in Table 3.2. The ^1H NMR data of **13b** are comparable to those observed for the free ligand. The methyl protons, H^1 and H^3 , of the isopropyl substituent on the thione appear at 1.57 ppm as a doublet due to coupling with proton H^2 . Spectral integration show that $\text{H}^1/\text{H}^3/\text{H}^6/\text{H}^7$ have the same chemical shift at δ 1.39 indicating their chemical equivalence. A slight downfield shift of $\Delta\delta$ 0.18 is observed for these protons compared to the free ligand. The coupling constant of 7.2 Hz for this doublet is approximately the same as the free ligand and rhodium complexes.¹⁶ Protons H^2/H^5 and H^9/H^{11} exhibit downfield shift of $\Delta\delta$ 0.20 and 0.14, respectively after coordination. The broad and weak intensity signal at δ 5.77 is assigned

¹⁷ N. Kuhn and T. Kratz, *Synthesis*, 1993, **6**, 561.

to the methine protons H² and H⁵. The downfield shift observed for these protons is $\Delta\delta$ 0.20 with respect to the free ligand.

No signal corresponding to the thione carbon, C⁴, in complex **13b** was obtained in the ¹³C NMR spectrum. The ¹³C NMR signals of C¹⁰ and C⁸ show downfield shift of $\Delta\delta$ 3.8. The pentafluorophenyl carbons of the C₆F₅ unit appear at about the same chemical shifts observed for the precursor Au(C₆F₅)(tht). The sizes of the coupling constants are comparable to those of the precursor.

The coordination of the thione ligand is evident both from the ¹H and the ¹³C NMR spectra, since signals corresponding to the tht ligand are not observed at all.

3.2.2.3 [Au(C₆F₅){S=C¹NHCH₂CH₂NH}], **13c**

Table 3.3 ¹H and ¹³C NMR data of compound **13c** in methanol-d₄ and the free ligand in DMSO-d₆¹⁸

Assignment	δ (ppm) (multiplicity, J(Hz))	δ (ppm) (multiplicity, J(Hz))
¹H NMR		
N-H	7.94	not observed
H ² and H ³	3.51 (4H, s)	3.51 (4H, s)
¹³C NMR		
C ¹		185.5
C ² and C ³		45.7
C ₆ F ₅		not observed

¹⁸ SDBS web: <http://www.aist.go.jp/RIODBS/SDBS> (National Institute of Advanced Industrial Science and Technology, 04 August 2005)

The ^1H and ^{13}C NMR data of compound **13c** are summarised in Table 3.3. The ^1H NMR signals corresponding to the N-H is not visible in a concentrated methanol- d_3 solution due to the strong signals from the solvents. The broad signal appearing at 3.57 ppm is assigned to the protons H^2/H^3 . No change in chemical shift was observed with respect to the signals of the free ligand in DMSO-d_6 .

Signals at δ 45.7 and 185.5 in the ^{13}C NMR spectrum are assigned to C^2/C^3 and the thione carbon C^1 , respectively. These signals do not show any significant change in chemical shift upon coordination.

Furthermore, the absence of the ^1H and ^{13}C NMR signals corresponding to the ligand tht indicate that, the substitution of the weakly coordinated thioether by the ligand 2-imidazolidinethione had occurred.

3.2.2.4 $[\text{Cl}_3\text{Au}\{\text{S}=\overline{\text{CN}(\text{Me})\text{C}(\text{Me})=\text{C}(\text{Me})\text{N}(\text{Me})}\}],$ **14a** and $[\text{Cl}_3\text{Au}\{\text{S}=\overline{\text{CN}(i\text{-Pr})\text{C}(\text{Me})=\text{C}(\text{Me})\text{N}(i\text{-Pr})}\}],$ **14b**

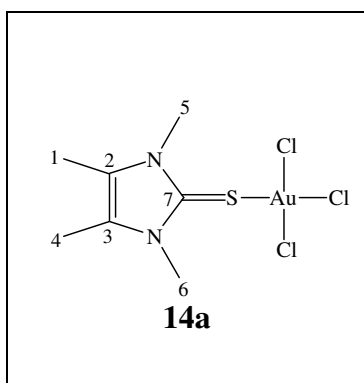
The chemical shifts in the ^1H and ^{13}C NMR spectra of the adduct **14a** are summarised in Table 3.4. Two broad signals are observed for the methyl protons in the ^1H NMR spectrum. Methyl protons H^5 and H^6 appear at 4.00 ppm. The signals for these protons exhibit a downfield shift of $\Delta\delta$ 0.52 compared to the protons of the free ligand and the gold(I) complex in Table 3.1. The broad signal at 2.38 ppm is assigned to the methyl protons H^1 and H^4 since they are chemically equivalent. These protons show a downfield shift of $\Delta\delta$ 0.32 when compared to the free ligand (Table 3.1).

The ^{13}C NMR spectrum of the neutral gold(III) complex displays a very weak signal at 137.6 ppm for the thione carbon C^7 . An upfield shift of $\Delta\delta$ 23.0 is observed with respect to the signal of the free ligand due to the reduction in double bond character of the thione C^7 . The signals for C^2 and C^3 show a noticeable downfield change in chemical shift of $\Delta\delta$ 10.0 from the signals of the free ligand because of the increase in double bond character of their C-N bond (Scheme 3.8).^{19,20} The signals for C^5/C^6 and C^1/C^4 remain approximately the same as those of the free ligand and the corresponding gold(I) complex.

¹⁹ E. S. Raper, *Coord. Chem. Rev.*, 1985, **61**, 115.

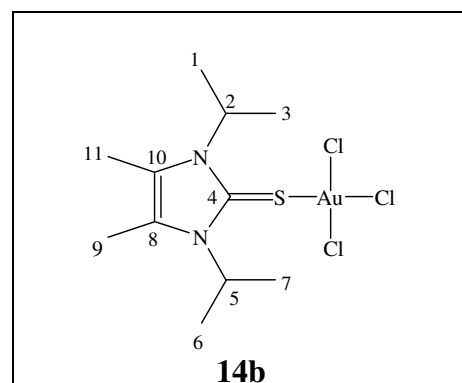
²⁰ M. N. Akhtar, A. A. Isab, M. S. Hussain and A. R. Al-Afraj, *Trans. Met. Chem.*, 1996, **21**, 553.

Table 3.4 ^1H and ^{13}C NMR data of compound **14a** in CD_2Cl_2



Assignment	δ (ppm) (multiplicity, J(Hz))
^1H NMR	
H^5 and H^6	4.00 (6H, s)
H^1 and H^4	2.38 (6H, s)
^{13}C NMR	
C^7	137.6
C^2 and C^3	130.9
C^5 and C^6	34.2
C^1 and C^4	9.3

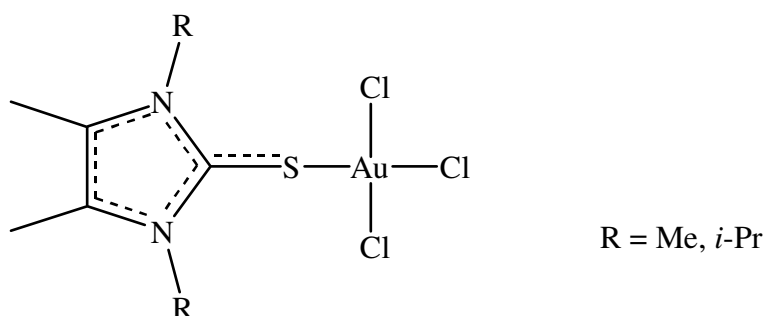
Table 3.5 ^1H and ^{13}C NMR data of compound **14b** in CDCl_3



Assignment	δ (ppm) (multiplicity, J(Hz))
^1H NMR	
H^2 and H^5	5.44 (2H, sep, $^3J_{\text{H}^2-\text{H}^5} = 7.9$ Hz)
H^9 and H^{11}	2.33 (6H, s)
H^1 , H^3 , H^6 and H^7	1.57 (12H, d, $^3J_{\text{H}^1,3-\text{H}^6,7} = 7.1$ Hz)
^{13}C NMR	
C^4	139.1
C^8 and C^{10}	129.6
C^2 and C^5	52.9
C^1 , C^3 , C^6 and C^7	20.9
C^9 and C^{11}	10.7

The ^1H and ^{13}C NMR spectra of adduct **14b** are summarised in Table 3.5. Three broad signals are observed in the ^1H NMR spectrum. The appearance of only one septet signal at δ 5.44 is characteristic of H^2 and H^5 coupled by pairs of methyl protons H^1/H^3 and H^6/H^7 , respectively indicating that the pair of protons is chemically equivalent. The broad signal at δ 2.33 and the doublet at δ 1.57 are assigned unequivocally to the methyl protons H^9 and H^{11} and the methyl protons H^1 , H^3 , H^6 and H^7 , respectively based on their spectral integrations and coupling constants. The downfield shifts observed for the methyl protons H^9 and H^{11} and the second group of methyl protons H^1 , H^3 , H^6 and H^7 (on the isopropyl substituent) are $\Delta\delta$ 0.20 and 0.18, respectively. The coupling constant for H^2/H^5 and that of the methyl protons (H^1 , H^3 , H^6 or H^7) is 7.9 Hz which is comparable to the free ligand (Table 3.2).

The signal for the thione carbon C⁴ (C=S) of the adduct appears at 139.1 ppm. It exhibits a significant upfield shift of $\Delta\delta$ 21.2 with respect to C⁴ of the free ligand due to the reduction in double bond character of the thione. The downfield shift of $\Delta\delta$ 8.1 representing carbons C⁸ and C¹⁰ with respect to the free ligand is more significant than **13b** because of the increase in double bond character of the C=N group.



Scheme 3.8

The chemical shift changes of the thione carbons C⁷ of **14a** and C⁴ of **14b** resonances are larger than the shift changes of C² and C³ of **14a** and C⁸ and C¹⁰ of **14b** indicating that the gold(III) is bound *via* the thione group and not the N of the ligands. The decreased double bond character of the thiones (C=S) by charge delocalisation (Scheme 3.8) indicate that thiole-thione equilibrium, where the thiole forms stronger bonding than the thione form.^{19,20}

Mass spectrometry

FAB MS, ESI MS and EI MS data of **13a**, **13b** and **13c** are summarised in Table 3.6. The FAB MS of complex **13a** exhibits a weak signal for the molecular ion peak $[\text{Au}(\text{C}_6\text{F}_6)\{\text{S}=\overline{\text{CN}(\text{Me})\text{C}(\text{Me})=\text{C}(\text{Me})\text{N}(\text{Me})}\}]^+$ at m/z 520. The peak at m/z 509 corresponds to $[\text{Au}\{\text{S}=\overline{\text{CN}(\text{Me})\text{C}(\text{Me})=\text{C}(\text{Me})\text{N}(\text{Me})}\}_2]^+$. A base peak corresponding to $[\text{Au}\{\text{S}=\overline{\text{CN}(\text{Me})\text{C}(\text{Me})=\text{C}(\text{Me})\text{N}(\text{Me})}\}]^+$ also appears at m/z 353 as a result of the loss of one of the thione ligands from $[\text{Au}\{\text{S}=\overline{\text{CN}(\text{Me})\text{C}(\text{Me})=\text{C}(\text{Me})\text{N}(\text{Me})}\}_2]^+$ or after the expulsion of $[\text{C}_6\text{F}_5]$ from the molecular ion. The succeeding peak at m/z 292 results from a fragment $[\text{Au}\{\text{S}=\overline{\text{CNC}=\text{CN}}\}]^+$ after the loss of four methyl groups.

Table 3.6 Mass spectrometry data of compounds **13a**, **13b** and **13c**

<i>m/z</i>	Intensity (%)	Fragment ion
13a		
843	10 (FAB MS)	$[(C_6F_6)_2Au\{S=\overline{CN(Me)C(Me)=C(Me)N(Me)}\}_2]^+$
520	7	$[M]^+$
509	11	$[Au\{S=\overline{CN(Me)C(Me)=C(Me)N(Me)}\}_2]^+$
353	45	$[Au\{S=\overline{CN(Me)C(Me)=C(Me)N(Me)}\}]^+$
292	18	$[Au\{S=\overline{CNC=CN}\}]^+$
13b		
621	16 (FAB MS)	$[Au\{S=\overline{CN(i-Pr)C(Me)=C(Me)N(i-Pr)}\}_2]^+$
576	7 (EI and FAB MS)	$[(C_6F_5)Au\{S=\overline{CN(i-Pr)C(Me)=C(Me)N(i-Pr)}\}]^+$
409	50 (FAB MS)	$[Au\{S=\overline{CN(i-Pr)C(Me)=C(Me)N(i-Pr)}\}]^+$
212	100 (EI and FAB MS)	$[S=\overline{CN(i-Pr)C(Me)=C(Me)N(i-Pr)}]^+$
170	20 (EI and FAB MS)	$[S=\overline{CN(i-Pr)C(Me)=C(Me)N}]^+$
13c		
735	95 (ESI MS)	$[(C_6F_5)_2Au\{S=\overline{CNHCH_2CH_2NH}\}_2]^+$
561	8 (ESI MS)	$[(C_6F_5)Au\{S=\overline{CNHCH_2CH_2NH}\}_2]^+$
401	100 (ESI MS)	$[Au\{S=\overline{CNHCH_2CH_2NH}\}_2]^+$

The molecular ion of $[(C_6F_5)Au\{S=\overline{CN(i-Pr)C(Me)=C(Me)N(i-Pr)}\}]^+$, **13b** is observed at *m/z* 576. The peak at *m/z* 621 results from a homoleptic rearrangement of the cationic complex to form $[Au\{S=\overline{CN(i-Pr)C(Me)=C(Me)N(i-Pr)}\}_2]^+$. A peak appearing at *m/z* 353 corresponds to the fragment $[Au\{S=\overline{CN(i-Pr)C(Me)=C(Me)N(i-Pr)}\}]^+$. The peak at *m/z* 353 corresponds to $[(C_6F_5)Au]^+$. The base peak of **13b** at *m/z* 212 corresponds to the free ligand.

An ESI MS spectrum for sample **13c** displays a peak at *m/z* 735 that corresponds to $[(C_6F_5)_2Au\{S=\overline{CNHCH_2CH_2NH}\}_2]$ and the loss of $[C_6F_5]$ unit results in a peaks at *m/z* 561 and the base peak due to the homoleptic rearrangement at *m/z* 401.

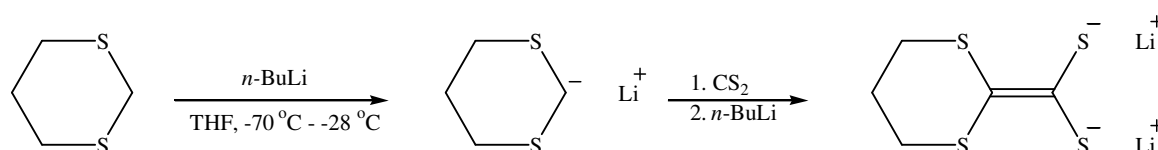
Table 3.7 Mass spectrometry data of compounds **14a** and **14b**

<i>m/z</i>	Intensity (%)	Fragment ion
14a		
509	8	$[\text{Au}\{\text{S}=\overline{\text{CN}(\text{Me})\text{C}(\text{Me})=\text{C}(\text{Me})\text{N}(\text{Me})}\}_2]^+$
353	4	$[\text{Au}\{\text{S}=\overline{\text{CN}(\text{Me})\text{C}(\text{Me})=\text{C}(\text{Me})\text{N}(\text{Me})}\}]^+$
329	3	$[\text{Au}\{\text{S}=\overline{\text{CNC}(\text{Me})=\text{C}(\text{Me})\text{N}}\}]^+$
289	5	$[\text{Au}\{\text{S}=\overline{\text{CNC}=\text{CN}}\}]^+$
157	8	$[\text{S}=\overline{\text{CN}(\text{Me})\text{C}(\text{Me})=\text{C}(\text{Me})\text{N}(\text{Me})}]^+$
125	5	$[\text{S}=\overline{\text{CNC}(\text{Me})=\text{C}(\text{Me})\text{N}}]^+$
14b		
691	3	$[(\text{Cl}_2)\text{Au}\{\text{S}=\overline{\text{CN}(i\text{-Pr})\text{C}(\text{Me})=\text{C}(\text{Me})\text{N}(i\text{-Pr})}\}_2]^+$
621	17	$[\text{Au}\{\text{S}=\overline{\text{CN}(i\text{-Pr})\text{C}(\text{Me})=\text{C}(\text{Me})\text{N}(i\text{-Pr})}\}_2]^+$
409	10	$[\text{Au}\{\text{S}=\overline{\text{CN}(i\text{-Pr})\text{C}(\text{Me})=\text{C}(\text{Me})\text{N}(i\text{-Pr})}\}]^+$
212	26	$[\text{S}=\overline{\text{CN}(i\text{-Pr})\text{C}(\text{Me})=\text{C}(\text{Me})\text{N}(i\text{-Pr})}]^+$
169	7	$[\text{S}=\overline{\text{CN}(i\text{-Pr})\text{C}(\text{Me})=\text{C}(\text{Me})\text{N}}]^+$
126	7	$[\text{S}=\overline{\text{CNC}(\text{Me})=\text{C}(\text{Me})\text{N}}]^+$

The FAB MS data for the neutral thione gold(III) complexes **14a** and **14b** are summarised in Table 3.7. The fragmentation pattern of the neutral complex **14b** indicates that a four coordinate gold(III) ion, $[(\text{Cl}_2)\text{Au}\{\text{S}=\overline{\text{CN}(i\text{-Pr})\text{C}(\text{Me})=\text{C}(\text{Me})\text{N}(i\text{-Pr})}\}_2]^+$ at *m/z* 691 is a result of rearrangement between the fragment ions in the mass spectrometer. A common trend for both complexes **14a** and **14b** is observed in the fragmentation patterns. Peaks at *m/z* 509 and 621, which respectively correspond to the homoleptic rearrangement products $[\text{Au}(\text{thione})_2]^+$ (Table 3.7). Both the homoleptically rearranged products of $[\text{Au}(\text{thione})_2]^+$ fragment further by loss of one of the thione ligands to give a peak at *m/z* 329 or 409 corresponding to $[\text{Au}\{\text{S}=\overline{\text{CNC}(\text{Me})=\text{C}(\text{Me})\text{N}}\}]^+$ or $[\text{Au}\{\text{S}=\overline{\text{CN}(i\text{-Pr})\text{C}(\text{Me})=\text{C}(\text{Me})\text{N}(i\text{-Pr})}\}]^+$. Subsequent fragment ions of the respective ligands appear at *m/z* 157 or 212.

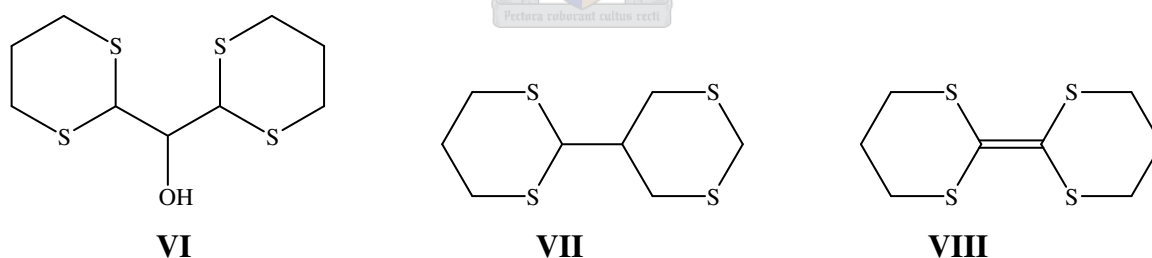
3.2.3 Cationic sulphonium complexes of gold(I)

The intermediate compound dilithio-1,3-dithiane-2-carbodithioate, $[\text{Li}_2\text{S}_2\text{C}=\overline{\text{CSCH}_2\text{CH}_2\text{CH}_2\text{S}}]$, was prepared from reaction of 1,3-dithiane in THF with *n*-BuLi at $-70\text{ }^\circ\text{C}$ to $-28\text{ }^\circ\text{C}$ and the addition of a similar mole quantity of CS_2 followed by the subsequent addition of a second portion of *n*-BuLi to obtain a red dianion solution (Scheme 3.9).²¹ The mixture was kept under an inert atmosphere for 1 h while the temperature was maintained at $-75\text{ }^\circ\text{C}$.



Scheme 3.9

Of note is that certain side reactions of 1,3-dithiane have been reported. The alkanol, di(1,3-dithian-2-yl)methanol **VI**, and dimers such as 2,2'-bi(1,3-dithianyl), **VII**, and 2,2'-bidithianyliden, **VIII**, (Scheme 3.4) were obtained in the preparation of 2-lithio-1,3-dithiane due to the presence of the oxidising impurity in *n*-BuLi (perhaps *n*-BuOOLi), excess of *n*-BuLi, air or moisture.^{22,23,24,25}



Scheme 3.10

The $[\{\text{Li}_2\text{S}_2\text{C}=\overline{\text{CSCH}_2\text{CH}_2\text{CH}_2\text{S}}]$ prepared as described above was used directly for reaction with $(\text{ClAu})_2\text{dppm}$ or $(\text{ClAu})_2\text{dppe}$, while the temperature was maintained at $-75\text{ }^\circ\text{C}$. In our procedure, a suspension of similar mole quantities of bis $[(\text{ClAu})_2\text{dppm}]$ or

²¹ D. M. Baird and R. D. Bereman, *J. Org. Chem.*, 1981, **46**, 458.

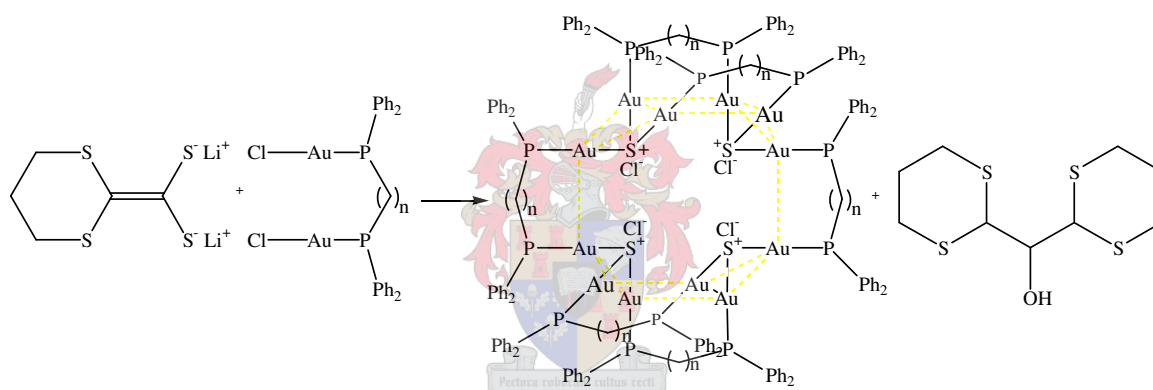
²² (a) N. P. Argade, B. G. Hazra and P. L. Joshi, *Synth. Comm.*, 1996, **26**, 2797. (b) C. A. Keal and M. A. Sackville, *J. Chem. Res. (M)*, 1986, 2501.

²³ R. B. Bates, L. M. Kroposki and D. E. Potter, *J. Org. Chem.*, 1972, **37**, 4.

²⁴ J. Thiem and H.-P. Wessel, *Liebigs Ann. Chem.*, 1983, 2173.

²⁵ I. Stahl, *Chem. Ber.*, 1985, **118**, 4857.

$[(\text{ClAu})_2\text{dppe}]$ in THF was transferred to the intermediate dianion $[\text{Li}_2\text{S}_2\text{C}=\overline{\text{CSCH}_2\text{CH}_2\text{CH}_2\text{S}}]$ and stirred for 2 h at $-75\text{ }^\circ\text{C}$. The temperature of the reaction mixtures was then raised to room temperature slowly and the solvent removed under vacuum. The residues were redissolved in dichloromethane and filtered through Celite. Crystallisation from a dichloromethane solution by slow evaporation at $-20\text{ }^\circ\text{C}$ afforded light yellow crystals of the polynuclear cationic tetrameric sulphonium complex of **15a** (Scheme 3.11) indicating that an oxidation reaction might have occurred. Colourless crystals of di(1,3-dithian-2-yl)methanol were also isolated from a dichloromethane solution of **15a** by slow evaporation at room temperature. These cationic complexes are stable in air and are soluble in THF, dichloromethane and acetone but insoluble in *n*-pentane, *n*-hexane and diethyl ether. The ^1H and ^{13}C NMR data indicate that the residues contain a derivative of an unknown product that contains *n*-butyl group.



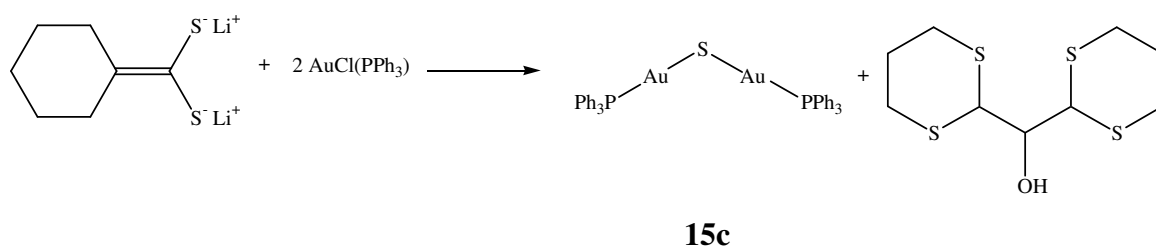
15a, $n = 1$ and

15b, $n = 2$

Scheme 3.11

A similar procedure as for **15a** and **15b** was followed using the triphenylphosphinegold(I) chloride, $\text{AuCl}(\text{PPh}_3)$. Protection from air and other oxidising agents in these experiments was absolutely necessary. A light yellow residue containing a cationic monomeric sulphonium complex (trinuclear gold(I) complex) was obtained. The final crude product obtained from this reaction is soluble in THF, dichloromethane and acetone and insoluble in diethyl ether, *n*-pentane and *n*-hexane. Crystallisation from dichloromethane solution layered with *n*-pentane afforded colourless crystals at $-20\text{ }^\circ\text{C}$ suitable for single crystal X-ray analysis. According to the ^1H and ^{13}C NMR spectra, the mixture also contained by-products of 1,3-dithiane derivatives and other unknown by-products incorporating the *n*-

butyl group. Single crystal X-ray analysis also enabled us to isolate and determine the molecular structure of the known gold(I) sulphide complex, $S(AuPPh_3)_2$, indicating that oxidation of the intermediate products might have occurred during the reaction. Whereas, the ESI MS results clearly indicated the presence of a monomeric cationic sulphonium complex, $[S(AuPPh_3)_3]^+$, this peak could have resulted from the fragment ion rearrangement within the mass spectrometer. ^{13}C NMR data confirmed that di(1,3-dithian-2-yl)methanol is one of the products (Scheme 3.12).



Scheme 3.12

3.2.4 Spectroscopic characterisation of compounds 15a - 15c

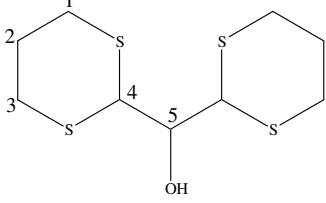
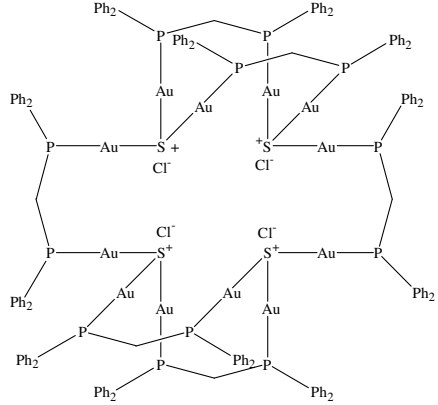
NMR spectroscopy

3.2.4.1

$(Cl)S-\{AuP(Ph_2)CH_2P(Ph)_2Au\}_2-S(Cl)-\{AuP(Ph_2)CH_2P(Ph)_2Au\}-S(Cl)-\{AuP(Ph_2)CH_2P(Ph)_2Au\}_2-S(Cl)-\{AuP(Ph_2)CH_2P(Ph)_2Au\}$, **15a** and di(1,3-dithian-2-yl)methanol

The 1H , ^{13}C and ^{31}P NMR data of compound **15a** and di(1,3-dithian-2-yl)methanol are summarised in Table 3.8. The 1H and ^{13}C NMR data show complicated spectra due to unknown by-products of 1,3-dithiane derivatives such as di(1,3-dithian-2-yl)methanol, 2,2'-bis(1,3-dithianyl) or 2,2'-bisdithianylidene and other by-products of ring opening. A broad doublet at 7.68 -7.18 ppm is assigned to the phenyl ring protons.²¹⁻²⁵ The signals for protons H^1 and H^3 representing the derivative of 1,3-dithiane are obscured by the strong signals from the methylene protons of the dppm ligand at 2.80 ppm and it is difficult to characterise them fully. The methylene CH_2 protons appear upfield with respect to the signals for the CH_2 group in the precursor, $[(AuCl)_2dppm]$ which normally appear at 3.60 ppm. Signals at 3.44 – 4.07 ppm and 2.03 ppm are tentatively assigned to the protons H^4/H^5 and H^2 , respectively.

Table 3.8 ^1H and ^{13}C NMR data of compound **15a** in CD_2Cl_2 and di(1,3-dithian-2-yl)methanol

		 <p style="text-align: center;">15a</p>
Assignment	$\delta(\text{ppm})$ (multiplicity, J(Hz))	$\delta(\text{ppm})$ (multiplicity, J(Hz))
<p>^1H NMR</p> <p>H^4 and H^5 H^1 and H^3 H^2 $(\text{Ph}_2)\text{P}\underline{\text{C}}\text{H}_2\text{P}(\text{Ph}_2)$ Ph</p>	<p>4.07 - 3.44 (2H, bm) not observed 2.03 (2H, s)</p>	<p>2.78 (12H, t, $^2J_{\text{H-H}} = 7.35$ Hz) 7.63 - 7.23 (240H, m)</p>
<p>^{13}C NMR</p> <p>C^4 and C^5 C^1 and C^3 C^2 $(\text{Ph}_2)\text{P}\underline{\text{C}}\text{H}_2\text{P}(\text{Ph}_2)$ C^{meta} C^{para} C^{ortho} C^{ipso}</p>	<p>35.5 32.1 26.2</p>	<p>36.9 134.1 (bs) 132.2 (bs) 129.6 (bs) 127.3 (d, obscured)</p>
<p>^{31}P NMR</p>		<p>28.32 (b)</p>

The ^{13}C NMR signals of the phenyl groups resonated as broad signals with in the range of 134.1 – 127.3 ppm with no significant change in chemical shift. ^{13}C NMR data show two signals typical for the 1,3-dithiane derivative at 35.5 ppm and 32.1 ppm and are assigned to C^4/C^5 and C^1/C^3 , respectively.

The ^{31}P NMR displayed a broad signal at 35.00 - 25.00 ppm. Two shoulders at 28.61 ppm and 28.03 ppm reveal the presence of three types of phosphorous atoms. This could be due

to ring flopping of the $\text{Au}_2(\mu\text{-dppe})$ rings, as is commonly observed in other complexes $[\text{M}_2(\mu\text{-dppe})_2]$.²⁶

3.2.4.2

$(\text{Cl})\text{S}-\{\text{AuP}(\text{Ph})_2(\text{CH}_2)_2\text{P}(\text{Ph})_2\text{Au}\}_2-\text{S}(\text{Cl})-\{\text{AuP}(\text{Ph})_2(\text{CH}_2)_2\text{P}(\text{Ph})_2\text{Au}\}_2-\text{S}(\text{Cl})-\{\text{AuP}(\text{Ph})_2(\text{CH}_2)_2\text{P}(\text{Ph})_2\text{Au}\}_2-\text{S}(\text{Cl})-\{\text{AuP}(\text{Ph})_2(\text{CH}_2)_2\text{P}(\text{Ph})_2\text{Au}\}_2-\text{S}(\text{Cl})-\{\text{AuP}(\text{Ph})_2(\text{CH}_2)_2\text{P}(\text{Ph})_2\text{Au}\}_2$, **15b** and di(1,3-dithian-2-yl)methanol

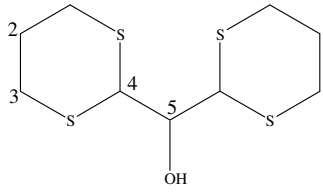
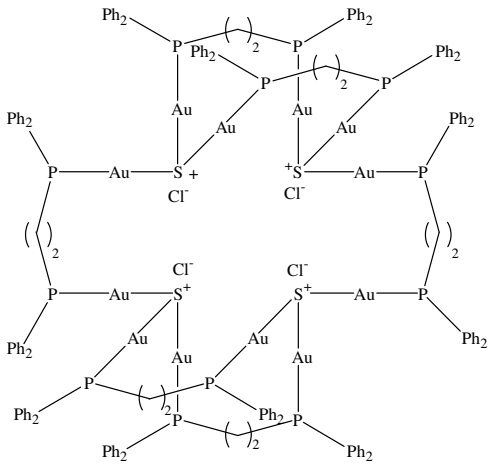
The ^1H , ^{13}C and ^{31}P NMR data of complex **15b** and di(1,3-dithian-2-yl)methanol are summarised in Table 3.9. The ^1H and ^{13}C NMR spectra are complicated due to the presence of unknown products as well as large numbers of protons from the cation. In the ^1H NMR spectrum the phenyl protons H^{ortho} , H^{meta} and H^{para} give a multiplet of signals at 7.72 - 7.44 ppm. The signal for the bridging ethylene protons $(\text{CH}_2)_2$ are complicated due to a fluxional (dynamic exchange) process.²⁷ Simultaneously, a broad signal at 2.80 ppm appearing as a shoulder on the signal for the ethylene protons of the dppe is assigned tentatively to H^1 and H^3 of the 1,3-derivative. The signals at δ 3.54 and 2.45 are similarly assigned to the protons of 1,3-dithiane derivative H^4 and H^2 , respectively.

The signals appearing at 132.6 ppm, 131.1 ppm, 129.6 ppm and 127.1 ppm in the ^{13}C NMR spectrum are assigned to the phenyl carbons C^{meta} , C^{para} , C^{ortho} and C^{ipso} , respectively. The coupling constants $J_{\text{C-P}}$ of the phenyl carbons are similar to those observed for $(\text{AuCl})_2\text{dppe}$. The bridging ethylene carbons, $(\text{CH}_2)_2$, correspond to the signal at 40.9 ppm, showing a slight downfield change in chemical shift with respect to the precursor complex $(\text{AuCl})_2\text{dppe}$. Signals corresponding to the 1,3-dithienyl derivative are observed as very weak signals and show a slight downfield change in chemical shift. Signals at 35.5 ppm, 32.1 ppm and 26.2 ppm are assigned to the carbons C^4/C^5 , C^1/C^3 and C^2 of the 1,3-dithianyl derivative. Only one signal has been detected for each carbon atom for C^{para} and C^{ipso} .

²⁶ (a) C. T. Hunt and A. L. Balch, *Inorg. Chem.*, 1981, **20**, 2267. (b) A. Blagg, A. T. Hutton, P. G. Pringle and B. L. Shaw, *J. Chem. Soc., Dalton Trans.*, 1984, 1815.

²⁷ M.-C. Brandys, M. C. Jennings and R. J. Puddephatt, *J. Chem. Soc., Dalton Trans.*, 2000, 4601.

Table 3.9 ^1H and ^{13}C NMR data of compound **15b** in CD_2Cl_2 and di(1,3-dithian-2-yl)methanol

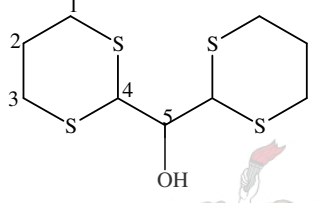
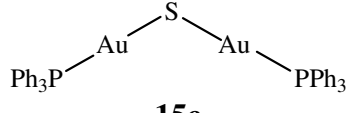
		 <p style="text-align: center;">15b</p>
Assignment	$\delta(\text{ppm})$ (multiplicity, J(Hz))	$\delta(\text{ppm})$ (multiplicity, J(Hz))
<p>^1H NMR</p> <p>H^4 and H^5 H^1 and H^3 H^2 $\text{H}[(\text{Ph}_2\text{P}(\underline{\text{C}}\text{H}_2)_2\text{P}(\text{Ph}_2)]$ Ph</p> <p>^{13}C NMR</p> <p>C^4 C^1 and C^3 C^2 $[(\text{Ph}_2\text{P}(\underline{\text{C}}\text{H}_2)_2\text{P}(\text{Ph}_2)]$ C^{meta} C^{para} C^{ortho} C^{ipso}</p> <p>^{31}P NMR</p>	<p>3.54 (2H, bs) 2.80 (4H, bs) 2.45 (2H, bs)</p> <p>35.5 32.1 26.2</p> <p>40.9 132.6 (d, $^3\text{J}_{\text{C-P}} = 28.8$ Hz) 131.1 (d, obscured) 129.6 (d, $^2\text{J}_{\text{C-P}} = 13.9$ Hz) 127.1 (d, obscured)</p>	<p>2.72 (24H, m) 7.72 - 7.44 (240H, b)</p> <p>37.76, 35.29, 21.87</p>

The ^{31}P NMR spectrum of compound **15b** shows three different types of phosphorous signals at δ 37.76, 35.29 and 21.87 probably due to ring flopping of the Au_2dpppe and symmetry of the molecule. The first two signals show a downfield change in chemical shift with respect to the signal in the ^{31}P NMR of the precursor gold(I) complex, which appears at 32.45 ppm.

3.2.4.3 [S(AuP(Ph₃)₂)]₂, **15c** and di(1,3-dithian-2-yl)methanol

The ¹H, ¹³C and ³¹P NMR spectra of compound **15c** and di(1,3-dithian-2-yl)methanol are summarised in Table 3.10. They show complicated signals. The multiplet of signals at 7.44 - 7.56 ppm is assigned to the phenyl protons H^{ortho}, H^{meta} and H^{para} of **15c**. The signals at δ 4.26, 2.99 and 2.66 are assigned to the protons H⁴/H⁵, H¹/H³ and H² of the di(1,3-dithian-2-yl)methanol or any of the derivatives of the 1,3-dithianyl product that may also contribute to these complications (Scheme 3.10).

Table 3.10 ¹H and ¹³C NMR data of compound **15c** and di(1,3-dithian-2-yl)methanol in CDCl₃

Assignment	δ(ppm) (multiplicity, J(Hz))	δ(ppm) (multiplicity, J(Hz))	
<div style="display: flex; justify-content: space-around; align-items: center;"> <div style="text-align: center;">  </div> <div style="text-align: center;">  <p>15c</p> </div> </div>			
¹H NMR			
H ⁴ , and H ⁵	4.26 (2H, s)	7.44 - 7.56 (30, m)	
H ¹ and H ³	2.99 (2H, m)		
H ²	2.66 (1H, m)		
Ph			
¹³C NMR			
C ⁵	75.4	130.8 (d, ¹ J _{C-P} = 249.8 Hz)	
C ⁴	47.9		
C ^{1,3}	27.8		
C ²	25.9		
C ^{ipso}			134.8 (d, ³ J _{C-P} = 14.1 Hz)
C ^{meta}			132.0 (d, obscured)
C ^{para}			129.7 (d, ² J _{C-P} = 11.2 Hz)
C ^{ortho}			
³¹P NMR		34.97	

In the ¹³C NMR spectrum the signals for the phenyl carbons appear as expected and no significant change in chemical shift is observed with respect to the precursor AuCl(PPh₃).

The coupling constants, J_{C-P} , are similar to those reported for AuCl(PPh₃). The signals at δ 75.4, 47.9, 27.8 and 25.9 are assigned to the carbons C⁵, C⁴, C¹/C³ and C² in di(1,3-dithian-2-yl)methanol, respectively.^{16,17}

The largest signal in the ³¹P NMR spectrum has the same chemical shift as the starting material AuCl(PPh₃). An additional signal at 35.00 ppm of very low intensity is observed.

Mass Spectrometry

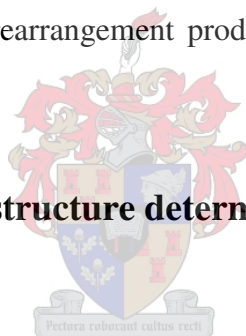
Table 3.11 Mass spectrometric data of compounds **15a**, **15b** and **15c**

<i>m/z</i>	Intensity (%)	Fragment ion
15a		
842	3	[S-{AuPPh ₂ CH ₂ PPh ₂ Au}-S] ⁺
811	10	[{AuPPh ₂ CH ₂ PPh ₂ Au}-S] ⁺
777	2	[AuPPh ₂ CH ₂ PPh ₂ Au] ⁺
580	10	[PPh ₂ CH ₂ PPh ₂ Au] ⁺
459	4	[AuPPh ₃] ⁺
384	6	[Ph ₂ PCH ₂ PPh ₂] ⁺
307	4	[PPhCH ₂ PPh ₂] ⁺
121	28.5	[S(CH ₂) ₃ SCH ₂] ⁺
15b		
857	2	[S-{AuPPh ₂ CH ₂ CH ₂ PPh ₂ Au}-S] ⁺
825	7	[{AuPPh ₂ CH ₂ CH ₂ PPh ₂ Au}-S] ⁺
791	1	[AuPPh ₂ CH ₂ CH ₂ PPh ₂ Au] ⁺
594	3	[AuPPh ₂ CH ₂ CH ₂ PPh ₂] ⁺
459	2	[AuPPh ₃] ⁺
321	3	[Ph ₂ PCH ₂ CH ₂ PPh] ⁺
15c		
1409	100	[S{AuPPh ₃ } ₃] ⁺
721	20	[Au(PPh ₃) ₂] ⁺

The mass spectrometric data of the cationic sulphonium complexes **15a** (FAB MS), **15b** (FAB MS) and **15c** (ESI MS) are summarised in Table 3.15. The molecular ions of the polynuclear (12) tetrameric cationic sulphonium complexes **15a** and **15b** are not observed. However, peaks at m/z 842 or 857 correspond to fragments of the bulky tetrameric cationic sulphonium complexes namely $[\text{S-AuP}(\text{Ph}_2)\text{CH}_2\text{P}(\text{Ph})_2\text{Au-S}]^+$ or $[\text{S-AuP}(\text{Ph}_2)\text{CH}_2\text{CH}_2\text{P}(\text{Ph})_2\text{Au-S}]^+$, of **15a** or **15b**, respectively. Again, both ions fragment further by stepwise loss of the S atoms with peaks corresponding to $[\text{AuPPh}_2\text{CH}_2\text{PPh}_2\text{Au}]^+$ and $[\text{AuPPh}_2\text{CH}_2\text{CH}_2\text{PPh}_2\text{Au}]^+$ at m/z 777 or 791, respectively. Peaks at m/z 307 or 321 indicate loss of one phenyl group from dppm and dppe, *i.e.* $[(\text{Ph})\text{PCH}_2\text{P}(\text{Ph})_2]^+$ or $[(\text{Ph})\text{PCH}_2\text{CH}_2\text{P}(\text{Ph})_2]^+$.

A peak for the 1,3-dithiane appears at m/z 121 in residue **15a** only. The molecular ion corresponding to **15c** was not observed, however, the base peak of the monomeric cationic sulphonium complex $[\text{S}\{\text{Au}(\text{PPh}_3)\}_3]^+$, appears at m/z 1409. A further fragment corresponding to the homoleptic rearrangement product, $[\text{Au}(\text{PPh}_3)_2]^+$ is indicated by a signal at m/z 721.

3.3 Crystal and molecular structure determinations by means of X-ray diffraction



The molecular and crystal structures of thione gold(I) and gold(III) complexes **13a**, **13b** and **14b** and the cationic sulphonium complex **15a** are discussed in the following subsections 3.3.1 – 3.3.4. All hydrogen atoms of **13b** and **15a** are omitted for clarity. Similarly, the chlorine counter ions and the phenyl rings (represented by one carbon each) are also omitted for clarity. Molecular interactions are also reported for **13a**, **13b** and **14b** only. Molecular structures of **15a** and di(1,3-dithian-2-yl)methanol were isolated and determined by X-ray analysis from the reaction between $(\text{AuCl})_2\text{dppm}$ and dilithio-1,3-dithiane-2-carbodithioate, $[\text{Li}_2\text{S}_2\text{C}=\overline{\text{CS}}\text{CH}_2\text{CH}_2\text{CH}_2\text{S}]$. Only **15a** is reported in this study, since the alkanol di(1,3-dithian-2-yl)methanol is already known.²⁸

²⁸ P. C. B. Page, D. J. Chadwick, M. B. Van Niel and D. Westwood, *Acta Crystallogr., Sec. C*, 1987, **C43**, 803.

3.3.1 The crystal and molecular structure of 13a

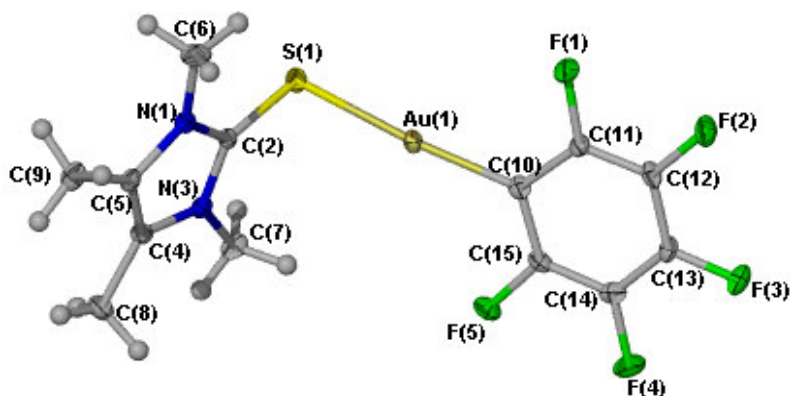


Figure 3.1 Drawing of the molecular structure of **13a**.

Compound **13a** crystallised from a diethyl ether solution layered with *n*-pentane in the monoclinic space group $P2_1/n$ as light yellow crystals at $-20\text{ }^\circ\text{C}$. Selected bond distances and angles are listed in Table 3.12. The molecular structure of **13a** is shown in Figure 3.1. The X-ray analysis shows that the ligand is coordinated through the thione sulfur. The Au(1)–C(10) bond length [2.019(4) Å] is comparable to that in other existing thione gold(I) complexes.²⁹ The Au–S bond length [2.304(11) Å] is in agreement with the values obtained for [Au(C₆F₅){S=CN(H)C(CH₃)=C(H)S}],²⁹ but slightly shorter than that in dihydrogenbis(2-mercapto-1-methylimidazole-3-yl)borato-1-triphenylphosphine)gold(I).³⁰ No intermolecular aurophilic Au–Au interaction is observed probably due to the repulsive forces of the lone pair of electrons in the thione sulfur, *i.e.*, the Au(1)–Au(1) separation [5.547 Å] observed is out of the range for aurophilic interaction. The S(1)–C(2) bond length of [1.726(4) Å] shows slight elongation with respect to the uncoordinated ligand [1.690 Å].³¹ This might be the result of electron density transfer from the C=S group of the ligand to the electrophilic gold(I) metal centre upon formation of the Au(1)–S(1) bond.

Coordination at the gold atom slightly deviates from linearity and the bond angle C(10)–Au(1)–S(1) [175.56(12)°] is comparable to dicyano-bis(imidazolidine-2-thione)-digold(I).³² The torsion angles Au(1)–S(1)–C(2)–N(3) [–73.8(4)°] and Au(1)–S(1)–C(2)–N(1) [111.6(3)°] indicate that the plane consisting of Au(C₆F₅) is tilted towards one side of

²⁹ S. Cronje, H. G. Raubenheimer, H. S. C. Spies, C. Esterhuysen, H. Schmidbaur, A. Schier and G. J. Kruger, *Dalton Trans.*, 2003, 2859.

³⁰ A. A. Mohamed, D. Rabinovich and J. P. Fackler, *Acta Crystallogr., Sect. E. Struct. Rep.*, 2002, **58**, 726.

³¹ N. Kuhn, J. Fahl, R. Famzi and M. Steimann, *Z. Kristallogr.*, 1998, **213**, 434.

³² F. B. Stacker and D. Britton, *Acta Crystallogr., Sect. C: Cryst. Struct. Commun.*, 2000, **56**, 798.

the ligand. The dihedral angle between the planes defined by coordination centre and the imidazoline ring is 64.06° .

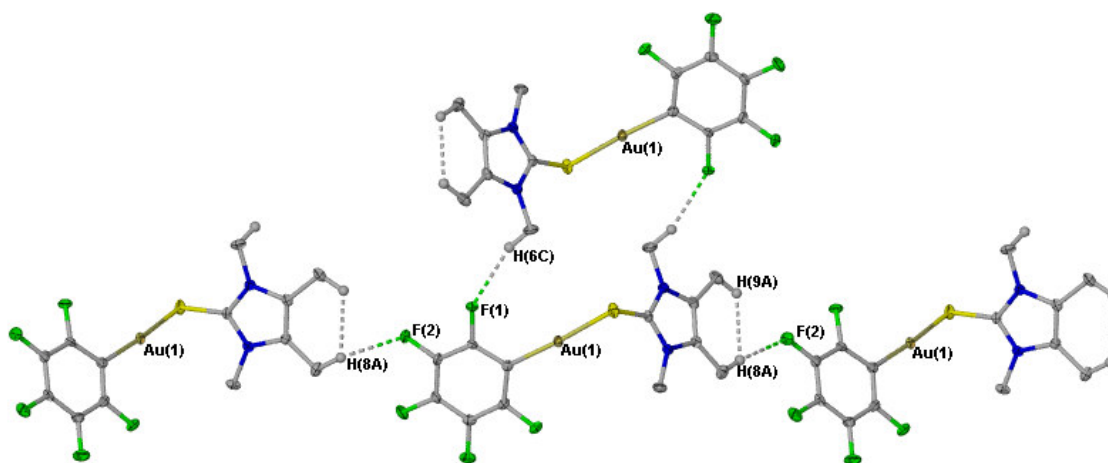


Figure 3.2 Diagram of **13a** showing intermolecular and intramolecular interactions.

The H(8A)---F(2) and H(6C)---F(1) distance indicate the shortest intermolecular interactions within the range of hydrogen bonding.

The packing diagrams of the molecules of **13a** along the b-axis (A) and c-axis (B) are shown in Figure 3.3. When the unit cell packing is viewed down the crystallographic b-axis, molecules are stacked symmetrically on top of each other alternatingly, *i.e.*, molecules in one layer are oriented in one direction, whereas the molecules in the next layer are oriented in the opposite direction. This shows that two molecules on successive layers are related by a centroid just lying in a space between the molecules.

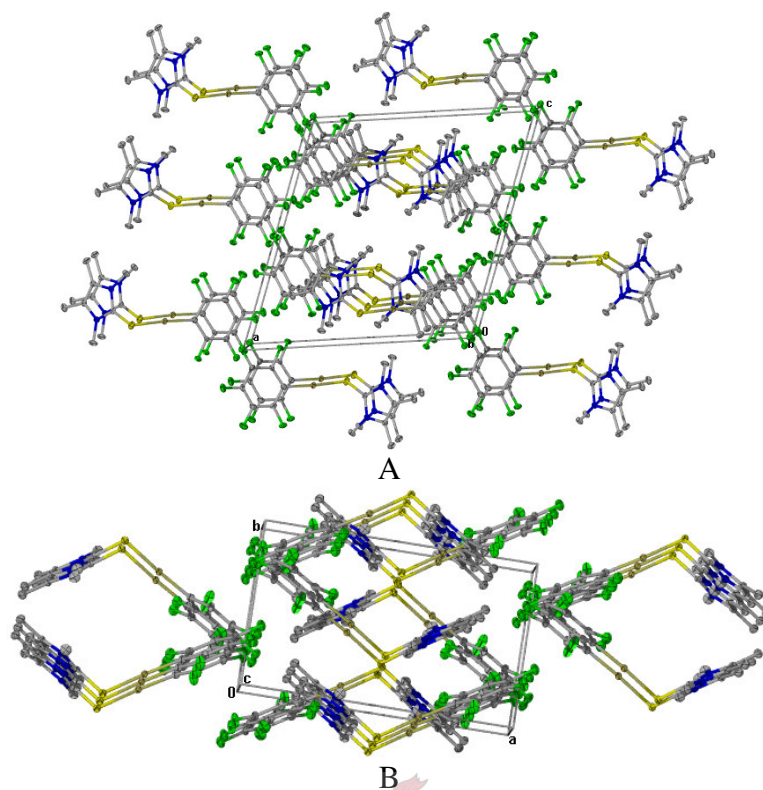


Figure 3.3 Packing diagram of the molecules of **13a** along the b-axis (A) and c-axis (B).

Table 3.12 Selected bond lengths (Å) and angles (°) for compound **13a**

Au(1)–C(10)	2.019(4)	N(1)–C(2)	1.341(5)
Au(1)–S(1)	2.3044(11)	N(1)–C(5)	1.392(5)
S(1)–C(2)	1.726(4)	N(1)–C(6)	1.460(5)
N(3)–C(2)	1.349(5)	C(5)–C(4)	1.351(6)
N(3)–C(4)	1.385(5)	C(5)–C(9)	1.506(6)
N(3)–C(7)	1.463(5)	C(4)–C(8)	1.485(6)
C(10)–Au(1)–S(1)	175.56(12)	C(5)–N(1)–C(6)	124.9(4)
C(2)–S(1)–Au(1)	104.71(14)	N(1)–C(2)–N(3)	106.7(3)
C(15)–C(10)–Au(1)	124.5(3)	N(1)–C(2)–S(1)	126.4(3)
C(11)–C(10)–Au(1)	122.3(3)	N(3)–C(2)–S(1)	126.8(3)
C(2)–N(3)–C(4)	109.9(3)	C(4)–C(5)–N(1)	107.0(4)
C(2)–N(3)–C(7)	123.8(4)	N(1)–C(5)–C(9)	121.5(4)
C(4)–N(3)–C(7)	126.3(3)	C(5)–C(4)–N(3)	106.8(4)
C(2)–N(1)–C(5)	109.7(3)	N(3)–C(4)–C(8)	123.3(4)
C(2)–N(1)–C(6)	125.4(4)		

3.3.2 The crystal and molecular structure of 13b

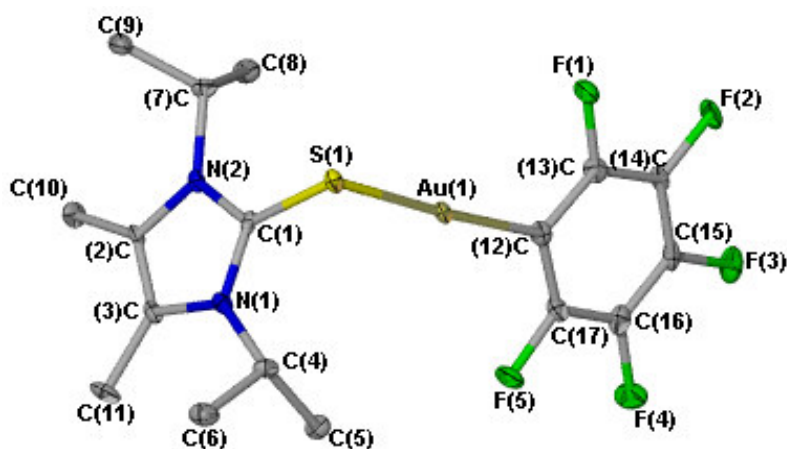


Figure 3.4 Drawing of the molecular structure of **13b**.

Compound **13b** crystallised from a dichloromethane solution layered with *n*-hexane in the monoclinic space group *C2/c* as colourless crystals at -20 °C. Selected bond lengths and bond angles are listed in Table 3.13. The molecular structure of **13b** is shown in Figure 3.4. The basic molecular structure shows a monomeric complex where the ligand is coordinated *via* the S atom. The N(1)–C(1) and N(2)–C(1) bond lengths [1.354(7) and 1.351(7) Å respectively] are normal.³³ The coordination effect slight elongation of the C–S bond length [1.733(6) Å] when compared to the uncoordinated ligand, but is shorter than the typical C–S single bond distance 1.819 Å. The C–S bond lengths of **13a** and **13b** have shown similar effects upon coordination. The Au(1)–S(1) bond length [2.3170(13) Å] lies within the expected range of [2.28 - 2.320 Å]. Many gold(I) thiolates (also drugs) typically have a linear S–Au–S entity with Au–S bond distances of about 2.29 Å.³⁴ No significant Au(1)–Au(1) interaction is present in **13b**.

The geometry at the coordination centre C(12)–Au(1)–S(1) [176.50(16)°] deviates slightly from linearity by 3.50°. The C(1)–S(1)–Au(1) bond angle of 101.00(18)° indicates lone-pair bonding-pair repulsion on the sulfur atom. The torsion angles N(1)–C(1)–S(1)–Au(1) [83.04°] and N(2)–C(1)–S(1)–Au(1) [95.00°] indicate that the plane S–AuC₆F₅ is slightly

³³ N. Burford, A. D. Phillips, H. A. Spinney, K. N. Robertson, T. S. Cameron and R. McDonald, *Inorg. Chem.*, 2003, **42**, 4949.

³⁴ C. F. Shaw, in *Gold: Progress in Chemistry, Biochemistry and Technology*, ed. H. Schmidbaur, John Wiley & Sons, Chichester, **1999**, p. 259.

tilted to one side of the imidazoline ring. The dihedral angle [79.93°] comprises the planes of the coordination centre and the imidazoline centre.

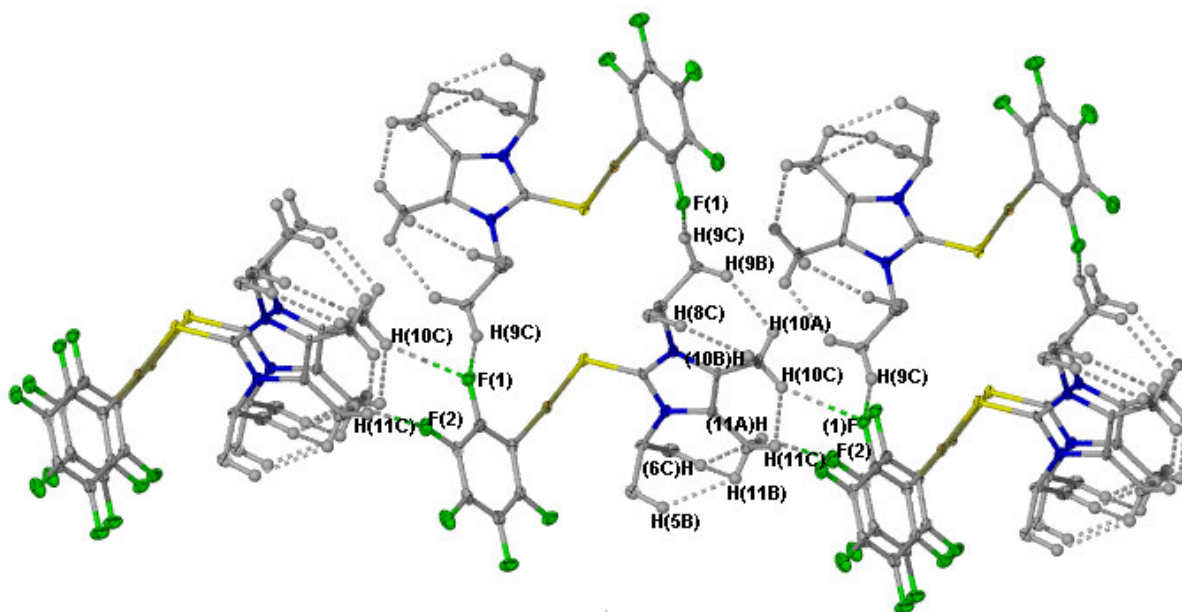


Figure 3.5 Diagram of **13b** showing intermolecular and intramolecular interactions.

Figure 3.5 shows intermolecular and intramolecular interactions. The intermolecular interactions between the neighbouring molecules of **13b** lie within the range of hydrogen bonding: F(2)---H(11A) [1.463 Å], F(1)---H(10C) [2.561 Å] and F(1)---H(9C) [2.592 Å]. All these intermolecular interactions influence the molecular packing.

The molecular packing for **13b** along the crystallographic b-axis (A) and c-axis (B) is shown in Figure 3.6. Molecules are stacked exactly on top of each other when viewed down the crystallographic b-axis, whereas, along the c-axis molecules are stacked on top of each other in an alternating fashion, *i.e.*, molecules in one layer are oriented in the opposite direction to the molecules on the following layer.

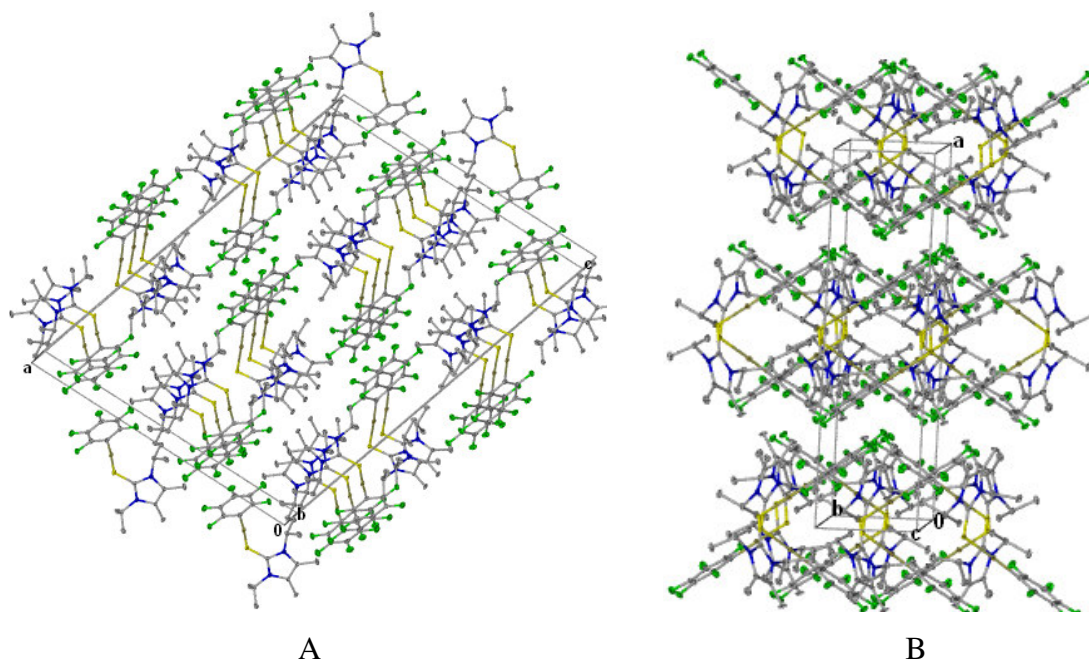


Figure 3.6 Packing diagram of the molecules of **13b** along the b-axis (A) and the c-axis (B).

Table 3.13 Selected interatomic bond lengths (Å) and angles (°) for compound **13b**

Au(1)–C(12)	2.023(6)	N(1)–C(4)	1.490(7)
Au(1)–S(1)	2.3170(13)	N(2)–C(1)	1.351(7)
S(1)–C(1)	1.733(6)	N(2)–C(2)	1.393(7)
N(1)–C(1)	1.354(7)	N(2)–C(7)	1.505(6)
N(1)–C(3)	1.395(7)	C(3)–C(2)	1.362(7)
C(12)–Au(1)–S(1)	176.50(16)	N(1)–C(4)–C(6)	111.4(5)
C(1)–S(1)–Au(1)	101.00(18)	N(1)–C(4)–C(5)	110.6(4)
C(1)–N(1)–C(3)	108.7(4)	C(2)–C(3)–N(1)	107.7(5)
C(1)–N(1)–C(4)	122.2(5)	N(1)–C(3)–C(11)	124.3(5)
C(3)–N(1)–C(4)	129.1(4)	C(3)–C(2)–N(2)	106.4(5)
C(1)–N(2)–C(2)	109.7(4)	N(2)–C(2)–C(10)	125.5(5)
C(1)–N(2)–C(7)	122.3(5)	N(2)–C(7)–C(9)	111.7(5)
C(2)–N(2)–C(7)	127.9(5)	N(2)–C(7)–C(8)	110.2(4)
N(2)–C(1)–N(1)	107.4(5)	C(17)–C(12)–Au(1)	124.1(4)
N(2)–C(1)–S(1)	126.3(4)	C(13)–C(12)–Au(1)	122.0(4)
N(1)–C(1)–S(1)	126.3(4)		

3.3.3 The crystal and molecular structure of 14b

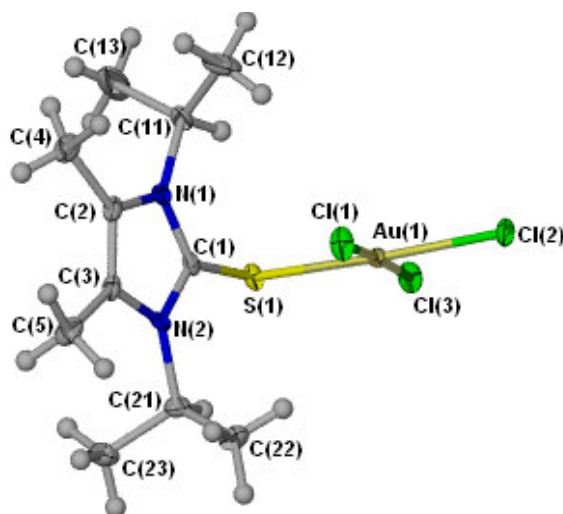


Figure 3.7 Drawing of the molecular structure of **14b**.

Compound **14b** crystallised from a dichloromethane solution layered with *n*-pentane in the orthorhombic space group $Pna2_1$ as red crystals. Selected bond lengths and angles are listed in Table 3.14. The molecular structure of **14b** is shown in Figure 3.7. Coordination of the ligand *via* the S atom has caused slight distortion at the coordination centre.

The Au(1)–Cl(2) bond length [2.3248(14) Å], is somewhat longer than the Au(1)–Cl(1) and Au(1)–Cl(3) bond lengths of 2.2780(16) and 2.2901(17) Å, respectively, due to the *trans* influence of the sulfur atom. Generally the Au–Cl bond lengths in **14b** are comparable to the Au–Cl bond lengths observed in AuCl₃(S=CHNMe₂) [2.244(12) – 2.290(12) Å].⁵ The Au(1)–S(1) bond length [2.3112(15) Å] is comparable to the Au–S bond length reported for **13b** [2.3170(13) Å] and [AuCl₃(S=CHNMe₂)] [2.296(12) Å]. The C(1)–S(1) bond length of [1.725(7) Å] is again slightly longer compared to the free ligand bond length [1.69 Å].

The gold atom is four-coordinate and the geometry at the coordination centre S(1)–Au(1)–Cl(2) [173.73(9)°] indicates significant deviation from linearity. The Cl(1)–Au(1)–S(1) and Cl(3)–Au(1)–S(1) bond angles of [95.68(8) and 82.93(8)°], where the two chlorine atoms are oriented in *cis*-positions show a slight deviation from the ideal geometry, whereas, the bond angles Cl(1)–Au(1)–Cl(2) [89.72(8)°] and Cl(3)–Au(1)–Cl(2) [91.80(8)°] are more or less the same although they appear with slight deviation from

[90.00°]. The C(1)–S(1)–Au(1) bond angle [106.88°] indicates the lone-pair bonding-pair repulsion on the sulfur atom. The torsion angles N(1)–C(1)–S(1)–Au(1) [86.00°] and N(2)–C(1)–S(1)–Au(1) [-97.29°] indicate that the plane of coordination defined by Au(1), Cl(1), Cl(2), Cl(3) and S(1) dissects the plane consisting of the imidazole ring between C(2) and C(3). Similarly, the dihedral angle [84.08°] between the coordination plane defined by Au(1), Cl(1), Cl(2), Cl(3), S(1) and the imidazole ring comprising N(1), C(2), C(3), N(2), C(1) and S(1) reveals the same observation.

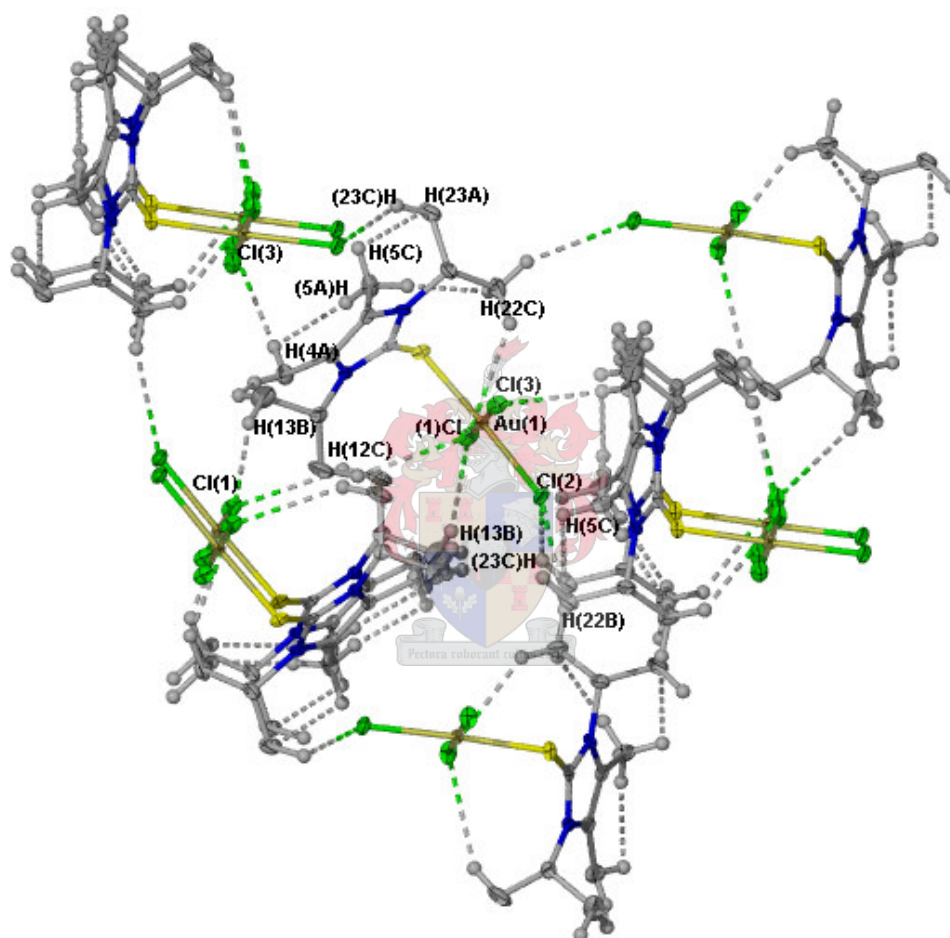


Figure 3.8 Diagram of **14b** showing intermolecular and intramolecular interactions.

Figure 3.8 depicts intermolecular and intramolecular interactions in such a way that the central molecule interacts with several neighbouring molecules within the range of hydrogen bonding.

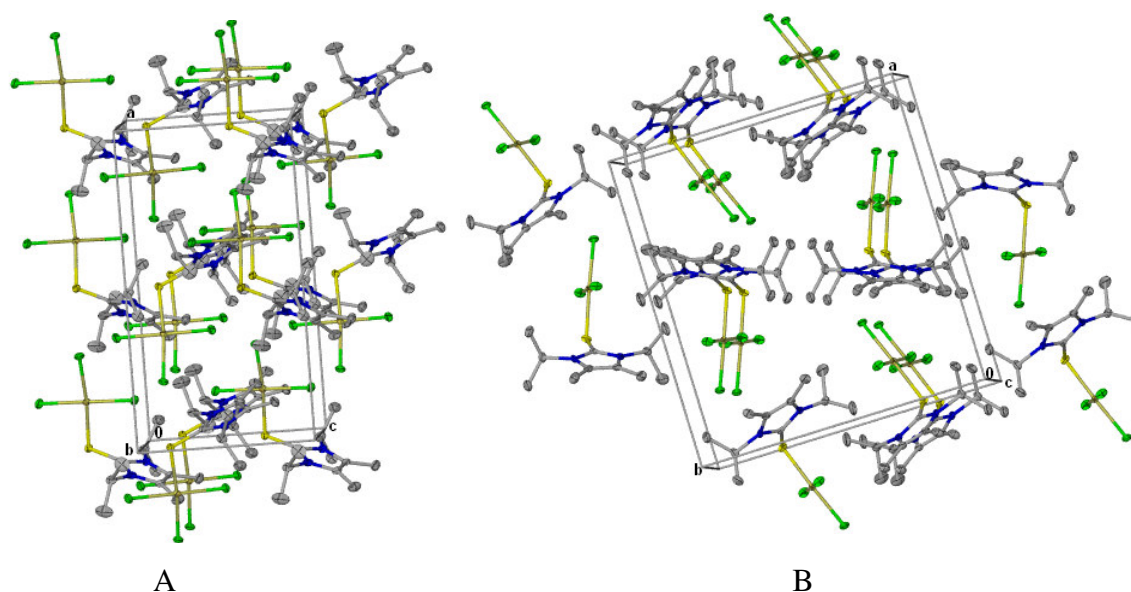


Figure 3.9 Packing diagram of the molecules of **14b** along the b-axis (A) and the c-axis (B).

The molecular packing diagram of **14b** is shown in Figure 3.9 along the crystallographic b-axis (A) and c-axis (B) of the unit cell. Molecules along the b-axis are stacked on top of each other in an alternating fashion, *i.e.*, molecules in one layer are oriented in the opposite direction to the molecules in the following layer. The molecules, however, are stacked on top of each other when viewed down the crystallographic c-axis.

Table 3.14 Selected interatomic bond lengths (Å) and angles (°) for compound **14b**

Au(1)–Cl(1)	2.2780(16)	N(2)–C(21)	1.497(7)
Au(1)–Cl(3)	2.2901(17)	C(3)–C(2)	1.350(9)
Au(1)–S(1)	2.3112(15)	C(3)–C(5)	1.482(9)
Au(1)–Cl(2)	2.3248(14)	N(1)–C(1)	1.345(8)
S(1)–C(1)	1.725(7)	N(1)–C(2)	1.376(8)
N(2)–C(1)	1.357(8)	N(1)–C(11)	1.486(8)
N(2)–C(3)	1.383(9)		
Cl(1)–Au(1)–Cl(3)	177.38(6)	C(1)–N(1)–C(2)	108.9(5)
Cl(1)–Au(1)–S(1)	95.68(8)	C(1)–N(1)–C(11)	122.3(5)
Cl(3)–Au(1)–S(1)	82.93(8)	N(1)–C(1)–N(2)	107.7(5)
Cl(1)–Au(1)–Cl(2)	89.72(8)	N(1)–C(1)–S(1)	126.7(5)

(continued...)

Cl(3)–Au(1)–Cl(2)	91.80(8)	N(2)–C(1)–S(1)	125.5(5)
S(1)–Au(1)–Cl(2)	173.73(9)	N(1)–C(11)–C(12)	111.3(6)
C(1)–S(1)–Au(1)	106.9(2)	N(1)–C(11)–C(13)	111.5(5)
C(1)–N(2)–C(3)	108.3(5)	N(2)–C(21)–C(22)	110.9(5)
C(1)–N(2)–C(21)	122.4(5)	N(2)–C(21)–C(23)	111.5(5)
C(3)–N(2)–C(21)	129.2(6)	C(3)–C(2)–N(1)	107.7(6)
C(2)–C(3)–N(2)	107.4(6)	N(1)–C(2)–C(4)	125.6(7)
N(2)–C(3)–C(5)	124.9(6)		

3.3.4 The crystal and molecular structure of 15a

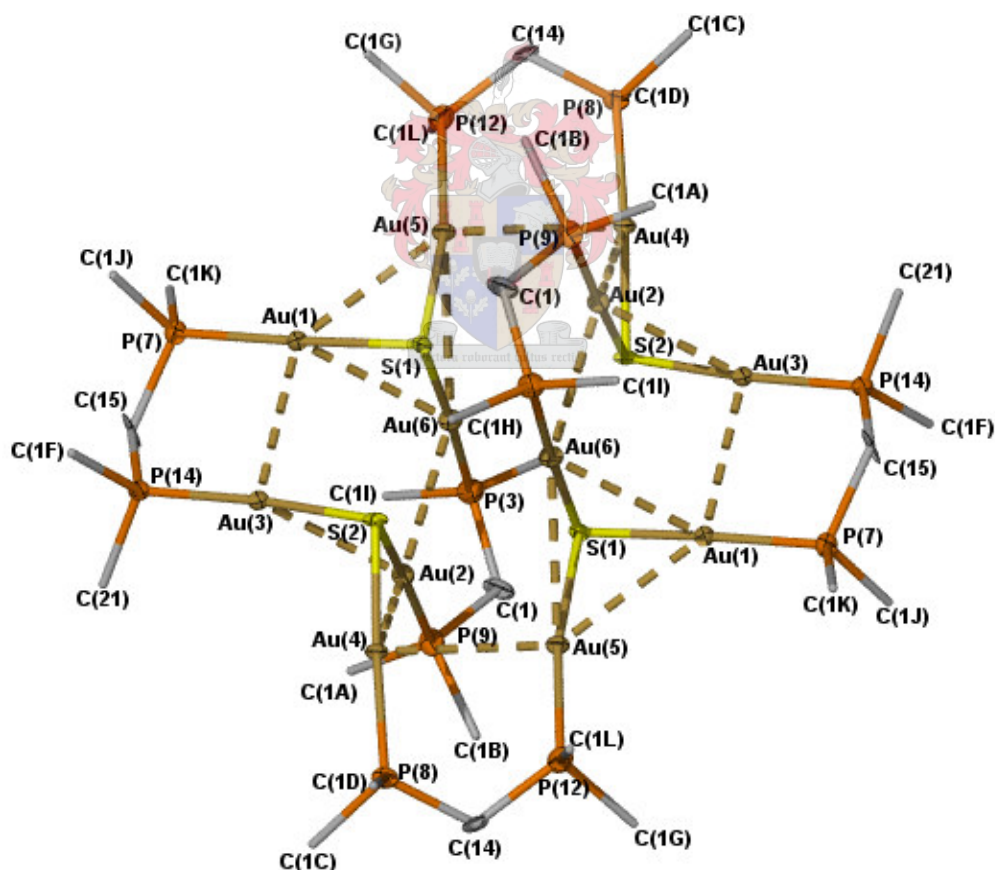


Figure 3.10 Drawing of the molecular structure of **15a**.

Compound **15a** crystallised in the monoclinic space group $P2_1/n$ as light yellow crystals from a dichloromethane solution by slow evaporation at $-20\text{ }^\circ\text{C}$. Selected bond lengths and

angles are listed in Table 3.15. The molecular structure of the dodecanuclear tetracationic sulphonium complex **15a** is shown in Figure 3.10. The molecular structure of the cationic sulphonium gold(I) complex shows a large cavity within the ring but no anion or solvent molecules are enclosed. The inefficient solid state packing and evaporation of the solvent led to poor data quality. Nevertheless, the data were sufficient to determine the structure of the cation carrying a positive charge of four.

Four sulfur atoms are coplanar and a crystallographic centre of inversion occurs at their centre. The four Au₃S units are linked by six bridging dppm ligands but are not identical: two have bond angles approaching 90° whereas the other two have one angle wider than 100°. Neither are the gold atoms in similar geometry arrangements. Au(3) and Au(4) exhibit only two aurophilic interactions each whereas all the other gold atoms have three. Furthermore, the gold atoms Au(1)–Au(3)–Au(2)–Au(6) are arranged in a square planar geometry with separation of *ca.* 3.105 Å. The deviation from the least square plane defined by Au(1)–Au(3)–Au(2)–Au(6) is found to be 0.0016 Å. The intramolecular Au–Au contacts shown in the structure range between 2.9834(15) - 3.2922(15) Å. Similarly, three gold atoms Au(1), Au(5) and Au(6) form trigonal planar geometry with Au–Au bond lengths averaging *ca.* 3.221 Å comparable to the intramolecular Au–Au bond lengths [2.83 - 3.409 Å] observed in [S(Au PPh₃)₃]PF₆, [(μ-Au₂dppf)₂]₂[OTf]₂, (dppf = bis(diphenylphosphanyl)ferrocene and [Au₁₂(μ₃-S)(μ-dppm)₆]X₄, (X = PF₆, ClO₄).^{35,36} No deviation from the least square plane defined by these atoms is found. The Au–S bond lengths range between 2.315(6) and 2.365(6) Å, which is in the range observed for Au-μ₃-sulfido complexes but longer than those found in μ₂-sulfido systems and shorter than those in μ₄-sulfido systems.¹⁴

The internal bond angles formed by the trigonal planar Au(1), Au(5) and Au(6) are *ca.* 60° each indicating a geometry of an equilateral triangle. The Au–S–Au angles range from 79.19 to 104.8°. The presence of a long Au(3)–Au(4) bond length of 3.678 Å and large bond angle Au(3)–S(2)–Au(4) [104.8(3)°] is probably due to the steric demands of the dppm ligands. The Au(I) centres are two coordinate and the geometry around the coordination centre of each Au(I) deviates from linearity significantly: S(2)–Au(2)–P(9)

³⁵ V. W.-W. Yam, E. C.-C. Cheng and K.-K. Cheung, *Angew. Chem. Int. Ed.*, 1999, **38**, 197.

³⁶ (a) M. Desmet, H. G. Raubenheimer and G. J. Kruger, *Organometallics*, 1997, **16**, 3324. (b) P. G. Jones, G. M. Sheldrick and E. Hädicke, *Acta. Crystallogr. Sect. B*, 1986, **36**, 2777.

[172.67°], S(2)–Au(3)–P(14) [173.48°], S(2)–Au(4)–P(8) [174.50°], S(1)–Au(1)–P(7) [177.98°], S(1)–Au(5)–P(12) [169.10°] and S(1)–Au(6)–P(3) [176.36°].

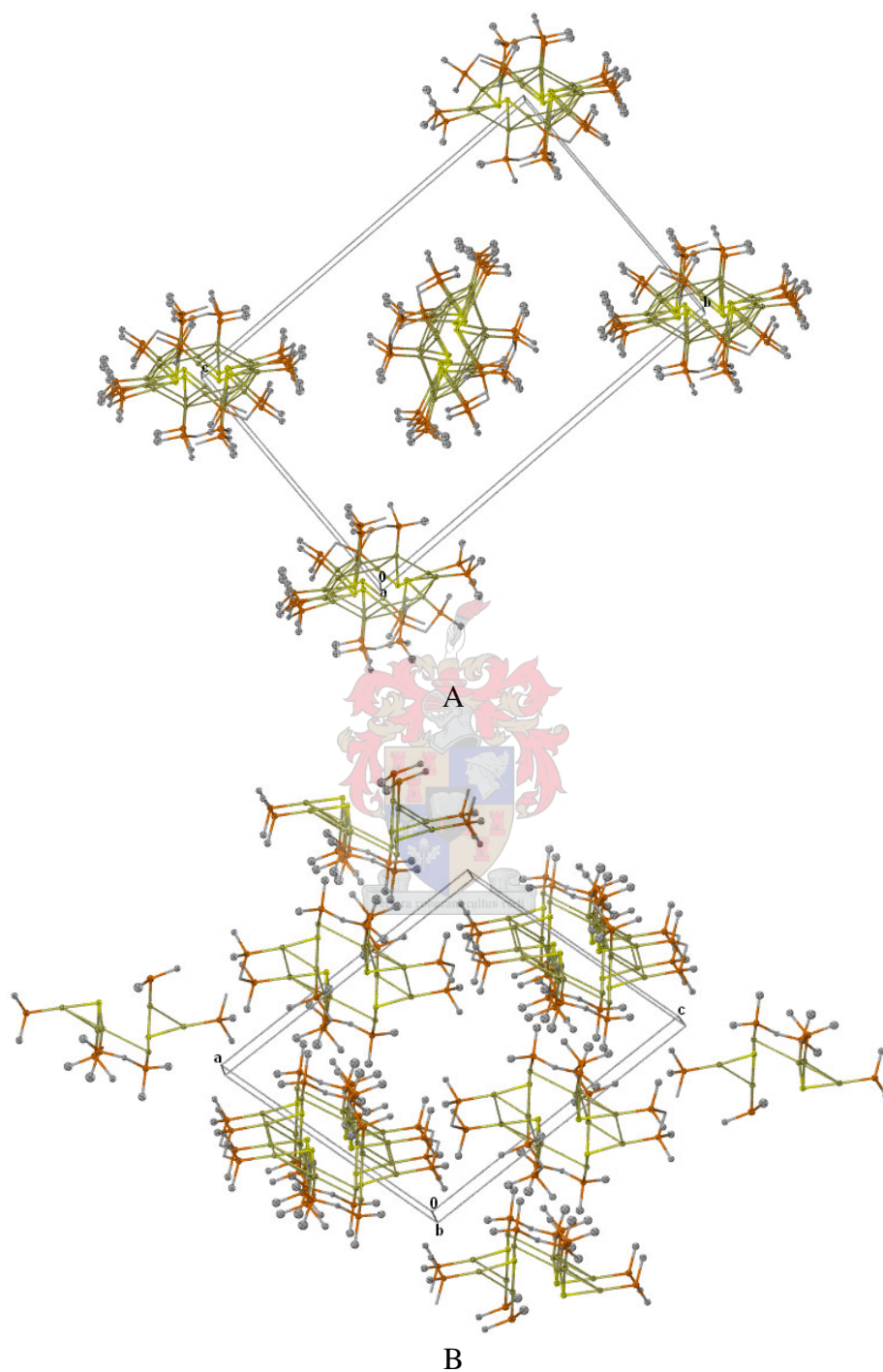


Figure 3.11 Packing diagram of the molecules of **15a** along the a-axis (A) and the b-axis (B)

Table 3.15 Selected interatomic bond lengths (Å) and angles (°) for compound **15a**

Au(1)–P(7)	2.270(7)	Au(2)–Au(6)	3.1232(15)
Au(1)–S(1)	2.323(6)	S(2)–Au(4)	2.315(6)
Au(1)–Au(3)	3.1220(14)	S(2)–Au(3)	2.329(7)
Au(1)–Au(6)	3.1845(14)	Au(3)–P(14)	2.265(7)
Au(1)–Au(5)	3.1839(14)	Au(3)–Au(1)	3.1220(14)
S(1)–Au(5)	2.316(6)	P(3)–Au(6)	2.267(8)
S(1)–Au(6)	2.351(7)	Au(4)–P(8)	2.265(7)
Au(2)–P(9)	2.259(7)	Au(4)–Au(5)	3.2394(14)
Au(2)–S(2)	2.365(6)	Au(5)–P(12)	2.260(8)
Au(2)–Au(4)	2.9834(15)	Au(5)–Au(6)	3.2922(15)
Au(2)–Au(3)	2.9927(14)	Au(6)–Au(2)	3.1232(15)
<hr/>			
P(7)–Au(1)–S(1)	178.0(2)	Au(3)–S(2)–Au(2)	79.2(2)
Au(3)–Au(1)–Au(6)	87.55(4)	P(14)–Au(3)–S(2)	173.2(2)
Au(3)–Au(1)–Au(5)	137.69(4)	Au(2)–Au(3)–Au(1)	92.52(4)
Au(6)–Au(1)–Au(5)	62.26(3)	P(8)–Au(4)–S(2)	174.5(3)
Au(5)–S(1)–Au(1)	86.7(2)	Au(2)–Au(4)–Au(5)	68.01(3)
Au(5)–S(1)–Au(6)	89.7(2)	P(12)–Au(5)–S(1)	169.4(3)
Au(1)–S(1)–Au(6)	85.9(2)	Au(1)–Au(5)–Au(4)	145.88(4)
P(9)–Au(2)–S(2)	172.5(3)	Au(1)–Au(5)–Au(6)	58.88(3)
Au(4)–Au(2)–Au(3)	75.99(4)	Au(4)–Au(5)–Au(6)	87.11(3)
Au(4)–Au(2)–Au(6)	145.06(5)	P(3)–Au(6)–S(1)	176.6(3)
Au(3)–Au(2)–Au(6)	91.00(4)	Au(2)–Au(6)–Au(1)	88.93(4)
Au(4)–S(2)–Au(3)	104.8(3)	Au(2)–Au(6)–Au(5)	136.38(4)
Au(4)–S(2)–Au(2)	79.19(19)	Au(1)–Au(6)–Au(5)	58.86(3)

The packing of the cations of **15a** along the crystallographic a-axis (A) and b-axis (B) is shown in Figure 3.11. All the phenyl groups on the phosphines and the counter ions Cl⁻ are omitted for clarity. The cations are stacked on top of each other when viewed down the crystallographic a-axis and b-axis. Along the a-axis the cations are packed on top of each other in such a way that the crystallographic centre of inversion (at the centroid of the four co-planar sulfur atoms) aligns itself at the corner of the unit cell and along the centre of the unit cell. The cations when viewed down the crystallographic b-axis are packed on top

of each other along the four sides of the unit cell forming a tunnel-like empty space along the centre of the unit cell.

3.4 Conclusions and future work

The reaction of thiones such as 1,3,4,5-tetramethyl-1,3-dihydro-imidazole-2-thione and 1,3-diisopropyl-4,5-dimethyl-1,3-dihydro-imidazole-2-thione with Au(tht)(C₆F₅) afforded new thione gold(I) complexes by a simple substitution of the weakly coordinated tetrahydrothiophene. NMR spectroscopic data confirmed the substitution reactions. Unfortunately the signals for the thione-carbons in the gold(I) complexes were not always observed despite the fact that fairly concentrated solutions were used in this study. The crystal and molecular structures of the complexes [Au(C₆F₅){S=CN(Me)C(Me)=C(Me)N(Me)}], **13a**, [Au(C₆F₅){S=CN(*i*-Pr)C(Me)=C(Me)N(*i*-Pr)}], **13b** and an adduct of the gold(III) chloride thione complex [AuCl₃{S=CN(*i*-Pr)C(Me)=C(Me)N(*i*-Pr)}], **14b**, were determined by X-ray diffraction. The Au(I) complexes are linear and the gold centre is bonded to the exocyclic S atom of the thione ligand.

Neutral complexes of gold(III) thiones were obtained by reacting HAuCl₄ with thione ligands (1,3,4,5-tetramethyl-1,3-dihydro-imidazole-2-thione and 1,3-diisopropyl-4,5-dimethyl-1,3-dihydro-imidazole-2-thione resulting in elimination of HCl. The molecular structure obtained from the single crystal X-ray analysis for [Cl₃Au{S=CN(*i*-Pr)C(Me)=C(Me)N(*i*-Pr)}]⁺, **14b**, indicated the coordination of the complex through the sulfur atom of the ligand affording a square planar geometry at the coordination centre of the gold(III) like a typical soft metal d⁸-complex.

Attempts to prepare $\overline{\text{S-(CH}_2\text{)}_3\text{-S-C=C-S-Au-PPh}_2\text{-(CH}_2\text{)}_n\text{-PPh}_2\text{-Au-S}}$ (where n = 1, 2; **IX** and **X**) and $\overline{\text{S-(CH}_2\text{)}_3\text{-S-C=C-(S-Au-PPh}_3\text{)}_2}$ by reacting (ClAu)₂dppm, (ClAu)₂dppe or AuCl(PPh₃) with dilithio-1,3-dithiane-2-carbodithioate, [Li₂S₂C=CSC₂H₄S], led to unexpected clusters of tetrameric cationic sulphonium complexes **15a** and **15b**. However, reaction between AuCl(PPh₃) and dilithio-1,3-dithiane-2-carbodithioate furnished the monomeric cationic sulphonium complex, [S{AuP(Ph₃)₃}₃]⁺Cl⁻, **15c**. NMR spectroscopic data of **15a**, **15b** and **15c** indicated the presence of more than one product in the respective samples prepared. One of the by-products consistently observed in the

NMR spectra was identified by X-ray analysis as di(1,3-dithian-2-yl)methanol. Dimer by-products or derivatives of 1,3-dithiane such as 2,2'-bidithianylidene and 2,2-di(1,3-dithianyl) could also be present in the mixture. Autoxidation of the intermediate [2-(1,3-dithianyl)]lithium by oxygen to an alcohol, lability of the C-S bond and the strong affinity of gold towards sulfur in particular, are among the assumed factors, which determine the formation of the final products.

The new sulphonium gold clusters have unusual bonding characteristics although they were not obtained by rational syntheses. They represent interesting structures that deserve further attention in future.

3.5 Experimental

3.5.1 Materials and methods

All preparations were carried out under an inert atmosphere of nitrogen or argon, using standard vacuum-line and Schlenk techniques. Solvents were dried by standard methods as mentioned in Chapter 2 and distilled under nitrogen before use.

AuCl(tht) was prepared as described in the literature.³⁷ Au(C₆F₅)(tht) was prepared according to a procedure described in the literature, by reacting (LiC₆F₅) with Au(Cl)(tht).^{38,39} Reagents dppm, dppe, PPh₃ and C₆F₅Br were obtained commercially from Aldrich and used without further purification. (AuCl)₂dppm and (AuCl)₂dppe⁴⁰ were prepared by a substitution reaction of AuCl(tht) with dppm and dppe, in 2:1 ratio, respectively, and AuCl(PPh₃) was prepared by reacting H₂AuCl₄ with PPh₃.⁴¹ Heterocyclic thione ligands such as 1,3-diisopropyl-4,5-dimethyl-1,3-dihydro-imidazole-2-thione and 1,3,4,5-tetramethyl-1,3-dihydro-imidazole-2-thione were prepared according to a method described by Kuhn and Kartz.¹⁸ 1,3-dithiane is commercially available from Fluka or it can also be prepared as described in literature.⁴² Carbon disulfide was obtained

³⁷ (a) R. Usón, A. Laguna and M. Laguna., *Inorg. Synth.*, 1989, **26**, 85. (b) R. Usón, A. Laguna, J. Vicente, *J. Organomet. Chem.*, 1977, **131**, 471.

³⁸ R. Usón and A. Laguna, *Inorg. Synth.*, 1982, **21**, 72.

³⁹ R. Usón, A. Laguna and M. Laguna, *Inorg. Synth.*, 85, **26**, 1989.

⁴⁰ M.-C. Brandys, M. C. Jennings and R. J. Puddephatt, *J. Chem. Soc., Dalton Trans.*, 2000, 4601.

⁴¹ M. I. Bruce, B. K. Nicholson and O. B. Shawkataly, *Inorg. Synth.*, 1989, **26**, 325.

⁴² Y. Wan, A. N. Kurchan, L. A. Barnhurst and A. G. Kutateladze, *Org. Lett.*, 2000, **2**, 8.

commercially distilled and stored on molecular sieve (4 Å) prior to use. *n*-BuLi was obtained commercially from Fluka and standardised prior to use.⁴³

Note: Due to impurities present in the final product mixtures of **15a**, **15b** and **15c**, melting points and yields are only reported for analytically pure compounds.

3.5.2 Preparations

3.5.2.1 Preparation of $[\text{Au}(\text{C}_6\text{F}_5)\{\text{S}=\overline{\text{CN}(i\text{-Pr})\text{C}(\text{Me})=\text{C}(\text{Me})\text{N}(i\text{-Pr})}\}], \mathbf{13b}$

A solution of 1,3-diisopropyl-4,5-dimethyl-1,3-dihydro-imidazole-2-thione (0.23 g, 0.40 mmol) in diethyl ether was transferred to a solution of Au(tht)(C₆F₅) (0.23 g, 0.40 mmol) in diethyl ether. The reaction mixture was stirred at room temperature for 2.5 h. The solvent was removed under vacuum. A colourless residue was obtained in high yield. The crude product was recrystallised from dichloromethane solution layered with *n*-hexane at -20 °C. Colourless crystals suitable for single crystal X-ray analysis were obtained.

Compound: **13b** Yield: 0.21 g (92 %) Melting point: 145 °C

3.5.2.2 Preparation of $[\text{Au}(\text{C}_6\text{F}_5)\{\text{S}=\overline{\text{CN}(\text{Me})\text{C}(\text{Me})=\text{C}(\text{Me})\text{N}(\text{Me})}\}], \mathbf{13a}$ and $[\text{Au}(\text{C}_6\text{F}_5)\{\text{S}=\overline{\text{CNHCH}_2\text{CH}_2\text{NH}}\}], \mathbf{13c}$

A solution of 1,3,4,5-tetramethyl-1,3-dihydro-imidazole-2-thione (0.070 g, 0.45 mmol) in dichloromethane or 2-imidazolidinethione [$\text{S}=\overline{\text{CNHCH}_2\text{CH}_2\text{NH}}$] (0.088 g, 0.86 mmol) in acetone was transferred to a similar mole amount of Au(C₆F₅)(tht) (0.21 g, 0.41 mmol) or (0.37 g, 0.85 mmol), respectively both in THF. The reaction solution of **13a** was filtered through Celite and the solvent was removed under vacuum. The residue was treated with diethyl ether and filtered over MgSO₄. The solvent was removed under vacuum. Light yellow crystals of **13a** suitable for X-ray analysis were obtained from a dichloromethane solution layered with *n*-pentane at -20 °C.

Compound: **13a** Yield: 0.23 g (98 %) Melting point: 147 °C

13c Yield: 0.33 g (83 %) Melting point: 205 °C

⁴³ W. R. Winkle, J. M. Langsinger and R. C. Ronald, *J. Chem. Soc., Chem. Comm.*, 1980, 87.

3.5.2.3 Preparation of $[\text{AuCl}_3\{\text{S}=\text{CN}(\text{i-Pr})\text{C}(\text{Me})=\text{C}(\text{Me})\text{N}(\text{i-Pr})\}]$, **14b**

An ethanol solution of 1,3-diisopropyl-4,5-dimethyl-1,3-dihydro-imidazole-2-thione (0.15 g, 0.7 mmol) was transferred to a solution of $\text{HAuCl}_4 \cdot 4\text{H}_2\text{O}$ (0.29 g, 0.71 mmol) in the same solvent. An immediate red precipitate was formed and filtered off and washed several times with diethyl ether. The residue was crystallised from a dichloromethane solution layered with diethyl ether at $-20\text{ }^\circ\text{C}$. Red needle like crystals suitable for single crystal X-ray analysis were obtained.

Compound: **14b** Yield: 0.31 g (85 %) Melting point: 185 - 189 $^\circ\text{C}$

3.5.2.4 Preparation of $[\text{AuCl}_3\{\text{S}=\text{CN}(\text{Me})\text{C}(\text{Me})=\text{C}(\text{Me})\text{N}(\text{Me})\}]$, **14a**

Procedure 3.4.5 was repeated for a different thione ligand, 1,3,4,5-tetramethyl-1,3-dihydro-imidazole-2-thione (0.11 g, 0.70 mmol), and with an equivalent quantity of $\text{HAuCl}_4 \cdot 4\text{H}_2\text{O}$ (0.29 g, 0.70 mmol) both dissolved in ethanol. The residue was recrystallised from dichloromethane solution layered with diethyl ether at $-20\text{ }^\circ\text{C}$.

Compound: **14a** Yield: 0.28 g (87 %) Melting point: 172 - 178 $^\circ\text{C}$

3.5.2.5 Oxidation of the cyclic 1,3-dithiane-2-carbodithioate gold(I) complex to $(\text{Cl})\text{S}-\{\text{AuP}(\text{Ph}_2)\text{CH}_2\text{P}(\text{Ph})_2\text{Au}\}_2-\text{S}(\text{Cl})-\{\text{AuP}(\text{Ph}_2)\text{CH}_2\text{P}(\text{Ph})_2\text{Au}\}-\text{S}(\text{Cl})-\{\text{AuP}(\text{Ph}_2)\text{CH}_2\text{P}(\text{Ph})_2\text{Au}\}_2-\text{S}(\text{Cl})-\{\text{AuP}(\text{Ph}_2)\text{CH}_2\text{P}(\text{Ph})_2\text{Au}\}$, **15a**

An *n*-BuLi (0.56 mmol, 1.6 M) solution in *n*-hexane was added drop wise from a syringe to a solution of 1,3-dithiane (0.067 gm, 0.56 mmol) in THF at $-70\text{ }^\circ\text{C}$. This solution was stirred for 1.5 h, during this period the reaction temperature of the ice-bath was slowly raised to $-30\text{ }^\circ\text{C}$ to complete the lithiation process. The temperature was again lowered down to $-70\text{ }^\circ\text{C}$ prior to the addition of carbon disulphide, CS_2 , (0.030 g, 0.024 cm^3) via syringe. At this stage the solution turned from colourless to light yellow. Simultaneously the second portion of *n*-BuLi was transferred all at once after the addition of the CS_2 . The temperature of the red dianion solution was allowed to rise slowly to $-30\text{ }^\circ\text{C}$ in 1.5 to 2 h, stirred for 30 min at this temperature and cooled down again to $-70\text{ }^\circ\text{C}$.

A suspension of (AuCl)₂dppm (0.34 g, 0.40 mmol) in THF at -70 °C was transferred to the red solution containing the intermediate dilithio-1,3-dithiane-2-carbodithioate. The reaction mixture was stirred at -70 °C for 2 h and the temperature was allowed to rise slowly to room temperature. The ice-bath was removed and the mixture stirred for 2 h at room temperature. The solvent was stripped under vacuum. The crude product was re-dissolved in dichloromethane and filtered through Celite to remove insoluble matter. The solvent was stripped again under vacuum and the residue was washed with diethyl ether. A dichloromethane solution was left to crystallise by slow evaporation.

3.5.2.6 Oxidation of the cyclic 1,3-dithiane-2-carbodithioate gold(I) complex to
(Cl)S—{AuP(Ph₂)(CH₂)₂P(Ph)₂Au}₂—S(Cl)—{AuP(Ph₂)(CH₂)₂P(Ph)₂Au}—S(Cl)—
{AuP(Ph₂)(CH₂)₂P(Ph)₂Au}₂—S(Cl)—{AuP(Ph₂)(CH₂)₂P(Ph)₂Au}, **15b**

The cationic complex **15b** was prepared from [(AuCl)₂dppe] (0.36 g, 0.42 mmol) and 1,3-dithiane (0.067 g, 0.56 mmol) in a similar fashion to **15a**. Crystallisation by slow evaporation from dichloromethane solution at -20 °C afforded rectangular light yellow crystals.

3.5.2.7 Oxidation of the acyclic 1,3-dithiane-2-carbodithioate gold(I) complex to
[S(Au(PPh₃))₂], **15c.**

The procedure was repeated as above with two mole quantities of AuCl(PPh₃) (0.30 g, 0.61 mmol) and dilithio-1,3-dithiane-2-carbodithioate in THF. Crystallisation from dichloromethane solution layered with *n*-pentane at -20 °C afforded light yellow crystals suitable for X-ray analysis.

3.5.3 X-ray structure determinations

The crystal data collection and refinement details for complexes **13a**, **13b**, **14b** and **15a** are summarised in Table 2.28 and Table 2.29. All data sets were collected on a Bruker SMART-Apex diffractometer using graphite monochromated Mo-K α radiation ($\lambda = 0.71073 \text{ \AA}$).⁴⁴ All measurements were made at 100 K. Data reduction was carried out with standard methods from the software package Bruker SAINT.⁴⁵ Empirical corrections were

⁴⁴ SMART Data collection software (version 5.629), Bruker AXS Inc., Madison, WI, 2003.

⁴⁵ SAINT, Data reduction software (version 6.45) Bruker AXS Inc., Madison, WI, 2003.

performed using SCALEPACK and SMART.⁴⁶ For adsorption corrections the data were treated with SADABS.^{47,48} The program X-Seed⁴⁹ was used as a graphical interface for structure solution and refinement with direct methods using SHELX. All non-hydrogen atoms were refined anisotropically by full-matrix least squares calculations on F^2 using SHELXL-97. The hydrogen atoms were fixed in calculated positions. POV-Ray for Windows was used to generate the various figures of the six compounds at the 50% probability level.

Additional information concerning the X-ray work is available from Prof H. G. Raubenheimer, Department of Chemistry, University of Stellenbosch.



⁴⁶ L.J. Ferrugia, *J. Appl. Crystallogr.*, 1999, **32**, 837.

⁴⁷ R.H. Blessing, *Acta Crystallogr., Sect. A*, 1995, **51**, 33.

⁴⁸ SADABS (version 2.05) Bruker AXS Inc., Madison, WI, 2002.

⁴⁹ (a) L. J. Barbour, *J. Supramol. Chem.*, 2001, **1**, 189. (b) J. L. Atwood and L. J. Barbour, *Cryst. Growth Des.*, 2003, **3**, 3.

Table 3.16 Crystallographic data for complexes **13a**, **13b** and **14b**

	13a	13b	14b
Empirical formula	C ₁₃ H ₁₂ AuF ₅ N ₂ S	C ₁₇ H ₂₀ AuF ₅ N ₂ S	C ₁₁ H ₂₀ AuCl ₃ N ₂ S
Formula weight (g.mol ⁻¹)	520.27	574.36	515.67
Crystal system	Monoclinic	Monoclinic	Orthorhombic
Space group	<i>P2₁/n</i>	<i>C2/c</i>	<i>Pna2₁</i>
a (Å)	13.941(2)	22.2148(16)	14.7853(18)
b (Å)	7.8954(13)	5.7654(4)	13.7779(17)
c (Å)	14.425(2)	29.879(2)	8.0774(10)
α (°)	90.00	90.00	90.00
β (°)	108.843(3)	107.1190(10)	90.00
γ (°)	90.00	90.00	90.00
Volume (Å ³)	1502.7(4)	1596.9(4)	1645.5(4)
Z	4	8	4
Calculated density (g.cm ⁻³)	2.300	2.086	2.082
Wave length (Å)	0.71073	0.71073	0.71073
Temperature (K)	100(2)	100(2)	100(2)
Absorption coefficient (mm ⁻¹)	2.521	9.540	2.082
Crystal size (mm ³)	0.15 x 0.10 x 0.10	0.20 x 0.15 x 0.10	0.25 x 0.05 x 0.05
2θ _{max} (°)	52.7	56.6	51.4
Index range, <i>hkl</i>	-17 ≤ <i>h</i> ≤ 16 -9 ≤ <i>k</i> ≤ 9 -18 ≤ <i>l</i> ≤ 14	-29 ≤ <i>h</i> ≤ 12 -7 ≤ <i>k</i> ≤ 7 -33 ≤ <i>l</i> ≤ 39	-18 ≤ <i>h</i> ≤ 14 -16 ≤ <i>k</i> ≤ 16 -9 ≤ <i>l</i> ≤ 9
Reflections collected	8439	10645	8415
No. of independent reflections	3055 (R _{int} = 0.0288)	4212 (R _{int} = 0.0339)	2866 (R _{int} = 0.0332)
Parameters	203	237	169
Goodness of fit	1.034	1.036	0.981
Largest peak	1.80	3.16	0.97
Deepest hole	-0.71	-1.47	-0.59
R ₁ (F _o > 2σF _o)	0.0253	0.0379	0.0227
wR ₂	0.0597	0.0714	0.0452

Table 3.17 Crystallographic data for complex **15a**

	15a
Empirical formula	$C_{150}H_{132}Au_{12}Cl_4P_{12}S_4$
Formula weight (g.mol ⁻¹)	4937.8
Crystal system	Monoclinic
Space group	$P2_1/n$
a (Å)	16.156(2)
b (Å)	29.312(4)
c (Å)	19.790(2) Å
α (°)	90.00
β (°)	106.501(3)
γ (°)	90.00
Volume (Å ³)	8985.8(19)
Z	4
Calculated density (g.cm ⁻³)	1.108
Wave length (Å)	0.71073
Temperature (K)	100(2)
Absorption coefficient (mm ⁻¹)	9.931
Crystal size (mm ³)	0.30 x 0.20 x 0.10
$2\theta_{max}$ (°)	56.6
Index range, <i>hkl</i>	$-20 \leq h \leq 20$ $-36 \leq k \leq 37$ $-12 \leq l \leq 26$
Reflections collected	55705
No. of independent reflections	20456 ($R_{int} = 0.1089$)
Parameters	658
Goodness of fit	0.982
Largest peak	9.78
Deepest hole	-3.72
R_1 ($F_o > 2\sigma F_o$]	0.1091
w R_2	0.2629

Chapter 4

New cationic and neutral imine complexes of gold(I) derived from HBBTM and HBBOM

4.1 Introduction and aims

4.1.1 General

Studies of gold(I) complexes have focused on their anti-arthritic, anti-tumour and anti-HIV activities. The coordination of gold(I) to *N*-donor ligands such as purines, pyrimidines and five-membered heterocycles may be biologically important.¹

The 'theory' of soft and hard acids and bases (HSAB) classifies gold as a soft metal, hence, with a slight tendency to bond to *N*-containing ligands. The relative strength of the gold non-metal bonds can be estimated from the *trans*-influence they exert on a ligand *trans* to it. The sequence deduced for the *trans*-influence, $P > C > S > Cl > N > O > F$, indicates that the gold atom binds more effectively to the atom with the higher donor strength.² As expected gold(I) complexes with imine ligands have limited stability due to the unsuitability of the soft metal centre to interact with the hard nitrogen donor. Certain factors such as aurophilic interactions or the formation of N-H...X hydrogen bonds provide stabilisation to these compounds in the solid state.³

N-coordinated gold(I) complexes have been obtained by treatment of [Au(C₆F₅)(tht)] with 4-methylthiazole and piperidine.⁴ Similarly, the reactions of AuCl(tht) with imine ligands such as 4,4-dimethyl-2-(2'-thienyl)oxazole, 4,4-dimethyl-2-(phenyl)oxazole, 1-methyl-2-(2-pyridinyl)imidazole, 1-methyl-2-(phenyl)imidazole, 4,4-dimethyl-2-(2'-thienyl)oxazole, 4,4-dimethyl-2-(phenyl)oxazole, 1-methyl-2-(2-pyridinyl)imidazole and

¹ C. F. Shaw III, in *Gold: Progress in Chemistry, Biochemistry and Technology*, ed. H. Schmidbaur, John Wiley & Sons, Chichester, 1999, p. 260.

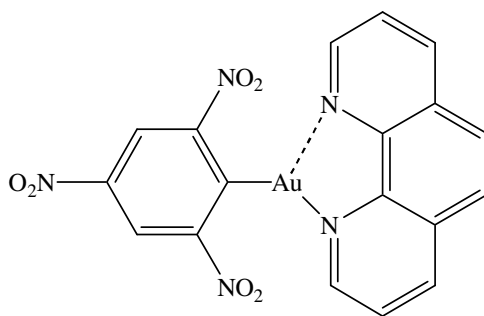
² H. Schmidbaur and Y. Inoguchi, *Z. Naturforsch.*, 1980, **B35**, 1329.

³ J. B. Melpolder and J. L. Burmeiter, *Inorg. Chim. Acta*, 1981, **49**, 115.

⁴ S. Cronje, H. G. Raubenheimer, H. S. C. Spies, C. Esterhuysen, H. Schmidbaur, A. Schier and G. J. Kruger, *Dalton Trans.*, 2003, 2859.

1-methyl-2-(phenyl)imidazole have also afforded *N*-coordinated gold(I) complexes by substituting the weakly coordinated thioether ligand (tht).⁵

Imine complexes of gold(I) with bidentate nitrogen ligands have been synthesised and are of the type $[\text{Au}(\text{C}_6\text{F}_4\text{-C}_6\text{F}_4\text{H})(\text{phen})]$, $[\text{Au}(\text{C}_6\text{F}_5)_2(\mu\text{-bipy})]$ and $\text{Au}(2,4,6\text{-}(\text{NO}_2)_3\text{C}_6\text{H}_2)(\text{dmphen})$, **I** (dmphen = 2,9-dimethyl-phen).¹ **I** shows pseudotricoordination with trigonal planar geometry.



Scheme 4.1

Amine complexes stabilised with phosphine ligands of the type $[\text{Au}(\text{L})(\text{PR}_3)]^+$ have also recently been isolated for 2-amino-thiazoline, histidine, benzimidazole and several other ligands. Similarly, dinuclear gold(I) complexes for diamines such as $(i\text{-Pr})\text{NH}(\text{CH}_2)_2\text{NH}(i\text{-Pr})$ and 1,4-piperazine are known.⁶

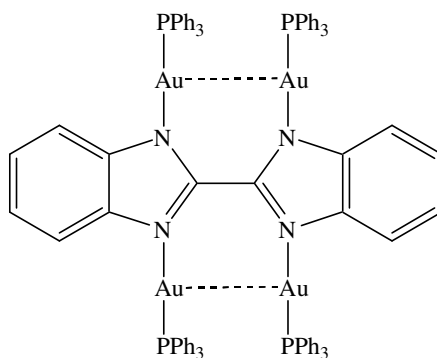
Gold(I) complexes, $[\text{AuL}(\text{PR}_3)]$ with anionic *N*-donor ligands have been obtained for several nitrogen donor ligands such as 4-nitroaniline, oxopurine and 1-amino-anthracene-9,10-dione.⁷ Tetranuclear complexes of the type $[\text{Au}_2(\mu\text{-L})(\text{PR}_3)]$, **II**, with a pyrazole derivative and nucleobases or nucleosides as ligands have also been obtained leading to aurophilic interactions (Scheme 4.2).⁷ Other examples include $[(\text{Ph}_3\text{P})\text{Au}(\text{bis}(\text{trimethyl})\text{amide})]$ and $[(\text{Ph}_3\text{P})\text{Au}(4\text{-nitro-anilide})]$. In the latter case both the monoaurated complex, $[(\text{Ph}_3\text{P})\text{Au}(\text{NHC}_6\text{H}_4\text{NO}_2)]$, and the diaurated complex,

⁵ M. Deetlefs, *Ph.D. Thesis*, University of Stellenbosch, 2001, p. 116.

⁶ M. C. Gimeno and A. Laguna, in *Silver and Gold: Comprehensive Coordination Chemistry II*, 1st ed., eds. in Chief J. A. McCleverty and T. J. Meyer, ed. D. E. Fenton, Elsevier Ltd./Elsevier Inc., Oxford/San Diego, 2004, p. 1034.

⁷ (a) R. Usón, J. Gimeno, J. Forines, F. Martinez and C. Fernández, *Inorg. Chim. Acta*, 1982, **63**, 91. (b) B. C. Tzeng, D. Li, S. M. Peng and C. M. Che, *J. Chem. Soc., Dalton Trans.*, 1993, 2365.

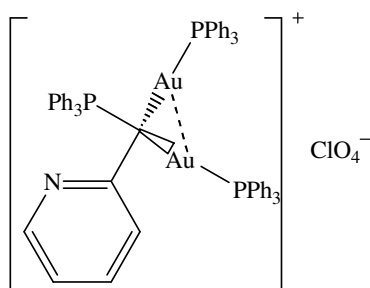
$[(\text{Ph}_3\text{PAu})_2(\text{NHC}_6\text{H}_4\text{NO}_2)]$ have been prepared. Other examples are known with L^- representing different substituents such as 2-pyridone, oxopurines, pyrazoles, imidazoles, benzimidazoles, tetrazoles and nucleobases or nucleosides.^{8,9} Several gold(I) complexes with azolyl ligands including a trinuclear $[\text{Au}(3,5\text{-Ph}_2\text{pz})]_3$ and the hexameric derivative, $[\text{Au}(3,5\text{-Ph}_2\text{pz})]_6$, have been isolated.⁶



II

Scheme 4.2

$\text{Au}(\text{acac})(\text{PPh}_3)$ is an important precursor in the synthesis of gold(I) complexes from methanide, sulfur and phosphorous donor ligands. $\text{Au}(\text{acac})(\text{PPh}_3)$ induces deprotonation and subsequent auration of a methylene group in phosphonium salts such as $[\text{Ph}_3\text{PCH}_2(\text{C}_5\text{H}_4\text{N}-2)]^+\text{ClO}_4^-$ to yield IV (Scheme 4.3).¹⁰



IV

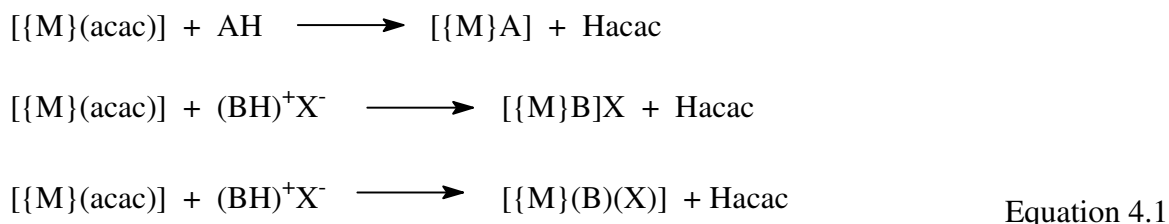
Scheme 4.3

⁸ J. Strähle, in *Gold: Progress in Chemistry, Biochemistry and Technology*, ed. H. Schmidbaur, John Wiley & Sons, Chichester, 1999, p. 319.

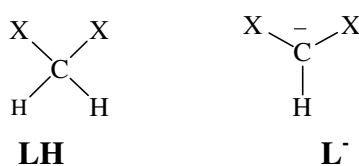
⁹ K. Nomiya, R. Noguchi, K. Ohsawa, T. Tsuda and M. Oda, *J. Inorg. Biochem.*, 2000, **78**, 363.

¹⁰ J. Vicente, M. T. Chicote, M. C. Lagunas and P. G. Jones, *J. Chem. Soc., Chem. Comm.*, 1991, **24**, 1730.

The complex $\text{Au}(\text{PPh}_3)(\text{acac})$ is a useful synthetic intermediate for many electrophilic substitution reactions yielding new compounds by acac protonation and substitution. Several reactions of such complexes with a protic acid AH or BH^+X^- , yield the coordination of the conjugate base A^- , B , or in the latter case (BH^+X^-) even both B and X^- by protonation of the acac ligand and replacing it with two different ligands as shown in Equation 4.1 below.¹¹



Bis(2-benzothiazolyl)methane, HBBTM and bis(2-benzoxazolyl)methane, HBBOM are very important heterocyclic ligands. Bis(heteroaryl)methanes in general and HBBTM and HBBOM in particular, have a reactivity pattern similar to that of β -diketones and malonic esters toward electrophilic reagents because of their active methylene groups. Substitution of one H atom by the less electron withdrawing AuL group decreases the acidity of the remaining H atom and makes it generally less active.^{12,13} These heterocyclic systems have been used both as neutral **LH** and anionic **L⁻** imine donor ligands in the preparative coordination chemistry of transition-metal ions (Scheme 4.4).



(X = benzothiazolyl, benzoxazolyl or other comparable heterocyclic system)

Scheme 4.4

Cationic complexes of the general formula $[\text{M}(\text{LH})_n]^{m+}$ are obtained from the neutral heterocyclic ligands **LH** and transition metal salts, whereas, the latter **L⁻** leads to the formation of neutral chelates of the type ML_n . The formation of one kind of complex

¹¹ (a) A. Abbotto, S. Bradamante, A. Facchetti and G. A. Pagani, *J. Org. Chem.*, 1998, **63**, 436. (b) A. Abbotto, S. Bradamante and G. A. Pagani, *Gazz. Chim. Ital.*, 1994, **124**, 301.

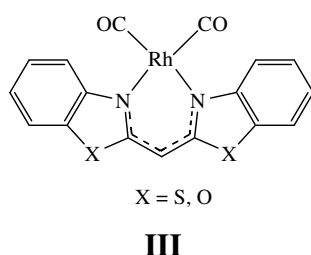
¹² J. Vicente and M. T. Chicote, *Coord. Chem. Rev.*, 1999, **193**, 1143.

¹³ F. Ragaini, M. Pizzotti, S. Cenini, A. Abbotto, G. A. Pagani and F. Demartin, *J. Organomet. Chem.*, 1995, **489**, 1107.

rather than the other depends critically on HL, the metal and the ancillary anion present in the starting metal salt.¹⁴

To account for the formation of the neutral complexes ML_n (where the ligand is present in its anionic form L^-) the acidity of the bridging CH_2 is expected to play a strategic role together with the stabilising energy of the metal-ligand coordination. The neutral chelates are obtained by deprotonation of the ligand LH, followed by metal salt coordination. The negative charge of the sp^2 hybridised methine carbon in the neutral chelates is then removed by delocalisation through the heterocyclic system.^{11,13}

Bases such as K_2CO_3 , NaH, NaOAc and *n*-BuLi have been reportedly used in the preparations of certain neutral chelates of HBBTM and HBBOM with some transition metals.¹¹⁻¹⁵ Neutral chelates $[ML_2]$ of divalent transition metals of Zn, Cu, Ni, Co and Hg were obtained by reaction of the metalacetates with HBBTM, HBBOM and other potential bidentate ligands.¹⁶ However, treatment of bis(2-benzothiazolyl)methane and bis(2-benzoxazolyl)methane with the acetates of poorly azaphilic transition-metal ions [e.g. Mn(II), Pb(II)] promotes oxidative dimerisation to the corresponding tetrakis(2-benzothiazolyl)ethane/ethene products.¹⁷ *cis*-[Rh(CO)₂(BBOM)] was prepared by addition of Na(BBOM) (generated from HBBOM and NaH) to $[Rh(CO)_2Cl]$.¹⁸ Similarly, in our laboratory neutral chelate complexes [Rh(cod)(BBTM)] and [Rh(CO)₂(BBTM)] were obtained and reported from the reaction of *n*-BuLi with HBBTM (Scheme 4.5).¹⁹



Scheme 4.5

¹⁴ A. Abbotto, S. Bradamante, A. Facchetti and G. A. Pagani, *J. Org. Chem.*, 2002, **67**, 5753.

¹⁵ H. B. Ammar, J. L. Nôtre, M. Salem, M. T. Kaddachi and P. H. Dixneuf, *J. Organomet. Chem.*, 2002, **662**, 63.

¹⁶ S. Bradamante, A. Facchetti and G. A. Pagani, *Gazz. Chim. Ital.*, 1996, **126**, 329.

¹⁷ C. Boga, A. C. Bonamartini, L. Forlani, E. Mezzina, A. Pompa, P. Sgarabotto, D. Spinelli and P. E. Todesco, *J. Chem. Res.*, 1999, **7**, 410.

¹⁸ F. Ragaini, M. Pizzotti, S. Cenini, A. Abbotto, G. A. Pagani and F. Demartin, *J. Organomet. Chem.*, 1995, **489**, 1107.

¹⁹ G. R. Julius, S. Cronje, A. Neveling, C. Esterhuysen and H. G. Raubenheimer, *Helv. Chim. Acta.* 2002, **85**, 3737.

The identity of the counter anion is also important and plays a significant role, in reactions with $[\{\text{Rh}(\text{CO})_2\text{Cl}\}_2]$ and palladium nitrate: $[\{\text{Rh}(\text{CO})_2\text{Cl}\}_2]$ does not react with neutral HBBOM whereas palladium nitrate affords a complex $[\text{Pd}(\text{HBBOM})(\text{NO}_3)_2]$.^{16,18}

Here, we report on the coordination properties of bisheteroaryl-methanes HBBTM and HBBOM behaving both as neutral ligands **LH**, affording salt complexes $[\text{M}(\text{LH})]^+$, and as anionic ligands **L**⁻, affording neutral chelates.

4.1.2 Aims and objectives

- The preliminary objective here was to investigate the coordination site of neutral chelates and cationic complexes of gold(I) with the heterocyclic ligands HBBTM and HBBOM by employing reagents such as *n*-BuLi and NaH. This study was planned around two methods, the first being deprotonation with *n*-BuLi in a stepwise fashion or NaH in one pot reaction to prepare neutral gold(I) complexes.
- Another question posed was: Would the acac-analogous BBTM and BBOM coordinate to gold *via* the central carbon to give new reagents that can be used in deprotonating substitution.
- Finally, to establish the synthetic utility of $[\text{Au}(\text{acac})(\text{PPh}_3)]$ in the preparation of neutral chelates of gold(I) by deprotonation of the active methylene protons in HBBTM and HBBOM and subsequent substitution of the weakly-bonded acetylacetonate ligand.

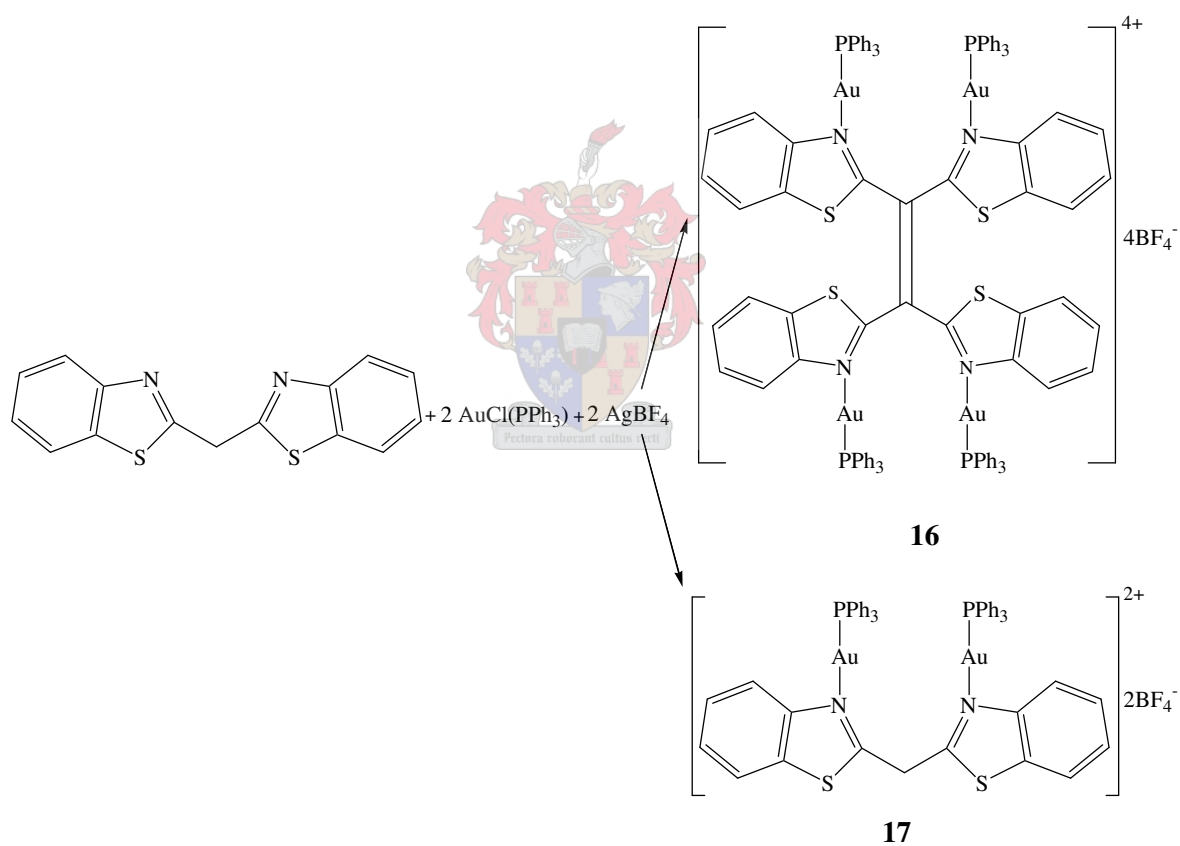
4.2 Results and discussions

4.2.1 Synthesis of cationic and neutral heterocyclic complexes of gold(I)

HBBTM and HBBOM were prepared by polyphosphoric acid-catalysed intermolecular condensation of dicarboxylic acid with *o*-aminothiophenol and *o*-aminophenol, respectively.^{20,21} A few approaches are attempted here to prepare cationic and neutral gold(I) complexes of the heterocyclic ligands of HBBTM and HBBOM.

²⁰ C. Ray and J. B. Braunwarth, *J. Org. Chem.*, 1961, **26**, 3434.

Cationic complexes **16** and **17** (Scheme 4.6) were obtained by adding two molar amounts of AgBF_4 in THF to a solution containing two molar amounts of $\text{AuCl}(\text{PPh}_3)$ and one molar amount of the ligand HBBTM in THF. After removal of all insoluble material by filtration through Celite, the solvent was removed under reduced pressure. The red residue was washed with diethyl ether several times. The residue is soluble in THF, dichloromethane and acetone, but poorly soluble in diethyl ether, *n*-pentane and *n*-hexane. Crystallisation of the residue from dichloromethane solution layered with diethyl ether at $-20\text{ }^\circ\text{C}$ yielded two different types of crystals, red and light-yellow, both suitable for single crystal X-ray analysis. Single crystal X-ray analysis was used to determine the molecular structures of the crystals.



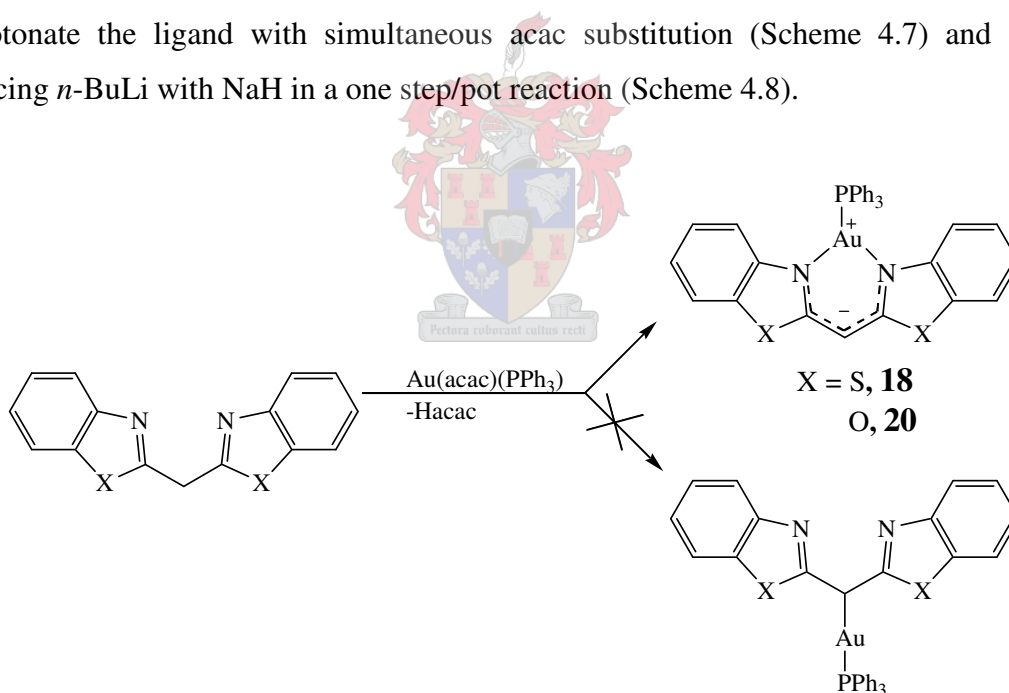
Scheme 4.6

These two products seem to be dependent on the reaction conditions. Reaction carried out under normal conditions, where air could possibly interfere in the reaction, afforded red crystals of **16** at higher yield in the mixture when compared to the light yellow crystals of

²¹ C. Ray and J. B. Braunwarth, U.S. Patent 3 250 780, 1966; [*Chem. Abs.*, 65 1966 7180g].

17. Although the mechanism is not clear, oxidative dimerisation of the ligand HBBTM to 2-(1,2,2-tri(benzo[*d*]thiazol-2-yl)vinyl)benzo[*d*]thiazole and coordination of each N atom with [Au(PPh₃)]⁺ to yield **16** seems to be a possible route. It was, however, noted that under maximum protection from air and moisture the light yellow crystals **17** were obtained at higher yield. Yet, a small amount of **16** was unavoidable and may be due to the presence of traces of air or an unspecified oxidising agent. The crystals of **16** and **17** are stable in air. The mechanism of oxidative dimerisation of the ligand and coordination to the metal centre would require an in-depth investigation. The mechanism could also include radical intermediates.

Attempts to obtain neutral complexes of HBBTM and HBBOM by deprotonating the ligands with *n*-BuLi and then adding AuCl(PPh₃) to the mixture were not successful (discussed in Section 4.4). Hence, two additional techniques were employed to obtain neutral complexes of gold(I) with HBBTM and HBBOM; (1) by using Au(acac)(PPh₃) to deprotonate the ligand with simultaneous acac substitution (Scheme 4.7) and (2) by replacing *n*-BuLi with NaH in a one step/pot reaction (Scheme 4.8).

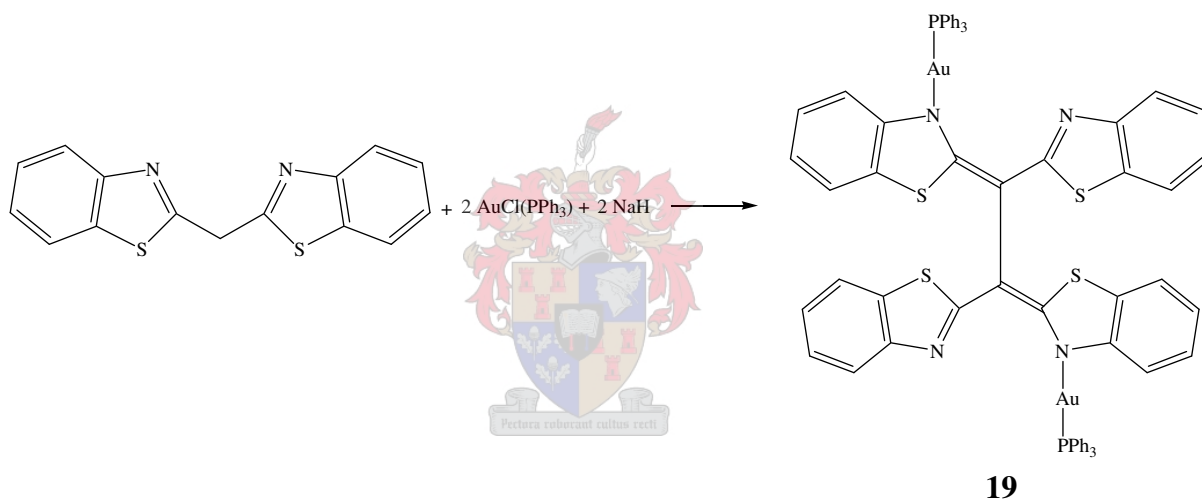


Scheme 4.7

The neutral chelate complex, **18**, was obtained in a good yield by treatment of HBBTM with similar mmol quantities of Au(acac)(PPh₃) in dichloromethane at room temperature. Several attempts to recrystallise the residue from dichloromethane solution layered with *n*-pentane or *n*-hexane at -20 °C afforded conglomerates of orange crystals which were not suitable for X-ray analysis. Nevertheless, ¹H, ¹³C and ³¹P NMR spectra and ESI MS data

of **18** correlate very well with the neutral chelate represented in Scheme 4.7. A similar reaction carried out with HBBOM will follow after the next paragraph.

An unexpectedly a high yield of the coupled neutral imine gold(I) complex, **19** (Scheme 4.8), was obtained by reacting a mixture of HBBTM and AuCl(PPh₃) in THF with the same mole quantity of NaH at -70 °C. The dinuclear complex **19** is soluble in THF, dichloromethane and acetone but insoluble in diethyl ether, *n*-pentane and *n*-hexane. Hence, crystallisation from dichloromethane solution layered with *n*-pentane afforded orange crystals of **19** suitable for X-ray analysis. Molecular structure determination of the complex by single crystal X-ray analysis revealed a dinuclear complex where a pair of gold atoms are bonded to the anionic-*N* donors of the tetrakis(2-benzothiazolyl)ethane.



Scheme 4.8

The reaction of Au(acac)(PPh₃) with similar mole quantities of HBBOM in methanol under ambient conditions afforded the first neutral chelate complex Au(BBOM)(PPh₃), **20**, at reasonable yield. The solvent was removed under reduced pressure and an orange residue was collected. The product is soluble in THF, acetone, methanol and dichloromethane but insoluble in diethyl ether, *n*-pentane and *n*-hexane. Light yellow crystals of the neutral chelate complex **20** were obtained by two methods, *i.e.*, crystallisation from a highly concentrated dichloromethane solution at -20 °C and by slow evaporation under ambient conditions. The fact that the complex was crystallised by slow evaporation in air defines the stability of the compound in atmospheric conditions.

4.2.2 Spectroscopic characterisation of compounds 16 - 20

NMR spectroscopy

In Section 4.2.1 it has been mentioned that the cationic complexes **16** and **17** could not be obtained in pure form, however, recrystallisation process enabled us to isolate sufficient crystals for X-ray analysis and determine the molecular structures (which will be discussed in-depth later in this chapter). As a result the ^1H , ^{13}C and ^{31}P NMR data in Sections 4.2.2.1 and 4.2.2.2 describe for the mixture of the compounds **16** and **17**.

4.2.2.1 $\{[(\text{AuPPh}_3)(\text{BT-N})]_2\text{C}=\text{C}\{(\text{BT-N})(\text{AuPPh}_3)_2\}^{4+}4[\text{BF}_4]^-$ (BT = benzothiazolyl), **16**

The ^1H , ^{13}C and ^{31}P NMR data of compound **16** are summarised in Table 4.1. The signals for the benzothiazolyl protons H^2 , H^5 , H^3 and H^4 are masked by the multiplet signals representing the phenyl protons at δ 7.64 - 7.56 and 7.54 - 7.48 of the main product, **16** and the low concentration product, **17**, respectively. Protons corresponding to the bridging methylene, CH_2 , group are absent in **16** as a result of the oxidative dimerisation of the carbanion to yield 2-(1,2,2-tri(benzo[*d*]thiazol-2-yl)vinyl)benzo[*d*]thiazole. A signal representing the methylene CH_2 of **17** is not observed due to the very low concentration.

The signals for the benzothiazolyl carbons C^1 and C^6 exhibit very weak and insignificant upfield shifts compared to the monomeric ligand. The bridging carbon, C^8 , resonates at 135.7 ppm which is downfield compared to the free ligand. This downfield shift ($\Delta\delta$ 97.0) with respect to the free ligand is, comparable to the analogous dimer tetrakis(2-benzothiazolyl)ethane (Section 4.4). Boga *et al.* investigated C-H/N-H tautomerism of tetrakis(2-benzothiazolyl)ethane and its oxidised product 2-(1,2,2-tri(benzo[*d*]thiazol-2-yl)vinyl)benzo[*d*]thiazole using NMR spectroscopy and reported similar observations.¹⁷ The signals for $\text{C}^{\textit{ipso}}$, $\text{C}^{\textit{meta}}$, $\text{C}^{\textit{para}}$ and $\text{C}^{\textit{ortho}}$ of the main product resonate at δ 131.7, 134.0, 133.0 and 130.0, respectively with insignificant change in chemical shift when compared to $\text{AuCl}(\text{PPh}_3)$. Low intensity signals of the phenyl carbon atoms representing trace products of **17** are also observed.

Table 4.1 ^1H and ^{13}C NMR data of compounds **16** and **17** in CDCl_3

Assignment	$\delta(\text{ppm})$ (multiplicity, J(Hz))	$\delta(\text{ppm})$ (multiplicity, J(Hz))
^1H NMR		
H^2	not observed	7.98 (4H, d, $^3J_{\text{H}2-\text{H}3} = 8.3$ Hz)
H^5	not observed	7.86 (4H, d, $^3J_{\text{H}5-\text{H}4} = 8.1$ Hz)
H^3	7.38 (4H, bs)	7.71 (4H, t, $^3J_{\text{H}3-\text{H}2,4} = 7.4$ Hz)
H^4	7.14 (4H, bs)	not seen
H^8		5.60 (2H, s)
Ph	7.64 - 7.56 (60H, m)	7.43 - 7.32 (30H, bd, $J = 43.1$ Hz)
^{13}C NMR		
C^7	166.6	172.5
C^1	150.2	150.3
C^6	134.9	135.23
C^2	126.1	126.7
C^5	125.3	126.0
C^3	123.5	123.3
C^4	123.0	121.4
C^8	135.7	36.4
C^{ipso}	131.7 (d, $J_{\text{C-P}} = 295.8$ Hz)	129.9 (d, $^1J_{\text{C-P}} = 358.4$ Hz)
C^{meta}	134.0 (d, $J_{\text{C-P}} = 7.3$ Hz)	133.9 (d, $^3J_{\text{C-P}} = 12.9$ Hz)
C^{para}	133.0 (d, obscured)	132.8 (d, obscured)
C^{ortho}	130.0 (d, $J_{\text{C-P}} = 7.1$ Hz)	129.8 (d, $^2J_{\text{C-P}} = 12.5$ Hz)
^{31}P NMR	47.09	31.35

Two broad signals are observed at δ 47.09 and 30.10 in the ^{31}P NMR indicating the presence of two products in the reaction mixture. The former signal showed a significant downfield shift of $\Delta\delta$ 13.00, whereas the latter showed only a slight shift of $\Delta\delta$ 4.00 with respect to $\text{AuCl}(\text{PPh}_3)$. Integration of the signals show that the signal at lower field (47.09 ppm) corresponding to **16** represents 71% of the mixture, whereas the signal at 30.10 ppm (representing **17**) contributes 29%.

4.2.2.2 $[(\text{PPh}_3\text{Au})(\text{BT}-N)_2\text{CH}_2]^{2+}2[\text{BF}_4]^-$ (BT = benzothiazolyl), **17**

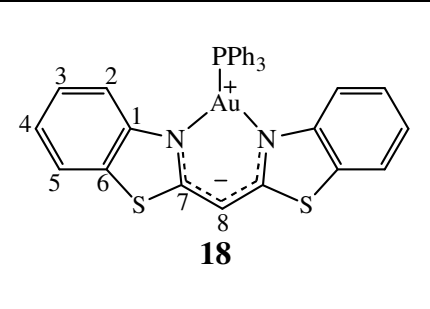
The ^1H , ^{13}C and ^{31}P NMR data of complex **17** are presented in Table 4.1. Generally, the signals of the protons corresponding to the benzothiazolyl groups shift slightly downfield compared to the free ligand. The signals for H^3 and H^4 are obscured by the multiplet of signals corresponding to the phenyl protons of **17** at 7.43 - 7.32 ppm and another set of phenyl proton signals resonate at 7.63 - 7.47 ppm indicating the presence of **16**. The bridging methylene protons shift slightly downfield upon coordination to 5.60 ppm in comparison to the free ligand (Table 2.18). Cationic complexes of rhodium reported by a member of our research group show that the protons of the methylene CH_2 group in the HBBTM are diastereotopic.¹⁹ However, in this regard the proton NMR signal for the CH_2 group of **17** is a sharp singlet indicating that these two protons are equivalent.

The signals in the ^{13}C NMR spectra are similar to those of **16**. Two sets of distinguishable signals are observed for the phenyl carbon atoms. The signals of the benzothiazolyl carbons show a slight change in chemical shifts with respect to the free ligand. However, ^{13}C NMR shift changes do not necessarily reflect local charge changes as the paramagnetic component of the chemical shift also contributes to the total chemical shift, unlike the chemical shift in the ^1H NMR spectra which is totally determined by the diamagnetic contribution of the chemical shift and thus reflects local charge movement.^{17,19} The signal at 36.4 ppm is assigned to the methylene carbon, C^8 . This signal shows a small upfield shift of $\Delta\delta$ 2.3 upon coordination.

The ^{31}P NMR spectra displayed two broad signals, more or less the same as reported for compound **16** (Table 4.1), at δ 46.67 and 31.35 indicating two products in the mixture. Integration of the signals indicated that the yield of complex **16** had decreased from 71% to 16.7%, whereas, the yield of complex **17** had increased from 29% to 83.3%. Nevertheless, pure products could not be isolated in large yields.

4.2.2.3 [(PPh₃)Au(BT-N)₂CH] (BT = benzothiazolyl), **18**

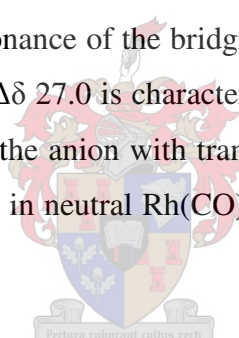
Table 4.2 ¹H and ¹³C NMR data of compound **18** in CDCl₃

Assignment	δ(ppm) (multiplicity, J(Hz))
 <p style="text-align: center;">18</p>	
¹H NMR	
H ²	8.05 (2H, d, ³ J _{H2-H3} = 7.6 Hz)
H ⁵	7.91 (2H, d, ³ J _{H2-H3} = 7.9 Hz)
H ³	Obscured by Ph ₃
H ⁴	Obscured by Ph ₃
H ⁸	6.60 (2H, s)
Ph	7.68 - 7.48 (15H, m)
¹³C NMR	
C ⁷	166.5
C ¹	154.0
C ⁶	136.6
C ²	126.8
C ⁵	125.9
C ³	123.6
C ⁴	122.3
C ⁸	39.1
C ^{ipso}	128.8 (d, obscured)
C ^{meta}	134.5 (d, ³ J _{C-P} = 13.5 Hz)
C ^{para}	132.6 (d, ⁴ J _{C-P} = 2.4 Hz)
C ^{ortho}	129.7 (d, ² J _{C-P} = 11.6 Hz)
³¹P NMR	33.67

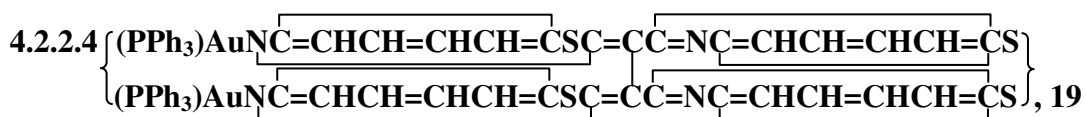
The ¹H, ¹³C and ³¹P NMR data of compound **18** are summarised in Table 4.2. The signals corresponding to the protons H³ and H⁴ are obscured by the phenyl protons of the phosphine ligand, although they are expected to shift slightly upfield upon coordination due to charge delocalisation. Two doublets at δ 8.05 and 7.91 are assigned to protons H² and H⁵, respectively. The coupling constants of H² and H⁵ are 7.6 Hz and 7.9 Hz respectively and are comparable to those of the free ligand (Table 2.18). A multiplet of

signals appearing at 7.68 - 7.48 ppm is assigned to the phenyl protons. The broad signal observed at 6.60 ppm is assigned to the bridging methine proton, H⁸. The conversion of the bridging methylene (ligand) to methine (chelate) after complexation is evident from both ¹H NMR integration (bridge versus ring protons) and the shift to low field ($\Delta\delta$ 1.67) of the methine proton signal compared to the methylene chemical shift of the free ligand. The absence of signals representing the methyl protons of acac, which usually appear at 2.22 ppm, and the methine proton, CH, at 4.37 ppm, indicates the quantitatively replacement of the acac ligand (Scheme 4.6).

The ¹³C NMR spectrum shows very weak signals at δ 166.0, 154.0 and 136.6 which are assigned to the benzothiazolyl group carbons C⁷, C¹ and C⁶, respectively. Signals for the corresponding phenyl carbons appear as expected with insignificant chemical shift changes with only one peak at 128.0 ppm observed for the C^{ipso}. The second signal is masked by the broad signals of C^{meta}. This observation has been quite common in most of the compounds discussed. The resonance of the bridging carbon, C⁸, appears at 66.2 ppm. The significant downfield shift of $\Delta\delta$ 27.0 is characteristic of the methine carbon C⁸ upon deprotonation and coordination of the anion with transition metals. This chemical shift is comparable to the resonance found in neutral Rh(CO)₂(BBTM) and other transition metal compounds.^{16,17}

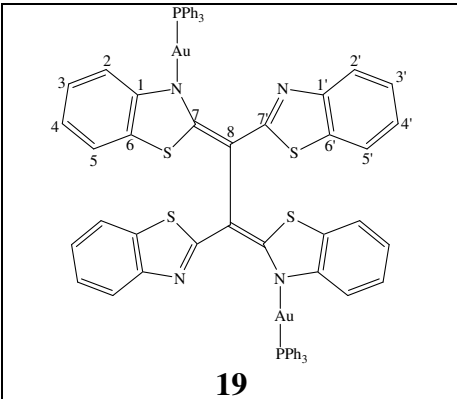


The ³¹P NMR spectrum of the complex has a strong signal at 33.66 ppm with $\Delta\delta$ 6.17 upfield shift compared to the precursor Au(acac)(PPh₃) indicating charge delocalisation of the formed carbanion.



The ¹H, ¹³C and ³¹P NMR spectra of complex **19** are summarised in Table 4.3. Protons H² and H⁵ of the benzothiazolyl groups, coordinated to gold *via* the anionic nitrogen, resonate at δ 8.38 and 7.98, respectively showing a small downfield shift of $\Delta\delta$ 0.35 and 0.20, respectively compared to the free ligand. However, protons H^{2'} and H^{5'} in the second benzothiazolyl group are unaffected by the charge transfer compared to the free ligand, hence their signals appear at δ 8.05 and 7.80, respectively.

Table 4.3 ^1H and ^{13}C NMR data of compound **19** in CDCl_3

Assignment	δ (ppm) (multiplicity, J(Hz))
 <p>19</p>	
^1H NMR	
H^2	8.38 (2H, dd, $^3J_{\text{H}^2-\text{H}^3} = 7.7$ Hz)
$\text{H}^{2'}$	8.05 (2H, dd, $^3J_{\text{H}^{2'}-\text{H}^{3'}} = 7.7$ Hz)
H^5	7.98 (2H, dd, $^3J_{\text{H}^5-\text{H}^4} = 7.7$ Hz)
$\text{H}^{5'}$	7.80 (2H, dd, $^3J_{\text{H}^{5'}-\text{H}^{4'}} = 7.7$ Hz)
$\text{H}^3, \text{H}^{3'}, \text{H}^4$ and $\text{H}^{4'}$	Obscured by Ph_3
Ph	7.54 - 7.41 (30H, m)
^{13}C NMR	
C^7	162.4
$\text{C}^{7'}$	163.9
C^1	153.5
$\text{C}^{1'}$	153.2
C^6	138.1
$\text{C}^{6'}$	137.1
C^2	127.5
C^5	126.5
C^3	124.5
C^4	122.4
C^8	134.5
C^{ipso}	130.5 (d, $^1J_{\text{C-P}} = 281.7$ Hz)
C^{meta}	134.3 (d, $^3J_{\text{C-P}} = 13.5$ Hz)
C^{para}	132.1 (d, $^4J_{\text{C-P}} = 2.5$ Hz)
C^{ortho}	129.4 (d, $^2J_{\text{C-P}} = 12.3$ Hz)
^{31}P NMR	34.60

A multiplet of signals at 7.54 - 7.44 ppm represents the phenyl protons of **19**. Signals corresponding to the protons $\text{H}^{3'}$ and $\text{H}^{4'}$ and H^3 and H^4 are obscured by the phenyl protons. The absence of signals corresponding to the bridging CH_2/CH protons, as well as

the appearance and significant down field shift of the bridging carbon C⁸ at δ 134.5 is an indication for the oxidative dimerisation of HBBTM to tetrakis(2-benzothiazolyl)ethane (Scheme 4.4).

Two sets of ¹³C NMR resonances are observed for the benzothiazolyl groups (representing the coordinated anionic imine-*N* and the uncoordinated groups, as the numbering scheme shows in Table 4.3). The signals corresponding to C⁷, C¹ and C⁶ at δ 162.4, 153.5 and 138.1, respectively have weak intensity. Whereas, the signals for C^{7'}, C^{1'} and C^{6'} have comparable chemical shifts to the free ligand since they are far from the coordination site.

The ³¹P NMR spectrum has only one broad signal at 34.60 ppm with negligible change in chemical shift when compared to the precursor AuCl(PPh₃).

4.2.2.5 [(PPh₃)Au(BO-*N*)₂CH] (BO = Benzoxazolyl), **20**

This is an example of a rare three-coordinate gold complex as will be further discussed when results of a crystal and molecular structure determination are presented.

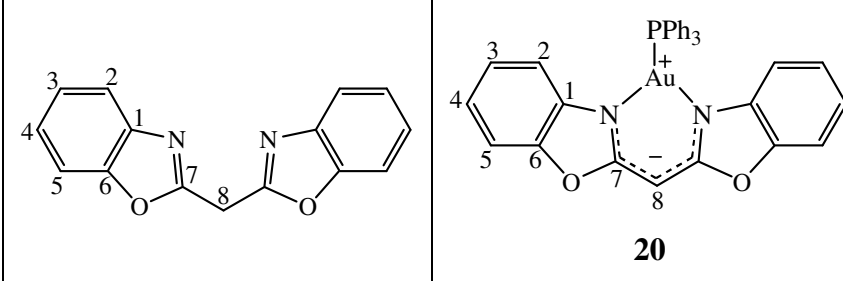
The ¹H, ¹³C and ³¹P NMR data for complex **20** are presented in Table 4.4. The resonance at 5.19 ppm, with a somewhat downfield ($\Delta\delta$ 0.55) from the signal for the CH₂ group of the free ligand is assigned to the methine proton, H⁸. This is due to the cationic gold units, Ph₃PAu⁺, which effectively remove the negative charge from the central carbon. The two benzoxazolyl groups are chemically equivalent, which indicates symmetric coordination to the gold ion. The signals for H⁵, H², H³ and H⁷ of the benzoxazolyl groups show an upfield shift of $\Delta\delta$ 0.5, 0.85, 0.56 and 0.48, respectively upon coordination with respect to the free ligand. The phenyl protons resonate at 7.66 - 7.48 ppm, slightly downfield from the precursor Au(acac)(PPh₃) which resonates at 7.56 - 7.40 ppm.²²

The signals for C¹ - C⁶ appear slightly upfield or downfield from the signals of the free ligand. This demonstrates clearly that the change in chemical shift in the ¹³C NMR spectrum of **20** does not necessarily reflect changes in charge. The bridging carbon atom, C⁸, resonates at 59.2 ppm, showing a significant downfield change in chemical shift of $\Delta\delta$ 29.3 upon deprotonation and coordination. The negative charge on the sp²-hybridised

²² J. Vicente and M.-T. Chicote, *Inorg. Synth.*, 1989, **32**, 172.

methine carbon, CH, in the complex is removed by delocalisation *via* the heteroatomic system to the electrophilic Ph_3PAu^+ .

Table 4.4 ^1H and ^{13}C NMR data of compound **20** in CDCl_3 .

Assignment	$\delta(\text{ppm})$ (multiplicity, J(Hz))	$\delta(\text{ppm})$ (multiplicity, J(Hz))
		
$^1\text{H NMR}$		
H ⁵	7.72 (2H, m)	7.21 (2H, d, $^3J_{\text{H}^5-\text{H}^4} = 7.8$ Hz)
H ²	7.56 (2H, m)	6.71 (2H, d, $^3J_{\text{H}^2-\text{H}^3} = 7.8$ Hz)
H ³	7.37 (2H, m)	6.81 (2H, t, $^3J_{\text{H}^3-\text{H}^{2,4}} = 7.8$ Hz)
H ⁴	7.37 (2H, m)	6.89 (2H, t, $^3J_{\text{H}^4-\text{H}^{3,5}} = 7.8$ Hz)
H ⁸	4.64 (2H, s)	5.19 (1H, s)
Ph		7.66 - 7.48 (15H, m)
$^{13}\text{C NMR}$		
C ⁷	160.7	168.6
C ¹	151.8	148.4
C ⁶	141.8	143.0
C ⁵	125.8	122.8
C ²	125.0	120.6
C ⁴	120.5	113.8
C ³	111.1	108.5
C ⁸	29.6	59.2
C ^{ipso}		127.0 (d, obscured)
C ^{meta}		134.2 (d, $^3J_{\text{C-P}} = 14.1$ Hz)
C ^{para}		131.6 (d, obscured)
C ^{ortho}		129.2 (d, $^2J_{\text{C-P}} = 11.3$ Hz)
$^{31}\text{P NMR}$		32.13

The signal resonating at δ 32.13 in the ^{31}P NMR spectrum appears upfield ($\Delta\delta$ 7.80) with respect to the value for the precursor $\text{Au}(\text{acac})(\text{PPh}_3)$, which normally appears at 39.83 ppm.²²

The absence of ^1H and ^{13}C NMR signals corresponding to the methyl, CH_3 , and methine, CH , groups of the acetylacetonate of the precursor, $\text{Au}(\text{acac})(\text{PPh}_3)$, are diagnostic of the substitution reaction of the acac by BBOM.

Mass spectrometry

The FAB-MS data of the cationic complexes **16** and **17** are given in Table 4.5. Molecular ions were not observed. The spectrum of complex **16** shows only one peak at m/z 136 which is assigned to $\{[\text{BT}]\text{CH}_2\}^+$. A weak intensity peak at m/z 999 for **17** appears to be equivalent to $[(\text{PPh}_3)_2\text{Au}\{\text{HBBTM}\}]^+$. The mass spectra for **17** are characterised by high intensity peaks for the homoleptic rearrangement product $[\text{Au}(\text{PPh}_3)_2]^+$ at m/z 721 and $[\text{Au}(\text{PPh}_3)]^+$ at m/z 459.

Table 4.5 Mass spectrometric data of compounds **16** and **17**

m/z	Intensity (%)	Fragment ion
16		
136	90	$\{[\text{BT}]\text{CH}_2\}^+$
17		
999	7	$[(\text{PPh}_3)_2\text{Au}\{\text{HBBTM}\}]^+$
721	90	$[\text{Au}(\text{PPh}_3)_2]^+$
459	43	$[\text{Au}(\text{PPh}_3)]^+$

The peaks observed in the ESI MS and EI MS spectra of the neutral complex **18** are summarised in Table 4.6. Here, the molecular ion $[\text{Au}(\text{BBTM})(\text{PPh}_3)]^+$ is clearly observed at m/z 740. Similar fragmentation patterns as above indicating loss of the $[\text{PPh}_3]^+$ gave rise to a weak signal at m/z 477 corresponding to $[\text{Au}(\text{BBTM})]^+$. The loss of the ligand BBTM from the complex gave rise to the peak at m/z 459 equivalent to $[\text{Au}(\text{PPh}_3)]^+$. Homoleptic rearrangement of the fragment ions again yields the peak corresponding to $[\text{Au}(\text{PPh}_3)_2]^+$ ions at m/z 721. The base peak in the ESI MS spectrum corresponds to the free ligand at m/z 282 after sequential loss of the PPh_3 ligand and Au atom. EI MS data also shows an extra signal at m/z 559 with a typical fragment for the dimeric 2-(1,2,2-tri(benzo[*d*]thiazol-

2-yl)vinyl)benzo[*d*]thiazole, which is followed by loss of one of the benzothiazolyl groups yielding a peak at *m/z* 426.

Table 4.6 Mass spectrometry data of compound **18**

<i>m/z</i>	Intensity (%)	Fragment ion
740	20 (ESI MS)	[(PPh ₃)Au{BT} ₂ CH] ⁺
721	2 (ESI MS)	[Au(PPh ₃) ₂] ⁺
559	9 (EI MS)	[(^a BT) ₂ C=C(BT) ₂] ⁺
477	1.5 (ESI MS)	[Au{BT} ₂ CH ₂] ⁺
459	1.5 (EI and ESI MS)	[Au(PPh ₃)] ⁺
426	44 (EI MS)	[(BT)C=C(BT) ₂] ⁺
282	100 (EI and ESI MS)	[{BT} ₂ CH ₂] ⁺
262	6 (EI and ESI MS)	[PPh ₃] ⁺
183	5 (EI and ESI MS)	[PPh ₂] ⁺
148	17 (EI and ESI MS)	[{BT}CH ₂] ⁺
109	3 (EI and ESI MS)	[PPh] ⁺

^aBT = benzothiazolyl group; the MS techniques used are indicated in brackets.

The FAB MS data of the neutral chelate complex **19** are summarised in Table 4.7. A very small peak at *m/z* 950 corresponding to [M] - 2PPh₃, as well as the loss of one Au atom that produces a peak at *m/z* 752 for the fragment [M - 2PPh₃ - Au] are observed. The fragmentation pattern contains a characteristic peak for trikis(2-benzothiazolyl)ethene at *m/z* 426. The peaks at *m/z* 721 and *m/z* 459 correspond to the homoleptic rearrangement product [Au(PPh₃)₂]⁺ and its fragment [Au(PPh₃)]⁺.

Table 4.7 Mass spectrometry data of compound **19**

<i>m/z</i>	Intensity (%)	Fragment ion
950	1	$\left[\text{AuNC}=\text{CHCH}=\text{CHCH}=\text{CSC}=\text{CC}=\text{NC}=\text{CHCH}=\text{CHCH}=\text{CS} \right]^+$ $\left[\text{AuNC}=\text{CHCH}=\text{CHCH}=\text{CSC}=\text{CC}=\text{NC}=\text{CHCH}=\text{CHCH}=\text{CS} \right]^+$
752	1	[{950}-Au] ⁺
721	5	[Au(PPh ₃) ₂] ⁺

(contd...)		
459	18	[Au(PPh ₃)] ⁺
426	20	[(BT) ₂ C=C(BT)] ⁺
109	10	[PPh] ⁺

4.3 Crystal and molecular structure determinations by means of X-ray diffraction

The molecular and crystal structures of the cationic complexes of **16** and **17** and the neutral complexes of **19** and **20** have been determined. The tetrafluoroborate counter ions of **16** and **17** are omitted for clarity. Similarly, the hydrogen atoms of molecular structures of **16** and **19** are omitted for clarity, while important hydrogen atoms are included in the molecular structures of **17** and **20**. All solvent molecules, except for **17**, are also omitted for clarity. Hydrogen atoms are also omitted from the packing diagrams of the complexes. Molecular interactions of **19** and **20** are reported for selected atoms.

4.3.1 The crystal and molecular structure of **16**

Compound **16** crystallised in the triclinic space group $P\bar{1}$ as red crystals from a dichloromethane solution layered with diethyl ether at -20 °C. Selected bond lengths and angles are listed in Table 4.8. The molecular structure of **16** is shown in Figure 4.1. Only the cationic structure is used in Figure 4.1 (A) and (B).

The fourazole rings are clearly shown as well as the imine-*N* coordination of all nitrogens to gold. The Au(1B)–Au(2B) and Au(1A)–Au(2A) bond lengths [3.792 and 4.004 Å, respectively] are longer than conventional aurophilic interactions [2.83 - 3.409 Å]²³ due to the steric demands by the triphenylphosphine ligands and interference from the co-crystallised solvent molecules and BF₄⁻ counter ions. The Au–P bond lengths in **16** lie within the range [2.229(3) – 2.246(3) Å], typical of two coordinate gold(I) centres.²⁴ The deviation from the least square plane defined by P(2A), Au(2A), N(2A), C(9A), C(10A), C(11A), C(12A), C(13A), C(14A), S(2A) and C(15A) [0.0672 Å] is relatively small when

²³ (a) M. Desmet, H. G. Raubenheimer and G. J. Kruger, *Organometallics*, 1997, **16**, 3324. (b) P. G. Jones, G. M. Sheldrick and E. Hädicke, *Acta. Crystallogr. Sect. B*, 1986, **36**, 2777.

²⁴ J. Strähle, in *Gold: Progress in Chemistry, Biochemistry and Technology*, ed. H. Schmidbaur, John Wiley & Sons, Chichester, 1999, p. 312.

compared to the deviations from the least square planes containing Au(1A) [0.2132 Å], Au(2B) [0.1081 Å] or Au(1B) [0.1746 Å] as coordination centres instead.

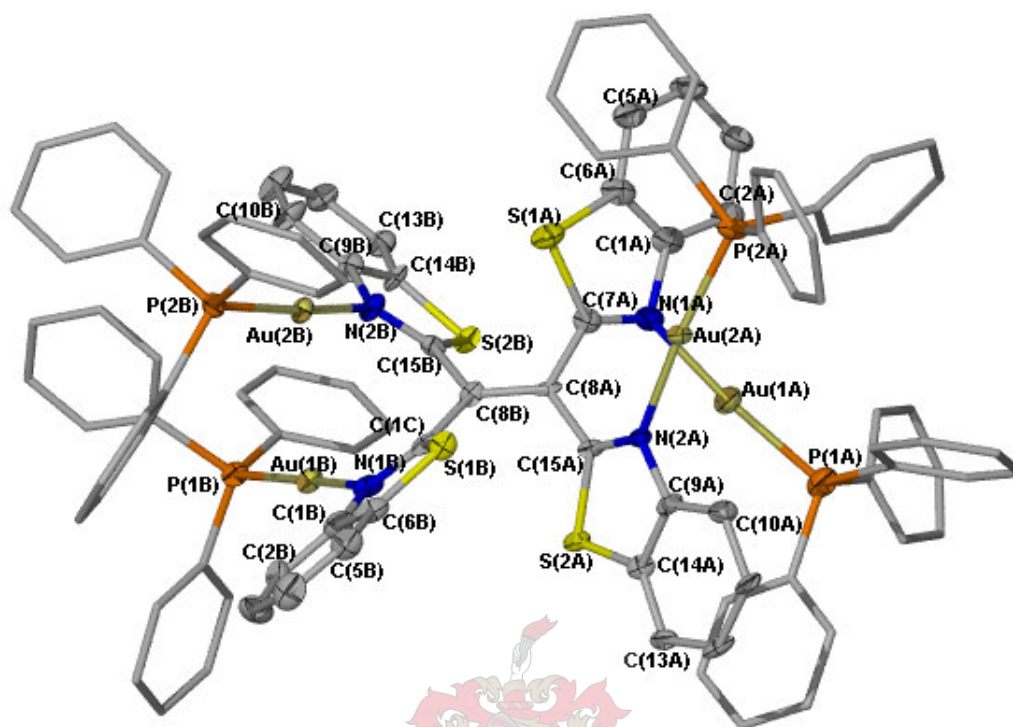


Figure 4.1 Drawing of molecular structure of **16**. All the phenyl groups are also represented as a bar line for clarity.

The bond lengths Au(1B)–N(1B) [2.093(9) Å], Au(2B)–N(2B) [2.068(9) Å], Au(2A)–N(2A) [2.085(8) Å] and Au(1A)–N(1A) [2.051(10) Å] are in the range generally observed for Au–N [2.050 - 2.105 Å] in the literature.²⁵ The bond lengths C(1C)–C(8B) [1.481(14) Å], C(15B)–C(8B) [1.480(14) Å], C(15A)–C(8A) [1.484(13) Å] and C(7A)–C(8A) [1.476(15) Å] indicate C–C single bonds.^{19,26} The C(8A)–C(8B) bond length of [1.359(14) Å] is typical for a C–C double bond. The N(1B)–C(1C) and N(2B)–C(15B) bond lengths [1.320(13) and 1.313(13) Å] are within the range observed for N–C double bonds, whereas N(2B)–C(9B) [1.415(14)] and N(1B)–C(1B) [1.388(14) Å] show partial double bond character, which may indicate that there is charge delocalisation occurring within the ring system.^{20,21} The bond lengths and angles in the thiazole units are similar to those reported for bis(bis(2-benzothiazolyl)methane)-zinc(II) (Zn(BBTM)₂) and

²⁵ J. Strähle, in *Gold: Progress in Chemistry Biochemistry and Technology*, ed. H. Schmidbaur, John Wiley & Sons, Chichester, 1999, p. 317.

²⁶ A. Abbotto, V. Alanzo, S. Brandamante, G. A. Pagani, C. Rizzoli and G. Calestani, *Gazz. Chim. Ital.*, 1991, **121**, 365.

[Rh(HBBTM)(cod)][BF₄] and [Rh (HBBTM)(CO)₂][BF₄].^{20,21} Collectively, all this data indicates that the ligand has undergone oxidative dimerisation.

The geometries about the coordination centres P(2A)–Au(2A)–N(2A) [174.1(2)°], P(1A)–Au(1A)–N(1A) [173.7(3)°], P(2B)–Au(2B)–N(2B) [171.1(2)°] and P(2B)–Au(2B)–N(2B) [173.2(3)°] deviate slightly from linearity and are comparable to the mono- and binuclear gold(I) amido compounds of purine derivatives [166.3(1) - 177.8(1)°].²⁷ The torsion angles N(1B)–C(1C)–C(8B)–C(15B) [44.4(15)°] and N(2B)–C(15B)–C(8B)–C(1C) [44.4(15)°] indicate the benzothiazolyl groups are not co-planar, similarly the torsion angles N(2A)–C(15A)–C(8A)–C(7A) [46.0(14)°] and N(2B)–C(15B)–C(8B)–C(1C) [44.4(15)°] show that C(7A) and C(15A) of the benzothiazolyl groups attached to the same carbon C(8A) are not co-planar. The torsion angles for similar atoms but considering S instead of the N atom, range between [-137.90 to -129.52°]. Hence, all the torsion angles around the azolyl groups indicate that they are not co-planar. The dihedral angles [81.31 and 76.04°] between the planes of the benzothiazolyl groups connected to C(8A) and C(8B), respectively also indicate that they are not co-planar.

The molecular diagram of **16** shows a number of intermolecular interactions within the range of hydrogen bond, however due to the intertwined nature of the counter ions BF₄⁻, the cations and solvent molecules, the diagram could not be presented here. Solvent molecules and BF₄⁻ counter ions play a role in the molecular packing. The H(43A)---C(74A) separation [2.886 Å] lies within the range for hydrogen bonding indicating intermolecular interaction. The Cl(31)---H(33A) separation [2.741 Å] indicates the shortest intermolecular contact between one of the solvent molecules and a phenyl group. Also Au(1B)---F(2D) and Au(1A)---F(3D) bond distances [3.058 Å] are among the short contacts observed within the sum of the van der Waals radii.

The packing diagrams of the molecules of **16** in the unit cell along the crystallographic a-axis(A) and b-axis(B) are shown in Figure 4.2. The BF₄⁻ counter ions and solvent molecules (dichloromethane) are omitted for clarity. The molecules are stacked on top of each other along the crystallographic a-axis and b-axis.

²⁷ U. E. I. Horvath, S. Cronje, J. M. McKenzie, L. J. Barbour and H. G. Raubenheimer, *Z. Naturforsch.*, 2004, **59b**, 1605.

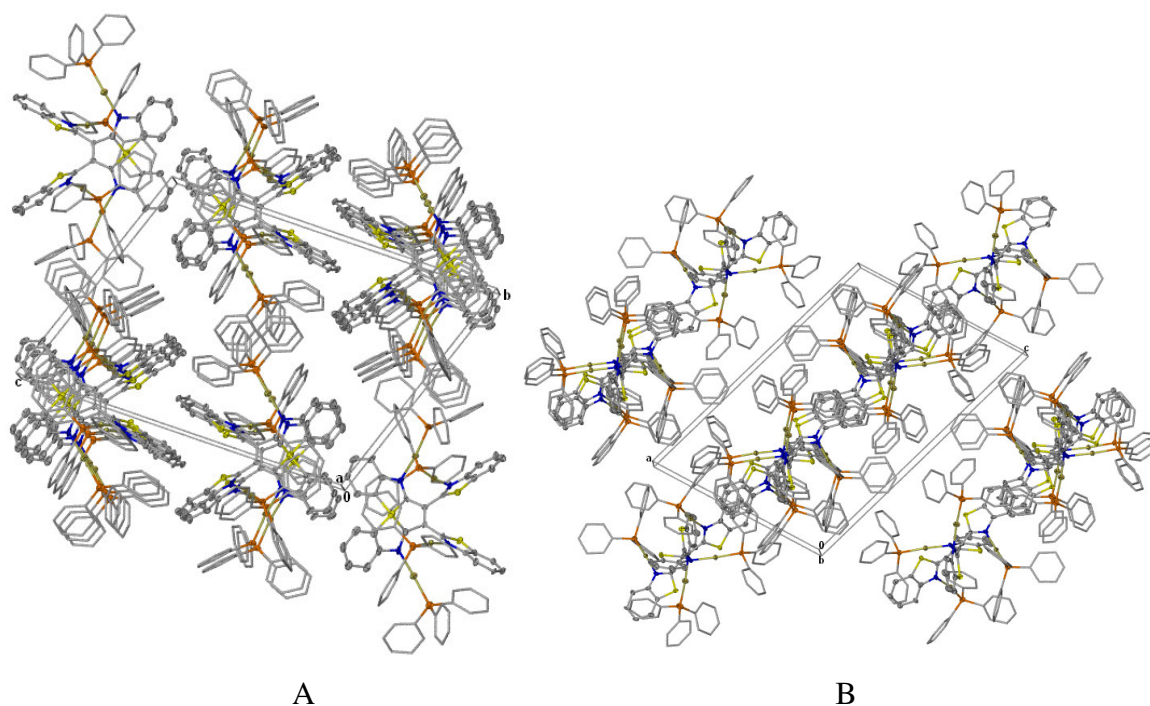


Figure 4.2 Packing diagram of the molecules of **16** along the a-axis (A) and b-axis (B).

Table 4.8 Selected bond lengths (Å) and angles (°) for **16**

Au(2A)–N(2A)	2.085(8)	N(2A)–C(9A)	1.377(12)
Au(2A)–P(2A)	2.239(3)	N(1B)–C(1C)	1.320(13)
Au(2B)–N(2B)	2.068(9)	N(1B)–C(1B)	1.388(14)
Au(2B)–P(2B)	2.229(3)	N(2B)–C(15B)	1.313(13)
Au(1B)–N(1B)	2.093(9)	N(2B)–C(9B)	1.415(14)
Au(1B)–P(1B)	2.240(3)	C(15A)–C(8A)	1.484(13)
Au(1A)–N(1A)	2.051(10)	C(15B)–C(8B)	1.480(14)
Au(1A)–P(1A)	2.246(3)	C(8A)–C(8B)	1.359(14)
S(2A)–C(14A)	1.713(11)	C(8A)–C(7A)	1.476(15)
S(2B)–C(15B)	1.724(10)	N(1A)–C(7A)	1.312(14)
S(1B)–C(6B)	1.721(12)	N(1A)–C(1A)	1.457(14)
N(2A)–C(15A)	1.328(13)	C(1C)–C(8B)	1.481(14)
N(2A)–Au(2A)–P(2A)	174.1(2)	N(2A)–C(15A)–S(2A)	114.4(7)
N(2B)–Au(2B)–P(2B)	171.1(2)	C(8A)–C(15A)–S(2A)	121.0(8)
N(1B)–Au(1B)–P(1B)	173.2(3)	C(8B)–C(8A)–C(7A)	120.1(9)

(continued...)	173.7(3)	C(8B)–C(8A)–C(15A)	121.8(9)
N(1A)–Au(1A)–P(1A)	90.2(5)	C(7A)–C(8A)–C(15A)	118.0(9)
C(14A)–S(2A)–C(15A)	112.1(9)	C(15B)–C(8B)–C(1C)	117.4(9)
C(15A)–N(2A)–C(9A)	127.3(7)	C(2A)–C(1A)–N(1A)	124.4(12)
C(15A)–N(2A)–Au(2A)	120.5(7)	C(6A)–C(1A)–N(1A)	112.9(11)
C(9A)–N(2A)–Au(2A)	110.4(9)	C(5A)–C(6A)–C(1A)	118.9(12)
C(15B)–N(2B)–C(9B)	129.0(7)	C(5A)–C(6A)–S(1A)	128.4(11)
C(15B)–N(2B)–Au(2B)	120.1(7)	C(1A)–C(6A)–S(1A)	112.7(9)
C(9B)–N(2B)–Au(2B)	124.5(9)		
N(2A)–C(15A)–C(8A)			

4.3.2 The crystal and molecular structure of 17

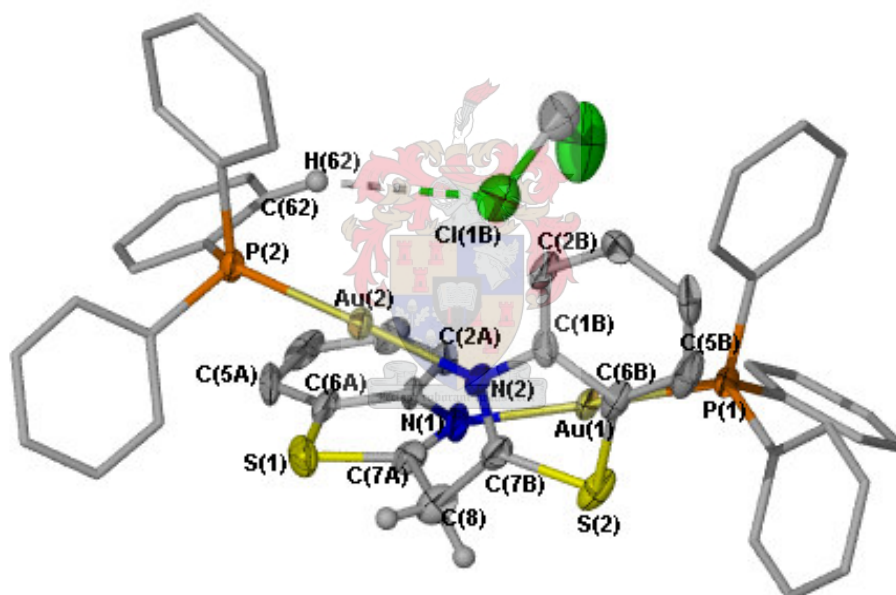


Figure 4.3 Drawing of molecular structure of 17.

Compound **17** crystallised in the monoclinic space group $C2/c$ as light yellow crystals from a dichloromethane solution layered with diethyl ether at $-20\text{ }^{\circ}\text{C}$. Selected bond lengths and angles are listed in Table 4.9. The molecular structure of **17** is shown in Figure 4.3. In the cationic complex the neutral ligand coordinates with two monovalent gold atoms *via* its imine-*N* atoms. All the dichloromethane solvent molecules and the BF_4^- counter ions are omitted from the diagram for clarity. A short contact with in the range of hydrogen bonding between a solvent molecule and the cation is also shown in the diagram.

The average Au–N bond length [2.087 Å] and Au–P [2.247 Å] are comparable to the bond lengths obtained for **16** and related compounds in the CCD database.¹⁸ Bond lengths between atoms of the heterocyclic rings correspond with those discussed for **16**. One of the BF₄⁻ counter ions shows disorder. The separation observed for Au(1)–Au(2) [5.039 Å] does not reflect effective intramolecular aurophilic interactions. One of the hydrogen atoms, H(10B) (not indicated), of the solvent molecules interacts with C(35) of the phenyl group at 2.826 Å and the chlorine atom, Cl(1B), of the same solvent interacts with another phenyl proton, H(62), at 2.896 Å. These separations fall within the range of hydrogen bonding and van der Waals criteria.²⁸ The planes defined by the coordination centres and the benzothiazolyl groups deviate from the indicated least square planes P(1), Au(1), C(7A), N(1), C(1A), C(2A), C(3A), C(4A), C(5A), C(6A) and S(1) [0.0490 Å] and P(2), Au(2), C(7B), N(2), C(1B), C(2B), C(3B), C(4B), C(5B), C(6B) and S(2) [0.0332 Å].

The geometry at the coordination centres N(2)–Au(2)–P(2) [178.6(3)°] and N(1)–Au(1)–P(1) [178.4(3)°] slightly deviate from the ideal linearity. Although, the geometry at the methylene bridge, C(8), with bond angles between [107.7 – 108.8°] are within the range of tetrahedral geometry, the C(7B)–C(8)–C(7A) bond angle [113.7(10)°] deviates slightly. The torsion angles N(1)–C(7A)–C(8)–C(7B) [51.9(16)°] and N(2)–C(7B)–C(8)–C(7A) [59.8(15)°] show that the benzothiazolyl units are not co-planar. The torsion angles of P(1)–Au(1)–N(1)–C(7A) [-96(10)°] and P(2)–Au(2)–N(2)–C(7B) [-3(10)°] indicate that the planes of the coordination centre are not in the same plane with respect to the benzothiazolyl groups. The dihedral angles between the planes defined by the benzothiazolyl groups connected to the bridging C(8) is 88.60°, indicating that the benzothiazolyl groups are perpendicular to each other.

Figure 4.4 shows the molecular packing of the molecules of **17** viewed down the crystallographic a-axis. All the phenyl groups are omitted for clarity and represented by only one carbon (the *ipso*-C). Solvent molecules and the counter ions, BF₄⁻, are also omitted from the diagram. Molecules are stacked on top of each other along the a-axis in an alternating fashion. Molecular packing when viewed down the crystallographic b-axis and c-axis also shows that molecules are stacked on top of each other.

²⁸ A. Khan, *J. Phys. Chem.*, 2000, **104**, 11268.

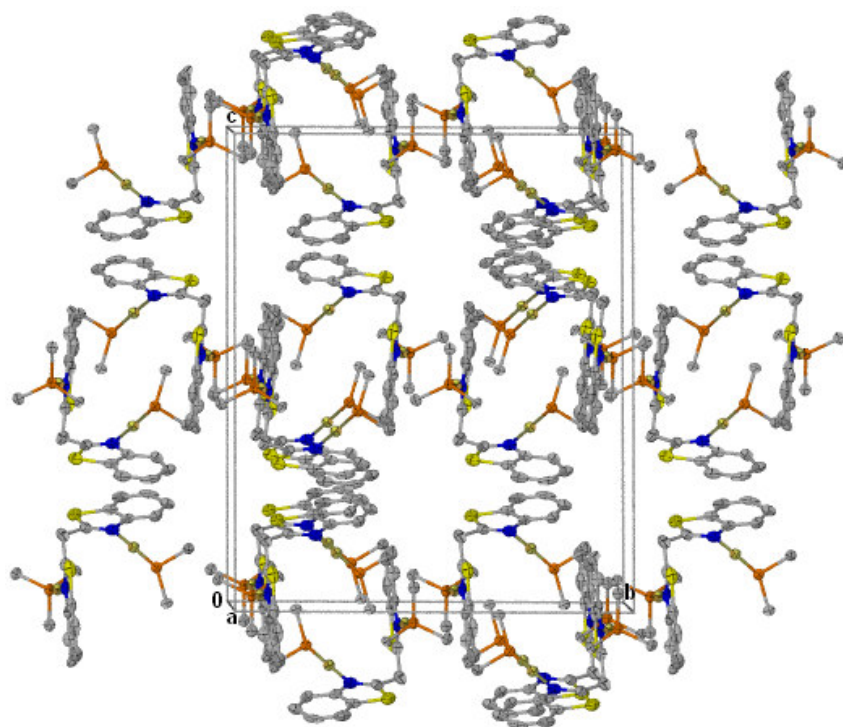


Figure 4.4 Packing diagram of the molecules of **17** along the a-axis.

Table 4.9 Selected bond lengths (Å) and angles (°) for **17**.

Au(2)–N(2)	2.079(9)	N(2)–C(7B)	1.300(14)
Au(2)–P(2)	2.245(3)	N(2)–C(1B)	1.397(15)
Au(1)–N(1)	2.095(9)	N(1)–C(7A)	1.274(14)
Au(1)–P(1)	2.249(3)	N(1)–C(1A)	1.401(15)
S(1)–C(7A)	1.726(13)	C(8)–C(7A)	1.536(17)
S(1)–C(6A)	1.750(14)	C(8)–C(7B)	1.537(18)
S(2)–C(6B)	1.717(14)	C(8)–H(8A)	0.9700
S(2)–C(7B)	1.719(12)	C(8)–H(8B)	0.9700
Pectora coherent cultus cecit			
N(2)–Au(2)–P(2)	178.6(3)	C(7B)–C(8)–H(8B)	108.8
N(1)–Au(1)–P(1)	178.4(3)	H(8A)–C(8)–H(8B)	107.7
C(7A)–S(1)–C(6A)	88.7(6)	N(2)–C(7B)–C(8)	124.1(11)
C(6B)–S(2)–C(7B)	90.2(6)	N(2)–C(7B)–S(2)	115.0(10)
C(7B)–N(2)–C(1B)	111.3(10)	C(8)–C(7B)–S(2)	120.9(9)
C(7B)–N(2)–Au(2)	123.5(8)	C(2A)–C(1A)–C(6A)	120.6(11)
C(1B)–N(2)–Au(2)	125.0(8)	C(2A)–C(1A)–N(1)	126.1(10)
C(7A)–N(1)–C(1A)	111.8(10)	C(6A)–C(1A)–N(1)	113.3(11)

(continued...)

C(7A)–N(1)–Au(1)	127.6(9)	C(1B)–C(6B)–C(5B)	119.1(12)
C(1A)–N(1)–Au(1)	120.6(8)	C(1B)–C(6B)–S(2)	109.6(10)
C(7A)–C(8)–C(7B)	113.7(10)	C(5B)–C(6B)–S(2)	131.3(10)
C(7A)–C(8)–H(8A)	108.8	N(1)–C(7A)–C(8)	127.1(11)
C(7B)–C(8)–H(8A)	108.8	N(1)–C(7A)–S(1)	116.6(9)
C(7A)–C(8)–H(8B)	108.8	C(8)–C(7A)–S(1)	116.2(9)

4.3.3 The crystal and molecular structure of **19**

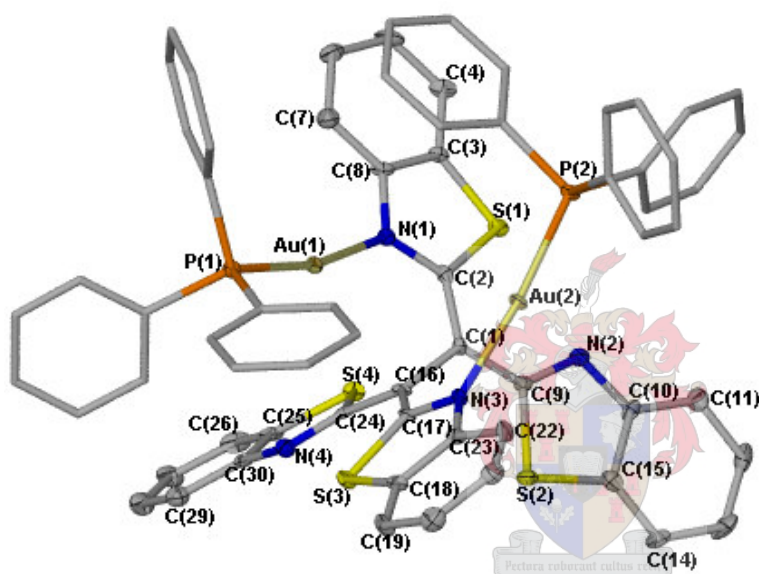


Figure 4.5 Drawing of molecular structure of **19**.

Compound **19** crystallised in the triclinic space group $P\bar{1}$ as light yellow crystals from a dichloromethane solution layered with *n*-hexane at -20 °C. Selected bond lengths and angles are listed in Table 4.10. The molecular structure of the dinuclear complex **19**, with an anionic *N*-donor ligand, is shown in Figure 4.5. Solvent molecules are omitted for clarity and the phenyl groups are represented as bar lines. Figure 4.5 depicts the molecular structure which consists of four 2-benzothiazolyl groups connected by C–C bonds analogous to an ethane functionality.

The C(1)–C(16) bond length [1.474(7) Å] compares very well to the C–C single bond observed for tetrakis(2-benzothiazolyl)ethane.¹⁴ The C(1)–C(2) and C(1)–C(9) bond lengths [1.400(7) and 1.418(7) Å], respectively are similar to the phenyl C–C bond.

Similarly, C(16)–C(24) and C(16)–C(17) bond lengths lie in the range from 1.377(7) to 1.421(7) Å. These bond lengths show slight elongation with respect to the natural C–C double bond and are shorter than a C–C single bond, indicating charge delocalisation. The N(1)–C(2) and N(2)–C(9) bond lengths [1.335(7) and 1.312(7) Å, respectively] are comparable to partial double bonds indicating π -delocalisation in the N(1)–C(2)–C(1)–C(9)–N(2) system. The N(3)–C(17) bond length [1.348(6) Å] also indicates partial double bond character, whereas N(4)–C(24) [1.306(7) Å] is typically within the range of a double bond.

The fact that the C(1)–C(9) and C(16)–C(24) bond lengths [1.418(7) and 1.427(71) Å, respectively] are slightly longer than the C(1)–C(2) and C(16)–C(17) distances of 1.400(7) and 1.377 Å, respectively indicates that the heterocyclic rings containing the electrophilic group, Ph₃PAu⁺ are more affected by the charge delocalisation. This means that the C–N bond should also be affected, which is indeed the instance: both C(2)–N(1) and C(17)–N(3) bond lengths of 1.335(7) and 1.348(6) Å are appreciably longer than similar distances in the free rings. (certainly some double bond delocalisation towards the two rings also occurs), *i.e.*, C(9)–N(2) and C(24)–C(4) are shorter by *ca.* 0.02 - 0.04 Å.^{24,29} Deviations from the least square planes defined by P(1), Au(1), N(1), C(8), C(7), C(6), C(5), C(4), C(3), S(1) and C(2) [0.0942 Å] and P(2), Au(2), N(3), C(23), C(22), C(21), C(20), C(19), C(18), S(3) and C(17) [0.2437 Å] indicate that the degree of deviations vary from one to the other. The Au–Au distance [3.985 Å] is too far for an aurophilic interaction probably due to the aforementioned factors (intermolecular interaction with solvent molecules, the steric bulkiness of the triphenylphosphine ligands and the rotation along the C(1)–C(6) bond). The Au–N bond lengths are practically similar ranging from [2.056(4) to 2.062(4) Å] and are comparable to those of **16**, **17**, 9*H*-purin-9-ate and 9*H*-purin-6-ylamine-9-ate.^{19,25} The Au–P bond length [2.222(16) Å] is as expected and is comparable to the value in previous compounds **16** and **17**.

The geometry at the coordination centre P–Au–N [168.12(13)°] considerably deviates from linearity. The angles around C(1) and C(16) [117.6(5) – 122.0(5)°] lie within the range of trigonal planar geometry. The torsion angles of C(24)–C(16)–C(1)–C(9) [-95.91°] and C(17)–C(16)–C(1)–C(2) [-116.63°] indicate that the benzothiazolyl groups are

²⁹ F. Ragaini, M. Pizzotti, S. Cenini, A. Abbotto, G. A. Pagani and F. Demartin, *J. Organomet. Chem.*, 1995, **489**, 1107.

not co-planar. The analysis of molecular models and optimisation of molecular geometries through semi empirical calculations (AMI) show structures in which the dihedral angles between the benzothiazolyl groups of tetrakis(2-benzothiazolyl)ethane is *ca.* 90°. ¹⁴ The dihedral angles defined by the benzothiazolyl groups connected to the same carbon atom (C(1) and C(16)) resulted in unusually small angles [14.89 and 15.83°, respectively] compared to the previous compounds and those discussed in Section 4.4.3.

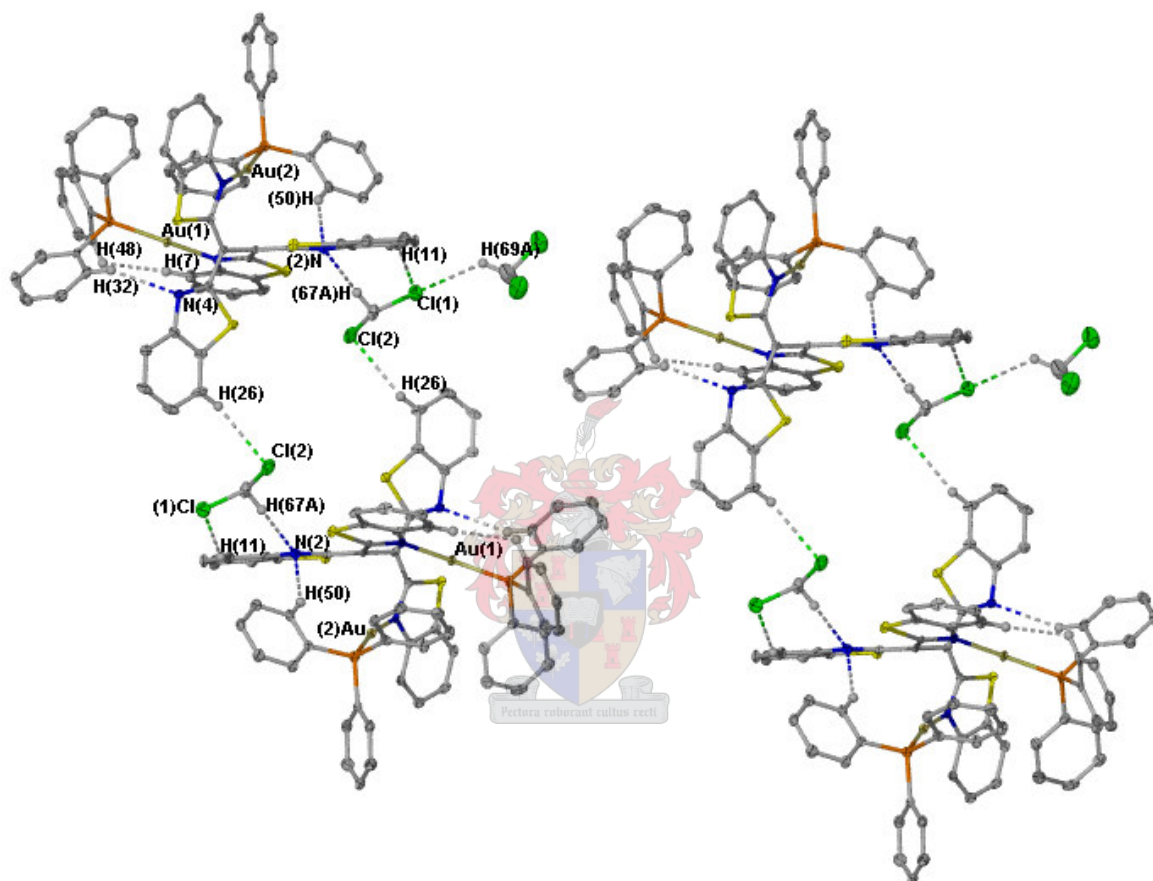


Figure 4.6 Diagram of **19** showing intermolecular and intramolecular interactions.

Figure 4.6 shows intermolecular and intramolecular interactions between the molecules of **19**. The separation between atoms N(4)–H(32) [2.654 Å] and N(2)–H(50) [2.483 Å] indicate intramolecular interactions within the range of hydrogen bonding. The separations observed H(26)–Cl(2) [2.900 Å], N(2)–H(67A) [2.575 Å] and H(11)–Cl(1) [2.857 Å] are also within the range for hydrogen bonds. The diagram also shows the intermolecular interactions mainly centred between the solvent molecules and molecules of **19**. In other words, the solvent molecules act as spacers between two molecules of **19**.

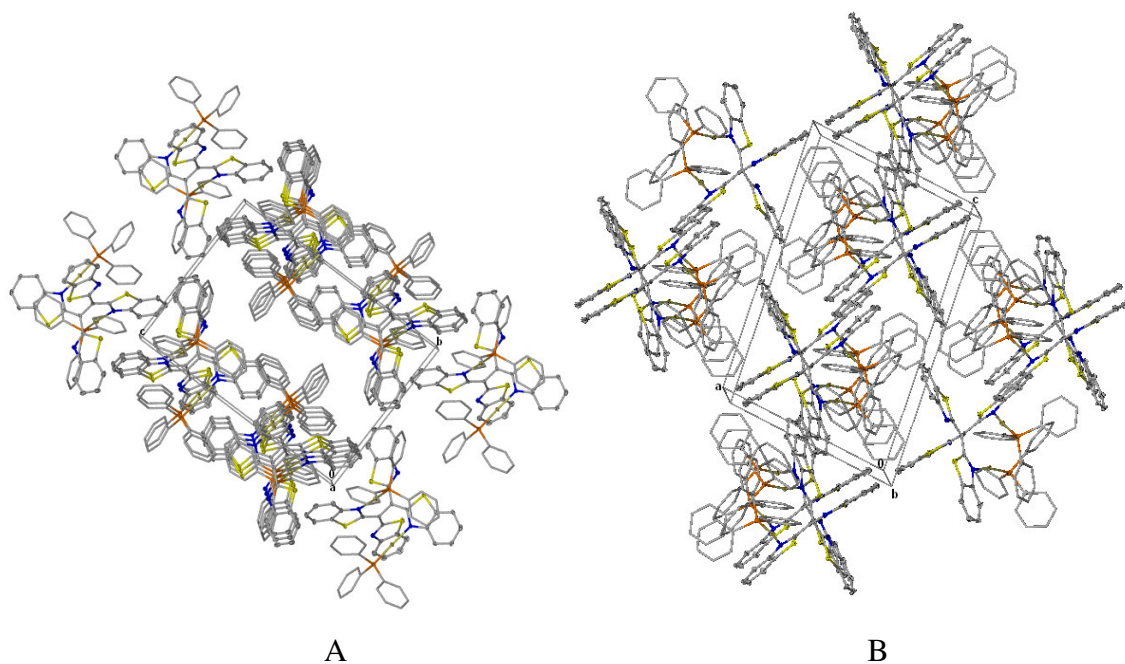


Figure 4.7 Packing diagram of the molecules of **19** along the a-axis (A) and b-axis (B).

Figure 4.7 illustrates the packing of the molecules of **19** down the crystallographic a-axis (A) and b-axis (B). Solvent molecules are omitted from the unit cell packing diagram. The unit cell packing viewed down the crystallographic b-axis shows molecules are stacked on top of each other. When the unit cell packing is viewed down the crystallographic a-axis molecules are stacked on top of each other along two parallel sides, leaving a tunnel-like channel.

Table 4.10 Selected bond lengths (Å) and angles (°) for **19**

Au(1)–N(1)	2.056(4)	S(2)–C(9)	1.758(5)
Au(1)–P(1)	2.2220(16)	C(1)–C(16)	1.473(7)
S(1)–C(3)	1.732(6)	N(2)–C(9)	1.312(7)
S(1)–C(2)	1.747(5)	N(2)–C(10)	1.386(7)
N(1)–C(2)	1.335(7)	N(3)–C(17)	1.348(6)
N(1)–C(8)	1.392(7)	N(3)–C(23)	1.372(7)
C(1)–C(2)	1.400(7)	C(16)–C(17)	1.377(7)
C(1)–C(9)	1.418(7)	C(16)–C(24)	1.421(7)
S(2)–C(15)	1.729(6)	Au(2)–N(3)	2.062(4)
N(1)–Au(1)–P(1)	167.31(13)	C(55)–P(2)–Au(2)	111.71(19)

(continued...)

C(3)–S(1)–C(2)	90.3(3)	C(49)–P(2)–Au(2)	117.98(19)
C(43)–P(1)–Au(1)	106.56(18)	C(61)–P(2)–Au(2)	109.22(18)
C(31)–P(1)–Au(1)	118.10(19)	C(9)–N(2)–C(10)	111.6(5)
C(37)–P(1)–Au(1)	116.1(2)	N(1)–C(2)–C(1)	124.4(5)
C(2)–N(1)–C(8)	112.2(5)	N(1)–C(2)–S(1)	112.7(4)
C(2)–N(1)–Au(1)	126.7(4)	C(1)–C(2)–S(1)	122.7(4)
C(8)–N(1)–Au(1)	120.7(4)	C(18)–S(3)–C(17)	90.1(3)
C(2)–C(1)–C(9)	122.0(5)	C(17)–N(3)–Au(2)	121.6(3)
C(2)–C(1)–C(16)	119.1(5)	C(23)–N(3)–Au(2)	122.6(3)
C(9)–C(1)–C(16)	117.6(5)	C(1)–C(9)–S(2)	117.3(4)
N(3)–Au(2)–P(2)	168.93(13)	C(11)–C(10)–N(2)	125.9(5)
C(15)–S(2)–C(9)	89.9(3)	N(2)–C(10)–C(15)	114.9(5)

4.3.4 The crystal and molecular structure of **20**

Compound **20** crystallised in the triclinic space group $P\bar{1}$ as light yellow crystals from a concentrated dichloromethane solution at $-20\text{ }^{\circ}\text{C}$. Selected bond lengths and angles are listed in Table 4.11. The molecular structure of **20** is shown in Figure 4.8. The structure shows a rare three-coordinated gold(I) complex. The diagram shows the anionic ligand coordinated bidentately *via* the imine-*N* to the gold atom.

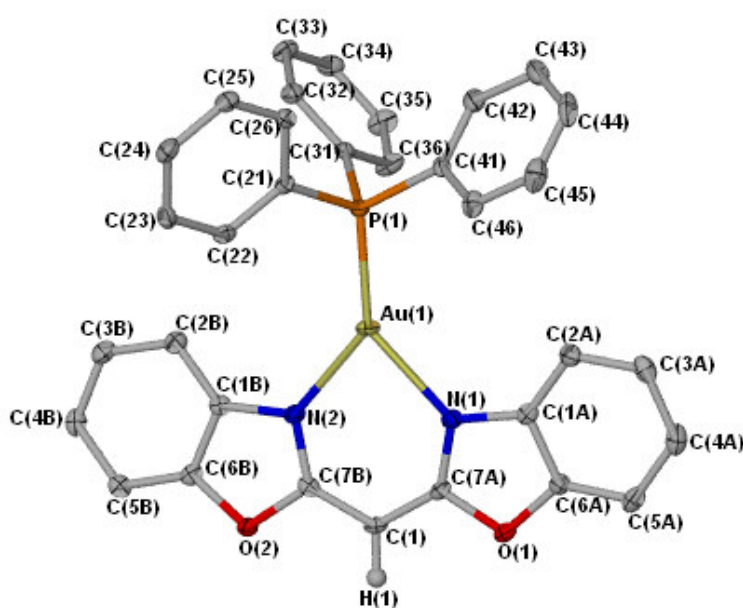


Figure 4.8 Drawing of molecular structure of **20**.

The N(2)–C(7B) and N(1)–C(7A) distances of 1.329(4) and 1.333(4) Å, respectively are slightly shorter than C–N single bonds and longer than C–N double bonds. Similarly, C(1)–C(7A) and C(1)–C(7B) have bond lengths of 1.382(4) and 1.391(4) Å, respectively that fall between single and double bond lengths. Collectively these bond lengths indicate π -delocalisation in the N(1)–C(7A)–C(1)–C(7B)–N(2)–C(1) system. The mean Au–N bond length [2.229 Å] significantly deviates from **16**, **17** and **19**, where the average Au–N bond lengths for each compound has been measured as 2.074(9), 2.087(9) and 2.059(4) Å, respectively. This slight elongation of Au–N bond length from the normal distance observed in the other compounds is due to the charge delocalisation within the six-membered metallacycle.

The geometry about the coordination centre, Au(1), P(1)–Au(1)–N(1), P(1)–Au(1)–N(2), and N(1)–Au(1)–N(2) with bond angles of 140.31(6), 137.05(6) and 82.35(8)°, respectively indicated a slightly distorted trigonal planar geometry. The six membered heterometallacycle has an envelope conformation formed by Au(1)–N(1)–C(7A)–C(1A)–C(7B)–N(2), wherein the backbone formed by N(1)–C(7A)–C(1)–C(7B)–N(2) [0.0201 Å] deviates slightly from the least square plane. The deviation from the least square plane defined by atoms P(1), Au(1), N(1), C(7A), C(1), C(7B) and N(2) is 0.0540 Å. The torsion angle Au(1)–N(2)–C(1B)–C(2B) [11.7(4)°] is relatively greater than the torsion angle Au(1)–N(1)–C(1A)–C(2A) [0.28°]. The trigonal planar C(7A)–C(1)–C(7B) bond angle [122.2(2)°] is comparable to a similar angle in bis(2-benzoxazolyl)methane-*N,N'*dicarbonylrhodium.¹⁰ The dihedral angle [6.80°] between the planes containing the benzoxazolyl groups (C(1), C(7A), N(1), C(1A), C(2A), C(3A), C(4A), C(5A), C(6A), O(1) and (C(1), C(7B), N(2), C(1B), C(2B), C(3B), C(4B), C(5B), C(6B), O(2))) is also very small compared to the dihedral angle between the azolyl groups connected to the same carbon atom in compounds **16** and **17**.

The intermolecular Au(1)–Au(1) distance [5.482 Å] indicates no aurophilic interaction. The Au(1) and C(1) of two molecules in successive layers are arranged parallel, but pointing in opposite directions. The steric demand by the triphenylphosphine ligands and interference due to solvent molecules are probably the contributing factors in precluding the aurophilic interactions. Molecular interactions H(22)–O(1), Cl(5)–H(2A) and Cl(5)–H(44) at distances of 2.550, 2.883 and 2.899 Å, respectively are observed within the range of hydrogen bonding.

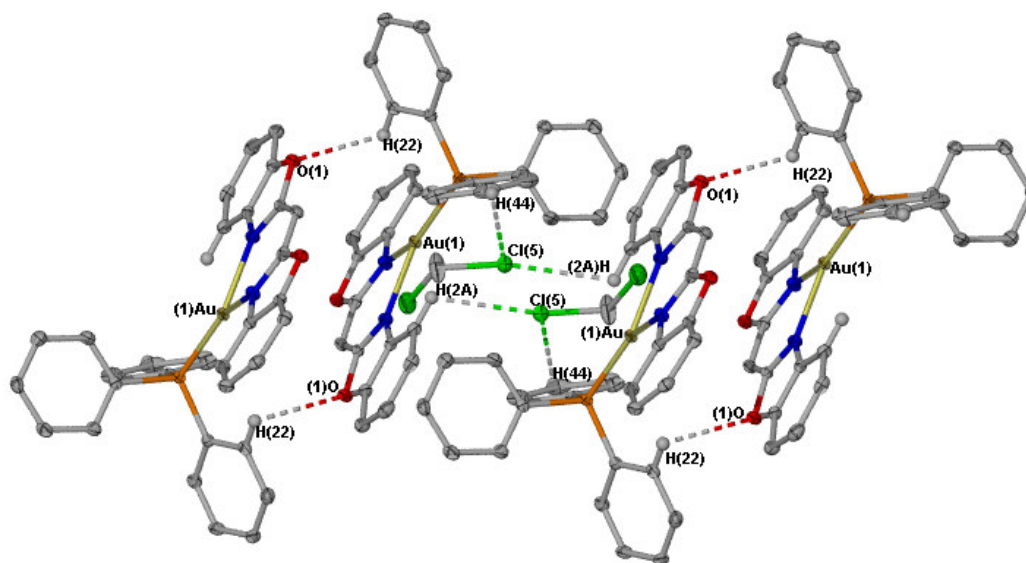


Figure 4.9 Diagram of **20** showing intermolecular interactions

Figure 4.9 depicts the intermolecular interactions between molecules of **20**. Two molecules are parallel but pointing in opposite directions separated by short contacts between O(1) and H(22) [1.550 Å]. Solvent molecules also act as a bridging units between two molecules as shown in Figure 4.9: Cl(5)–H(2A) [2.883 Å] and H(44)–Cl(5) [2.899 Å].

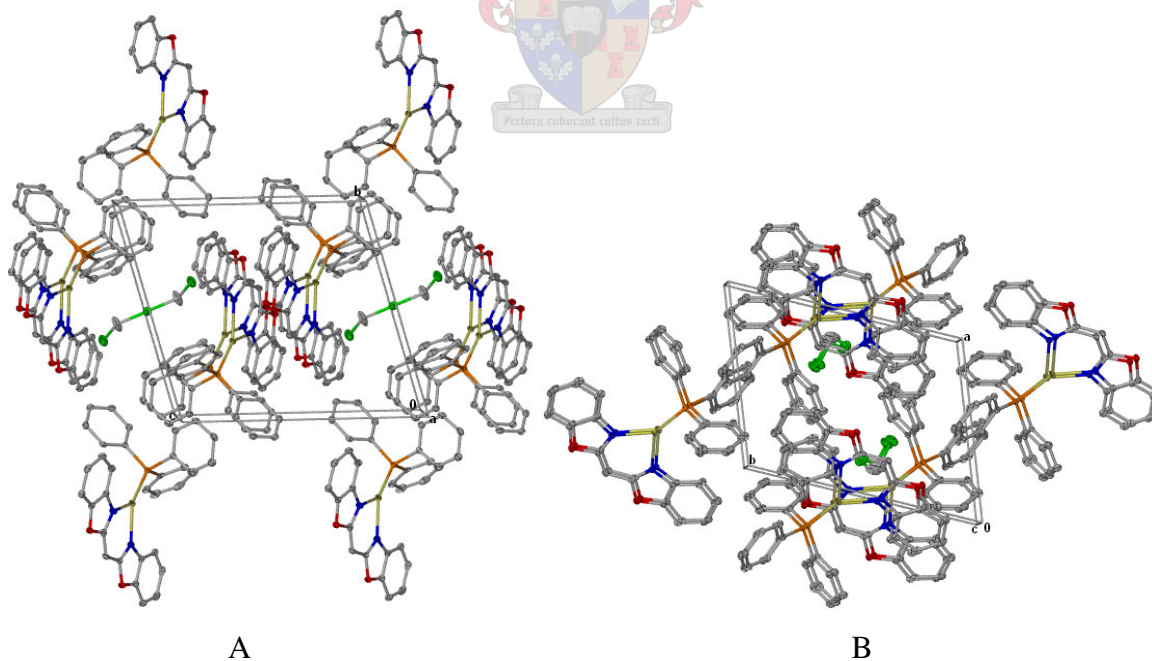


Figure 4.10 Packing diagram of the molecules of **20** along the a-axis (A) and c-axis (B).

Packing of the molecules of **20** when viewed down the crystallographic a-axis and c-axis is shown in Figure 4.10. Molecules are stacked on top of each other in an alternating

fashion when viewed down the crystallographic c-axis. Molecules in one layer are oriented in one direction, while molecules in the next layer occur in the opposite direction.

Table 4.11 Selected bond lengths (Å) and angles (°) for **20**

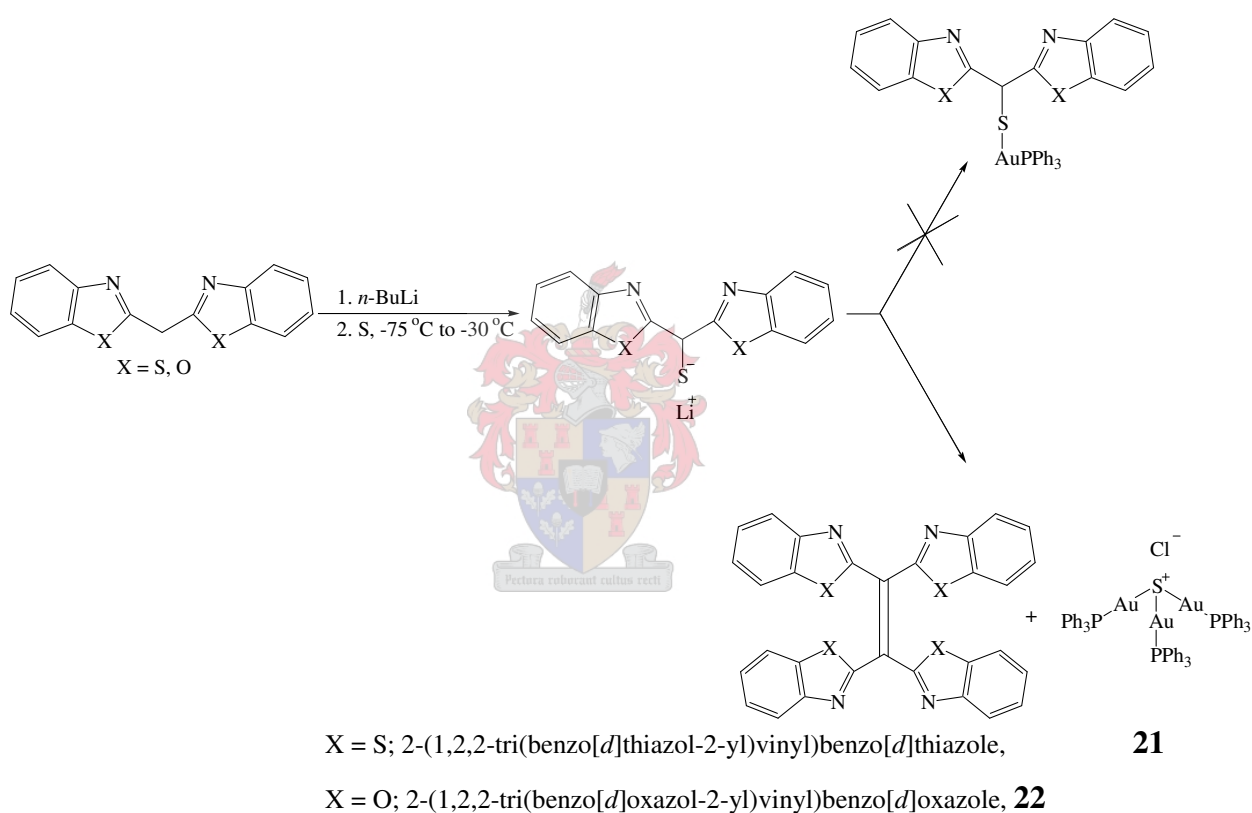
Au(1)–P(1)	2.2073(7)	N(2)–C(7B)	1.329(4)
Au(1)–N(1)	2.226(2)	N(2)–C(1B)	1.396(4)
Au(1)–N(2)	2.231(2)	N(1)–C(7A)	1.333(4)
O(2)–C(7B)	1.385(3)	N(1)–C(1A)	1.397(4)
O(2)–C(6B)	1.385(3)	C(7B)–C(1)	1.391(4)
O(1)–C(6A)	1.382(3)	C(7A)–C(1)	1.382(4)
O(1)–C(7A)	1.386(3)	C(1)–H(1)	0.9498
P(1)–Au(1)–N(1)	140.31(6)	O(1)–C(6A)–C(1A)	108.1(2)
P(1)–Au(1)–N(2)	137.05(6)	N(2)–C(7B)–O(2)	112.6(2)
N(1)–Au(1)–N(2)	82.35(8)	N(2)–C(7B)–C(1)	129.8(3)
C(21)–P(1)–Au(1)	115.00(9)	O(2)–C(7B)–C(1)	117.6(2)
C(31)–P(1)–Au(1)	111.62(9)	N(1)–C(7A)–C(1)	129.9(3)
C(41)–P(1)–Au(1)	116.43(9)	N(1)–C(7A)–O(1)	112.3(2)
C(7B)–O(2)–C(6B)	105.1(2)	C(1)–C(7A)–O(1)	117.9(2)
C(6A)–O(1)–C(7A)	105.3(2)	C(5B)–C(6B)–O(2)	128.0(3)
C(7B)–N(2)–C(1B)	105.9(2)	O(2)–C(6B)–C(1B)	108.0(2)
C(7B)–N(2)–Au(1)	127.10(18)	C(2B)–C(1B)–N(2)	132.0(3)
C(1B)–N(2)–Au(1)	126.44(18)	C(6B)–C(1B)–N(2)	108.4(2)
C(7A)–N(1)–C(1A)	106.0(2)	C(7A)–C(1)–H(1)	118.9
C(7A)–N(1)–Au(1)	127.58(18)	C(7B)–C(1)–H(1)	119.0
C(1A)–N(1)–Au(1)	126.38(18)	C(2A)–C(1A)–N(1)	131.8(3)
C(5A)–C(6A)–O(1)	128.0(3)	C(6A)–C(1A)–N(1)	108.3(2)

4.4 Results and discussions for the oxidative dimerisation of HBBTM and HBBOM

In the previous sections we have discussed the syntheses and characterisation of new cationic as well as neutral gold(I) complexes of HBBTM and HBBOM. We also attempted

other approaches to the preparation of neutral gold(I)thiolate complexes of HBBTM and HBBOM (Scheme 4.9 and Scheme 4.10). However, due to some unspecified redox reactions oxidative dimerisation products like, 2-(1,2,2-tri(benzo[*d*]thiazol-2-yl)vinyl)benzo[*d*]thiazole and 2-(1,2,2-tri(benzo[*d*]oxazol-2-yl)vinyl)benzo[*d*]oxazole were formed. In the following sections we include all the experimental details and the scientific data related to the transformations:

4.4.1 Unexpected oxidative dimerisation of HBBTM and HBBOM

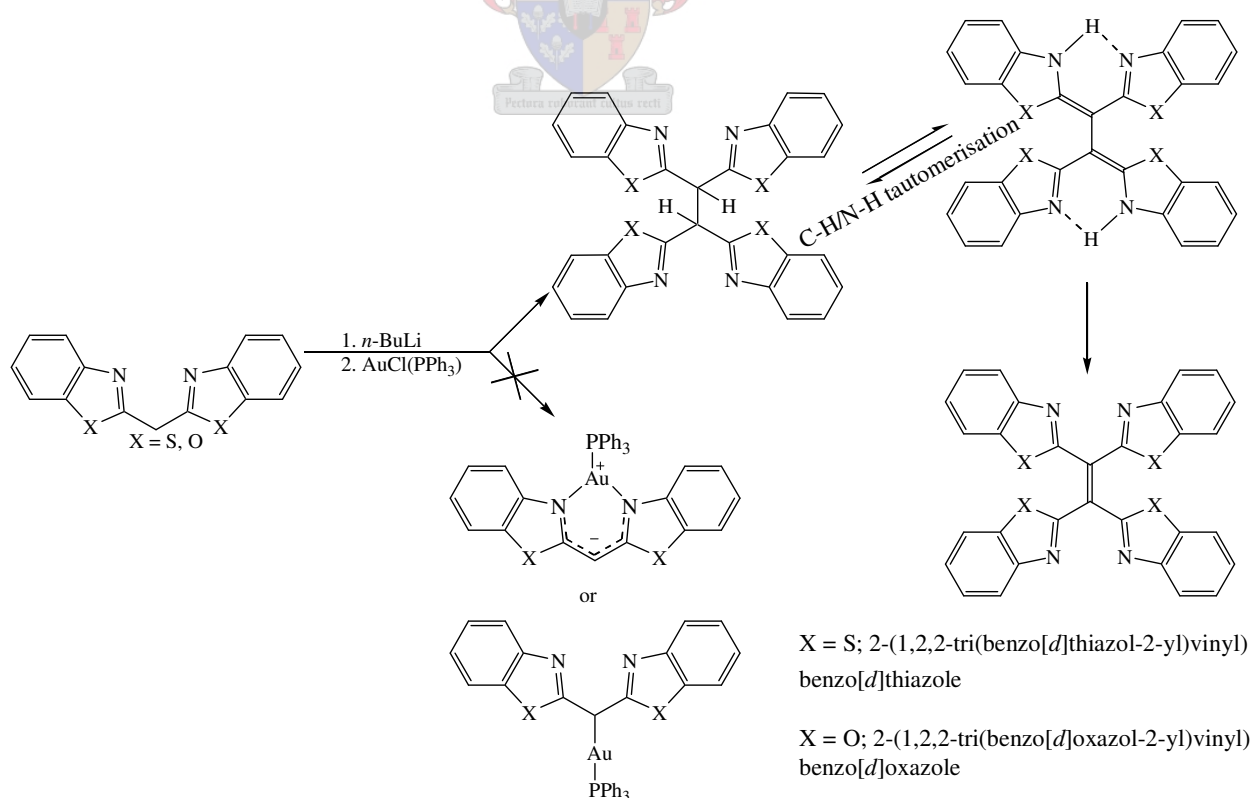


Scheme 4.9

The dimeric tetrakis(2-benzothiazolyl)ethane, 2-(1,2,2-tri(benzo[*d*]oxazol-2-yl)vinyl)benzo[*d*]oxazole and cationic sulfonium gold(I) complex (μ_3 -sulfide[triphenylphosphinegold])chlorate, [S(Au(PPh₃))₃]⁺Cl⁻ were obtained after treatment of the respective ligands, HBBTM or HBBOM, in THF with similar mmol amounts of *n*-BuLi at -70 °C, followed by the addition of excess amounts of sulfur and AuCl(PPh₃) at an interval of 30 min. After the solvent was removed at reduced pressure the residues were washed with diethyl ether. The final products dissolve very well in THF,

dichloromethane and acetone. A mixture of orange and colourless crystals was obtained from dichloromethane solution layered with *n*-pentane at -20 °C. Selectively the orange crystals were investigated by single crystal X-ray analysis and the molecular structures show 2-(1,2,2-tri(benzo[*d*]oxazol-2-yl)vinyl)benzo[*d*]oxazole. The FAB MS and ESI MS investigations also indicated a second product equivalent to the cationic sulphonium complex, $[\text{S}(\text{Au}(\text{PPh}_3))_3]^+\text{Cl}^-$, however, no X-ray analysis was performed.

A solution of HBBTM or HBBOM in THF was treated with an *n*-BuLi solution in *n*-hexane at -70 °C and resulted in blue fluorescence during the process of deprotonation characteristic of charge delocalisation. A solution of AuCl(PPh₃) in THF was transferred to the mixture and stirred for 2 h. The solvent was removed under vacuum. The products dissolve very well in THF, dichloromethane and chloroform. The ³¹P NMR data for this mixture indicated the presence of the dinuclear gold(I) complex **18**. Crystallisation of the residue from chloroform solution layered with *n*-hexane at -20 °C afforded a mixture of yellow and orange crystals. The molecular structure obtained (for X = S) by single crystal X-ray studies for the yellow crystals show the oxidative dimerisation of the ligand HBBTM to 2-(1,2,2-tri(benzo[*d*]thiazol-2-yl)vinyl)benzo[*d*]thiazole.



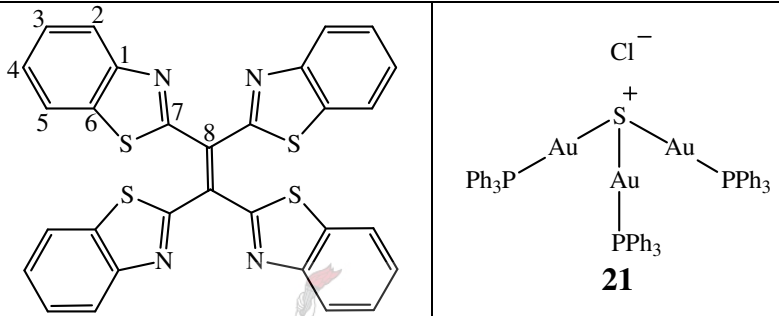
Scheme 4.10

4.4.2 Spectroscopic characterisation of 2-(1,2,2-tri(benzo[*d*]thiazol-2-yl)vinyl)benzo[*d*]thiazole, [S(AuP(Ph₃))₃]⁺Cl⁻, **21 and 2-(1,2,2-tri(benzo[*d*]oxazol-2-yl)vinyl)benzo[*d*]oxazole, **22****

NMR spectroscopy

4.4.2.1 [(BT)₂C=C(BT)₂] (BT = benzothiazolyl), and [S(AuP(Ph₃))₃]⁺Cl⁻, **21**

Table 4.12 ¹H and ¹³C NMR data of {BT}₂C=C{BT}₂ and [S(Au(PPh₃))₃]⁺Cl⁻, **21** in CDCl₃

Assignment	δ(ppm) (multiplicity, J(Hz))	δ(ppm) (multiplicity, J(Hz))
		
¹H NMR		
H ²	7.98 (4H, m)	7.56 – 7.44 (45H, m)
H ⁵	7.89 (4H, m)	
H ³	Obscured by Ph ₃	
H ⁴	Obscured by Ph ₃	
Ph		
¹³C NMR		
C ⁷	165.0	128.1 (d, obscured) 132.8 (d, ³ J _{C-P} = 10.9 Hz) 132.2 (d, ⁴ J _{C-P} = 3.2 Hz) 129.1 (d, ² J _{C-P} = 12.2 Hz)
C ¹	153.7	
C ⁶	137.6	
C ²	126.9	
C ⁵	125.9	
C ³	124.7	
C ⁴	122.3	
C ⁸	Obscured by Ph ₃	
C ^{ipso}		
C ^{meta}		
C ^{para}		
C ^{ortho}		
³¹P NMR		43.68

The ^1H , ^{13}C and ^{31}P NMR data of 2-(1,2,2-tri(benzo[*d*]thiazol-2-yl)vinyl)benzo[*d*]thiazole and $[\text{S}\{\text{Au}(\text{PPh}_3)_3\}]^+\text{Cl}^-$, **21** are summarised in Table 4.12. The ^1H and ^{13}C NMR investigations for the reaction products obtained in Scheme 4.10 are quite similar to those reaction products obtained in Scheme 4.9, thus the analytical discussions of the two Schematic reactions are divided into two according to the similarities of the proposed products. However, differences have also been considered between ^{31}P NMR spectra and are treated accordingly. The ^{31}P NMR data for the reaction products obtained according to Scheme 4.10 revealed similar chemical shifts to that of the dinuclear gold(I) complex **19**. This hints that one may also carefully isolate complex **19** by a recrystallisation. As a result in this report we only have considered the ^{31}P NMR of those products obtained in Scheme 4.9.

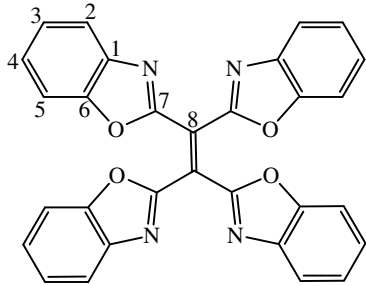
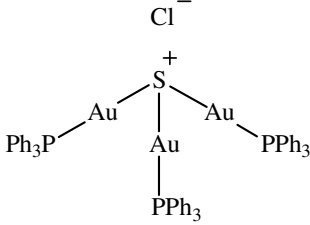
The protons H^2 and H^5 resonate at δ 7.98 and 7.89, respectively. Two sets of multiplets at δ 7.76 - 7.69 and 7.56 - 7.44 are assigned for the phenyl protons. The signals for H^3 and H^4 are obscured by two sets of strong signals of the phenyl groups of the cationic sulphonium complex, $[\text{S}(\text{AuP}(\text{Ph}_3))_3]^+\text{Cl}^-$. A very weak signal at 4.93 ppm characteristic for the methylene protons, CH_2 , indicates the presence of unreacted ligand. However, comparison of spectral integration of the signal with respect to the benzothiazolyl protons H^2 and H^5 shows that the concentration of the CH_2 is extremely low, thus indicating that oxidative dimerisation product of the ligand HBBTM to 2-(1,2,2-tri(benzo[*d*]thiazol-2-yl)vinyl)benzo[*d*]thiazole has a higher yield.

The ^{13}C NMR spectrum shows two sets of signals for the benzothiazolyl groups indicating the presence of two possible products. The signal corresponding to the methine carbon, CH , does not appear at the expected region.²³ This indicates that the oxidative dimerisation of HBBTM to 2-(1,2,2-tri(benzo[*d*]thiazol-2-yl)vinyl)benzo[*d*]thiazole has occurred, although the corresponding signal for C^8 is obscured by the strong signals from the triphenylphosphine ligand. One of the signals corresponding to the doublets for $\text{C}^{\textit{ipso}}$ at 133.7 ppm is obscured by the high intensity signals for the other phenyl carbon atoms.

The ^{31}P NMR spectrum shows three singlet signals at 43.68 ppm (64 %), 33.81 ppm (33 %), and 28.42 ppm (3.0 %). The signal with the highest intensity at 43.68 ppm (64 %) is assigned to $[\mu_3\text{-sulfide}(\text{triphenylphosphinegold}(\text{I}))]\text{chlorate}$, $[\text{S}(\text{Au}(\text{PPh}_3))_3]^+\text{Cl}^-$.

4.4.2.2 {BO}₂C=C{BO}₂ (BO = benzoxazolyl), **22** and [S(Au(PPh₃))₃]⁺Cl⁻

Table 4.13 ¹H and ¹³C NMR data of {BO}₂C=C{BO}₂, **22** and [S(Au(PPh₃))₃]⁺Cl⁻ in CDCl₃

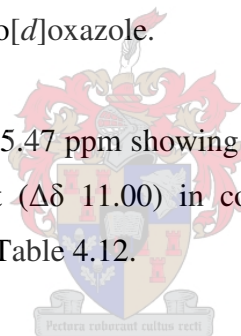
	 <p style="text-align: center;">22</p>	
Assignment	δ(ppm) (multiplicity, J(Hz))	δ(ppm) (multiplicity, J(Hz))
¹H NMR		
H ⁵	7.73, (4H, tm, ³ J _{H5-H4} = 13.5 Hz)	7.51 - 7.40 (45H, m)
H ²	7.71, (4H, tm, ³ J _{H2-H3} = 13.3 Hz)	
H ³	Obscured by Ph ₃	
H ⁴	Obscured by Ph ₃	
H ⁸	Obscured by Ph ₃	
Ph	Obscured by Ph ₃	
¹³C NMR		
C ⁷	168.3	not observed
C ¹	149.2	
C ⁶	141.2	
C ⁵	123.6	
C ²	120.5	
C ⁴	112.1	
C ³	111.0	
C ⁸	134.8	
C ^{ipso}		
C ^{meta}		
C ^{para}		132.4, (d, ³ J _{C-P} = 10.4 Hz)
C ^{ortho}		131.7, (d, ⁴ J _{C-P} = 3.1 Hz)
		128.6, (d, ² J _{C-P} = 13.9 Hz)
³¹P NMR		45.47

¹H, ¹³C and ³¹P NMR data of the mixture of the products, **22** and [S(Au(PPh₃))₃]⁺Cl⁻ are summarised in Table 4.13. Predominantly the mixture contains the signals corresponding to the 2-(1,2,2-tri(benzo[*d*]oxazol-2-yl)vinyl)benzo[*d*]oxazole and [μ₃-sulfido-tris(triphenylphosphine gold)]chlorate, [S(Au(PPh₃))₃]⁺Cl⁻. The ¹H NMR signals of H³ and

H⁴ of the benzothiazolyl group are obscured by the phenyl protons. Multiplets of signals at δ 7.73 and 7.71 are assigned to the protons H⁵ and H², respectively. The multiplet of signals observed at 7.51 - 7.40 ppm are comparable to the signals reported for the phenyl protons in [μ_3 -sulfido-tris(triphenylphosphine gold)]chlorate, [S(Au(PPh₃))₃]⁺Cl⁻ (Table 4.12). Neither the signal corresponding to the methine proton, CH, nor the methylene, CH₂, protons are observed, indicating that oxidative dimerisation of HBBOM to 2-(1,2,2-tri(benzo[*d*]oxazol-2-yl)vinyl)benzo[*d*]oxazole has taken place.

The ¹³C NMR spectrum has been complicated due the presence of a mixture of products. The chemical shifts and coupling constants for the phenyl carbons are similar to **21**, but the signal for the C^{*ipso*} is obscured by the strong and broad intensity signal for C^{*ortho*}. No signals are observed corresponding to the methylene carbon, CH₂, as well as for the methine carbon, CH. A signal at 134.8 ppm is assigned to the sp² C⁸, this indicates that the bridging carbon atom, C⁸, has undergone oxidative dimerisation to 2-(1,2,2-tri(benzo[*d*]oxazol-2-yl)vinyl)benzo[*d*]oxazole.

³¹P NMR shows a broad signal at 45.47 ppm showing only one type of phosphorous atom. The downfield shift is significant ($\Delta\delta$ 11.00) in comparison with AuCl(PPh₃) and is comparable to the data reported in Table 4.12.



Mass spectrometry

The FAB MS data for the residue containing a mixture of the products are summarised in Table 4.14. The FAB mass spectrum shows a peak with the highest intensity at m/z 1410 corresponding to the cation [μ_3 -sulfide(triphenylphosphinegold(I))], [S(Au(PPh₃))₃]⁺. The fragmentation pattern of this cation shows the loss of one [PPh₃]⁺ at m/z 1147 to give [AuS[Au(PPh₃)₂]⁺. The peaks at m/z 721 and m/z 459 are characteristic of the homoleptically-rearranged [Au(PPh₃)₂]⁺ and [Au(PPh₃)]⁺ products. The peak at m/z 426 corresponds to the fragment [(BT)₂C=C(BT)]⁺ (BT = benzothiazolyl) obtained after the loss of a benzothiazolyl group from 2-(1,2,2-tri(benzo[*d*]thiazol-2-yl)vinyl)benzo[*d*]thiazole. The peak at m/z 281 is due to the free ligand. The FAB MS data obtained for **22** were not clear, hence no data are reported.

Table 4.14 Mass spectrometric data for the mixture of $\{\text{BT}\}_2\text{C}=\text{C}\{\text{BT}\}_2$ and $[\text{S}(\text{Au}(\text{PPh}_3))_3]^+\text{Cl}^-$, **21**

<i>m/z</i>	Intensity (%)	Fragment ion
1410	19	$[\text{S}[\text{Au}(\text{PPh}_3)]_3]^+$
1147	3	$[\text{AuS}[\text{Au}(\text{PPh}_3)]_2]^+$
950	1.5	$[\text{S}[\text{Au}(\text{PPh}_3)]_2]^+$
721	5	$[\text{Au}(\text{PPh}_3)_2]^+$
459	19	$[\text{Au}(\text{PPh}_3)]^+$
426	2	$[(\text{BT})_2\text{C}=\text{C}(\text{BT})]^+$
281	17	$[\{\text{BT}\}_2\text{CH}_2]^+$
109	12	$[\text{PPh}]^+$

4.4.3 The crystal and molecular structures of 2-(1,2,2-tri(benzo[*d*]thiazol-2-yl)vinyl)benzo[*d*]thiazole, **11** and 2-(1,2,2-tri(benzo[*d*]oxazol-2-yl)vinyl)benzo[*d*]oxazole, **22**

Compounds 2-(1,2,2-tri(benzo[*d*]thiazol-2-yl)vinyl)benzo[*d*]thiazole and 2-(1,2,2-tri(benzo[*d*]oxazol-2-yl)vinyl)benzo[*d*]oxazole crystallised in the monoclinic space groups $P2_1/n$ and $P2_1/c$, respectively as light yellow crystals from concentrated dichloromethane solutions layered with *n*-pentane at -20°C . Selected bond lengths and angles are listed in Table 4.15 and Table 4.16. The molecular structures for 2-(1,2,2-tri(benzo[*d*]thiazol-2-yl)vinyl)benzo[*d*]thiazole (A) and 2-(1,2,2-tri(benzo[*d*]oxazol-2-yl)vinyl)benzo[*d*]oxazole (B) are shown in Figure 4.11. The compounds have similar bond lengths and angles for analogous atoms with in the ranges of the indicated standard deviations. One of the differences noticed, however is the co-crystallisation of pair of solvent molecules linked by intermolecular interactions comparable to the hydrogen bonding with the 2-(1,2,2-tri(benzo[*d*]thiazol-2-yl)vinyl)benzo[*d*]thiazole. The molecular structure in Figure 4.11 shows that the four azolyl groups are connected by C(1)–C(1) and the symmetrically identical groups are arranged in *trans* position. The mean C(1)–C(1) bond length of $1.357(3) \text{ \AA}$ in both compounds confirms the oxidative dimerisation of bis(2-benzothiazolyl)methane, HBBTM and bis(2-benzoxazolyl)methane, HBBOM to 2-(1,2,2-tri(benzo[*d*]thiazol-2-yl)vinyl)benzo[*d*]thiazole and 2-(1,2,2-tri(benzo[*d*]oxazol-2-yl)vinyl)benzo[*d*]oxazole, respectively.

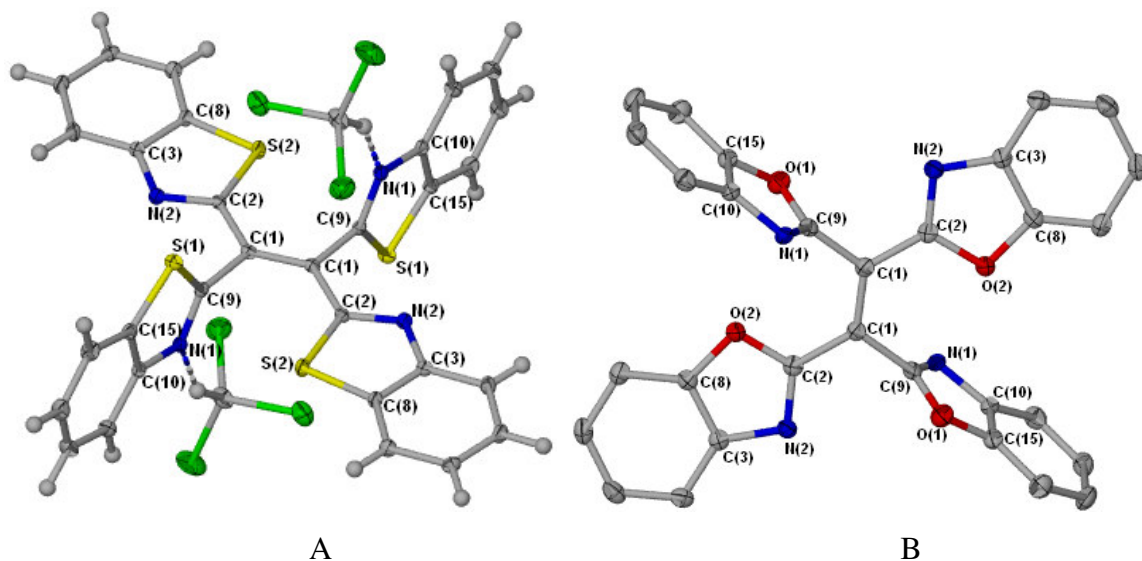


Figure 4.11 Drawing of molecular structure of 2-(1,2,2-tri(benzo[*d*]thiazol-2-yl)vinyl)benzo[*d*]thiazole (A) and 2-(1,2,2-tri(benzo[*d*]oxazol-2-yl)vinyl)benzo[*d*]oxazole (B).

The mean C(1)–C(9) and C(1)–C(2) bond lengths of 1.49(2) and 1.462(2) Å, respectively correspond to a C–C single bond. Similarly N(1)–C(9) and N(2)–C(2) bond lengths of 1.297(2) and 1.304(2) Å, respectively are equivalent to double bonds and are fairly short when compared to N(1)–C(10) and N(2)–C(3) bond lengths of 1.394(2) and 1.388(2) Å corresponding to single bonds. The bond lengths and angles in the benzene and 1,3-thiazole rings are as expected. The deviation of the plane defined by C(1), N(1), C(10), C(11), C(12), C(13), C(14), C(15), O(1) and C(9) for 2-(1,2,2-tri(benzo[*d*]oxazol-2-yl)vinyl)benzo[*d*]oxazole from the least square plane is 0.0258 Å.

The mean bond angles C(1)–C(1)–C(2) [125.76(18)°], C(1)–C(1)–C(9) [120.91(18)°] and C(2)–C(1)–C(9) [113.30(13)°] indicate trigonal planar geometry around C(1) and are comparable to the bond angles obtained by tetrakis(2-benzothiazoly)ethane.¹⁵ S(1)–C(15)–C(10) [109.45(12)°] and S(2)–C(8)–C(3) [109.32(12)°] are in accordance with 2-(1,2,2-tri(benzo[*d*]thiazol-2-yl)vinyl)benzo[*d*]thiazole and similarly also O(1)–C(15)–C(10) [107.80(13)°] and O(2)–C(8)–C(3) [107.76(13)°] are in accordance with 2-(1,2,2-tri(benzo[*d*]oxazol-2-yl)vinyl)benzo[*d*]oxazole. The dihedral angle [85.35°] between the planes defined by the benzothiazolyl groups attached to the C(1) deviates slightly from 90°. Similarly, the dihedral angle comprising the planes of the benzoxazolyl groups

attached to the same C(1) atom is 74.44° . The torsion angles defined by C(9)–C(1)–C(1)–C(9) [180°] and C(2)–C(1)–C(1)–C(2) [180°] indicate the symmetrically identical benzothiazolyl and benzoxazolyl groups attached to C(1) are related by a centroid that lies between the bridging C(1) atoms.

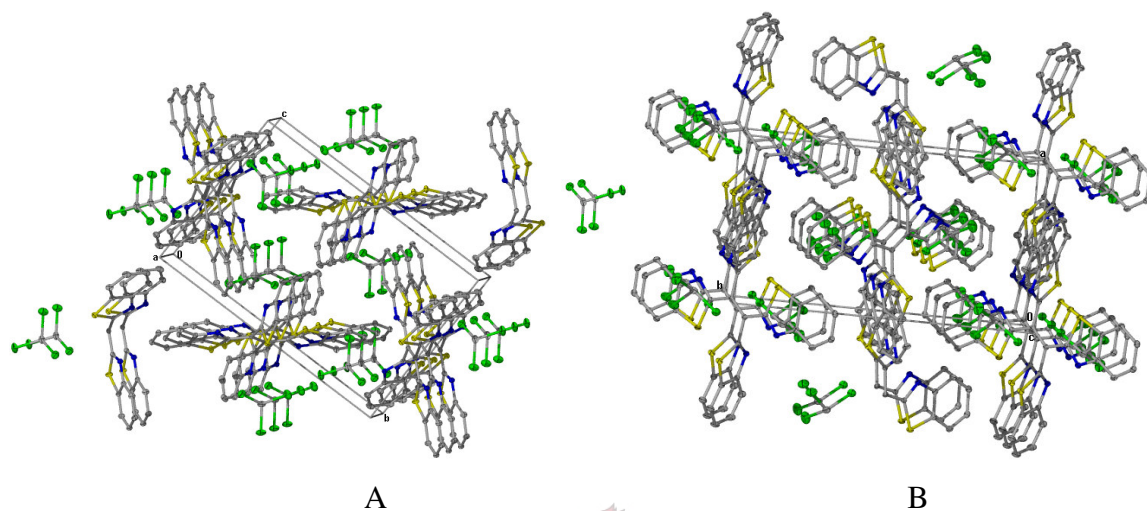


Figure 4.12 Packing diagram of the molecules of 2-(1,2,2-tri(benzo[*d*]thiazol-2-yl)vinyl)benzo[*d*]thiazole along the *a*-axis (A) and *c*-axis (B).

Molecular packing of 2-(1,2,2-tri(benzo[*d*]thiazol-2-yl)vinyl)benzo[*d*]thiazole molecules along the crystallographic *a*-axis and *c*-axis are shown in Figure 4.12. The unit cell packing when viewed down the crystallographic *a*-axis and *c*-axis shows the molecules are stacked along these axes.

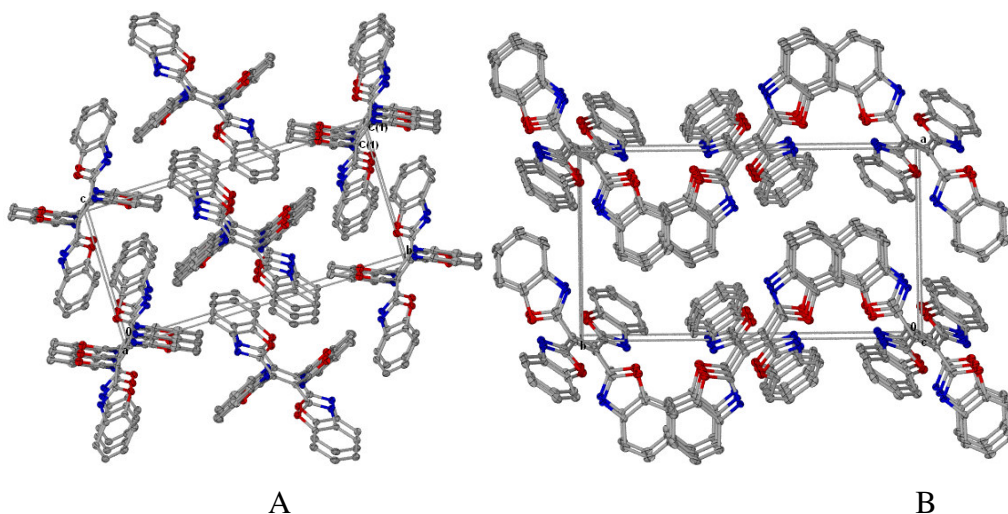


Figure 4.13 Packing diagram of the molecules of 2-(1,2,2-tri(benzo[*d*]oxazol-2-yl)vinyl)benzo[*d*]oxazole along the *a*-axis (A) and *c*-axis (B).

Molecular packing of 2-(1,2,2-tri(benzo[*d*]oxazol-2-yl)vinyl)benzo[*d*]oxazole molecules along the crystallographic a-axis (A) and c-axis (B) are shown in Figure 4.13. Molecules along the crystallographic a-axis and c-axis are stacked on top of each other and have similar packing features to those of 2-(1,2,2-tri(benzo[*d*]thiazol-2-yl)vinyl)benzo[*d*]thiazole along the crystallographic c-axis (Figure 4.13).

Table 4.15 Selected bond lengths (Å) and angles (°) for 2-(1,2,2-tri(benzo[*d*]thiazol-2-yl)vinyl)benzo[*d*]thiazole

S(1)–C(15)	1.7320(18)	C(2)–S(2)	1.7540(16)
S(1)–C(9)	1.7453(17)	C(3)–C(4)	1.403(2)
N(2)–C(2)	1.307(2)	C(3)–C(8)	1.408(2)
N(2)–C(3)	1.381(2)	C(9)–C(1)	1.498(2)
N(1)–C(9)	1.294(2)	C(8)–S(2)	1.7314(17)
N(1)–C(10)	1.391(2)	C(10)–C(15)	1.404(2)
C(2)–C(1)	1.467(2)	C(1)–C(1)	1.358(3)
C(15)–S(1)–C(9)	88.89(8)	C(3)–C(8)–S(2)	109.32(12)
C(2)–N(2)–C(3)	111.11(14)	N(1)–C(10)–C(11)	125.10(16)
C(9)–N(1)–C(10)	110.42(14)	N(1)–C(10)–C(15)	114.89(15)
N(1)–C(9)–C(1)	123.02(15)	C(11)–C(10)–C(15)	120.01(16)
N(1)–C(9)–S(1)	116.33(12)	C(1)–C(1)–C(2)	126.74(19)
C(1)–C(9)–S(1)	120.64(12)	C(1)–C(1)–C(9)	120.40(19)
C(7)–C(8)–C(3)	121.73(15)	C(2)–C(1)–C(9)	112.84(14)
C(7)–C(8)–S(2)	128.95(13)		

Table 4.16 Selected bond lengths (Å) and angles (°) for 2-(1,2,2-tri(benzo[*d*]oxazol-2-yl)vinyl)benzo[*d*]oxazole

O(2)–C(2)	1.3620(18)	N(1)–C(10)	1.3971(18)
O(2)–C(8)	1.3823(18)	C(10)–C(15)	1.386(2)
O(1)–C(9)	1.3367(19)	C(1)–C(1)	1.356(3)
O(1)–C(15)	1.3866(18)	C(1)–C(2)	1.457(2)
N(2)–C(2)	1.3005(19)	C(1)–C(9)	1.482(2)
N(2)–C(3)	1.3952(19)	C(8)–C(3)	1.392(2)
N(1)–C(9)	1.3033(19)		

(continued...)

C(2)–O(2)–C(8)	103.67(11)	O(2)–C(2)–C(1)	120.16(13)
C(2)–N(2)–C(3)	104.27(12)	O(2)–C(8)–C(7)	128.45(14)
C(1)–C(1)–C(2)	124.78(17)	O(2)–C(8)–C(3)	107.76(13)
C(1)–C(1)–C(9)	121.41(17)	C(7)–C(8)–C(3)	123.78(14)
C(2)–C(1)–C(9)	113.75(12)	C(8)–C(3)–C(4)	120.44(14)
N(2)–C(2)–O(2)	115.83(13)	C(8)–C(3)–N(2)	108.47(13)
N(2)–C(2)–C(1)	123.99(13)	C(4)–C(3)–N(2)	131.08(14)

4.5 Conclusions and further work

In this chapter complexes of gold(I) derived from the formally bidentate ligands HBBTM and HBBOM as well as products of side reactions have been described. Products obtained were unfortunately not always pure but, nevertheless, X-ray diffraction studies allowed their unequivocal characterisation. During the course of reaction between HBBTM, Au(PPh₃)Cl and AgBF₄ the ligand HBBTM underwent oxidative dimerisation to an alkene derivative, 2-(1,2,2-tri(benzo[*d*]thiazol-2-yl)vinyl)benzo[*d*]thiazole and binds to four Ph₃PAu⁺ units yielding [{(AuPPh₃)(BT-*N*)₂C=C{(BT-*N*)(AuPPh₃)}₂]⁴⁺4[BF₄]⁻, **16**, and a second product [{(AuPPh₃)(BT-*N*)₂CH₂]²⁺2[BF₄]⁻, **17** was also isolated and characterised from the mixture.

When ligands HBBTM and HBBOM deprotonated with Ph₃PAu(acac), both form unique three-coordinated gold compounds [(PPh₃)Au{BT-*N,N*}₂CH], **18** and [(PPh₃)Au{BO-*N,N*}₂CH], **20** by utilising both their *N*-atoms. Another neutral gold(I) complex (Ph₃P)AuNC=CHCH=CHCH=CSC=C(BT)–(BT)C=CSC=CHCH=CHCH=CNAu(PPh₃), **19** with an anionic donor ligand was obtained by treating HBBTM and AuCl(PPh₃) with NaH in a one-pot reaction. Structural analysis by X-ray diffraction indicates that the bond bridging the C–C atoms has single bond [1.474(7) Å].

Further work should involve other gold substrates and specifically compounds of the type LAuCl with L a labile ligand (THT or Me₂S). In the same fashion as before, unprecedented homoleptic compounds and the bonding herein could be investigated.

HBBTM and HBBOM deprotonated with *n*-BuLi prior to the addition of AuCl(PPh₃) afforded 2-(1,2,2-tri(benzo[*d*]thiazol-2-yl)vinyl)benzo[*d*]thiazole and tetrakis(2-benzoxazolyl)ethene, respectively. The oxidative dimerisation of the carbanions of the intermediates and the spontaneous oxidation of the tautomeric C-H/N-H tetrakis(2-benzothiazolyl)ethane and tetrakis(2-benzoxazolyl)ethane are responsible for these transformations. Other attempts to prepare thiolategold(I) complexes of Au(SBBTM)(PPh₃) or Au(SBBOM)(PPh₃) by deprotonation of HBBTM or HBBOM with *n*-BuLi followed by insertion of sulfur into the carbanion intermediates (C–Li) and reaction with AuCl(PPh₃) led to oxidative dimerisation of the ligands and formation of the cationic sulphonium complex, [S(AuPPh₃)₃]⁺Cl⁻. ¹H, ¹³C and ³¹P NMR, ESI MS and single crystal X-ray analysis were used to characterise these products.

Further work should be carried out to establish in more ways than one how HBBTM and HBBOM differ from acacH in their reaction with metal complexes.

4.6 Experimental

4.6.1 Materials and methods



All reactions were carried out under an atmosphere of nitrogen or argon using Schlenk techniques. Solvents were dried by standard methods as mentioned in Chapter 2 and distilled under nitrogen prior to use. AuCl(PPh₃)³⁰ was prepared as described in the literature from PPh₃ and HAuCl₄. Au(acac)(PPh₃) was prepared from Tl(acac) and AuCl(PPh₃).¹³ Tl(acac) was prepared from Tl₂CO₃ and Hacac,¹³ it is also commercially available from Aldrich. HBBTM and HBBOM were prepared according to procedures in the literature.^{9,10} The following compounds were obtained commercially from Aldrich and used without further purification: AgBF₄, S₈ and NaH (which was carefully washed with *n*-hexane and diethyl ether). *n*-BuLi (Fluka) was standardised prior to use.³¹

Note: Due to impurities present in the final product mixtures of **21** and **22**, melting points and yields are only reported for analytically pure compounds.

³⁰ M. I. Bruce, B. K. Nicholson and O. B. Shawkataly, *Inorg. Synth.*, 1989, **26**, 325.

³¹ W. R. Winkle, J. M. Langsinger and R. C. Ronald, *J. Chem. Soc., Chem. Comm.*, 1980, 87.

4.6.2 Preparations

4.6.2.1 Preparation of $[\{\text{Ph}_3\text{PAu}(\text{BT}-N)\}_2\text{C}=\text{C}\{\text{BT}-N\}\text{AuPPh}_3\}_2]^{4+}4[\text{BF}_4]^-$, **16** and $[\{\text{Ph}_3\text{PAu}(\text{BT}-N,N)\}_2\text{CH}_2]^{2+}2[\text{BF}_4]^-$, **17**

A mixture of HBBTM (0.10 g, 0.36 mmol) and AuCl(PPh₃) (0.36 g, 0.72 mmol) in THF was transferred to a solution of AgBF₄ (0.40 g, 0.72 mmol) in THF at room temperature. A white precipitate of AgCl formed immediately. The reaction mixture was stirred at room temperature for > 20 h. The solvent of the red THF solution was removed under vacuum and the residue was washed several times with diethyl ether. The residue containing insoluble substances was re-dissolved in dichloromethane and filtered through Celite to remove the AgCl precipitate. The product was crystallised from dichloromethane and diethyl ether by diffusion at -20 °C. Red and light yellow crystals suitable for molecular structure determination were obtained.

Compound: **16** Yield: 1.5 g (71 %) Melting point: 150 - 153 °C (decomposed)

17 Yield: 0.83 g (83 %) Melting point: 135 °C (decomposed)

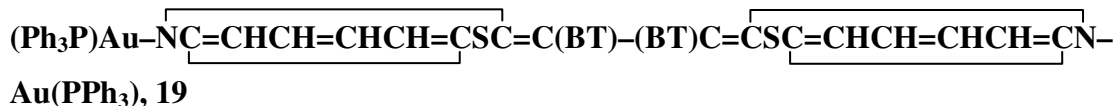
4.6.2.2 Preparation of $\text{PPh}_3\text{Au}(\text{BT}-N,N)_2\text{CH}$, **18**

A solution of HBBTM (0.084 g, 0.30 mmol) in THF was transferred to a suspension of Au(acac)(PPh₃) (0.10 g, 0.18 mmol) in the same solvent. The mixture was stirred at room temperature for more than 20 h. The solvent was stripped under vacuum. The oily residue was treated with a mixture of *n*-pentane and minimum amount of dichloromethane and the solvent was removed in *vacuo*. This step was repeated several times until a residue free of the acetylacetonate was obtained. Finally, the residue was dissolved in the minimum of dichloromethane and precipitated by adding an excess of *n*-pentane. The yellow residue was filtered off and collected.

Compound: **18** Yield: 0.10 g (75 %)

Melting point: 110 °C (decomposed)

4.6.2.3 Preparation of



A suspension of an excess of NaH was transferred to a mixture of HBBTM (0.10 g 0.36 mmol) and AuCl(PPh₃) (0.18 g, 0.36 mmol) in THF at -60 °C. The reaction mixture was stirred for 30 min and the dry-ice bath was removed. The reaction mixture was stirred at room temperature for 3 h. The orange mixture was stirred overnight at room temperature. The solvent was removed under vacuum and the orange residue was washed with *n*-hexane. The residue was re-dissolved in dichloromethane and filtered through Celite to remove NaCl and the excess of NaH. The solvent was reduced under vacuum to approximately 5.0 cm³ and the product precipitated by the addition of an excess of *n*-hexane. The residue was recrystallised from dichloromethane and *n*-pentane by slow diffusion at -20 °C.

Compound: **19** Yield: 0.45 g (84 %) Melting point: 128 - 131 °C (decomposed)

4.6.2.4 Preparation of [(PPh₃)Au{BO}₂CH], 20

The same procedure as in Section 4.4.2 above was repeated with HBBOM (0.088 g, 0.35 mmol) and Au(acac)(PPh₃) (0.17 g, 0.31 mmol) in methanol. A concentrated solution of dichloromethane at -20 °C afforded light yellow crystals.

Compound: **20** Yield: 0.14 g (64 %) Melting point: 130 °C (decomposed)

4.6.2.5 {BT}₂C=C{BT}₂ and [S(AuP(Ph₃))₃]⁺Cl⁻, 21

A solution of HBBTM (0.15g, 0.53 mmol) in diethyl ether was cooled down to -78 °C in a dry-ice bath. A solution of *n*-BuLi in *n*-hexane (0.40 cm³ of 1.4 M) was added from a syringe drop wise while stirring. Luminescence was observed. The temperature was raised to -30 °C and an excess of S₈ suspended in diethyl ether was added to this mixture. The luminescent solution turned red immediately and was stirred for another 30 min at the same temperature. A suspension of AuCl(PPh₃) in the same solvent was transferred to the mixture. The temperature was raised slowly to room temperature and finally the ice-bath was removed and the mixture was stirred overnight at room temperature. A yellow

precipitate was filtered off and washed with ether. The mother liquor was collected and stripped under vacuum and an orange residue was obtained.

4.6.2.6 $\{\text{BO}\}_2\text{C}=\text{C}\{\text{BO}\}_2$, **22** and $[\text{S}(\text{AuP}(\text{Ph}_3))_3]^+\text{Cl}^-$

A THF solution of HBBOM (0.075 g, 0.30 mmol) was cooled to $-78\text{ }^\circ\text{C}$ followed by the drop wise addition of a *n*-BuLi solution in *n*-hexane (0.25 cm^3 of 1.4 M). The temperature was then slowly raised to room temperature. A suspension of an excess of S_8 in THF was transferred to the mixture, which was already cooled down to $-78\text{ }^\circ\text{C}$ again. After stirring for 1 h, a solution of $\text{AuCl}(\text{PPh}_3)$ (0.15 g, 0.33 mmol) in THF was transferred to the mixture. The reaction mixture was warmed slowly. Finally, the cooling bath was removed and the orange mixture stirred at room temperature. The solvent was removed under vacuum. The residue was extracted with diethyl ether, dichloromethane and THF. The extracts were filtered through Celite and evacuated to dryness.

4.6.3 X-ray structure determinations

The crystal data collection and refinement details for complexes **16**, **17**, **19**, **20**, 2-(1,2,2-tri(benzo[*d*]thiazol-2-yl)vinyl)benzo[*d*]thiazole and tetrakis(2-benzoxazoly)ethene are summarised in Table 2.28 and Table 2.29. All data sets were collected on a Bruker SMART-Apex diffractometer using graphite monochromated Mo- $\text{K}\alpha$ radiation ($\lambda = 0.71073\text{ \AA}$).³² All measurements were made at 100 K, except **17** and **22** were measured at 273 K. Data reduction was carried out with standard methods from the software package Bruker SAINT.³³ Empirical corrections were performed using SCALEPACK and SMART.³⁴ For adsorption corrections the data were treated with SADABS.^{35,36} The program X-Seed³⁷ was used as a graphical interface for structure solution and refinement with direct methods using SHELX. All non-hydrogen atoms were refined anisotropically by full-matrix least squares calculations on F^2 using SHELXL-97. The hydrogen atoms were fixed in calculated positions. POV-Ray for Windows was used to generate the various figures of the six compounds at the 50% probability level.

³² SMART Data collection software (version 5.629), Bruker AXS Inc., Madison, WI, 2003.

³³ SAINT, Data reduction software (version 6.45) Bruker AXS Inc., Madison, WI, 2003.

³⁴ L.J. Ferrugia, *J. Appl. Crystallogr.*, 1999, **32**, 837.

³⁵ R.H. Blessing, *Acta Crystallogr., Sect. A*, 1995, **51**, 33.

³⁶ SADABS (version 2.05) Bruker AXS Inc., Madison, WI, 2002.

³⁷ (a) L. J. Barbour, *J. Supramol. Chem.*, 2001, **1**, 189. (b) J. L. Atwood and L. J. Barbour, *Cryst. Growth Des.*, 2003, **3**, 3.

Additional information concerning the X-ray work is available from Prof H. G. Raubenheimer, Department of Chemistry, University of Stellenbosch.

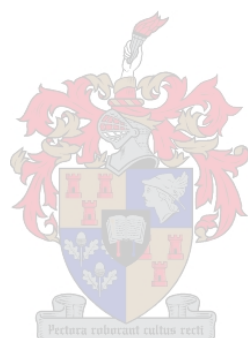


Table 4.17 Crystallographic data for complexes **16**, **17** and **19**

	16	17	19
Empirical formula	C ₁₀₇ H ₈₅ Au ₄ B ₄ Cl ₁₀ F ₁₆ N ₄ P ₄ S ₄	C ₁₀₈ H ₉₂ Au ₄ B ₃ Cl ₁₂ F ₁₄ N ₄ P ₄ S ₄	C ₆₉ H ₅₂ Au ₂ Cl ₆ N ₄ P ₂ S ₄
Formula weight (g.mol ⁻¹)	3168.52	3209.67	1733.96
Crystal system	Triclinic	Monoclinic	Triclinic
Space group	<i>P</i> $\bar{1}$	<i>C2/c</i>	<i>P</i> $\bar{1}$
a (Å)	16.3698(13)	27.8737(12)	12.723(5)
b (Å)	18.0679(14)	18.8516(8)	13.593(6)
c (Å)	23.7823(19)	24.2529(11)	19.108(8)
α (°)	102.239(2)	90	88.815(7)
β (°)	102.7390(10)	112.1550(10)	80.273(7)
γ (°)	111.094(2)	90	77.976(7)
Volume (Å ³)	6064.2(8)	11803.1(9)	3185(2)
Z	2	4	2
Calculated density (g.cm ⁻³)	1.735	1.806	1.808
Wave length (Å)	0.7107	0.71073	0.71073
Temperature (K)	100(2)	273(2)K	100(2)
Absorption coefficient (mm ⁻¹)	5.236	5.423	5.081
Crystal size (mm ³)	0.25 x 0.07 x 0.04	0.25 x 0.10 x 0.10	0.20 x 0.10 x 0.10
$2\theta_{\max}$ (°)	51.4	56.6	51.4
Index range, <i>hkl</i>	-19 ≤ <i>h</i> ≤ 19 -22 ≤ <i>k</i> ≤ 22 -28 ≤ <i>l</i> ≤ 28	-17 ≤ <i>h</i> ≤ 36 -24 ≤ <i>k</i> ≤ 23 -32 ≤ <i>l</i> ≤ 30	-15 ≤ <i>h</i> ≤ 15 -16 ≤ <i>k</i> ≤ 13 -23 ≤ <i>l</i> ≤ 23
Reflections collected	62159	36260	19977
No. of independent reflections	22897 (<i>R</i> _{int} = 0.0704)	13449 (<i>R</i> _{int} = 0.0914)	11851 (<i>R</i> _{int} = 0.0270)
Parameters	1378	691	784
Goodness of fit	1.101	1.001	1.039
Largest peak	6.71	3.54	1.53
Deepest hole	-3.00	-3.00	-1.19
<i>R</i> ₁ (<i>F</i> _o > 2σ <i>F</i> _o)	0.0617	0.0715	0.0341
w <i>R</i> ₂	0.1637	0.1561	0.0777

Table 4.18 Crystallographic data for complexes **20**, $\{\text{BT}\}_2\text{C}=\text{C}\{\text{BT}\}_2$, **11** and $\{\text{BO}\}_2\text{C}=\text{C}\{\text{BO}\}_2$, **22**

	20	11	22
Empirical formula	$\text{C}_{68}\text{H}_{52}\text{Au}_2\text{Cl}_4\text{N}_4\text{O}_4\text{P}_2$	$\text{C}_{32}\text{H}_{20}\text{Cl}_6\text{N}_4\text{S}_4$	$\text{C}_{30}\text{H}_{16}\text{N}_4\text{O}_4$
Formula weight ($\text{g}\cdot\text{mol}^{-1}$)	1586.81	801.46	496.47
Crystal system	Triclinic	Monoclinic	Monoclinic
Space group	$P\bar{1}$	$P2_1/n$	$P2_1/c$
a (Å)	9.4960(6)	9.9553(16)	9.2697(9)
b (Å)	12.9445(8)	16.299(3)	16.1943(16)
c (Å)	13.1761(8)	11.5485(19)	8.0332(8)
α (°)	74.6170(10)	90.00	90.00
β (°)	88.2130(10)	115.400(2)	104.395(2)
γ (°)	70.6180(10)	90.00	90.00
Volume (Å ³)	1470.21(16)	1692.7(5)	1168.1(2)
Z	1	2	2
Calculated density ($\text{g}\cdot\text{cm}^{-3}$)	1.792	1.572	1.412
Wave length (Å)	0.71073	0.71073	0.71073
Temperature (K)	100(2)	100(2)	273(2)
Absorption coefficient (mm^{-1})	5.275	0.786	0.096
Crystal size (mm^3)	0.30 x 0.25 x 0.10	0.35 x 0.25 x 0.15	0.30 x 0.25 x 0.15
$2\theta_{\text{max}}$ (°)	50.7	56.5	56.5
Index range, hkl	$-11 \leq h \leq 11$ $-15 \leq k \leq 15$ $-15 \leq l \leq 15$	$-12 \leq h \leq 12$ $-21 \leq k \leq 21$ $-15 \leq l \leq 14$	$-12 \leq h \leq 12$ $-17 \leq k \leq 21$ $-10 \leq l \leq 17$
Reflections collected	14625	19055	6984
No. of independent reflections	5356 ($R_{\text{int}} = 0.0227$)	4019 ($R_{\text{int}} = 0.0370$)	2714 ($R_{\text{int}} = 0.0213$)
Parameters	405	208	172
Goodness of fit	1.058	1.072	1.062
Largest peak	1.07	0.83	0.36
Deepest hole	-0.48	-0.62	-0.29
R_1 ($F_o > 2\sigma F_o$)	0.0195	0.0378	0.0482
wR_2	0.0474	0.0907	0.1167